Determining the spatial and temporal distribution of macro- and microplastics in soil and their impact on soil function.

RAMAGE, S.J.F.F.

2024

DETERMINING THE SPATIAL AND TEMPORAL DISTRIBUTION OF MACRO- AND MICROPLASTICS IN SOIL AND THEIR IMPACT ON SOIL FUNCTION

STUART JOHN FREDERICK FORDE RAMAGE

PhD

2024

DETERMINING THE SPATIAL AND TEMPORAL
DISTRIBUTION OF MACRO- AND MICROPLASTICS IN SOIL
AND THEIR IMPACT ON SOIL FUNCTION

STUART JOHN FREDERICK FORDE RAMAGE

A thesis submitted in partial fulfilment of the requirements of
Robert Gordon University
for the degree of Doctor of Philosophy

This research programme was carried out in collaboration with
The James Hutton Institute

October 2024

Declaration

I declare that the work presented in this thesis is my own, except where otherwise acknowledged, and has not been submitted in any form for another degree or qualification at any other academic institution.

Information derived from published or unpublished work of others has been acknowledged in the text and a list of references is given.

Stuart J. F. F. Ramage

Acknowledgements

Abstract

Microplastics are long-term anthropogenic terrestrial ecosystem stressors which are ubiquitous in the natural environment, found in all ecological niches including aquatic and terrestrial environments. Consequently, microplastics have been found within organisms and plants, where they have the potential to induce adverse effects. Little is known of microplastic distribution in Scotland (or worldwide), their fate over time, and how they interact with organic pollutants or the impact of these interactions on soil function. It was the overarching aim of this project to determine the extent of macro- and microplastics in Scottish surface soils, both spatially and temporally, and evaluate the impact of microplastics on soil function and ecosystem services.

The novel high-gradient magnetic separation (HGMS) methodology was developed to overcome the challenges faced using the commonly used density separation method and improve recovery rates of all microplastic types, compositions, and sizes, regardless of soil type. HGMS was able to recover microplastics consistently across different soil types and their recovery rates ranged between 91- 96% which was statistically higher than the achieved by density separation (0-89%; p < 0.05). The HGMS method not only allowed for the recovery of high-density microplastics, but it also showed capability for recovering fibres held in fibre-soil aggregate complexes. The HGMS method was then applied to investigate the fate of microplastics in a long-term sewage sludge study, and to determine spatial distribution of microplastics on a national scale.

Sewage sludges applied to agricultural soils are sources of microplastic pollution, however, little is known about the accumulation, persistence, or degradation of these microplastics over time. In a long-term study (25 years), the abundance and degradation of microplastics was assessed in soils sampled biennially from an experimental field managed under an improved grassland regime following the application of five different sewage sludges. Microplastic abundance, dominated by fibres, significantly increased by 1417-3700% following sewage sludge applications (p < 0.05) with abundance remaining relatively constant over time (22 years) (p > 0.05). Fibres degraded over time, showing the greatest reduction in size, highlighting the possibility that fibres release secondary micro(nano)plastics. Films were also highly susceptible to degradation, while other microplastic morphologies were more resistant. Coloured fibres showed dye loss over time, which possibly leached into soil. The sludges contained different microplastic compositions (e.g., polyester, polyurethane), reflecting the possible different sources of the sludges. This evidence is useful in informing regulation on sewage sludge use and management, and in assessing the fate and impact of microplastics in soil.

The first national-scale study on microplastic prevalence in soils was conducted using the National Soils Inventory of Scotland. Results highlighted that microplastic 'hotspots' could be identified through distribution mapping which demonstrated that geography played a role in microplastic distribution e.g., spatial variation in land use or rural locations impacted by tourism. Fibres were the most abundant microplastic morphology (≥ 88.91%). Microplastic data was correlated to anthropogenic, topographical, soil physicochemical, and environmental factors which influenced microplastic

distribution in Scotland. Largely, land use was a significant factor in the distribution of microplastics such that high-intensity land management resulted in higher microplastic pollution (average 3756 microplastics L^{-1} soil) compared to unmanaged soils (average 562 microplastics L^{-1} soil) ($p < 0.05$). Microplastics were also correlated with persistent organic pollutants (r_S = 0.18-0.46), including compounds linked to plastic manufacturing and degradation, suggesting that microplastics may contribute to pollution of these contaminants through leaching or that they share a common anthropogenic source.

Further, sorption and desorption kinetics of 16 priority polycyclic aromatic hydrocarbons (PAHs) were investigated using two different sizes of polyethylene microfilms derived from mulch film mixed into an agricultural soil. Sorption data fitted a first order equilibrium model while desorption data fitted an exponential decay model. Sorption and desorption kinetics were influenced by physico-chemical properties of PAHs, and no significant differences between the rate of sorption or desorption were observed. Decreases in soil organic matter indicated that smaller-sized microfilms sequestered a higher amount of PAHs (3.36% decrease compared to 2.93% for the larger microfilm) and sorption to microfilms prevented soil acidification likely caused through microbial degradation (2.67% decrease in soil pH opposed to 4.10%).

The effect of microfilms, chrysene, and chrysene-bound microfilms on ecosystem function (soil respiration) and microbial activity (substrate-induced respiration) was then investigated. The treatment groups showed differences in function and activity with chrysene inducing reduced soil respiration and microbial activity ($p < 0.05$), microfilms inducing increased soil respiration and microbial activity, and chrysene-bound microfilms not significantly changing ecosystem function compared to a soil negative control. These were attributed to changes in the microbial biomass. Evaluation of the microbial community composition through sequencing of the 16S rRNA gene showed differences in the microbial communities was more pronounced at a lower taxonomic level (family) and that there were significant changes in beta diversity of the microbial communities between treatments ($p < 0.05$). Sorption of chrysene to microfilms appear to limit the availability of chrysene to soil micro-organisms and may alleviate the immediate effects of chrysene. However, this may pose a greater threat as chrysene could be slowly released into the soil environment and persist over a prolonged period.

Key findings are discussed throughout this thesis, which highlight the importance of understanding the extent and impact of microplastics in Scotland to enable future work to be conducted and inform future mitigation and remediation strategies for the protection of one of Scotland's most valuable natural assets.

Keywords: Microplastics; soil; pollution; persistence; degradation; persistent organic pollutants; sorption kinetics; ecosystem function; microbial activity; Scotland

Research outputs

Published papers:

- Ramage S.J.F.F., Pagaling E., Haghi R.K., Dawson L.A., Yates K., Prabhu R., Hillier S., Devalla S. Rapid extraction of high- and low-density microplastics from soil using high-gradient magnetic separation. *Science of The Total Environment*. 2022; 831, 154912. DOI: https://doi.org/10.1016/j.scitotenv.2022.154912

Oral conference presentations:

- Robert Gordon University's 3 Minute Thesis competition (2023)
  - Runner-up of 8 participants
- 9th Annual European Network of Forensic Science Institutes – Animal, Plant and Soil Traces Working Group meeting (2022), "*Microplastics in Scottish soils: A new method to reveal their fate and their applicability to forensic science*"
- RGU School of Engineering Alumni event (2022), "*A novel approach to extracting microplastics from soil using high-gradient magnetic separation*"
- Postgraduate Hutton Symposium (2021), "*Rapid extraction of high- and low-density microplastics from soil using high-gradient magnetic separation*"
  - Awarded the *James Hutton Limited Innovation Prize*
- Raman Optronics Webinar Series 2021 (2021), "*Development of an automated method for enumeration of Nile Red-stained microplastics in soil using fluorescence microscopy*"
- Microplastics eConference 2020 (2020), "*Challenges in the separation of microplastics from terrestrial soils*"
- Postgraduate Hutton Symposium (2020), "*Determining the spatial and temporal distribution of macro- and microplastics in soil and their impact on soil function*"
- 5th Annual Scottish Student Forensic Research Symposium (2019), "*Assessing the problems & potential value of microplastics in soil as trace evidence*"
  - *Awarded 1st prize*.

Poster conference presentations:

- 44th TB Macaulay Lecture (2023), "*Application of sewage sludge to soil results in the accumulation, persistence, and degradation of microplastics in soil: evidence from a 25-year study*"
- SEFARI (2023), "*Forensics and micropollutants: plasticisers and microplastics*"
- 22nd World Congress of Soil Science (2022), "*Rapid extraction of high- and low-density microplastics from soil using high-gradient magnetic separation*"
- 11th Scottish Symposium on Environmental Analytical Chemistry RSC (2020), "*High-gradient magnetic separation of microplastics from environmental matrices*"
- Environmental and Biochemical Science internal review (2020) – poster presentation, "*Determining the spatial and temporal distribution of macro- and microplastics in soil and their impact on soil function*".

Awards and achievements:

- Runner-up in Robert Gordon University's 3 Minute Thesis competition (2023)
- PhD research on microplastic extraction from soils included in the Scottish Government's RESAS 2016-2022 highlights report (https://www.gov.scot/publications/2016-22-rural-affairs-food-environment-research-programme-evaluation-highlights-report/)
- Awarded funding to undertake a course in Next-Generation Sequencing data analysis following a competitive internal grant application (James Hutton Institute – "*Post-graduate Student Conference and Training Fund*") totalling £789 (2022)
- James Hutton Limited Innovation Prize (2021) – for the development of a novel method of microplastic extraction from soil (and other matrices) using modified iron nanoparticles and high-gradient magnetic separation, improving recovery rates compared to conventional methods
- 1st prize for oral presentation, Scottish Student Forensic Research Symposium (2019) – see "Oral conference presentations".

Contents

List of tables

Chapter 6

List of figures

The PE microplastics used here contained aluminium trihydrate (gibbsite) (troughs around 3500 cm^{-1} region) – a common plastic flame-retardant filler (Shah et al., 2014).

Chapter 4

appearing with ragged edges (E-F). The panels are labelled with the year that the soil was sampled.

Chapter 5

Chapter 1: Introduction

1.1 Motivation for research

Plastics are one of the largest mass-produced man-made materials ever produced across the world since its first introduction in the 1950s. Because of their increasing affordability, durability, and versatility, global production of resins and fibres have increased significantly from 2 Mt in the 1950s to 368 Mt (excluding synthetic fibre production) in 2019 (PlasticsEurope, 2020) at an estimated growth rate of 8.5% per annum, accumulating to a total of around 7800 Mt plastic produced worldwide. Half of which has been produced since 2002 alone.

Geyer et al. (2017) reported that of the total plastic waste generated, only 9% was recycled, 12% incinerated, and a significant proportion was disposed of in landfills or accumulated in the natural environment (79%). Plastic constitutes 54% by mass of the anthropogenic waste materials released into the environment (Hoellein et al., 2014). Projected figures estimate that by 2050, the natural environment and landfills will retain 12,000 Mt of plastic waste (Geyer et al., 2017). Furthermore, due to a high volume of single use plastics, the amount of plastic waste in 2015 was estimated to be approximately 6300 Mt (Geyer et al., 2017). Single use plastics accounted for over a third of global plastic production in 2017 (Jefferson, 2019). The terrestrial environment in particular faces an unparalleled threat whereby annual plastic release to land is estimated to be 4-23 times greater by mass than that released to oceans (Horton et al., 2017).

Plastics have many diverse uses, however, the highest demand for plastic is in the packaging industry (39.6%) (PlasticsEurope, 2020). The use of plastic is also in demand for building and construction (20.4%), automotive components (9.6%), electronics (6.2%), household, leisure, and sports (4.1%), agriculture (3.4%), and miscellaneous uses such as medical appliances and mechanical engineering (16.7%). As such, there are many different polymer types available which offer a range of desirable properties depending on their intended application. Thermoplastics, a class of polymers that repeatedly melt when heated and harden when cooled, represent 84.6% of registered polymers (PlasticsEurope, 2020). Thermoplastics include polymers such as polyethylene, polypropylene, polyvinyl chloride, polyethylene terephthalate, and polystyrene. The other class of plastics are thermosets which are polymers that, once heated, undergo a chemical change to form a three-dimensional network which do not allow the plastic to be remelted or reformed after cooling, and

Table 1.1: Table of common plastics featured in this thesis, their densities and structures, and their common uses (PlasticsEurope, 2020). Structures were generated using ChemDraw.

Name	Structure	Density (g/cm^3)	Type	Common uses
Polyethylene	[repeating unit: –C(H)(H)–C(H)(H)–]$_n$	0.88-0.96	Thermoplastic	Food packaging, reusable bags, trays and containers, agricultural film, toys, pipes, houseware
Polypropylene	[repeating unit: –C(H)(CH$_3$)–C(H)(H)–]$_n$	0.86-0.95	Thermoplastic	Food packaging, pipes, automotive components, bank notes, tree guards
Polyethylene terephthalate	[repeating unit: –C(=O)–C$_6$H$_4$–C(=O)–O–C(H)(H)–C(H)(H)–O–]$_n$	1.37-1.46	Thermoplastic	Containers for liquids and foods
Polyvinyl chloride	[repeating unit: –C(H)(H)–C(H)(Cl)–]$_n$	1.40	Thermoplastic	Window frames, construction materials, pipes, cable insulation, water sport equipment
Polystyrene	[repeating unit: –C(H)(C$_6$H$_5$)–C(H)(H)–]$_n$	0.96-1.05	Thermoplastic	Food packaging, building insulation, electrical equipment
Polytetrafluoro-ethylene	[repeating unit: –C(F)(F)–C(F)(F)–]$_n$	2.20	Thermoplastic	Cable coating, valves, non-stick coatings, automotive components, electrical appliances
Polymethyl methacrylate	[repeating unit: –C(H)(CH$_3$)–C(H)(COOCH$_3$)–]$_n$	1.17-1.20	Thermoplastic	Touch screens, glass substitute, electrical appliances
Polyurethane	[repeating unit: –C(=O)–N(H)–C(H)(H)–C(H)(H)–N(H)–C(=O)–O–C(H)(H)–C(H)(H)–O–]$_n$	0.08-0.30	Thermoset	Building insulation, footwear, furniture
Acrylic fibre	[repeating unit: –C(H)(CN)–C(H)(H)–]$_n$	1.25-1.34	Thermoset	Clothing, textiles
Nylon fibre	[repeating unit: –C(=O)–(CH$_2$)$_4$–C(=O)–N(H)–(CH$_2$)$_6$–N(H)–]$_n$	1.08-1.62	Thermoplastic	Clothing, textiles
Polyester fibre	[repeating unit: –C(=O)–C$_6$H$_4$–C(=O)–O–C(H)(H)–C(H)(H)–O–]$_n$	1.38	Thermoset	Clothing, textiles

include plastics such as polyurethanes, polyesters, acrylics, and phenol-formaldehydes. Examples of a range of common plastics, their structures, type, and other information is presented in Table 1.1.

The properties of each type of plastic can reflect the operational lifetime of that plastic product. For example, the affordability, versatility, chemical resistance, and durability of thermoplastics such as polyethylene, polypropylene, and polyethylene terephthalate, make them ideal materials for packaging. However, packaging materials are largely single-use, therefore, the operational lifetime of these plastic items is relatively short before the item is quickly disposed. Single-use plastics are accountable for over a third of global plastic production (Jefferson, 2019), but has doubled in production since 2000 with 40% of production dominated by packaging materials (Chen et al., 2021). Chen et al. (2021) also reported that 32% of single-use plastic packaging is released to the natural environment. The properties that make plastics highly desirable materials for household, commercial, and industrial use also make plastics extremely resistant to degradation in the natural environment.

Continued large-scale production of plastics, their rapid consumption and poor waste management, and very low environmental degradability has led to a significant accumulation of plastic waste within the terrestrial environment (Ng and Obbard, 2006). Herein lies an unprecedented environmental and ecological concern, whereby the slow degradation of plastic waste through mechanical, chemical, or biological processes leads to the formation and release of microplastics (<5 mm in size) into the terrestrial environment which can have negative consequences for the biophysical environment and human health. Scotland has a large and diverse variety of land uses, topographical features, and soil types and physicochemical properties. As such, microplastic pollution has the potential to be extremely complex due to the many factors which can influence their abundance, distribution, size, degradation, and interaction with pollutants and soil microbes. The James Hutton Institute also houses the National Soils Archive of Scotland containing archived samples and surface soils taken from across the whole of Scotland. These soils are supplemented with large datasets. These unique resources and databases allow for the investigation of microplastics in Scottish soils both temporally and spatially, providing an unparalleled insight into microplastic pollution in Scotland, and understand factors which may influence and drive microplastic pollution in Scotland.

1.2 Research aim and objectives

The overarching aim of this project was to determine the extent of macro- and microplastics (plastics > 5 and ≤ 5 mm in size, respectively) in Scottish surface soils, both spatially and temporally, and evaluate the impact of microplastics on soil function and ecosystem services. The following objectives were set out to meet this aim:

1. Develop a novel method for improved extraction of microplastics from soil to be applied to soil samples throughout the project.
2. Measure microplastics in archived soils collected from sewage sludge-treated land (1994-2019) to investigate their fate over time.
3. Measure microplastics in soils archived in the National Soils Inventory for Scotland to determine the prevalence of microplastics in Scotland on a national spatial scale.
4. Map microplastic distribution and investigate factors that influence microplastic distribution (e.g., land use, soil type, environmental and biological factors) using multivariate statistics.
5. Determine the sorption and desorption kinetics of organic contaminants with microplastics and investigate the impact of microplastics carrying organic pollutants on soil function and ecosystem services using microbial respiration, microbial activity (MicroResp^{TM}), and microbial community structure (16S rRNA gene sequencing).

1.3 Thesis structure

The thesis is structured as follows:

Chapter 2: This chapter presents a comprehensive literature review of the background in plastic pollution, and in particular, microplastic pollution in the terrestrial environment, and the subsequent known consequences of microplastic interactions in soils. This chapter establishes the knowledge gaps this project intended to address.

Chapter 3: A novel extraction method for improving microplastic recoveries from soil matrices is presented in this chapter. The extraction method developed combined the use of surface-modified iron nanoparticles for magnetic tagging of microplastics and high-gradient magnetic separation (HGMS), a commonly used technique in soil science. The performance of the developed method was tested against that of the commonly used density separation method which is subject to several hindrances

in microplastic recoveries from soil. The developed HGMS method out-performed the density separation method and overcame the problems associated with this method.

Chapter 4: The developed HGMS method was applied to archived soils dating from 1994 to 2019 to investigate the fate of microplastics over time in soils treated with sewage sludge. This chapter provides the first high temporal resolution data of the accumulation, persistence, and degradation of microplastics over a 25-year period. This study is also the first to report the appearance of partially dyed fibres, whereby the dye in the fibres may have been degraded or leached into the soil which may lead to toxic effects in the soil environment. The weathering of microplastics over time was also assessed by scanning electron microscopy and Fourier-transform infrared spectroscopy analysis.

Chapter 5: The first national scale study of the distribution of microplastics in soil is presented in this chapter. Microplastics were recovered from surface soils obtained from the National Soils Inventory for Scotland using the developed HGMS method, and their abundance and distribution was mapped. Environmental and anthropogenic factors which may affect microplastic distribution were extensively assessed, as well as the relationships of microplastics with persistent organic pollutants measured in the soils which are associated with plastic production and degradation.

Chapter 6: This chapter investigated the sorption and desorption kinetics of sixteen (16) polycyclic aromatic hydrocarbons (PAHs) with different sizes of polyethylene microfilms derived from mulching film in an agricultural soil. It is the first study to investigate PAHs sorption in a true soil matrix under environmentally realistic conditions and also one of the few to report desorption kinetics of PAHs in a soil-microfilm system. The size of microplastics affect the sorption and desorption rates for different molecular sizes of PAHs. The potential impact of these interactions on the physicochemical properties of soil was investigated and discussed.

Chapter 7: The impact of the interactions of PAHs with microplastics was further explored in this chapter by elucidating the combined effects of microplastics and PAHs on soil microbial community structure and activity. Soil respiration measurements indicated that ecosystem function was decreased in chrysene treatments and elevated in microfilm treatments. The presence of microfilms in the chrysene-bound microfilm treatment indicated that they alleviated the negative impact of chrysene.

Substrate-induced respiration confirmed the findings in soil respiration suggesting that microbial activity was hindered by chrysene, elevated by microfilms, and neutralised in the chrysene-bound microfilm treatments. Furthermore, glucose-induced respiration suggested that microbial biomass was depleted by chrysene, increased by microfilms, and slightly increased in chrysene-bound treatments. Analysis of the 16S rRNA gene sequences confirmed changes in the microbial community compositions between treatments, with changes pronounced at a lower taxonomic level (i.e., family). An increase in rarer taxa was observed in the chrysene treatment which are attributed to polycyclic aromatic hydrocarbon degradation.

Each chapter has its own introduction covering the background information and addressing the necessity for researching each topic. Each chapter also includes their own materials and methods, results and discussion, and conclusion sections, along with their own references and supplemental data (appendices) where appropriate. All results from throughout this thesis are summarised and drawn together in Chapter 8.

1.4 References

Chen Y., Awasthi A.K., Wei F., Tan Q., Li J. Single-use plastics: Production, usage, disposal, and adverse impacts. *Science of The Total Environment*. 2021; 752, 141772. DOI: https://doi.org/10.1016/j.scitotenv.2020.141772

Geyer R., Jambeck J.R. and Law K.L. Production, use, and fate of all plastics ever made. *Science Advances*. 2017; 3(7), 25–29. DOI: https://doi.org/10.1126/sciadv.1700782

Hoellein T., Rojas M., Pink A., Gasior J., Kelly J. Anthropogenic litter in Urban freshwater ecosystems: Distribution and microbial interactions. *PloS One*. 2014; 9, e98485. DOI: https://doi.org/10.1371/journal.pone.0098485

Horton A.A., Walton A., Spurgeon D.J., Lahive E., Svendsen C. Microplastics in freshwater and terrestrial environments: Evaluating the current understanding to identify the knowledge gaps and future research priorities. *Science of The Total Environment*. 2017; 586, 127-141. DOI: https://doi.org/10.1016/j.scitotenv.2017.01.190

Jefferson M. Whither Plastics? – Petrochemicals, plastics and sustainability in a garbage-riddled world. *Energy Research and Social Science*. 2019; 56, 101229. DOI: https://doi.org/10.1016/j.erss.2019.101229

Ng K.L., Obbard, J.P. Prevalence of microplastics in Singapore's coastal marine environment. *Marine Pollution Bulletin*. 2006; 52(7), 761–767. DOI: https://doi.org/10.1016/j.marpolbul.2005.11.017

Parolini M., et al. Microplastic Contamination in Snow from Western Italian Alps. *International Journal of Environmental Research and Public Health*. 2021; 18, 768. DOI: https://doi.org/10.3390/ijerph18020768

PlasticsEurope. 2020. *Plastics – the Facts 2020: An analysis of European plastics production, demand and waste data.* [online]. Brussels: PlasticsEurope. Available from: Plastics - the Facts 2020 • Plastics Europe [Accessed 01 February 2021].

Chapter 2: Literature Review

2.1 Microplastics

Microplastics are ecosystem stressors defined as pieces of plastic which are ≤ 5 mm in size (diameter), while macroplastics are those > 5 mm and nanoplastics are those ≤ 1 mm. Furthermore, microplastics can be classified as primary or secondary microplastics. Primary microplastics are purposefully manufactured for use in cosmetic or personal care products and within industrial processes, and secondary microplastics are the products of degradation from larger pieces of plastic (Wang et al., 2019a).

Microplastics can be categorised based on their morphology. These morphologies are predominantly fibres, fibre bundles, films, flakes, particles, and fragments (Figure 2.1A-F, respectively). For this project, the following definitions from Rochman et al. (2019) were used. Fibres were defined as flexible textile fibres of equal thickness throughout their length, while fibre bundles were defined as tightly wound masses of entangled fibres which could not be separated. Films were defined as flat, thin pieces of plastic that were malleable, whereas flakes were defined as flat, thin pieces of plastic that were not malleable. Particles were defined as spherical in shape with a smooth surface, but also included hemispheres (i.e., fragmented spheres). Finally, fragments were defined as rigid microplastics which had irregular or angular shapes.

2.1.1 Sources of (micro)plastics in the terrestrial environment

The terrestrial environment includes soil, its interface with air, and its associated biological communities (Tarazona and Ramos-Peralonso, 2014). Soil is composed of minerals, organic matter, gas, water, and living organisms, and serves main functions including nutrient cycling, carbon storage and turnover, regulation of biotic processes and promotion of biodiversity, sustaining plant and crop systems, and water and air filtration (Hatfield et al., 2017). There are many different soil types which are classified based on their texture (particle size distribution), mineralogy content, and organic matter content. Scotland, in particular, has a large variety and diversity of soil types ranging from highly organic and acidic soils (peats) to fertile brown earth soils to podzols and gleys (The James Hutton Institute, 2023).
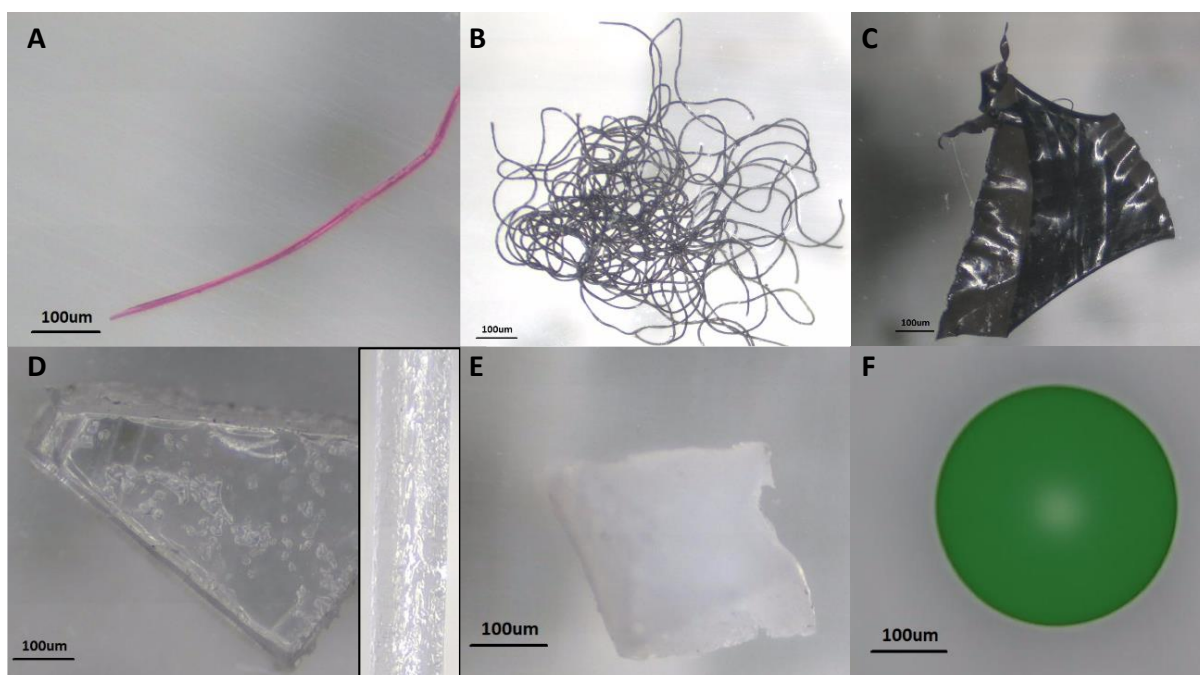
Figure 2.1: Images of the microplastic morphologies observed in this project. Images are: (A) fibre, (B) fibre bundle, (C) film, (D) flake with side profile (width), (E) fragment, and (F) particle. Images were taken using an Olympus BX53M microscope fitted with a YenCam HD camera.

There are many pathways for plastic pollution (including microplastics) to continuously enter the terrestrial environment directly or indirectly. Agriculture has been identified as a potentially significant source of plastic waste and a sink for microplastic pollution, with annual global plastic use in agricultural production estimated at 12.5 million tonnes (FAO, 2021). Mulch film is a globally used technology due to the improvements in crop health and yield, amongst other benefits (Yang et al., 2021). However, the retrieval of mulch film is difficult and laborious, and often leads to macro-sized film residues remaining in the soil which become a source of microplastics. Other uses of film include wrapping for silage which similarly becomes a source of agricultural microplastics. Another pathway for microplastic pollution in agricultural soils is through the application of soil amendments such as sewage sludge or compost which contain high abundances of microplastics (Xu et al., 2020; Ramage et al., 2022). Sewage sludges are the biosolid waste material of the wastewater treatment process which results from the settling of the solid waste material which includes microplastics originating from industrial or household wastewater (e.g., synthetic fibres from clothing and microbeads from personal care products) (Carr et al., 2016). It is then commonly applied to agricultural soils worldwide as a fertiliser because it is rich in organic matter and macro- and micronutrients, which benefit soil fertility and function (Elmi et al., 2020), inadvertently transferring these microplastics into the soil. Composts contain microplastics as a result of improper disposal and inadequate waste management (Bläsing and Amelung, 2018). The final

main source of agricultural microplastic is through irrigation from natural water bodies or repurposed wastewater effluent (Jian et al., 2020).

Soils also receive large quantities of plastic waste through littering and illegal dumping of waste leading to microplastic production, which can then be translocated through wind action and surface run-off or flooding (Kim et al., 2006). Furthermore, atmospheric deposition is also one of the most significant sources of soil microplastics. Owing to their light weight, microplastics can be transported through the atmosphere by wind and subsequently deposited in soils (Allen et al., 2019). Rainfall has been identified as an important factor influencing microplastic deposition, with increased rainfall resulting in higher microplastic fallout (Dris et al., 2016; Xie et al., 2020). This is also true for snowfall (Zhang et al., 2020).

2.1.2 Microplastic formation, degradation, and persistence

Once exposed to the soil environment is simultaneously degraded through abiotic (chemical, physical) and biotic processes. The degree of chemical degradation of microplastics varies depending on the polymer type, the presence of additives such as UV stabilisers or anti-oxidants within the polymer matrix, as well as the medium in which the microplastic is present (Song et al., 2017). UV irradiation (photodegradation or photo-oxidation) is a key driver to (micro)plastic degradation in surface water and coastal areas (Bläsing and Amelung, 2018), however, exposure of (micro)plastic pollution to UV radiation and oxygen is limited to only those present on the soil's surface or at shallow soil depths due to soil impediment (Beltrán-Sanahuja et al., 2021; Huang et al., 2021). As such, degradation of plastics may be a slower process in soil compared to aquatic environments. Photo-oxidation leads to the alteration in polymer chemical structure by forming oxygen containing functional groups but more importantly, UV light has sufficient energy to overcome the bond dissociation energies of C-C and C-H bonds of the basic polymer backbone (375 and 420 kJ mol^{-1}, respectively) leading to the formation of free radicals (Krueger et al., 2015; Song et al., 2017). This bond dissociation leads to microplastic surface embrittlement (i.e., crack formation) which weakens the structural integrity of microplastics and promotes fragmentation. Hydrolysis is another route for the chemical degradation of microplastics.

The chemical composition of microplastics, however, dictate the influence of chemical degradation. For example, polyethylene's backbone is exclusively C-C single bonds (Table 1.1) and are resistant to photo-

oxidation (Chamas et al., 2020), however, any impurities introduced during manufacturing, prior weathering, and any unsaturated C=C bonds which may be present can act as chromophores which are readily oxidised into functional groups which are susceptible to photo-oxidation. On the other hand, polymers such as polyethylene terephthalate is composed of two alternating subunits, ethylene glycolate and terephthalate, linked by ester bonds (Table 1.1). These subunits are more susceptible to photo-oxidation and, albeit slow, may chemically degrade faster than polyethylene. Under acidic conditions, the hydrolysis of polyethylene terephthalate is accelerated, and due to the formation of carboxylic acids, the pH of the local soil may drop leading to autocatalytic acceleration (Chamas et al., 2020).

Physical abrasion is also a driving factor in degradation, however, movement and abrasion in soil is minimal or non-existent except in predominantly agricultural soils whereby mechanical fragmentation can occur due to practices such as tilling (Zhou et al., 2020).

Various soil microbial communities can also biodegrade microplastics, and Pathak and Navneet (2017) reported that this occurs in sequential steps. These are: bio-deterioration (the alteration of the polymer's chemical and physical properties), bio-fragmentation (breakdown of polymers into simple units such as monomers and dimers by catalytic enzymatic cleavage), assimilation (uptake of these simpler molecules by microorganisms), and mineralisation (oxidised metabolite production e.g., CO_2, CH_4, H_2O, organic acids). As with chemical degradation, biodegradation of polymers depends upon their physical and chemical properties (e.g., molecular weight and crystallinity) as well as soil conditions such as available oxygen and soil pH, but also on the microbial species within the community (Pathak and Navneet, 2017). Aerobic conditions are favourable for microbial degradation as oxygen acts as an electron acceptor and produces greater energy (Gu, 2003), and the presence of oxygen will also aid in potential photo-oxidative degradation which in turns promotes better microbial degradation (Krueger et al., 2015). Anaerobic conditions are prevalent in deeper layers of soil, therefore, the efficiency of biodegradation will decrease. Biodegradation is an important remedial process for microplastic pollution in soil as not only does it cause physical fragmentation, but it also produces smaller molecules which act as carbon sources which soil microbes can utilise for energy by metabolising these molecules through enzymatic systems (Li et al., 2023a). Both bacteria and fungi can degrade microplastics, however, fungi have been reported to show greater biodegradability, possibly related to the extra- and intra-cellular enzymes which they secrete (Zhu et al., 2023).

As a result of the slow degradative processes and the poor conditions within soils that result in low microplastic degradability, microplastics can persist in the terrestrial environment for a significant period of time. For example, Bläsing and Amelung (2018) reviewed several studies which reported that only 0.4% of polyethylene and polypropylene degraded after 800 and 365 days in soil, respectively, while polyvinyl chloride displayed no degradation after 35 years. Soils are, therefore, referred to as a sink for microplastic pollution, as microplastic degradation is minimal and they accumulate rapidly over time.

The progress of microplastic degradation is not well understood, since all studies examine microplastics retrospectively from locations of known historical input (e.g., sewage sludge applications or mulch film usage) or have relatively short-term experiments simulating the natural environment. While these studies provide insight into the degradative process of microplastics, there is no current knowledge of microplastic degradation in high temporal resolution. High temporal resolution data such as this would allow researchers to understand the fate of microplastics over time and better inform understanding on the impact of microplastic pollution in soils.

2.1.3 Microplastic distribution

Microplastics are ubiquitous in soils, however, there are significant regional variations in microplastic distribution in soils which are influenced by anthropogenic or environmental factors. As outlined in section 2.2.2, agricultural soils are the most affected soils by anthropogenic activities which lead to high microplastic abundances. However, there are significant variations in microplastic abundance between agricultural soils in different regions with the same land use type. For example, a typical farm in Germany contained 3.7 ± 11.9 microplastics kg^{-1} topsoil (0-10 cm) (Harms et al., 2021), while 2462 ± 3767 microplastics kg^{-1} were recovered from an agricultural soil (0-10 cm) in China (Chen et al., 2022). The differences in abundances may be attributed to the amount of plastic used, plastic waste management, the history of plastic use, and type of plastics used on the farms.

Soils in remote locations with minimal human activity such as the Tibetan Plateau (China) (Feng et al., 2020) and Alp regions (Western Italy) (Parolini et al, 2021) can also be polluted with microplastics at significantly lower abundances compared to soils in locations with higher human activity such as agricultural soils. Büks and Kaupenjohann (2020) reported that soil microplastic abundances in rural locations can be 10 times lower than in soils in the vicinity of municipal areas. Microplastics in remote

locations with no population or industries are largely due to tourism with inputs from atmospheric deposition (Li et al., 2023a). Microplastic abundance is also negatively correlated with elevation (Zhou et al., 2021a).

Coastal soils have exhibited a large variation in microplastic abundance (e.g., 1.3 to 14712.5 microplastics kg^{-1} (Zhou et al., 2018)) whereby microplastic abundances are attributed to the distance of sampling location to the sea and atmospheric factors such as wave height and spray as well as prevailing winds, sea-based activities (e.g., mariculture, commercial fishing, recreational activities) as well as nearby land-based tourism and leisure, and the proximity and density of urban populations.

It is, therefore, evident that the many different land areas and uses, including population densities and environmental factors, have a substantial influence on the abundance and distribution of soil microplastic pollution. To date, only regional studies have been conducted (e.g., Corradini et al., 2021; Li et al., 2023b; Qiu et al., 2023) which is limited by the study area and the variety of human populations, anthropogenic activities, and land uses. However, no studies have been conducted on a national scale to understand the wider context of microplastic abundance in soil which would take into account the vast range of soil types, the variation between and within land uses, and environmental and biological factors which may influence the distribution and prevalence of microplastic pollutions.

2.2 Microplastic extraction and analysis

2.2.1 Extraction methods

To quantify and subsequently analyse microplastics, they must first be extracted from soils, however, this is a complicated task as soils are a complex solid matrix, with broad inter- and intra-sample density and particle size ranges (de Souza Machado et al., 2018). Despite extraction being the preliminary and, arguably, the most imperative step, there is currently no standardised method for microplastic extractions from soils which can lead to unknown variations in extraction recoveries when comparing studies as well as doubts into the degree of accuracy in the subsequent reporting of results.

The most commonly applied method for soil microplastic extraction is the density (or flotation) method. This method takes advantage of the difference in density between plastics and soil particles

(Zhang et al., 2019), with most plastic densities ranging from 0.9-2.3 g mL^{-1} while soil particles have higher densities around 2.6-2.7 g mL^{-1} (Prata et al., 2020a). Microplastics are separated from soil using saturated high-density salt solutions (e.g., NaCl, ZnCl$_2$, NaI, and CaCl$_2$ (1.2-1.8 g mL^{-1})) whereby lighter density microplastics float while denser soil particles settle after thorough mixing (Zhang et al., 2019). However, density separation causes the flotation of any light-density material. Soils contain high amounts of organic matter which is light in density (1.0-1.4 mL^{-1}) and commonly extracted with microplastics (Han et al., 2019). This can physically hinder the flotation of microplastics as well as interfere with subsequent analyses such as Fourier-transform infrared analysis (FTIR). Digestion steps are often required before or after density separation in order to remove co-extracted organic matter. This is achieved using a range of methods including acidic, alkaline, oxidising, or enzymatic digestion treatments. Of these treatments, oxidising treatments are the most common for soil organic matter digestion which utilise H$_2$O$_2$ due to its superiority at removing soil organic matter compared to acidic and alkaline treatments (Fan et al., 2023). Peroxide digestion can be improved by adding a Fe^{3+} catalyst to the H$_2$O$_2$ (creating Fenton's Reagent) which increases the efficiency of soil organic matter removal and also does not affect the microplastics compared to other digestion methods (Hurley et al., 2018). However, the frothing which occurs during the digestion process, or indeed the need for any additional steps in the extraction, can lead to the loss of extracted microplastics. While the density separation method has high recovery rates for low-density microplastics (Han et al., 2019; Liu et al., 2018; Scheurer and Bigalke, 2018; Zhang et al., 2018), high-density microplastics, such as polytetrafluoroethylene and polyvinyl chloride, are not easily recovered due to their densities being similar to bulk soil particles (Liu et al., 2018; Zhang et al., 2018). Salt solutions are also environmentally toxic which leads to issues with their disposal (Thomas et al., 2020).

Other extraction methods include elutriation which is similar to the density separation method, although, air or water is introduced at the bottom of an enclosed column promoting the flotation of light particles and deposition of heavier particles (Canensi et al., 2022). This method is effective in removing microplastics from sediments samples but is not very effective in soils due to the wider variability in particle size distributions within soils (Grause et al., 2022). Another extraction method, which does not rely on microplastic density but rather their ionic properties, is electrostatic separation (Felsing et al., 2018; Enders et al., 2020). Similar to elutriation, microplastic recovery is extremely effective in sediment samples, however, recovery efficiency is much lower in soils which are richer in minerals which impede the electrostatic attraction of microplastics. Magnetic extraction of microplastics also does not rely on microplastic density, but instead uses surface modified iron nanoparticles to bind to microplastics which in turn can be removed using magnets (Grbic et al., 2019).

Microplastic recoveries were not tested with soil, but the efficiency was low for sediments and the use of magnets caused the fragmentation and damage of microplastics. The choice of microplastic extraction technique for soils is, therefore, important as this initial step will have an impact on subsequent enumeration and analyses.

The methods outlined above each have their respective advantages for microplastic extraction from soil, however, all have their own drawbacks. Namely, differences in extractable of microplastics between different soil types and microplastic type, size, and size. It is important to have an extraction method with high recovery rates irrespective of these factors, particularly when assessing microplastics in Scottish soils, whereby there are many different types (see section 2.1.1).

2.2.2 Microplastic enumeration

Microplastics are commonly enumerated by traversing the filter paper (after density separation), containing the extracted microplastics which had been filtered onto them, under an optical microscope (Qiu et al., 2016), and during enumeration, microplastics can be categorised based on their morphology, colour, and size. As part of this enumeration step, Qiu et al. (2019) set out criteria which must be met when visually assessing whether an observed particulate is a microplastic before it can be included in enumeration:

- No visible cellular or organic structures;
- Fibres are of equal thickness throughout their length;
- Particulates display clear and homogenous colours;
- Transparent or white particulates must be assessed at high magnification and under fluorescence microscopy to exclude organic origins.

This is a quick and simple method for microplastic enumeration but is subject to the competency of the examiner, the influence of potential bias, and the visibility and size of the microplastics.

Fluorescence microscopy provides additional sensitivity and discrimination for both detecting and enumerating microplastics. Microplastics must first be stained with a fluorescent dye such as Nile Red in order to be visualised under the fluorescent microscope (Maes et al., 2017; Devalla et al., 2019), then once irradiated with blue excitation, the fluorescence emission of the stained microplastics can be observed through an orange filter. Caution must be taken when using Nile Red as the dye does not

specifically adsorb to microplastics and will also bind to organic matter due to its lipophilic nature (Grause et al., 2022), therefore, it is imperative that organic matter is digested prior to fluorescence microscopy. Alternatively, organic matter can be counter-stained with dyes such as DAPI (4,6-diamidino-2-phenylindole) so that it can be distinguished easily from other fluorescing material (i.e., microplastics) (Tarafdar et al., 2022). The increase in sensitivity in detection enables smaller sized microplastics to be detected and enumerated offering a greater advantage over optical microscopy. Furthermore, automated counting software has been developed to provide a quick, objective method of microplastic detection and enumeration with high sample throughput capabilities (Prata et al., 2019; Prata et al., 2020b).

2.2.3 Analytical methods

Spectroscopic techniques are used to identify the polymer types and confirm the particulate is indeed a microplastic. The most commonly used spectroscopic technique is Fourier-transform infrared (FTIR) due to its advanced characterisation capabilities and its ability to detect microplastics as small as 10 µm (depending on the method used e.g., FTIR microscopy, attenuated total reflectance (ATR)-FTIR) (Yang et al., 2021). ATR-FTIR can greatly improve the signal-to-noise ratio in the spectra generated from microplastic measurements (Wang et al., 2020a), however, this method requires physical contact of the probe with the microplastic which applies pressure which can subsequently damage the microplastic or account for potential losses of microplastics either during handling or from the pressure of the probe. FTIR microscopy offers lower detection limits (10 µm) compared to other FTIR methods and does not require physical contact with the microplastics and, as such, is the most commonly used technique for microplastic identification. FTIR also enables the assessment of microplastic weathering, whereby the resultant spectrum provides information in structural and chemical alterations (i.e., the addition, loss, or alteration of functional groups and changes in band intensities) (Phan et al, 2022; Zvekic et al., 2022).

Raman spectroscopy is a technique complimentary to FTIR which has the advantage of detecting microplastics as small as 1 µm with higher spectral resolution capabilities (as low as 500 nm) and can simultaneously identify microplastics fillers or pigments (Yang et al., 2021). However, Raman spectroscopy can be hindered by the presence of organic matter which produces a significant background fluorescence signal (Anger et al., 2018; Wang et al., 2020a; Yang et al., 2021), therefore, it is imperative to select appropriate extraction and digestion steps before spectroscopic identification.

Inorganic materials such as clay minerals also interfere with microplastic detection as well as the presence of adsorbed contaminants and the degree of weathering (Anger et al., 2018; Yang et al., 2021).

Scanning electron microscopy (SEM) is an advanced microscopic detection method which offers high resolution stereoscopic imaging of microplastics to gain morphological and topographic information of microplastics as well as provide chemical information (e.g., inorganic additives) using coupled detectors for energy dispersive X-ray analysis (Fries et al., 2013; Fan et al., 2023). Due to the high magnifying power of SEM, imaging can aid in distinguishing microplastics from organic materials and can also be used to assess the weathering of the surface of microplastics (cracks, pitting etc). SEM is a non-destructive technique, however, plastics are poor conductors so need to be coated in a highly conductively metal (e.g., gold) to improve the resolution and quality of the images (Vianello et al., 2013).

Chromatographic techniques such as pyrolysis gas chromatography – mass spectrometry (Pyr-GC-MS) are gaining popularity for analysing the structures of microplastics through analysing their thermal degradation products (Fries et al., 2013) as well as quantifying microplastics. Thermo-analytical techniques are advantageous as they do not require sample pretreatment and can sequentially provide information on the organic additives present in the microplastic (Qiu et al., 2016; Yang et al., 2021). However, these methods are destructive without providing information on the size, shape, or colour, and are limited by the microplastic size which can be manually inserted into the pyrolysis tube (Yang et al., 2021).

A comparison of the advantages and disadvantages of these methods of microplastic quantification and identification are summarised in Table 2.1.

2.3 Microplastic interactions with chemical pollutants

Due to the abundance, their collective large surface area, hydrophobicity, and persistence of microplastics, they have the potential to interact with other pollutants present in the soil such as organic contaminants and heavy metals and act as vectors for translocating and magnifying the levels of these contaminants.

Table 2.1: Comparison of methods for microplastic quantification and identification (summarised from Hanvey et al. (2017) and Huang et al. (2023)).

Technique	Advantages	Disadvantages
Optical Microscopy	• Simple • Low cost • Universally available • Low chemical hazard	• Time consuming and laborious • Accuracy subject to user competency • Not confirmatory (subjective) • Limited by visibility and microplastic size
Fluorescence Microscopy (fluorescent dyes)	• Increased sensitivity • Potential to couple with automated image processing software for quantification • Various dyes available including counterstains for identifying organic matter • Semi-qualitative	• Increased chemical hazard • Dyes not specific to microplastics (false positives) • Interferences from organic matter • Time consuming sample preparation and processing
Scanning Electron Microscopy	• High power of detection (high magnification) • Potential to automate • Simultaneous quantification, imaging of microplastic surfaces, and characterisation using coupled detectors	• Expensive sample preparation • Semi-destructive sample preparation • Cannot quantify per colour • Low work efficiency
Fourier-transform Infrared	• Fast technique • Potential to automate • Qualitative and quantitative • Provides information on weathering • Range of modes available to suit sample types (e.g., ATR, microscopy) • High sensitivity	• Limited to sizes > 10 μm • Some modes may be semi-destructive (e.g., compression during contact with ATR diamond)
Raman	• Qualitative and quantitative • Provides information on weathering • Range of modes available to suit sample types • Highly sensitive • Complementary to infrared analysis • Detection of microplastics < 10 μm	• Long analysis time • Lesser development for use for microplastic analysis compared to infrared analysis • Affected by presence of organic matter, inorganic minerals and adhered contaminants
Pyrolysis-Gas Chromatography-Mass Spectroscopy	• Pretreatment not required • Quantifiable based on composition • Provides information on polymerisation, degradation, additives	• Destructive • No information on size, morphology, or colour • Expensive

Heavy metals are soil pollutants derived from both natural and anthropogenic sources, however, the continuous polluting of soils with heavy metals due to anthropogenic sources leads to environmental degradation (Lu et al., 2012). Yu et al. (2020) describes microplastics as organic substances due to the backbone of the polymer consisting of carbon and hydrogen atoms which enhance the sorption capacity of heavy metals, simultaneously inhibiting their desorption capacity, which reduces the mobility of these metals in soil. Since microplastics are hydrophobic, they can absorb heavy metals by interacting with heavy metals ions at charged or polar regions of the microplastic as well as through the co-precipitation with hydrous metal oxides (Ashton et al., 2010; Holmes et al., 2012). The functional groups present in the polymer's chemical structure determine the sorption capacity of heavy metals (and other pollutants) to the microplastic's surface (Yu et al., 2020). The continuous absorption of heavy metals onto the surface of microplastics leads to the accumulation and concentration of heavy metal pollution in soils.

Of particular concern, microplastics strongly interact with persistent organic pollutants in soil. Organic pollutants (e.g., polycyclic aromatic hydrocarbons, plasticisers, and pesticides) can originate from a wide range of sources including fossil fuels, agricultural treatments, and emissions and can be released into the soil environment through treated wastewater discharge, sewage sludge applications, and direct application of pesticides and fertilisers (Duarte et al., 2018).

A large range of different organic contaminants can be sorbed onto the surface of microplastics through various complex sorption mechanisms including partitioning, surface sorption (hydrogen bonding, π-π and electrostatic interactions, and van der Waals force), and pore filling (Wang et al., 2020b; Chang et al., 2022). Several factors affect the sorption of organic contaminants including environmental factors (e.g., temperature, pH, dissolved organic matter), microplastic physicochemical characteristics (e.g., chemical composition, particle size, degree of aging/weathering, additives), and organic contaminant properties (e.g., polarity, molecular weight and structure, hydrophobicity, functional groups) (Xia et al., 2023). The weathering of microplastics increases the surface area for sorption of organic contaminants but it also increases oxygen-containing functional groups and hydrophilicity which can increase their sorption capacity for hydrophilic pollutants such as antibiotics, but on the contrary, decreases the sorption capacity for hydrophobic pollutants such as polycyclic aromatic hydrocarbons (Duan et al., 2021).

Of the many different classes of organic pollutants, there are a plethora of parent compounds, but their metabolites and breakdown products are also of environmental concern which can all interact with microplastics. It is for this reason that microplastic interactions with organic pollutants within soils are largely under-researched except for common global soil contaminants. No known studies have investigated the sorption and desorption behaviour of organic pollutants to microplastics in a true soil matrix as soil-based studies typically employ a soil suspension approach for sorption experiments which are not always environmentally realistic (e.g., Zhang et al., 2021; Li et al., 2022; Sahai et al., 2023; Yu et al., 2023) and often promote chemical interactions through sample agitation which rarely occurs in soils.

2.4 Environmental interactions and ecological impact of microplastics in soil

2.4.1 Effects of microplastics in soil

Microplastics can alter the physical properties of soils including their water holding capacity, bulk density, and soil structure (de Souza Machado et al., 2018; de Souza Machado et al., 2019) which consequently have an impact on many soil functions. For example, microplastic films promoted the formation of desiccation cracks in the surfaces of clay soils and significantly increased soil water evaporation due to the channels formed in the soil (Wan et al., 2019). This has implications for the tensile strength of soils and also impedes the translocation of chemical pollutants. Furthermore, the presence of microplastic fibres significantly decrease the formation of water stable aggregates which can then negatively alter the diversity of soil microenvironments (de Souza Machado et al., 2018). Alterations to the physical structure of soils caused by microplastics can have an impact on plant growth and development. For example, the decrease in soil bulk density enables plant root length to increase (de Souza Machado, 2019), however, microplastics themselves in turn decrease root diameter and root tissue density. Soil cracking can also inhibit plant growth (Li et al., 2020). Alterations to soil structure can also have profound effects on sustainability and metabolism of soil microbes leading to interrupted nutrient turnover and implications for soil fertility (Hartmann and Six, 2022).

The presence of microplastics in soils can adversely affect plants and crops through various pathways. Plants can directly uptake microplastics through crack-entry pathways in crop roots, whereby microplastics can enter the root vascular system (xylem) and transported from the roots via transpiration into the shoots (Li et al., 2020), providing a source for crop food chain transfer, bioaccumulation, and a potential direct pathway for the human consumption of microplastics.

Furthermore, microplastics have been documented to physically block cell wall pores or cell connections preventing the uptake and exchange of nutrients (Jiang et al., 2019). Consequently, the uptake of microplastics can increase cytotoxicity and genotoxicity as well as inducing oxidative damage through increased antioxidant enzyme activities. Furthermore, microplastic exposure also affects plant growth, development, redevelopment, and germination (Zhou et al., 2021b).

Microplastics act as additional man-made ecological niches in the natural environment (referred to as the "plastisphere" by several researchers; Figure 2.2), whereby microorganisms can form biofilms on the surface of the microplastic (Amaral-Zettler et al., 2020). At this interface, the microplastic surface may provide favourable conditions for the growth of tolerant microorganisms but inhibit the growth of intolerant microorganisms (Zhang et al., 2022). Gao et al. (2021) studied the effects of microplastic additions to soil on microbial community structure in an agricultural soil and reported that microbial biomass increased but their diversity was reduced. In particular, the abundance of gram-positive bacteria (e.g., *Nocardioidaceae*, *Amycolatopsis*, and *Aeromicrobium*) was elevated while the abundance of gram-negative bacteria (e.g., *Nitrospirales*, *Alphaproteobacteria*, and *Agrobacterium*) was reduced. This may be explained by the distinct microbiomes that form around microplastics that promote elevated numbers of resistant microorganisms and overall biomass, while subsequently reducing their diversity and promote novel hotspots for microbial communities in soils. Soil microorganisms are an integral part of soil ecosystems and important for soil health and function which makes them good bioindicators for soil quality, however, the consequences of microplastics altering microbial ecosystems are largely unknown for soil ecological functions and biochemical processes, particularly in agroecosystems (Zhang et al., 2022) and warrant investigation.

In addition to the effect microplastics induce in the terrestrial environment, the leaching of their additives can also cause detrimental effects. Additives, such as phthalates and bisphenol A, are added to plastics during manufacturing to improve the properties of the plastic for their intended purpose, however, these additives are known endocrine disruptors to soil vertebrates and invertebrates (e.g., increased estrogenic activity), as well as acting as carcinogenic agents in humans (Zhang et al., 2019). Soil microbial communities are also negatively impacted by plastic leachates, e.g., di (2-ethylhexyl) phthalate altered bacterial community structure diversity by the simultaneous decline and enrichment of different bacterial phyla and its monoester metabolite, mono (2-ethylhexyl) phthalate, exhibited higher toxicity than its parent compound (Zhu et al., 2018).
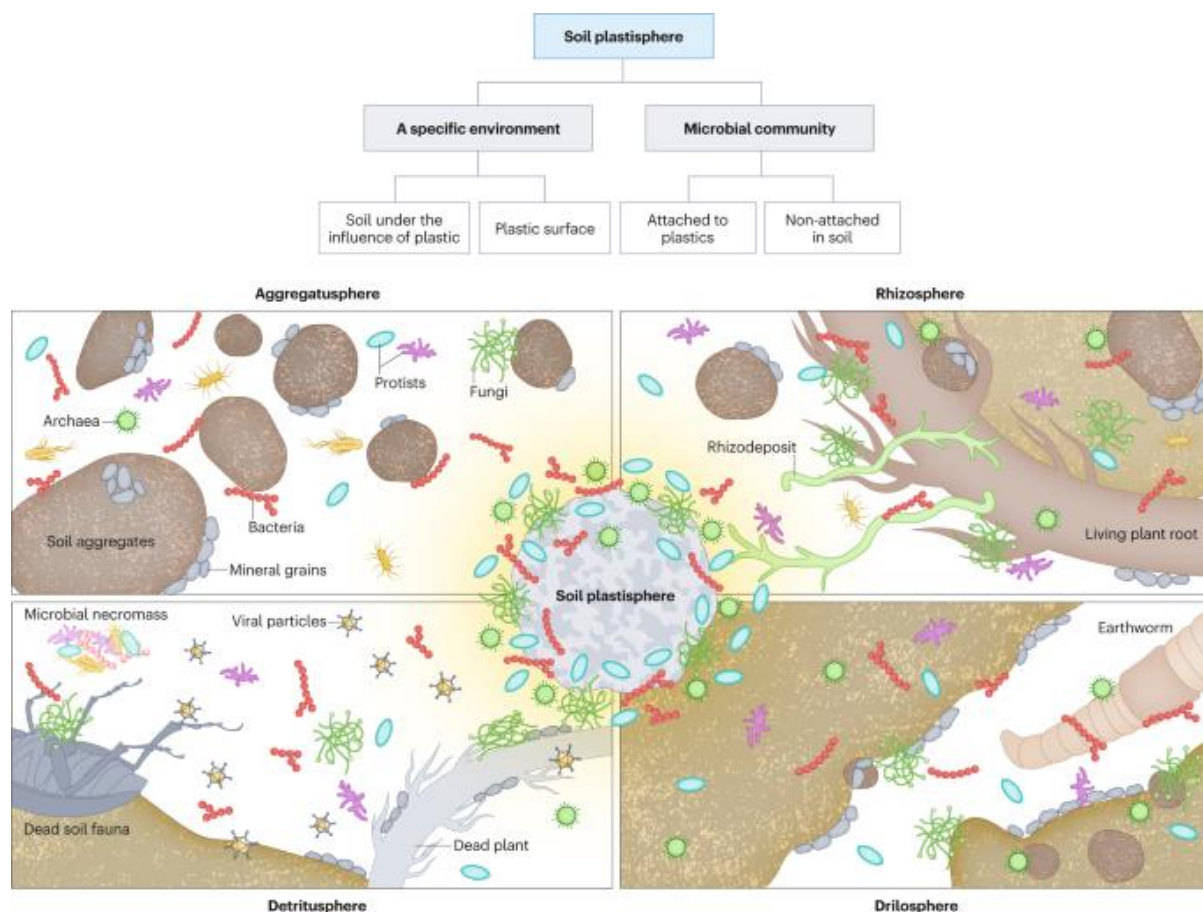
Figure 2.2: Soil plastisphere (Rillig et al. 2024 64-67 fig. 1).

2.4.2 Impact of microplastic interactions with organic pollutants in soil

Exposure of soil organisms such as earthworms and nematodes (Qiu et al., 2022) and plants (Li et al., 2020) to chemical pollutants can potentially be enhanced through the ingestion or incorporation of microplastics vectoring such pollutants. Microplastics have been reported to enhance the toxic effects of organic contaminants in plants (e.g., polystyrene microplastics reduced the uptake of phenanthrene in soybean but induced higher toxicity to soybean tissue at the cellular and molecular level (Xu et al., 2021a)). Organic contaminants have the potential to transfer from microplastics to soil biota (e.g., polybrominated diphenyl ethers transfer from polyurethane microplastics into earthworms (Gaylor et al., 2013)), however, depending on the pollutant and microplastic type, bioaccumulation of organic contaminants may decrease when bound to microplastics due to their interaction mechanisms, the conditions of the soil biota digestive system, and the length of exposure time in the gut (e.g., Wang et al., 2019b).

Both organic pollutants and microplastics are known to independently have adverse effects on soil microbial community structures (Cai et al., 2020; He et al., 2023), however, the co-exposure of organic pollutants sorbed to microplastics can elevate their toxicity and introduce additional synergistic effects. For example, the co-exposure of ciprofloxacin and polyethylene microplastics to soils led to a significant reduction in microbial community diversity, and the elevated abundance of various bacterial phyla resulted in the rapid depletion of soil nitrogen (Wang et al., 2020c). The degradation rate of ciprofloxacin was also significantly reduced in the presence of polyethylene microplastics (Wang et al., 2020c) suggesting that the environmental exposure of organic pollutants and their toxic impacts may be longer lasting when sorbed to microplastics than free organic pollutants in soil. Conversely, a study by Xu et al. (2021b) reported that polystyrene microplastics alleviated the negative effects of sulfamethazine on soil microbial communities through antagonistic effects, and similarly, in a study by Kleinteich et al. (2018) whereby the stresses induced by polycyclic aromatic hydrocarbons were alleviated when sorbed to polyethylene microplastics in sediment samples. The chemical composition of the microplastic as well as the chemical nature of the pollutant play a role in the sorption and desorption of organic contaminants (see section 1.4), although, it is hypothesised that this phenomenon is attributed to the formation of biofilms on the microplastic surface which act as a protective barrier between the organic contaminants and external soil environment (Kleinteich et al., 2018; Chang et al., 2022). However, the mechanisms and impact of the interactions of microplastics and organic contaminants in soil is still largely under-researched.

2.5 Summary

A detailed overview of microplastics, their interactions with soil microbes and other pollutants within the terrestrial environment, and the negative impact of microplastic interactions in soils has been presented. Methods of microplastic extraction and detection have also been discussed. Areas with knowledge gaps have been identified, in particular, the need for improved microplastic extraction from soils, the need to understand microplastic degradation over time, how microplastic abundance is influenced on a national scale, and how microplastics interact with organic contaminants and how this impacts soil microbes. Each chapter hereafter will reiterate these knowledge gaps and detail how each study addressed these issues and provide future perspectives to further address any more identified areas of interest as a result of the research conducted.

2.6 References

Allen S., Allen D., Phoenix V.R., Le Roux G., Jiménez P.D., Simonneau A., Binet S., Galop D. Atmospheric transport and deposition of microplastics in a remote mountain catchment. *Nature Geoscience*. 2019; 12, 339-344. DOI: https://doi.org/10.1038/s41561-019-0335-5

Amaral-Zettler L.A., Zettler E.R., Mincer T.J. Ecology in the plastisphere. *Nature Reviews Microbiology*. 2020; 18, 139-151. DOI: https://doi.org/10.1038/s41579-019-0308-0

Anger P.M., von der Esch E., Baumann T., Elsner M., Niessner R., Ivleva N.P. Raman microspectroscopy as a tool for microplastic particle analysis. *TrAC Trends in Analytical Chemistry*. 2018; 109, 214-226. DOI: https://doi.org/10.1016/j.trac.2018.10.010

Ashton K., Holmes L., Turner A. Association of metals with plastic production pellets in the marine environment. *Marine Pollution Bulletin*. 2010; 60, 2050-2055. DOI: https://doi.org/10.1016/j.marpolbul.2010.07.014

Beltrán-Sanahuja A., Benito-Kaesbach A., Sánchez-García N., Sanz-Lázaro C. Degradation of conventional and biobased plastics in soil under contrasting environmental conditions. *Science of The Total Environment*. 2021; 787, 147678. DOI: https://doi.org/10.1016/j.scitotenv.2021.147678

Bläsing M., Amelung W. Plastics in soil: Analytical methods and possible sources. *Science of the Total Environment*. 2018; 612, 422-435. DOI: http://dx.doi.org/10.1016/j.scitotenv.2017.08.086

Büks F., Kaupenjohann M. Global concentrations of microplastics in soils – a review. *SOIL*. 2020; 6, 649-662. DOI: https://doi.org/10.5194/soil-6-649-2020

Cai Y., Chen H., Yuan R., Wang F., Chen Z., Zhou B. Metagenomic analysis of soil microbial community under PFOA and PFOS stress. Environmental Research. 2020; 188, 109838. DOI: https://doi.org/10.1016/j.envres.2020.109838

Canensi S., Barucca G., Corinaldesi C. Extraction efficiency of different microplastic polymers from deep-sea sediments and their quantitative relevance. *Frontiers in Marine Science*. 2022, 9, 975875. DOI: https://doi.org/10.3389/fmars.2022.975875

Carr S.A., Lin J., Tesoro A.G. Transport and fate of microplastic particles in wastewater treatment plants. *Water Research*. 2016; 91, 174-182. DOI: https://doi.org/10.1016/j.watres.2016.01.002

Chamas A., Moon H., Zheng J., Qiu Y., Tabassum T., Jang J.H., Abu-Omar M., Scott S.L., Suh S. Degradation Rates of Plastics in the Environment. *ACS Sustainable Chemistry and Engineering*. 2020; 8, 3494-3511. DOI: https://doi.org/10.1021/acssuschemeng.9b06635

Chang J., Fang W., Liang J., Zhang P., Zhang G., Zhang H., Zhang Y., Wang Q. A critical review on interaction of microplastics with organic contaminants in soil and their ecological risks on soil organisms. *Chemosphere*. 2022; 306, 135573. DOI: https://doi.org/10.1016/j.chemosphere.2022.135573

Chen L., Yu L., Li Y., Han B., Zhang J., Tao S., Liu W. Spatial distributions, compositional profiles, potential sources, and influencing factors of microplastics in soils from different agricultural farmlands in China: a national perspective. *Environmental Science and Technology.* 2022; 56, 16964-16974. DOI: https://doi.org/10.1021/acs.est.2c07621

Corradini F., Casado F., Leiva V., Huerta-Lwanga E., Geissen V. Microplastics occurrence and frequency in soils under different land uses on a regional scale. *Science of the Total Environment*. 2021; 752, 141917. DOI: https://doi.org/10.1016/j.scitotenv.2020.141917

de Souza Machado A.A., Kloas W., Zarfl C., Hempel S., Rillig M.C. Microplastics as an emerging threat to terrestrial ecosystems. *Global Change Biology*. 2017; 24, 1405-1416. DOI: https://doi.org/10.1111/gcb.14020

de Souza Machado A.A., Lau C.W., Till J., Kloas W., Lehmann A., Becker R., Rillig M.C. Impacts of Microplastics on the Soil Biophysical Environment. *Environmental Science and Technology*. 2018; 52, 9656-9665. DOI: https://doi.org/10.1021/acs.est.8b02212

de Souza Machado A.A., Lau C.W., Kloas W., Bergmann J., Bachelier J.B., Faltin E., Becker R., Görlich A.S., Rillig M.C. Microplastics Can Change Soil Properties and Affect Plant Performance. *Environmental Science and Technology*. 2019; 53, 6044-6052. DOI: https://doi.org/10.1021/acs.est.9b01339

Devalla S., Joseph O., Prabhu R., 2019. Nile red-dye based analysis of synthetic fibres for forensic applications. In: H. Bouma, R. Prabhu, R.J. Stokes, and Y. Yitzhaky, eds. *Proceedings of the 3rd Counterterrorism, crime fighting, forensics, and surveillance technologies conference 2019: co-located with the Society of Photo-Optical Instrumentation Engineers (SPIE) Security and defence 2019 conference*. 9-12 September 2019. Strasbourg, France: Proceedings of the SPIE, 11166. Bellingham, WA: SPIE [online], article ID 111660Y. Available from: https://doi.org/10.1117/12.2536780

Dris R., Gasperi J., Saad M., Mirande C., Tassin B. Synthetic fibers in atmospheric fallout: A source of microplastics in the environment? *Marine Pollution Bulletin*. 2016; 104, 290-293. DOI: https://doi.org/10.1016/j.marpolbul.2016.01.006

Duan J., Bolan N., Li Y., Ding S., Atugoda T., Vithanage M., Sarkar B., Tsang D.C.W., Kirkham M.B. Weathering of microplastics and interaction with other coexisting constituents in terrestrial and aquatic

environments. *Water Research*. 2021; 196, 117011. DOI: https://doi.org/10.1016/j.watres.2021.117011

Duarte R.M.B.O., Maltos J.T.V., Senesi N., 2018. Organic Pollutants in Soils. In: A.C. Duarte, A. Cachada, T. Rocha-Santos, eds. *Soil Pollution*. Aveiro: Academic Press, pp. 103-126. DOI: https://doi.org/10.1016/B978-0-12-849873-6.00005-4

Elmi A., Al-Khaldy A., AlOlayan M. Sewage sludge land application: Balancing act between agronomic benefits and environmental concerns. *Journal of Cleaner Production*. 2020; 250, 119512. DOI: https://doi.org/10.1016/j.jclepro.2019.119512

Enders K., Tagg A.S., Labrenz M. Evaluation of Electrostatic Separation of Microplastics From Mineral-Rich Environmental Samples. *Frontiers in Environmental Science*. 2020; 8, 112. DOI: https://doi.org/10.3389/fenvs.2020.00112

Fan W., Qiu C., Qu Q., Hu X., Mu L., Gao Z., Tang X. Sources and identification of microplastics in soils. *Soil & Environmental Health*. 2023; 1, 100019. DOI: https://doi.org/10.1016/j.seh.2023.100019

FAO. 2021. *Assessment of agricultural plastics and their sustainability. A call for actio*n. Rome. https://doi.org/10.4060/cb7856en

Felsing C., Kochleus C., Buchinger S., Brennholt N., Stock F., Reifferscheid G. A new approach in separating microplastics from environmental samples based on their electrostatic behavior. *Environmental Pollution*. 2018; 234, 20-28. DOI: https://doi.org/10.1016/j.envpol.2017.11.013

Feng S., Lu H., Tian P., Xue Y., Lu J., Tang M., Feng W. Analysis of microplastics in a remote region of the Tibetan Plateau: Implications for natural environmental response to human activities. *Science of The Total Environment*. 2020; 739, 140087. DOI: https://doi.org/10.1016/j.scitotenv.2020.140087

Fries E., Dekiff J.H., Willmeyer J., Nuelle M.T., Ebert M., Remy D. Identification of polymer types and additives in marine microplastic particles using pyrolysis-GC/MS and scanning electron microscopy. *Environmental Science: Processes & Impacts*. 2013; 15, 1949-1956. DOI: https://doi.org/10.1039/C3EM00214D

Gaylor M.O., Harvey E., Hale R.C. Polybrominated Diphenyl Ether (PBDE) Accumulation by Earthworms (*Eisenia fetida*) Exposed to Biosolids-, Polyurethane Foam Microparticle-, and Penta-BDE-Amended Soils. *Environmental Science and Technology*. 2013; 47, 13831-13839. DOI: https://doi.org/10.1021/es403750a

Grause G., Kuniyasu Y., Chien M.F., Ilnoue C. Separation of microplastic from soil by centrifugation and its application to agricultural soil. *Chemosphere*. 2022; 288, 132654. DOI: https://doi.org/10.1016/j.chemosphere.2021.132654

Gu J.D. Microbiological deterioration and degradation of synthetic polymeric materials: recent research advances. *International Biodeterioration and Biodegradation*. 2003; 52, 69-91. DOI: https://doi.org/10.1016/S0964-8305(02)00177-4

Han X., Lu X., Vogt R.D. An optimized density-based approach for extracting microplastics from soil and sediment samples. *Environmental Pollution*. 2019; 254, 113009. DOI: https://doi.org/10.1016/j.envpol.2019.113009

Hanvey J.S., Lewis P.J., Lavers J.L., Crosbie N.D., Pozo K., Clarke B.O. A review of analytical techniques for quantifying microplastics in sediments. *Analytical Methods*. 2012; 9, 1369-1383. DOI: https://doi.org/10.1039/C6AY02707E

Harms I.K., Diekötter T., Troegel S., Lenz M. Amount, distribution and composition of large microplastics in typical agricultural soils in Northern Germany. *Science of The Total Environment*. 2021; 758, 143615. DOI: https://doi.org/10.1016/j.scitotenv.2020.143615

Hartmann M., Six J. Soil structure and microbiome functions in agroecosystems. *Nature Reviews Earth & Environment*. 2022; 4, 4-18. DOI: https://doi.org/10.1038/s43017-022-00366-w

Hatfield J.L., Sauer T.J., Cruse R.M., 2017. Soil: The Forgotten Piece of the Water, Food, Energy Nexus. In: D.L. Sparks, ed. *Advances in Agronomy*. Cambridge, MA: Academic Press. 1-46. DOI: https://doi.org/10.1016/bs.agron.2017.02.001

He R., Peng C., Jiang L., Han H., Chu Y.X., Wang J., Liu C.Y., Zhao N. Characteristic pollutants and microbial community in underlying soils for evaluating landfill leakage. *Waste Management*. 2023; 155, 269-280. DOI: https://doi.org/10.1016/j.wasman.2022.11.015

Holmes L.A., Turner A., Thompson R.C. Adsorption of trace metals to plastic resin pellets in the marine environment. *Environmental Pollution*. 2012; 42-48. DOI: https://doi.org/10.1016/j.envpol.2011.08.052

Huang D., Xu Y., Lei F., Yu X., Ouyang Z., Chen Y., Jia h., Guo X. Degradation of polyethylene plastic in soil and effects on microbial community composition. Journal of Hazardous Materials. 2021; 416, 126173. DOI: https://doi.org/10.1016/j.jhazmat.2021.126173

Huang Z., Hu B., Wang H. Analytical methods for microplastics in the environment: a review. *Environmental Chemistry Letters*. 2023; 21, 383-401. DOI: https://doi.org/10.1007%2Fs10311-022-01525-7

Hurley R.R, Lusher A.L., Olsen M., Nizzetto L. Validation of a Method for Extracting Microplastics from Complex, Organic-Rich, Environmental Matrices. *Environmental Science and Technology.* 2018; 52, 7409-7417. DOI: https://doi.org/10.1021/acs.est.8b01517

The James Hutton Institute, 2023. *Soils – Introduction*. [online]. Aberdeen: The James Hutton Institute. Available from: Soils | Exploring Scotland | The James Hutton Institute [Accessed 07 October 2023].

Jian M., Zhang Y., Yang W., Zhou L., Liu S., Xu E.G. Occurrence and distribution of microplastics in China's largest freshwater lake system. *Chemosphere*. 2020; 261, 128186. DOI: https://doi.org/10.1016/j.chemosphere.2020.128186

Jiang X., Chen H., Liao Y., Ye Z., Li m., Klobučar G. Ecotoxicity and genotoxicity of polystyrene microplastics on higher plant *Vicia faba*. *Environmental Pollution*. 2019; 250, 831-838. DOI: https://doi.org/10.1016/j.envpol.2019.04.055

Kleinteich J., Seidensticker S., Marggrander N., Zarfl C. Microplastics Reduce Short-Term Effects of Environmental Contaminants. Part II: Polyethylene Particles Decrease the Effect of Polycyclic Aromatic Hydrocarbons on Microorganisms. *International Journal of Environmental Research and Public Health*. 2018; 15, 287. DOI: https://doi.org/10.3390/ijerph15020287

Krueger M.C., Harms H., Schlosser D. Prospects for microbiological solutions to environmental pollution with plastics. *Applied Microbiology and Biotechnology*. 2015; 99, 8857-8874. DOI: https://doi.org/10.1007/s00253-015-6879-4

Li L., Luo Y., Li R., Zhou Q., Peijnenburg W.J.G.M., Yin N., Yang J., Tu C., Zhang Y. Effective uptake of submicrometre plastics by crop plants via a crack-entry mode. *Nature Sustainability*. 2020; 3, 927-937. DOI: https://doi.org/10.1038/s41893-020-0567-9

Li Z., Sun L., Wang H. Adsorption behaviour and mechanism of polycyclic aromatic hydrocarbons onto typical microplastics in a soil solution. *International Journal of Environmental Analytical Chemistry*. 2022. DOI: https://doi.org/10.1080/03067319.2022.2128791

Li Y., Liu Q., Junaid M., Chen G., Wang J. Distribution, sources, transportation and biodegradation of microplastics in the soil environment. *TrAC Trends in Analytical Chemistry*. 2023a; 164, 117106. DOI: https://doi.org/10.1016/j.trac.2023.117106

Li Z., Xu B., Zhang R., Wang F., Li L., Wang K., Zhang R., Jing X., Liu Y., Chen P. Effects of land use on soil microplastic distribution adjacent to Danjiangkou reservoir, China. *Chemosphere*. 2023b; 338, 139389. DOI: https://doi.org/10.1016/j.chemosphere.2023.139389

Liu M., Lu S., Song Y., Lei L., Hu J., Lv W., Zhou W., Cao C., Shi H., Yang X., He D. Microplastic and mesoplastic pollution in farmland soils in suburbs of Shanghai, China. *Environmental Pollution*. 2018; 242, 855-862. DOI: https://doi.org/10.1016/j.envpol.2018.07.051

Lu A., Wang J., Qin X., Wang K., Han P., Zhang S. Multivariate and geostatistical analyses of the spatial distribution and origin of heavy metals in the agricultural soils in Shunyi, Beijing, China. *Science of The Total Environment*. 2012; 425, 66-74. DOI: https://doi.org/10.1016/j.scitotenv.2012.03.003

Maes T., Jessop R., Wellner N., Haupt K., Mayes A.G. A rapid-screening approach to detect and quantify microplastics based on fluorescent tagging with Nile Red. *Scientific Reports*. 2017; 7, 44501. DOI: https://doi.org/10.1038/srep44501

Parolini M., et al. Microplastic Contamination in Snow from Western Italian Alps. *International Journal of Environmental Research and Public Health*. 2021; 18, 768. DOI: https://doi.org/10.3390/ijerph18020768

Pathak V.M., Navneet. Review on the current status of polymer degradation: a microbial approach. *Bioresources and Bioprocessing*. 2017; 4. DOI: https://doi.org/10.1186/s40643-017-0145-9

Phan S., Padilla-Gamiño J.L., Luscombe C.K. The effect of weathering environments on microplastic chemical identification with Raman and IR spectroscopy: Part I. polyethylene and polypropylene. *Polymer Testing*. 2022; 116, 107752. DOI: https://doi.org/10.1016/j.polymertesting.2022.107752

Prata J.C., Reis V., Maltos J.T.V., da Costa J.P., Duarte A.C., Rocha-Santos T. A new approach for routine quantification of microplastics using Nile Red and automated software (MP-VAT). *Science of The Total Environment*. 2019; 690, 1277-1283. DOI: https://doi.org/10.1016/j.scitotenv.2019.07.060

Prata J.C., da Costa J.P., Lopes I., Duarte A.C., Rocha-Santos T. Environmental exposure to microplastics: An overview on possible human health effects. *Science of The Total Environment*. 2020a; 702, 134455. DOI: https://doi.org/10.1016/j.scitotenv.2019.134455

Prata J.C., Alves J.R., da Costa J.P., Duarte A.C., Rocha-Santos T. Major factors influencing the quantification of Nile Red stained microplastics and improved automatic quantification (MP-VAT 2.0). *Science of The Total Environment*. 2020b; 719, 137498. DOI: https://doi.org/10.1016/j.scitotenv.2020.137498

Qiu Q., Tan Z., Wang J., Peng J., Li M., Zhan Z. Extraction, enumeration and identification methods for monitoring microplastics in the environment. *Estuarine, Coastal and Shelf Science*. 2016; 176, 102-109. DOI: http://dx.doi.org/10.1016/j.ecss.2016.04.012

Qiu Q., Tan Z., Wang J., Peng J., Li M., Zhan Z. Extraction, enumeration and identification methods for monitoring microplastics in the environment. *Estuarine, Coastal and Shelf Science*. 2019; 176, 102-109. DOI: https://doi.org/10.1016/j.ecss.2016.04.012

Qiu Y., Zhou S., Zhang C., Zhou Y., Qin W. Soil microplastic characteristics and the effects on soil properties and biota: A systematic review and meta-analysis. *Environmental Pollution*. 2022; 313, 120183. DOI: https://doi.org/10.1016/j.envpol.2022.120183

Qiu Y., Zhou S., Zhang C., Qin W., Lv C., Zou M. Identification of potentially contaminated areas of soil microplastic based on machine learning: A case study in Taihu Lake region, China. *Science of the Total Environment*. 2023; 877, 162891. DOI: http://dx.doi.org/10.1016/j.scitotenv.2023.162891

Ramage S.J.F.F., Pagaling E., Haghi R.K., Dawson L.A., Yates K., Prabhu R., Hillier S., Devalla S. Rapid extraction of high- and low-density microplastics from soil using high-gradient magnetic separation. *Science of The Total Environment*. 2022; 831, 154912. DOI: https://doi.org/10.1016/j.scitotenv.2022.154912

Rillig M.C., Kim S.W., Zhu Y.G. The soil plastisphere. *Nature Reviews Microbiology*. 2024; 22, 64-67. DOI: https://doi.org/10.1038/s41579-023-00967-2

Rochman C.M. *et al*. Rethinking microplastics as a diverse contaminant suite. Environmental Toxicity and Chemistry. 2019; 38, 703-711. DOI: https://doi.org/10.1002/etc.4371

Sahai H., Valverde M.G., Morales M.M., Hernando M.D., del Real A.M.A., Fernández-Alba A.R. Exploring sorption of pesticides and PAHs in microplastics derived from plastic mulch films used in modern agriculture. *Chemosphere*. 2023; 333, 138959. DOI: https://doi.org/10.1016/j.chemosphere.2023.138959

Scheurer M., Bigalke M. Microplastics in Swiss floodplain soils. *Environmental Science and Technology.* 2018; 52, 3591-3598. DOI: https://doi.org/10.1021/acs.est.7b06003

Song Y.K., Hong S.H., Jang M., Han G.M., Jung S.W., Shim W.J. Combined Effects of UV Exposure Duration and Mechanical Abrasion on Microplastic Fragmentation by Polymer Type. *Environmental Science and Technology*. 2017; 51, 4368-4376. DOI: https://doi.org/10.1021/acs.est.6b06155

Tarafdar A., Choi S.H., Kwan J.H. Differential staining lowers the false positive detection in a novel volumetric measurement technique of microplastics. *Journal of Hazardous Materials*. 2022; 432, 128755. DOI: https://doi.org/10.1016/j.jhazmat.2022.128755

Tarazona J.V. and Ramos-Peralonso M.J., 2014. Environmental Risk Assessment, Terrestrial. In: P. Wexler, ed. *Encyclopaedia of Toxicology*. Third edition. Cambridge, MA: Academic Press. 411-414. DOI: https://doi.org/10.1016/B978-0-12-386454-3.00560-1

Thomas B., Schütze B., Heinze W.M., Steinmetz Z. Sample preparation techniques for the analysis of microplastics in soil—a review. *Sustainability*. 2020; 12, 9074. DOI: https://doi.org/10.3390/su12219074

Vianello A., Boldrin A., Guerriero P., Moschino V., Rella R., Sturaro A., Da Ros L. Microplastic particles in sediments of Lagoon of Venice, Italy: First observations on occurrence, spatial patterns and identification. *Estuarine, Coastal and Shelf Science*. 2013; 130, 54-61. DOI: http://dx.doi.org/10.1016/j.ecss.2013.03.022

Wan Y., Wu C., Xue Q., Hui X. Effects of plastic contamination on water evaporation and desiccation cracking in soil. *Science of the Total Environment*. 2019; 654, 576-582. DOI: https://doi.org/10.1016/j.scitotenv.2018.11.123

Wang J., Liu X., Li Y., Powell T., Wang X., Wang G., Zhang P. Microplastics as contaminants in the soil environment: A mini-review. *Science of the Total Environment*. 2019a; 691, 848-857. DOI: https://doi.org/10.1016/j.scitotenv.2019.07.209

Wang J., Coffin S., Sun C., Schlenk D., Gan J. Negligible effects of microplastics on animal fitness and HOC bioaccumulation in earthworm *Eisenia fetida* in soil. *Environmental Pollution*. 2019b; 249, 776-784. DOI: https://doi.org/10.1016/j.envpol.2019.03.102

Wang W., Ge J., Yu X., Li H. Environmental fate and impacts of microplastics in soil ecosystems: Progress and perspective. *Science of The Total Environment*. 2020a; 708, 134841. DOI: https://doi.org/10.1016/j.scitotenv.2019.134841

Wang F., Zhang M., Sha W., Wang Y., Hao H., Dou Y., Li Y. Sorption Behavior and Mechanisms of Organic Contaminants to Nano and Microplastics. *Molecules*. 2020b; 25, 1827. DOI: https://doi.org/10.3390/molecules25081827

Wang J., Liu X., Dai Y., Ren J., Li Y., Wang X., Zhang P., Peng C. Effects of co-loading of polyethylene microplastics and ciprofloxacin on the antibiotic degradation efficiency and microbial community

structure in soil. *Science of The Total Environment*. 2020c; 741, 140463. DOI: https://doi.org/10.1016/j.scitotenv.2020.140463

Xia W., Rao Q., Deng X., Chen J., Xie P. Rainfall is a significant environmental factor of microplastic pollution in inland waters. *Science of The Total Environment*. 2020; 732, 139065. DOI: https://doi.org/10.1016/j.scitotenv.2020.139065

Xia Y., Niu S., Yu J. Microplastics as vectors of organic pollutants in aquatic environment: A review on mechanisms, numerical models, and influencing factors. *Science of the Total Environment*. 2023; 887, 164008. DOI: http://dx.doi.org/10.1016/j.scitotenv.2023.164008

Xu B., Liu F., Cryder Z., Huang D., Lu Z., He Y., Wang H., Lu Z., Brookes P.C., Tang C., Gan J., Xu J. Microplastics in the soil environment: occurrence, risks, interactions and fate – a review. *Critical Reviews in Environmental Science and Technology*. 2020; 50, 2175-2222. DOI: https://doi.org/10.1080/10643389.2019.1694822

Xu G., Liu Y., Yu Y. Effects of polystyrene microplastics on uptake and toxicity of phenanthrene in soybean. *Science of The Total Environment*. 2021a; 783, 147016. DOI: https://doi.org/10.1016/j.scitotenv.2021.147016

Xu M., Du W., Ai F., Xu F., Zhu J., Yin Y., Ji R., Guo H. Polystyrene microplastics alleviate the effects of sulfamethazine on soil microbial communities at different CO2 concentrations. *Journal of Hazardous Materials*. 2021b; 413, 125286. DOI: https://doi.org/10.1016/j.jhazmat.2021.125286

Yang L., Zhang Y., Kang S., Wang Z., Wu C. Microplastics in soil: A review on methods, occurrence, sources, and potential risk. *Science of The Total Environment*. 2021; 780, 146546. DOI: https://doi.org/10.1016/j.scitotenv.2021.146546

Yu H., Hou J., Dang Q., Cui D., Xi B., Tan W. Decrease in bioavailability of soil heavy metals caused by the presence of microplastics varies across aggregate levels. *Journal of Hazardous Materials*. 2020; 395, 122690. DOI: https://doi.org/10.1016/j.jhazmat.2020.122690

Yu B., Zhao T., Gustave W., Li B., Cai Y., Ouyang D., Guo T., Zhang H. Do microplastics affect sulfamethoxazole sorption in soil? Experiments on polymers, ionic strength and fulvic acid. *Science of the Total Environment*. 2023; 860, 160221. DOI: http://dx.doi.org/10.1016/j.scitotenv.2022.160221

Zhang S., Yang X., Gertsen H., Peters P., Salánki T., Geissen V. A simple method for the extraction and identification of light density microplastics from soil. *Science of The Total Environment*. 2018; 616-617, 1056-1065. DOI: https://doi.org/10.1016/j.scitotenv.2017.10.213

Zhang S., Wang J., Liu X., Qu F., Wang X., Wang X., Li Y., Sun Y. Microplastics in the environment: A review of analytical methods, distribution, and biological effects. *TrAC Trends in Analytical Chemistry*. 2019; 111, 62-72. DOI: https://doi.org/10.1016/j.trac.2018.12.002

Zhang Y., Kang S., Allen S., Allen D., Gao T., Sillanpää M. Atmospheric microplastics: A review on current status and perspectives. *Earth-Science Reviews*. 2020; 203, 103118. DOI: https://doi.org/10.1016/j.earscirev.2020.103118

Zhang C., Lei Y., Qian Y., Qiao J., Liu J., Li S., Dai L., Sun K., Guo H., Sui G., Jing W. Sorption of organochlorine pesticides on polyethylene microplastics in soil suspension. *Ecotoxicology and Environmental Safety*. 2021; 223, 112591. DOI: https://doi.org/10.1016/j.ecoenv.2021.112591

Zhang Y., Cai C., Gu Y., Shi Y., Gao X. Microplastics in plant-soil ecosystems: A meta-analysis. *Environmental Pollution*. 2022; 308, 119718. DOI: https://doi.org/10.1016/j.envpol.2022.119718

Zhou Q., Zhang H., Fu C., Zhou Y., Dai Z., Li Y., Tu C., Luo Y. The distribution and morphology of microplastics in coastal soils adjacent to the Bohai Sea and the Yellow Sea. *Geoderma*. 2018; 322, 201-208. DOI: https://doi.org/10.1016/j.geoderma.2018.02.015

Zhou Y., Wang J., Zou M., Jia Z., Zhou S., Li Y. Microplastics in soils: A review of methods, occurrence, fate, transport, ecological and environmental risks. *Science of The Total Environment*. 2020; 748, 141368. DOI: https://doi.org/10.1016/j.scitotenv.2020.141368

Zhou Y., He G., Jiang X., Yao L., Ouyang L., Liu X., Liu W., Liu Y. Microplastic contamination is ubiquitous in riparian soils and strongly related to elevation, precipitation and population density. *Journal of Hazardous Materials*. 2021a; 411, 125178. DOI: https://doi.org/10.1016/j.jhazmat.2021.125178

Zhou J., Wen Y., Marshall M.R., Zhao J., Gui H., Yang Y., Zeng Z., Jones D.L., Zang H. Microplastics as an emerging threat to plant and soil health in agroecosystems. *Science of The Total Environment*. 2021b; 787, 147444. DOI: https://doi.org/10.1016/j.scitotenv.2021.147444

Zhu F., Zhu C., Zhou D., Gao J. Fate of di (2-ethylhexyl) phthalate and its impact on soil bacterial community under aerobic and anaerobic conditions. *Chemosphere*. 2019, 216, 84-93. DOI: https://doi.org/10.1016/j.chemosphere.2018.10.078

Zhu J., Dong G., Feng F., Ye J., Liao C.H., Wu C.H., Chen S.C. Microplastics in the soil environment: Focusing on the sources, its transformation and change in morphology. *Science of The Total Environment*. 2023; 896, 165291. DOI: https://doi.org/10.1016/j.scitotenv.2023.165291

Zvekic M., Richards L.C., Tong C.C., Krogh E.T. Characterizing photochemical ageing processes of microplastic materials using multivariate analysis of infrared spectra. *Environmental Science: Processes & Impacts*. 2022; 24, 52-61. DOI: https://doi.org/10.1039/D1EM00392E

Chapter 3: Microplastic extraction method development and their detection

Microplastics are present in all environments, and concerns over their possible detrimental effects on flora and fauna have arisen. Density separation is commonly used to separate MPs from soils to allow MP quantification; however, it frequently fails to extract high-density MPs sufficiently, resulting in under-estimation of microplastic abundances. In this proof-of-concept study, a novel three-stage extraction method was developed, involving high-gradient magnetic separation and removal of magnetic soil (Stage 1), magnetic tagging of microplastics using surface modified iron nanoparticles (Stage 2), and high-gradient magnetic recovery of surface-modified microplastics (Stage 3). The method was optimised for four different soil types (loam, high-carbon loamy sand, sandy loam, high-clay sandy loam, and peat) spiked with different microplastic types (polyethylene, polyethylene terephthalate, and polytetrafluoroethylene) of different particle sizes (63 μm to 2 mm) as well as polyethylene fibres (2–4 mm). The optimised method achieved average recoveries of 95% for fibres and 90% for particles across all the soil types. These were significantly higher than recoveries achieved by density separation, particularly for fibres and high-density microplastics ($p < 0.05$). To demonstrate the practical application of the HGMS method, it was applied to a farm soil sample, and high-density microplastic particles were only recovered by HGMS. Furthermore, this study showed that HGMS can recover fibre-aggregate complexes. This improved extraction method will provide better estimates of microplastic quantities in future studies focused on monitoring the prevalence of microplastics in soils. The detection of microplastics using fluorescent dyes was also explored.

3.1 Introduction

To accurately assess microplastic contamination, it is important to extract both high- and low-density microplastics. This is a complicated task for soils as they are a complex solid matrix, with broad inter- and intra-sample density and particle size ranges (de Souza Machado et al., 2018a). Additionally, soils often contain high concentrations of organic material that form aggregates around microplastics making them difficult to extract (Bläsing and Amelung, 2018; Thomas et al., 2020; Zhang and Liu, 2018).

There are several methods that can be employed to extract microplastics from soil. Methods that do not rely on plastic density include electrostatic separation (Felsing et al., 2018; Enders et al., 2020) and elutriation (Claessens et al., 2013), however, they have mainly been tested on sediments. Electrostatic

separation achieved microplastic recoveries near 100% when applied to sediments (Felsing et al., 2018), however, microplastic recoveries were significantly reduced when the method was applied to mineral-rich soils (Enders et al., 2020). Moreover, there was great variability in recovery because it was dependent on microplastic particle size (Enders et al., 2020). Elutriation is extremely effective for microplastic removal in sediments (Claessens et al., 2013), however, Grause et al. (2022) reported that the method was not effective for microplastic extraction from soils due to the wider variability in particle size distributions within soils (Grause et al., 2022). The method also requires large amounts of liquid to fill the column which is impractical if solutions of higher density than water are desired. Another technique which involves the circulation of salt solutions through an enclosed system containing soil has proven highly effective at recovering microplastics (Liu et al., 2019).

Density separation takes advantage of the difference in density between plastics and soil particles (Zhang et al., 2019), and is a simple method that has become the most common approach for microplastic extraction from soil. The density range of most plastics is relatively low at 0.9-2.3 g/mL, while the densities of most soil particles are higher, averaging around 2.6-2.7 g/mL (Prata et al., 2020a). Density separation uses high-density salt solutions such as zinc bromide to resuspend soil, allowing microplastics to float while soil particles sink (Han et al., 2019; He at al., 2018; Liu et al., 2018; Masura et al., 2015; Scheurer and Bigalke, 2018; Zhang et al., 2018). While this method has high recovery rates for low-density microplastics (Han et al., 2019; Liu et al., 2018; Scheurer and Bigalke, 2018; Zhang et al., 2018), high-density microplastics, such as polytetrafluoroethylene and polyvinyl chloride, are not easily recovered due to their densities being similar to bulk soil particles (Liu et al., 2018; Zhang et al., 2018). Moreover, density separation suffers from co-extraction of organic matter (making enumeration difficult) (Hurley et al., 2018; Prata et al., 2019; Wang et al., 2018), long sample processing times (Liu et al., 2018; Scheurer and Bigalke, 2018; Zhang et al., 2018), and issues surrounding the salt solutions' environmental toxicity (Thomas et al., 2020). Since high-density microplastics represent > 20% of the global plastic demand (Plastics Europe, 2019), it is important to extract these microplastics to accurately determine the levels of terrestrial plastic pollution.

Grbic et al. (2019) developed an alternative method to extract microplastics involving magnetic separation using surface modified iron nanoparticles, extracting both high- and low-density microplastics. Their proof-of-concept work involved the surface modification (hydrophobisation) of iron nanoparticles with hexadecyltrimethoxysilane to enable them to bind to microplastics in environmental samples which were subsequently extracted using a neodymium magnet. Their work

did not include testing the recovery of microplastics from a terrestrial soil matrix. Instead, the method was tested using freshwater, seawater, and sediment; however, microplastic recovery in the sediment was lower with this method compared to that achieved through density separation (Grbic et al., 2019). Moreover, damage to the microplastics due to removal from the magnet was observed. The principle of magnetic separation using iron nanoparticles was further studied by Shi et al. (2022) for microplastic removal in water samples, though no details of the type of magnetic extraction system were supplied, and particles were removed from a simple water matrix rather than sediment or soil.

A technique known as high-gradient magnetic separation (HGMS) has the potential to improve recovery of microplastics from soil, and bypass the methodological issues associated with the previous magnetic extraction method (Grbic et al., 2019). HGMS is widely used to separate micro- and nano-scale particles in aqueous suspensions (Alves et al., 2019; Gerber and Birss, 1983; Hillier and Hodson, 1997; Mullins, 1977; Rikers et al., 1998; Watson, 1973; Yavuz et al., 2009), and is widely applied to various matrix separation processes including those in the medical (Bhakdi et al., 2010) and mining industries (Chun, 1995; Dahe, 2000; Ignjatović et al., 1995), and for water purification (Yavuz et al., 2006). Soils contain a vast array of minerals that, even if not ordinarily considered magnetic, are rendered magnetic in the HGMS system, and HGMS is often used to separate these 'paramagnetic' minerals from soils (Mullins, 1977). It has also been used to remediate soils from heavy metal contamination and radioactive wastes (Ebner et al., 1999; Rikers et al., 1998). HGMS systems typically consist of a column housing magnetically susceptible wires placed in an electromagnetic field. These wires dehomogenise the field, generating steep gradients that vary across the volume of any particles of appropriate size in the vicinity of the wires, thereby producing a net force on the particles. Particles are separated by the competition between magnetic forces on the one hand, and fluid drag or gravitational forces on the other. The use of an electromagnet is a useful component of the system as it allows the strength of the magnetic field to be adjusted for optimal separation of a wide range of particles with varying complexities, sizes, and magnetic susceptibilities. The use of an electromagnet also allows microplastics to be subsequently retrieved after extraction without damaging them by avoiding physical contact with the magnetic source.

In this proof-of-concept study, a novel alternative method for extracting microplastics from soil was developed, which uses the HGMS technique (Hillier and Hodson, 1997) in combination with the use of hydrophobised iron nanoparticles (Grbic et al., 2019) for binding to the surface of microplastics to facilitate high-gradient magnetic separation and subsequent recovery. The three-staged method

involves: Stage 1 – initial removal of inherently present magnetic soil particles; Stage 2 – tagging of microplastics with modified iron nanoparticles to render them magnetic; and Stage 3 – recovery of surface modified microplastics. In this method, the microplastics do not come into direct contact with the magnet, which avoids damage to the microplastics as had been observed in the previous permanent magnetic extraction method developed by Grbic et al. (2019). This novel HGMS method recovered both high- and low-density microplastics and fibres from soil, and recovered fibres that were partially embedded in soil aggregates. Furthermore, the developed method was less time-consuming, more cost-effective, and avoided the use of environmentally hazardous chemicals.

3.2 Materials and Methods

3.2.1 Soil sampling and soil chemistry

Five soil types were used to test and optimise the method: loam (Forfar, Angus), high-carbon loamy sand (Dunmaglass, Inverness), sandy loam (Boyndie, Aberdeenshire), high-clay sandy loam (Hartwood, North Lanarkshire), and peat (Balmoral, Aberdeenshire). These five soil types were tested as they represented the major soil types in Scotland which was crucial for the determination of the spatial distribution of microplastics at a national scale (see Chapter 5). All soils were air dried and sieved to < 2 mm. The optimised method was then tested on a farm soil sample from the Glensaugh Farm Research Facility (Laurencekirk, Aberdeenshire). A composite surface sample (0-10 cm) was collected from the farm (20 kg) using an auger from 50 locations in a field (1,144 m^2), air dried and sieved to < 2 mm. Surface samples were collected because they are more likely to contain microplastics. The field was used for livestock grazing. Within the field were several plots experimenting with the application of different types of sewage sludges. Samples were not collected from these sewage sludge-amended plots but were taken elsewhere in the field. However, the plots which were treated with sewage sludge were subjected to a temporal study in this project (see Chapter 4).

Glassware and metal tools were used throughout to avoid contamination from plastic utensils, with glassware heated in a muffle oven (450 °C) before use (Dris et al., 2018). Soil clay, silt and sand content were determined by laser diffraction (British Standards Institution, 2009) using a Mastersizer 3000 particle analyser with Hydro LV sample dispersion unit (Malvern Panalytical). Total carbon content was determined by an automated Dumas combustion procedure (Pella and Colombo, 1973) using a Flash 2000 Elemental Analyser. Soil chemistry data is given in Table 3.1. Particle size distribution and carbon content analyses were conducted in this study to accurately determine soil types derived from the soil

texture triangle. However, simple hand texturing procedures (Arshad et al., 1997) can be used effectively for determination of the likely experimental conditions required for the soil type concerned.

Table 3.1: Soil Chemistry. Particle size ranges for clay, silt, and sand, respectively, are indicated in the brackets.

Soil Type	Clay Content (%) (<2 μm)	Silt Content (%) (2-20 μm)	Sand Content (%) (20-2000 μm)	Carbon Content (%)	pH (in water)
Loam	10.07	43.17	46.76	3.00	5.17
High-carbon loamy sand	1.05	13.94	85.01	14.40	5.36
Sandy loam	4.98	21.55	73.47	2.33	5.08
High-clay sandy loam	21.00	20.00	59.00	4.79	5.45
Peat	-	-	-	47.77	3.61
Glensaugh (sandy loam)	3.40	37.82	58.78	7.36	5.73

3.2.2 High-Gradient Magnetic Separation (HGMS) System

The HGMS arrangement was an in-house, custom-built unit, essentially the same as used by Hillier and Hodson (1997). A 35 cm long magnetic steel collector wire (magnetic matrix; 1.6 mm diameter) was housed within glass tubing (2.5 cm i.d. and 40 cm long) and held using a clamp stand within a magnetic field generated with an electromagnet. The magnetic poles were 40 cm long and 3 cm apart to accommodate the glass tube and the magnetic flux density was set by adjusting the applied current from customised constant current power supplies derived from electrophoresis units (Figure 3.1). The maximum magnetic flux density achievable in this system with this pole gap was 0.53 Tesla. Rubber tubing (Nalgene™; 3/4 in i.d. x 25 cm long) was attached to the bottom of the glass tube and a lock-grip clamp was used here to allow the glass tube to be filled with HPLC grade ethanol (Rathburn, UK) and a separate clamp was used to separate the magnetic material from the non-magnetic material. Samples were added to the glass tubing via a glass funnel.
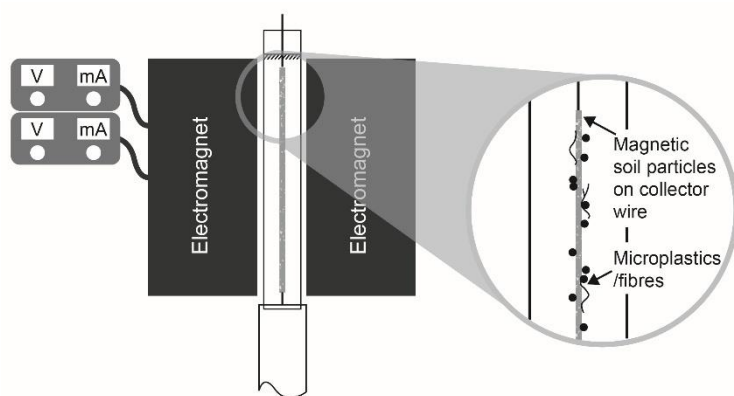
Figure 3.1: Schematic of the HGMS system showing the current suppliers, the electromagnet poles and column containing the collector wire and ethanol (denoted by the dashed line in the column) where there are microplastics adhered to the wire.

3.2.2.1 Stage 1: Removal of magnetic soil particles

Four mL of each dry soil was spiked with 30 individual microplastics or fibres and mixed thoroughly with a few drops of Milli-Q water to encourage adequate mixing and soil aggregation. Each microplastic type and size was tested with each soil type individually, giving a total of 245 individual tests. The microplastics tested were 63-75, 106-125, 300-355 and 600-710 μm polyethylene (PE) microspheres (Cospheric LLC, USA), 2-4 mm PE fibres, 2.0 x 2.0 x 0.4 mm polyethylene terephthalate (PET) flakes and 650-850 μm polytetrafluoroethylene (PTFE) fragments, which were prepared in the laboratory. Spiking reached a concentration of 1% (w/w) or less, which is a similar concentration to those found in the environment (de Souza Machado et al., 2018b). Once the spiked soils were dry again, they were mixed thoroughly to ensure there was no clumping or large aggregation. The soil samples were resuspended in 20 mL of ethanol (Figure 3.2). The magnetic flux densities were adjusted to locate the optimal conditions for magnetic soil particle removal for each soil (Figure 3.3; 0.29 Tesla for loam, 0.35 Tesla for high-carbon loamy sand, 0.53 Tesla for sandy loam, 0.16 Tesla for high-clay sandy loam, and 0.25 Tesla for peat). Each spiked soil sample was introduced to the magnetic field to allow magnetic soil particles to adhere to the collector wire (3 min settling time). The glass tube was agitated to dislodge any loosely adhered microplastics from the wire. The non-magnetic fraction (containing the microplastics) that had settled past the collector wire was separated from the magnetic material by a lock grip clamp attached to a flexible Nalgene™ tube and retained for Stages 2 and 3. The magnetic field was switched off and the magnetic soil fraction flushed out and discarded. This was repeated a second time. The collector wire was cleaned for Stage 3.
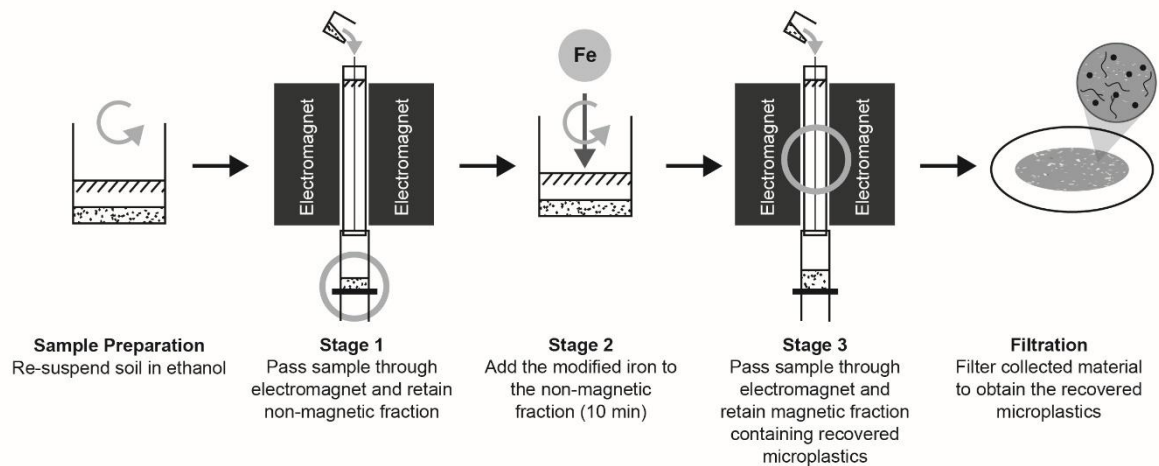
Figure 3.2: Schematic of the three-staged HGMS method.

3.2.2.2 Stage 2: Magnetisation of microplastics

Modified iron nanoparticles were prepared according to Grbic et al. (2019). Briefly, 0.16 g of iron nanoparticles (25 nm; Sigma-Aldrich) were mixed with 80 mL ethanol and 800 µL hexadecyltrimethoxysilane for 12 h on a Gallenkamp orbital shaker at 140 rev/min. The liquid was then decanted using a magnet to retain the iron nanoparticles at the bottom of the container, and the modified iron nanoparticles were then re-suspended in 20 mL Milli-Q water for storage. Approximately 10 mg of modified iron nanoparticles were added to the non-magnetic soil fraction retained from Stage 1 using a microspatula and incubated at room temperature for 10 min (with frequent stirring by hand with a glass rod) to allow binding of the iron nanoparticles to the microplastics (Figure 3.2).

3.2.2.3 Stage 3: Extraction of microplastics

The magnetic flux densities were adjusted to the optimal conditions for microplastic recovery for each soil (Figure 3.3): 0.39 Tesla for loam, 0.39 Tesla for high-carbon loamy sand, 0.53 Tesla for sandy loam, 0.39 Tesla for high-clay sandy loam, and 0.34 Tesla for peat. The sample was introduced to the HGMS system, and the magnetic fraction retained. The process was repeated for a second cycle with the non-magnetic fraction (adding another ~10 mg of modified iron nanoparticles). The retained fractions containing microplastics were filtered onto 1.2 µm Whatman GF/C glass microfibre membrane filters (Figure 3.2).

3.2.3 Density separation

Four mL of the test soils were spiked with microplastics and fibres as described above, resuspended in 50 mL of saturated zinc bromide solution (density ≈ 2.4 g mL^{-3}) and placed on an IKA® KS 260 basic rotary shaker at 300 rpm for 5 min and allowed to settle overnight. As with the HGMS method, a total of 245 individual spiked soil tests were processed by density separation.

Eight mL of soil from the Glensaugh Research Facility was used directly (i.e., without spiking) and processed in the same way as the test soils prior to extraction. Previously published studies using density separation as the extraction method used sample sizes of 5-10 g of soil (Corradini et al., 2019; Radford et al., 2021; Zhang et al., 2018), so the 8 g (equal to the 8 mL sample) used in this study aligns with this practice. Moreover, previously published studies tested soils in triplicate (Corradini et al., 2019; Han et al., 2019; Liu et al., 2018; Radford et al., 2021; Scheurer and Bigalke, 2018; Zhang et al., 2018), but for improved statistics, 7 replicates was used in this study.

Zinc bromide is a common salt solution and was used in this study as it has the potential to extract both high- and low-density microplastics (He et al., 2018; Liu et al., 2018; Scheurer and Bigalke, 2018; Zhang et al., 2018). The Milli-Q water used to make the saturated salt solution was filtered before preparation to minimise the possibility of any microplastic contamination. The solution was decanted and rinsed with excess solution using a glass pasture pipette while carefully inverting the beaker to reduce the potential loss of microplastics through their adhesion to the walls of the beaker. The decanted and rinsed solution was filtered as described above, and the process repeated a second time.

3.2.4 Quantification and identification of microplastics

Recovered material was treated with 10 mL 30% hydrogen peroxide (Sigma-Aldrich) for 1 h at 60 °C to remove organic matter from the microplastics, and then re-filtered. Microplastics were counted directly on the filter papers using a Nikon SMZ1500 stereo microscope (10x magnification). Both HGMS-recovered microplastics and density separation-recovered microplastics were quantified from 7 replicates per test soil type and microplastics extracted from the Glensaugh sample by HGMS and density separation were also quantified from 7 replicates. A blank measurement was also performed with all reagents only.
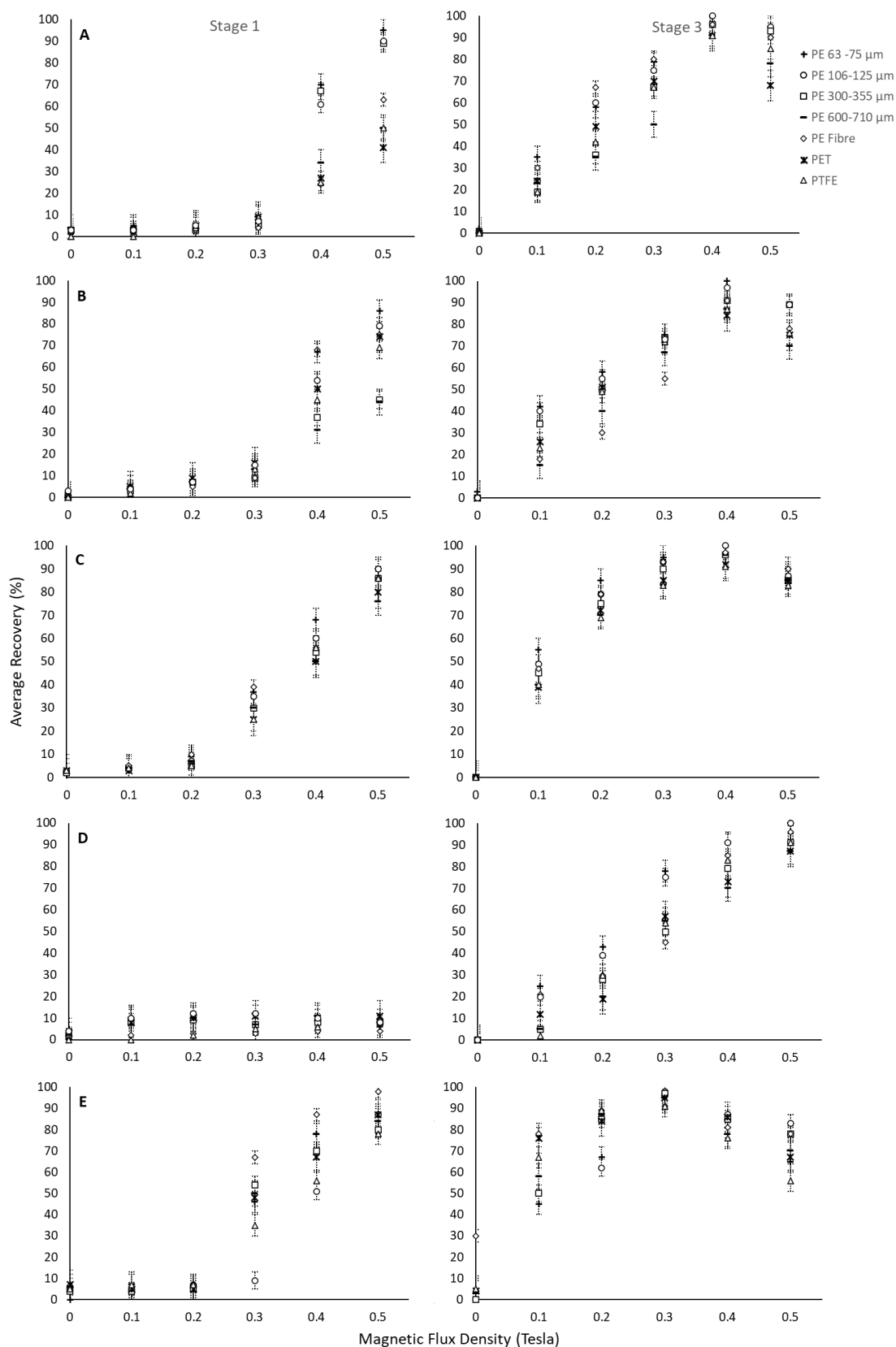
Figure 3.3: Influence of magnetic flux density (*x*-axis) on average microplastic recovery (*y*-axis) in (A) loam, (B) high-carbon loamy sand, (C) high-clay sandy loam, (D) sandy loam, and (E) peat for Stage 1 and Stage 3 of HGMS. Error bars indicate standard deviation.

Diamond attenuated Total Reflection - Fourier-Transform Infrared (DATR-FTIR) measurements of microplastics that were > 70 μm in size were carried out using a Bruker Vertex 70 FTIR spectrometer. To generate an IR spectrum, a DATR crystal with a single reflectance system was used. Data points in the range of 4000-400 cm^{-1} were recorded with a resolution of 4 cm^{-1} and an average of 200 scans. An air blank spectrum, with the same number of scans and resolution was recorded as the background spectrum before each measurement. Interpretation of the IR spectra was achieved using searchable in-house and commercial libraries of reference IR spectra.

3.2.5 Statistical analysis

Recovery of microplastics was calculated as a percentage of the total number of spiked microplastics. *T*-tests were performed to find the significance associated with the differences in microplastic recovery between the two methods (Welch, 1938). This is an appropriate statistical test to use when *n* is as small as 2 and the within-pair correlation is high (> 0.8) (de Winter, 2013). ANOVA was performed to find the significance associated with the differences in recovery of each microplastic type and fibres within each soil type for HGMS (Sthle and Wold, 1989). Microplastics were split into small-sized microplastics (63-75 μm PE and 2-4 mm PE fibres), medium-sized microplastics (106-125 μm PE and 300-355 μm PE), and large-sized microplastics (600-710 μm PE, 2.0 x 2.0 x 0.4 mm PET and 650-850 μm PTFE), for the ANOVA tests. All statistical tests were performed using R (version i386 4.0.0).

3.2.6 Detection of microplastics using fluorescent dye

The procedure for fluorescent detection of microplastics was followed from Stanton et al. (2019). A co-staining solution of Nile Red and 4′,6-diamidino-2-phenylindole (DAPI) was prepared by dissolving both dyes in a small volume of acetone before making the final solution in *n*-hexane to a concentration of 10 and 0.5 μg mL^{-1}, respectively. Filter papers from the Glensaugh soil samples were moistened using filtered Milli-Q water then treated with a few drops of the co-staining solution and left for 30 min in the dark. The filter papers were then rinsed with a few drops of Milli-Q water under vacuum to remove excess dye, then observed under a Leica DM5000B fluorescent microscope fitted with a Leica DFC310 FX camera using A4 (excitation wavelength 360/40 nm, emission wavelength 470/40 nm), L5 (480/40 nm, 527/30 nm), and N2.1 (515-560 nm, 590 nm) filter cubes.

3.3 Results and Discussion

3.3.1 Optimisation of microplastic recovery using the HGMS system

Stage 1 of the HGMS method was implemented to remove naturally paramagnetic minerals (Mullins, 1977) and prevent them coating the collector wire and blocking adherence of the microplastics. Stage 2 magnetically tagged microplastics by binding modified iron nanoparticles to their surface. Stage 3 recovered the microplastics that were hydrophobically attached to modified iron nanoparticles, which rendered them magnetic in the HGMS system.

Magnetic flux densities for Stages 1 and 3 were optimised for each soil type (Figure 3.3). Particle capture in an axial HGMS system, configured as herein, depends on the competition between gravity settling forces and magnetic forces (Watson, 1973), with the latter a function of both the magnetic susceptibility of any given particle (or aggregate) and its radius. This means that polymer type would not affect magnetic recovery using HGMS – this is determined only by particle size and the ability of the modified iron nanoparticles to bind to the surface of the microplastic. Plastics are diamagnetic (Keyser and Jefferts, 1989) and would ordinarily be repelled from the HGMS filter, but tagging with iron nanoparticles effectively renders them paramagnetic in the HGMS system. Grbic et al. (2019) reported that the iron nanoparticles bound to PE, PET, polypropylene, polyvinyl chloride, polystyrene and polyurethane, and this study has further demonstrated that iron nanoparticles also bind to both PTFE fragments and PE fibres (Figure 3.4). The microplastics selected in this work encompassed various chemical and physical properties, such as polar (PET) and non-polar (PE and PTFE) plastics, low-density (PE) and high-density (PET and PTFE) plastics, and different shapes (fibres, particles, flakes, fragments – see Figure 2.1 in Chapter 2) and sizes (63 μm to 2 mm) to demonstrate the ability of HGMS to extract plastics with different properties without significant reductions in their recovery.

Shi et al. (2022) reported that the hydrophobicity and crystallinity of microplastics affected the adsorption efficiency of the modified iron nanoparticles. The lower the hydrophobicity and crystallinity of the polymer, the lower the adsorption capacity of the iron nanoparticles, however, the polarity and pH of the background solution can influence this. Ethanol molecules are amphiphilic so have hydrophobic and hydrophilic properties. No significant differences in recovery of the plastic types were observed ($p > 0.05$), therefore, it was concluded that these physicochemical properties did not play a significant role in microplastic recovery in the HGMS system.

Differences in optimal conditions can be ascribed to factors such as different soil particle size distributions (Table 3.1), and differences in mineralogy and carbon content insomuch as this determines the magnetic susceptibility of the particles or aggregates present.

Both loam and high-carbon loamy sand had similar relationships between magnetic flux density and microplastic recovery (Figures 3.3A and 3.3B). In Stage 1, magnetic flux densities > 0.35 Tesla removed the most magnetic soil material, but this also removed > 40% of untreated microplastics. Studies have reported that microplastics bind to the surface of clay particles in soil (Pathan et al., 2020). This may account for the loss of some microplastics in Stage 1, particularly for the loam soil (10.07% clay; Table 3.1), due to paramagnetic clay particles being attracted to the collector wire. Some types of organic matter may also behave paramagnetically and become attracted to the collector wire, and at stronger magnetic flux densities, organic matter behaving diamagnetically may also be attracted to parts of the collector wire (Sokolowska et al., 2016). Microplastics have been found to adhere to the surface of vegetation/organic matter (Mateos-Cárdenas et al., 2021), therefore, any microplastics adhered to the surface of organic matter in the HGMS system has the potential to be removed through para- or diamagnetic attraction of the organic matter to the collector wire in Stage 1, particularly in soils containing a higher organic matter content such as the high-carbon loamy sand (14.4% carbon) and peat (47.77% carbon) (Table 3.1) used in this study. At 0.10-0.35 Tesla, a maximum of only 9% of untreated microplastics were removed. Therefore, an appropriate magnetic flux density was selected that allowed maximum removal of magnetic soil material, without causing significant losses of untreated microplastics. This was 0.29 and 0.35 Tesla for loam and high-carbon loamy sand, respectively.

The adherence of microplastic to organic matter and their subsequent removal was further supported when examining the removal rate of microplastics in the peat soil in Stage 1 (Figure 3.3E), whereby removal of untreated microplastics was greater at magnetic flux densities > 0.20 Tesla. This was due to the increased amount of organic matter present which resulted in increased interactions with untreated microplastics. Therefore, a magnetic flux density of 0.25 T was selected.

High-clay sandy loam displayed a similar pattern of behaviour to loam and high-carbon loamy sand for microplastic removal in Stage 1, however, the removal of untreated microplastics was higher at magnetic flux densities > 0.20 Tesla (Figure 3.3C). This was expected for this soil type as there was a

higher proportion of clay particles (21.00% clay; Table 3.1) that could adhere to the surface of microplastics, and so microplastics may have been removed at lower magnetic flux densities due to this clay-microplastic interaction. Therefore, a suitable magnetic flux density of 0.16 Tesla was selected for high-clay sandy loam.

By contrast, microplastic removal from sandy loam during Stage 1 remained constant across the range (Figure 3.3D) due to its low carbon and clay content, so 0.53 Tesla was selected for this soil type.

In Stage 3, microplastic recovery decreased at electromagnetic strengths > 0.4 Tesla for loam, high-carbon loamy sand, high-clay sandy loam, and peat due to larger volumes of soil particles and organic matter (that were not removed in Stage 1) adhering to the collector wire, likely because the resultant deposit effectively blocked the attraction of iron-bound microplastics. Therefore, to achieve optimum recovery of microplastics, a uniform 0.39 Tesla was selected for Stage 3 in the loam, high-carbon loamy sand, and high-clay sandy loam soils (Figures 3.3A-C), and 0.34 Tesla for the peat soil. For the sandy loam, optimal microplastic recovery occurred at the highest magnetic flux density (0.53 Tesla; Figure 3.1D) because most magnetic soil particles were removed during Stage 1.

3.3.2 Performance of the HGMS method

HGMS achieved significantly higher recoveries for both high- and low-density microplastics in all the test soil types compared to density separation ($p < 0.01$; Figure 3.4). The exception was recovery of PE (300-355 µm) in high-carbon loamy sand and sandy loam, and PE (600-710 µm) in high-clay sandy loam, which showed no statistical difference between the two methods ($p > 0.05$). A global t-test (i.e., a *t*-test performed on all 490 tests for microplastic recovery by density separation and HGMS) showed that overall, HGMS gave significantly higher microplastic recoveries than density separation ($p < 0.01$).

The average recovery of PE (63-75 µm) was 89±4% using density separation and 98±2% using HGMS. The recovery of PE (106-125 µm) was 89±4% using density separation and 96±3% using HGMS. The higher recoveries of these very small microplastics achieved by HGMS is important because small microplastics have greater detrimental impacts on organisms (Huerta-Lwanga et al., 2016; Ng et al., 2018) so it will allow future studies to consider impacts on soil biota. Moreover, small microplastics are usually difficult to handle in the laboratory, so they often get missed. Recovery of PE (300-355 µm) was

90±4% using density separation but 94±4% using HGMS. The recovery of PE (600-710 μm) was 90±6% using HGMS, but only 73±10% using density separation. PET had a recovery of 56±7% using density separation and 90±6% using HGMS. A significant improvement in recovery for the highest density polymer tested, PTFE, was observed using HGMS. PTFE was not recovered at all using density separation, but recoveries of 90±5% were achieved with HGMS. Density separation is often incapable of extracting high-density microplastics due to their density being similar to that of soil particles (Scopetani et al., 2020). High-density polymers are manufactured to be resistant to environmental, chemical, and thermal degradation. This can be achieved through their polymeric structures (e.g., the high bonding energy of C-F covalent bonds in PTFE (485 kJ/mol) renders the structure chemically inert), or through the addition of additives to improve their functionality. Due to their resistance to degradation in the environment, they will likely accumulate over time. Until recently, there has been a lack of attention to the presence of high-density microplastics in the environment despite their low degradability as well as their contribution of more than 20% of the global plastic demand (PlasticsEurope, 2019). Therefore, the recovery of high-density microplastics using HGMS is an important aspect as it will allow a more accurate determination of microplastic prevalence in soil.

HGMS also showed improved recovery for fibres (94±5%) compared to density separation (71±15%). Fibres are one of the most commonly occurring microplastics in both the terrestrial and marine environment (Corradini et al., 2019; Henry et al., 2019), therefore, it was important that the HGMS method was capable of extracting fibres.

Most HGMS recoveries had smaller standard deviations than density separation, (the exceptions were PE (106-125 μm) and PE (300-355 μm) where they were the same), indicating that HGMS has better reproducibility compared to both density separation and to the previous magnetic extraction method developed by Grbic et al. (2019) (±6-47%). There was no significant difference in recovery of small-sized microplastics (63-75 μm PE and 2-4 mm PE fibres), medium-sized microplastics (106-125 μm PE and 300-355 μm PE) or large-sized microplastics (600-710 μm PE, 2.0 x 2.0 x 0.4 mm PET and 650-850 μm PTFE) between the replicates in all five soil types (p > 0.05), indicating that the HGMS method is highly reproducible when extracting fibres and microplastics from these soil types. The exception was in the high-carbon loamy sand where there was a significant difference between replicates when recovering the small-sized microplastics, likely as a result of their removal in Stage 1 (p < 0.05) (Mateos-Cárdenas et al., 2021).
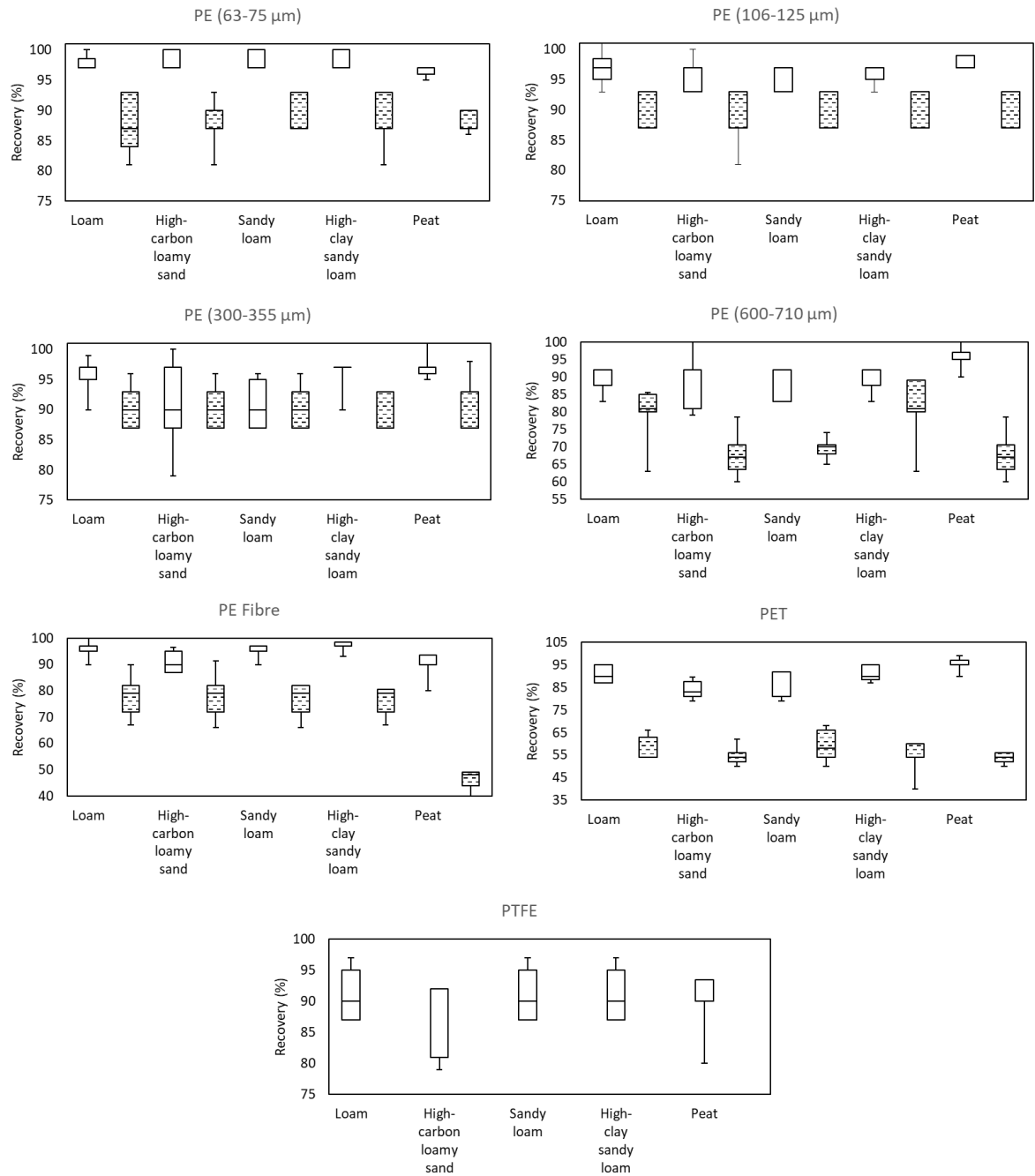
Figure 3.4: Box plots showing microplastic recovery (*y*-axis) using HGMS in each soil type (loam, high-carbon loamy sand, sandy loam, high-clay sandy loam, and peat) (*x*-axis) compared to density separation. White boxes represent results from HGMS, while the patterned boxes represent the results of density separation. Errors bars show standard deviation (n = 7).

Background levels of microplastics particles and fibres in the test soils were determined by HGMS and optical microscopy (at 10x magnification) to allow accurate measurements of microplastic recovery from the test soils used for both HGMS and density separation. Only fibres were detected in all test

soils except for the high-carbon loamy sand. No other microplastic morphologies were detected in the test soils. These contaminant fibres were bright and long so they were easily distinguished from the spiked fibres and were discounted from the recovery calculations. Blank control measurements showed that no microplastic or fibre contaminants were detected in any of the reagents (zinc bromide or ethanol containing modified iron nanoparticles) after filtration. All glassware was regularly heated in a muffle oven at 450 °C to reduce the potential for microplastic contamination (Dris et al., 2018). Therefore, the author is confident that the difference in recovery rates obtained from HGMS and density separation, respectively, were not a result of differences in background levels of microplastics or fibres in the test soils or reagents.

Taken together, HGMS achieved good microplastic recoveries irrespective of density, size, or shape of the microplastic under the conditions set using the optimal magnetic flux densities selected for each soil type. Several studies found high-density microplastics to be either low in quantity or absent in soil (Liu et al., 2018; Scheurer and Bigalke, 2018). This may reflect inefficient extraction methods, which subsequently under-estimated the true abundance of high-density microplastics. Implementation of the HGMS method in future studies has the potential to provide more accurate quantifications of microplastics and fibres.

The use of an electromagnet prevented fragmentation of microplastics. This is an improvement on the previous magnetic extraction method developed by Grbic et al. (2019), which reported fragmentation and damage of microplastics during their removal from the permanent magnet, which could result in over-estimation of microplastic abundance in real environmental samples. The removal of inherently present magnetic soil particles during Stage 1 is also a further improvement to the Grbic et al. (2019) method as it enabled better recovery rates of all microplastics tested.

3.3.3 Practical application of the HGMS method to a farm soil sample

The performance of the HGMS method was additionally tested against density separation using a sandy loam soil sample from the Glensaugh Farm Research Facility (Table 3.1). Agricultural soils have been identified as being a major 'hot-spot' for microplastic pollution due to land management practices such as sewage sludge amendment and the use of mulching film (Guo et al, 2020). Seven replicates of 8 g of soil were used for analysis, with the sample being split into two 4 g subsamples for HGMS. The magnetic flux densities selected were based on the parameters prescribed to the test soil types. The main factors considered in determining the magnetic flux densities for Stages 1 and 3 were the clay and carbon

content. Since the rate of microplastic recovery was sensitive to these soil factors (section 3.1), and the Glensaugh sample contained a higher carbon content (Table 3.1), weaker magnetic flux densities were used compared to the sandy loam test soil. Based on these factors, 0.35 and 0.39 Tesla for Stage 1 and 3, respectively, were selected for the Glensaugh sample and the extraction was carried out as described (section 2.3-2.6; Figure 3.2). HGMS extracted an average of 14±4 fibres and 3±1 microplastics per 8 g sample while density separation recovered an average of 8±3 fibres and 1±1 microplastics (Figure 3.5). Microplastics were predominantly films (potentially originating from the use of silage and haylage plastic wrapping) with the other microplastics being fragments and flakes. Fibres and microplastics may also have originated from microplastic pollution that drifted onto the field by wind transportation from nearby experimental soil amendment plots which are known to contain microplastics (Corradini et al., 2019; Gui et al., 2021; Rolsky et al, 2020; Vithanage et al., 2021).

The within-pair correlation between the microplastic recoveries with HGMS and density separation was high (> 0.8), which meant that Welch's *t*-test was an appropriate test to use when looking for significant differences in recoveries. This showed that there was a significant difference in microplastic recovery between the two methods ($p < 0.05$), likely due to microplastics becoming trapped by settling soil aggregates, reducing extraction efficiency during density separation (Zhang and Liu, 2018). Fibres
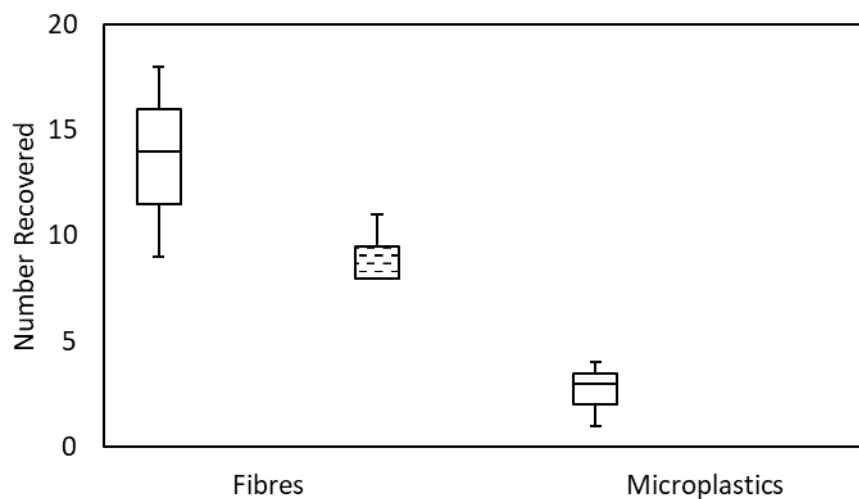
Figure 3.5: Box plot comparing the recovery of microplastics and fibres from the Glensaugh soil sample by HGMS and density separation. White boxes represent results from HGMS, while the patterned boxes represent the results of density separation. Error bars depict one standard deviation (n = 7).

recovered from the Glensaugh sample ranged from approximately 2 to 15 mm in length, while the dimensions of the particles ranged from approximately 90 to 450 µm, and the PE films were an average of approximately 3 x 1.5 x 0.1 mm. The microplastics and fibres recovered were of a different size, colour, and shape to those used during the method development stage, ruling out any possibility of cross-contamination. Fibres that were partially entrapped in soil aggregates were successfully recovered using HGMS (Figure 3.6), possibly due to the combined effects of the bound iron nanoparticles to the fibre's surface and the magnetically susceptible soil minerals within the aggregate. No such observation was seen with density separation. Density separation often fails to extract fibres or microplastics entrapped within aggregates (Bläsing and Amelung, 2018) due to their overall higher density. Disaggregation steps such as ultrasonication can be undertaken to improve microplastic recovery during density separation, however, the extent of ultrasonication is dependent on soil type and the aggregate's stability, and care must be taken to minimise further interference of the flotation of low-density soil organic matter caused during disaggregation (Thomas et al., 2020). Ultrasonication also has the potential to damage or fragment microplastics. This means that the developed HGMS method has the potential to offer extraction of these commonly observed fibre-aggregate complexes resulting in higher recoveries and a more accurate quantification of terrestrial fibre and microplastic pollution.

Figure 3.6: Photograph of a red fibre (identified predominantly as polyester by FTIR) partially embedded in a soil aggregate under the stereomicroscope recovered from the Glensaugh sample using the developed HGMS method.

ATR-FTIR was used to confirm the compositions of the microplastics recovered from the Glensaugh soil samples (Figure 3.7), where microplastics were ≥ 70 µm. As a control, FTIR analysis was also performed on modified iron-bound microplastics used to spike the soils. This was done to ensure the presence of

the bound modified iron nanoparticles on subsequently recovered microplastics did not interfere with FTIR measurements (Figure 3.8). Spectral interpretation identified predominantly PE, PET-glycol and polyester, or blends of these plastic types for recovered fibres, PE for films, and PE and PTFE for fragments, flakes, and particles. This demonstrated that other plastic types could be recovered using HGMS other than those tested during the method optimisation stage of this work. FTIR also confirmed that HGMS recovered both high- and low-density microplastics.

The application of HGMS to the Glensaugh farm sample demonstrated the effectiveness of the method to extract microplastics from soils. The higher recovery of microplastics and fibres by HGMS from soil will enable researchers and practitioners in the agricultural and food industries to understand the true impact of agricultural films and soil amendments on soil quality and health. It has been reported that the consumption of macroplastics (> 5 mm) and microplastics by sheep through grazing can occur (Beroit et al., 2021). Microplastics can also affect crop growth and yield (Khalid et al., 2020) or have the potential to be incorporated into crops, fruits, or vegetables (Conti et al., 2020; Dong et al., 2021; Li et al., 2020). Therefore, the developed HGMS method could potentially help with soil monitoring and subsequently inform the agriculture and food industries.
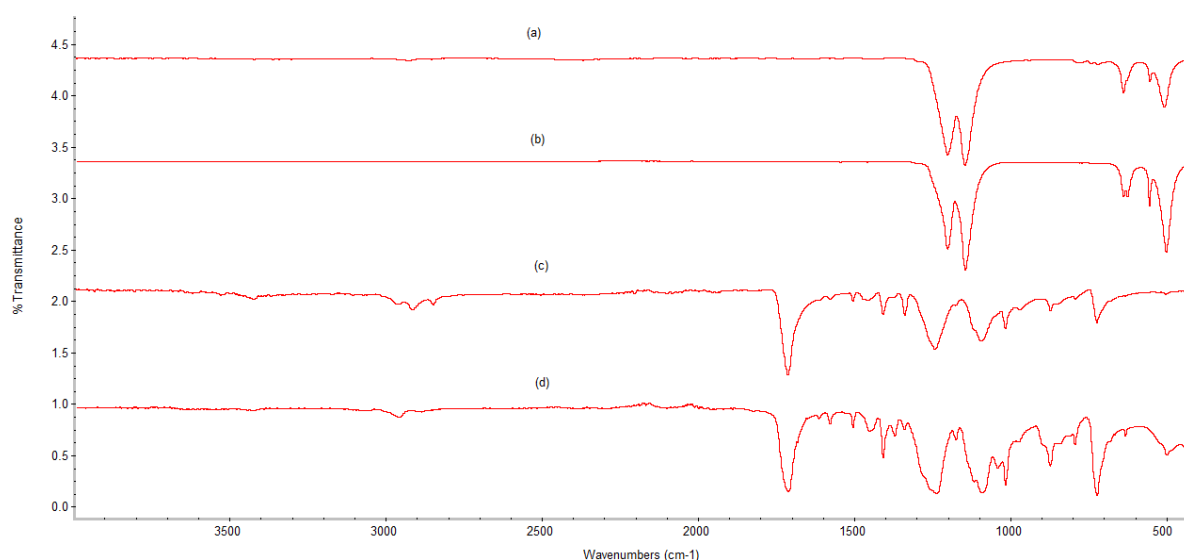
Figure 3.7: FTIR spectra of (a) a PTFE particle, and (c) a PET-glycol fibre recovered from the Glensaugh sample. Spectra (b) and (d) are their respective reference spectra.
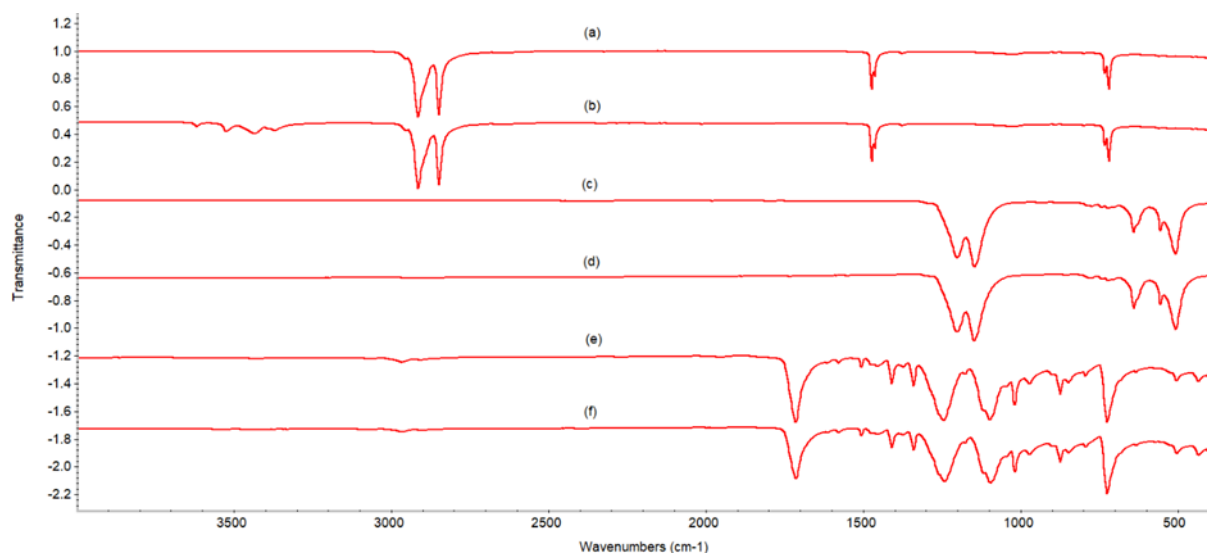
Figure 3.8: Comparison of reference FTIR spectra of (a) PE, (c) PTFE, and (e) PET to modified iron-bound (b) PE, (d) PTFE, and (f) PET microplastics recovered from a test soil. The PE microplastics used here contained aluminium trihydrate (gibbsite) (troughs around 3500 cm^{-1} region) – a common plastic flame-retardant filler (Shah et al., 2014).

3.3.4 Evaluation of the HGMS method

HGMS was a significantly faster method, taking ~30 min to process one sample, compared to 2-3 days for density separation. In this HGMS method, ethanol was used, which is readily biodegradable and non-toxic (Thomas et al., 2020), whereas density separation uses salt solutions that are toxic and have long lasting environmental effects (Thomas et al., 2020). Ethanol is also substantially cheaper than the salts used in density separation. Ethanol was used because it has a low specific density, which resulted in better dispersion of lighter microplastics into solution, improving both settling times, and contact times with the collector wire during Stages 1 and 3. Water was considered during development of the HGMS method, but this caused the flotation of lighter microplastics and fibres preventing them from reaching the collector wire within the electromagnetic field for high-gradient magnetic extraction in Stage 3 (data not shown). Ethanol also has minimal impacts on microplastics (Dawson et al., 2020).

This proof-of-concept study was intended to show the potential of HGMS to extract microplastics from soil. The HGMS system can be easily adapted by other researchers who wish to build on this concept. Various filter designs are available commercially (or are easy to make) to accommodate a range of separation requirements, from large to small sample volumes to ones designed for specific sizes or quantities of target components or types of matrices. Since HGMS works as a function of magnetic

forces and magnetic susceptibility and radius of the microplastic, a scaled-up system would simply require the quantity of modified iron nanoparticles and the capacity/throughput of the HGMS set-up to be adjusted appropriately. Larger HGMS systems have indeed been used in the mining industry (Chun, 1995; Dahe, 2000; Ignjatović et al., 1995) and laboratory HGMS systems of various sizes are available.

In summary, HGMS is a faster, safer, and cheaper extraction method; it is also a mature industrial technology (Alves et al., 2019; Gerber and Birss, 1983; Hillier and Hodson, 1997; Mullins, 1977; Rikers et al., 1998; Watson, 1973; Yavuz et al., 2009) that may be further optimised for microplastic separation on a larger scale.

A potential drawback of the novel HGMS method is that some knowledge of the soil composition and particle size may be required prior to microplastic extraction as this influences the parameters required for separation. However, it is possible to identify broad soil types relatively easily by hand texturing (Arshad et al., 1997). In this study, laser diffraction particle size analysis and Dumas combustion procedures were carried out to accurately determine soil particle size and carbon content, respectively. However, hand texturing would allow these extra analysis steps to be by-passed. This proof-of-concept work has already optimised HGMS conditions for five soil types (loam, high-carbon loamy sand, sandy loam, high-clay sandy loam, and peat), and so it likely that similar experimental conditions can be used for similar soil types by other researchers wishing to replicate this experimental set-up. Moreover, the conditions prescribed to the five test soil types were used as a benchmark for assigning magnetic flux densities to the Glensaugh farm sample, where the soil parameters differed to those in the test samples. Therefore, optimising a particular soil sample for recovery is not a time-consuming task. A further drawback is that some microplastics may be lost during Stage 1. Any untreated microplastics adhered to the collector wire or physically trapped in the magnetic deposit that accumulated on the wire in Stage 1 were discarded along with the magnetic soil particles, which likely accounted for the losses observed. Despite this, the novel HGMS method still out-performed the commonly used density separation method and previous magnetic extraction method (Grbic et al., 2019) with recoveries ranging between 83-100% for all the microplastics and fibres in this study.

3.3.5 Fluorescent detection of microplastics in HGMS-extracted soil

The use of fluorescent dyes for microplastic detection post-HGMS recovery was investigated. Nile Red was used for staining microplastics and DAPI was used as counter-stain to dye biological material which can also be stained by Nile Red due to its lipophilicity (Stanton et al., 2019). Similar to Stanton et al. (2019), green fluorescence (using the L5 filter) was most suitable for observing Nile Red-stained material while blue fluorescence (A4 filter) was most suitable for observing DAPI-stained material. The co-staining approach had considerable advantages in discriminating between potential microplastics and microscopic biological matter (e.g., fragments of plant material) (Figure 3.9). The fluorescence of particles using Nile Red in conjunction with the absence of fluorescence with DAPI confirmed that the particle was likely a microplastic (Figure 3.9A and B), however, would need confirmation using FTIR analysis. Due to the lipophilic nature of Nile Red, it has an affinity for biological material (lipid bilayer of cell membranes) (Stanton et al., 2019). The fluorescence of a particle with both Nile Red and DAPI (Figure 3.9C and D) confirmed the particle was of biological origin and could be discounted from microplastic enumeration and further analyses.

The number of possible microplastics detected by fluorescence was extremely high and required a long manual processing time. Furthermore, these potential microplastics were < 50 µm in size and could not be confirmed as microplastics by FTIR. It was deemed that the process would require optimisation and semi-automation for enumeration (e.g., using the MP-VAT 2.0 method developed by Prata et al. (2020b)). However, a substantial length of time would be needed to set up and optimise this methodology and would be out of scope for this project. Therefore, enumeration of microplastics was done by optical microscopy throughout this project.
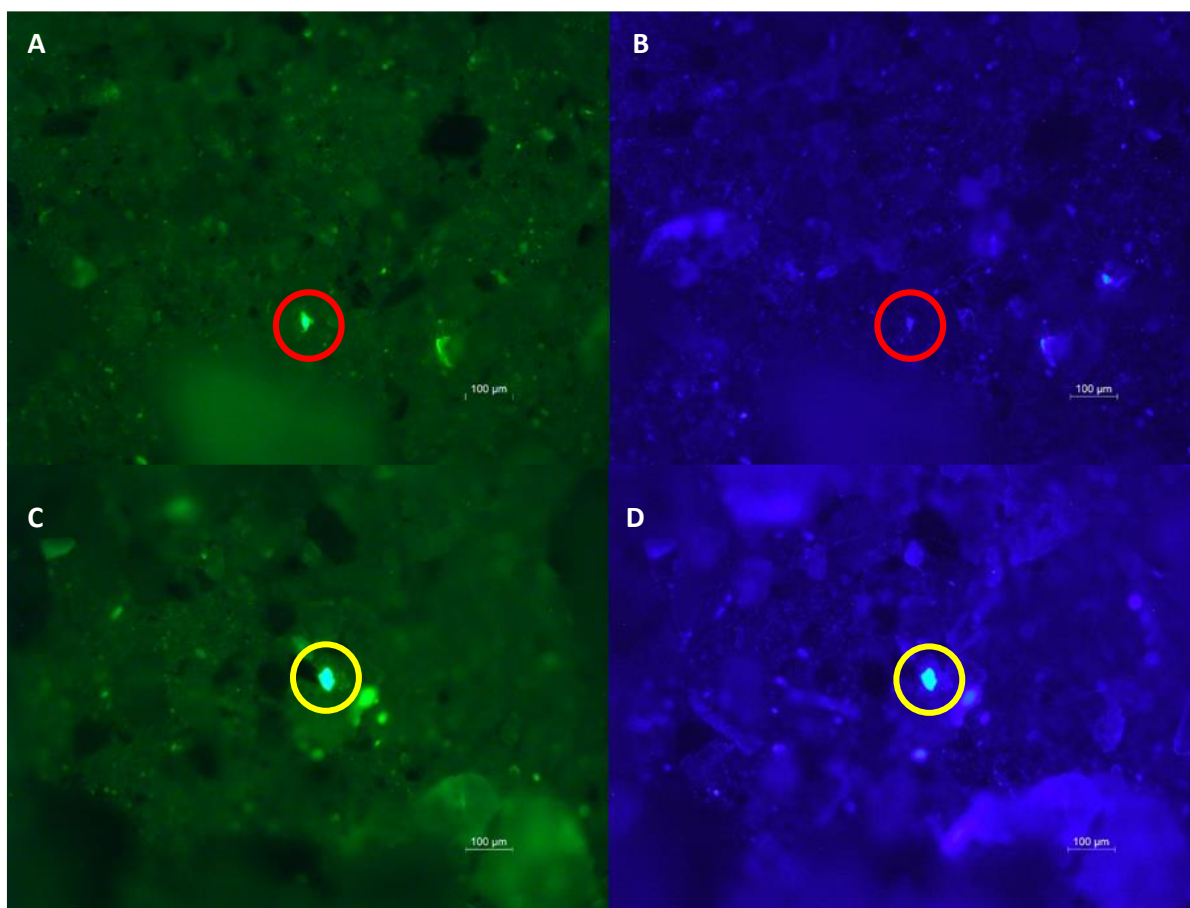
Figure 3.9: Fluorescent images of (A) a fluorescing microplastic stained with the Nile Red (circled in red), (B) the microplastic stained with DAPI not fluorescing (therefore confirmed to be a microplastic), (C) fluorescing biological material stained with the Nile Red (circled in yellow), and (D) fluorescing biological material stained with DAPI. Images A and C are observed using the L5 filter and images B and D are observed using the A4 filter.

3.4 Conclusion

The novel HGMS extraction method achieved high recoveries for both high- and low-density microplastics and fibres across a range of soil types. It is a fast and inexpensive method of extraction avoiding the use of expensive and toxic chemicals as used by the density separation method. This method was also capable of recovering fibre-aggregate complexes enabling more accurate enumeration of microplastic pollution in soils. Further work will be required to streamline the process (e.g., calibrate the set up to accommodate more soil types, larger sample volumes and optimise the design of the HGMS filter (collector wire)). However, even in a simple configuration, such as that used in the present investigation, this improved extraction method will provide an alternative quicker and more accurate method of quantifying and monitoring microplastic contamination in environmental

samples in future studies and would be beneficial for the food, agricultural and environmental sectors. This novel extraction method was applied to two studies, Chapter 4 for investigating the temporal distribution of microplastics and Chapter 5 for investigating the spatial distribution of microplastics. As these samples are finite and unique, it was important to have confidence that all microplastic work on these samples achieved optimal results, starting with their extraction.

The use of fluorescent dyes (Nile Red and DAPI) offered a substantial improvement in micro- and nanoplastic detection following HGMS extraction. However, the investment in the set up and optimisation of this was deemed to be out of scope for this project but warrants further investigation and implementation for future work.

3.5 References

Alves M.N., Miró M., Breadmore M.C., Macka M. Trends in analytical separations of magnetic (nano)particles. *Trends in Analytical Chemistry*. 2019; 114: 89-97. DOI: http://dx.doi.org/10.1016/j.trac.2019.02.026

Arshad M.A., Lowery B., Grossman B. Physical tests for monitoring soil quality. *Methods for assessing soil quality*. 1997; 49, 123-141. DOI: https://doi.org/10.2136/sssaspecpub49.c7

Beriot N., Peek J., Zornoza R., Geissen V., Huerta Lwanga E. Low density-microplastics detected in sheep faeces and soil: A case study from the intensive vegetable farming in Southeast Spain. *Science of The Total Environment*. 2021; 755, 142653. DOI: https://doi.org/10.1016/j.scitotenv.2020.142653

Bhakdi S.C., Ottinger A., Somsri S., Sratongno P., Pannadaporn P., Chimma P., Malasit P., Pattanapanyasat K., Neumann H.P.H. Optimized high gradient magnetic separation for isolation of Plasmodium-infected red blood cells. *Malaria Journal*. 2010; 9(38). DOI: https://doi.org/10.1186/1475-2875-9-38

Bläsing M., Amelung W. Plastics in soil: Analytical methods and possible sources. *Science of the Total Environment*. 2018; 612, 422-435. DOI: http://dx.doi.org/10.1016/j.scitotenv.2017.08.086

British Standards Institution (2009) *BS EN ISO 13320:2009: Particle size analysis – Laser diffraction methods*. Available at: https://www.iso.org/standard/44929.html (Accessed: 02 February 2021).

Chun Y.K. The removal of iron from hard pulverised kaolin by dry high-gradient magnetic separation. *Magnetic and Electrical Separation*. 1995; 6, 171-177.

Claessens M., Van Cauwenberghe L., Vandeghucte M.B., Janssen C.R. New techniques for the detection of microplastics in sediments and field collected organisms. *Marine Pollution Bulletin*. 2013; 70, 227-233. DOI: http://dx.doi.org/10.1016/j.marpolbul.2013.03.009

Conti G.O., Ferrane M., Banni M., Favara C., Nicolosi I., Cristaldi A., Fiore M., Zuccarello P. Micro- and nano-plastics in edible fruit and vegetables. The first diet risks assessment for the general population. *Environmental Research*. 2020; 187, 109677. DOI: https://doi.org/10.1016/j.envres.2020.109677

Corradini F., Meza P., Eguiluz R., Casado F., Huerta-Lwanga E., Geissen V. Evidence of microplastic accumulation in agricultural soils from sewage sludge disposal. *Science of the Total Environment*. 2019; 671, 411-420. DOI: https://doi.org/10.1016/j.scitotenv.2019.03.368

Dahe X. A large scale application of SLon magnetic separator in Meishan iron ore mine. *Magnetic and Electrical Separation*. 2000; 11, 1-8. DOI: https://doi.org/10.1080/10556910211967

Dawson A.L., Motti C.A., Kroon F.J. Solving a Sticky Situation: Microplastic Analysis of Lipid-Rich Tissue. *Frontiers in Environmental Science*. 2020; 8:563565. DOI: https://doi.org/10.3389/fenvs.2020.563565

de Souza Machado A.A., Kloas W., Zarfl C., Hempel S., Rillig M.C. Microplastics as an emerging threat to terrestrial ecosystems. Global Change Biology. 2018a; 24, 1405-1416. DOI: https://doi.org/10.1111/gcb.14020

de Souza Machado A.A., Lau C.W., Till J., Kloas W., Lehmann A., Becker R., Rillig M.C. Impacts of Microplastics on the Soil Biophysical Environment. *Environmental Science & Technology*. 2018b; 52, 9656-9665. DOI: https://doi.org/10.1021/acs.est.8b02212

de Winter J.C.F. Using the Student's t-test with extremely small sample sizes. *Practical Assessment, Research and Evaluation*. 2013; 18, Article 10. DOI: https://doi.org/10.7275/e4r6-dj05

Dong Y., Gao M., Qiu W., Song Z. Uptake of microplastics by carrots in presence of As (III): Combined toxic effects. *Journal of Hazardous Materials*. 2021; 411, 125055. DOI: https://doi.org/10.1016/j.jhazmat.2021.125055

Dris R., Gasperi J., Rocher V., Tassin B. Synthetic and non-synthetic anthropogenic fibers in a river under the impact of Paris Megacity: Sampling methodological aspects and flux estimations. *Science of the Total Environment*. 2018; 618, 157-164. DOI: https://doi.org/10.1016/j.scitotenv.2017.11.009

Ebner A.D., Ritter J.A., Nuñez L. High-gradient magnetic separation for the treatment of high-level radioactive wastes. *Separation Science and Technology*. 1999; 34, 1333-1350. DOI: https://doi.org/10.1080/01496399908951096

Enders K., Tagg A.S., Labrenz M. Evaluation of Electrostatic Separation of Microplastics From Mineral-Rich Environmental Samples. Frontiers in Environmental Science. 2020; 8, 122. DOI: https://doi.org/10.3389/fenvs.2020.00112

Felsing S., Kochleus C., Buchinger S., Brennholt N., Stock F., Reifferscheid G. A new approach in separating microplastics from environmental samples based on their electrostatic behavior. *Environmental Pollution*. 2018; 234, 20-28. DOI: https://doi.org/10.1016/j.envpol.2017.11.013

Gerber R.,Birss R.R., 1983, High Gradient Magnetic Separation: Chichester, U.K., John Wiley and Sons, 208 p.

Grause G., Kuniyasu Y., Chien M.F., IInoue C. Separation of microplastic from soil by centrifugation and its application to agricultural soil. *Chemosphere*. 2022; 132654. DOI: https://doi.org/10.1016/j.chemosphere.2021.132654

Grbic J., Nguyen B., Guo E., You J.B., Sinton D.L., Rochman C.M. Magnetic Extraction of Microplastics from Environmental Samples. *Environmental Science and Technology Letters*. 2019; 6: 68-72. DOI: https://doi.org/10.1021/acs.estlett.8b00671

Gui J., Sun Y., Wang J., Chen X., Zhang S., Wu D. Microplastics in composting of rural domestic waste: abundance, characteristics, and release from the surface of macroplastics. Environmental Pollution. 2021; 274, 116553. DOI: https://doi.org/10.1016/j.envpol.2021.116553

Guo J.J., Huang X.P., Xiang L., Wang Y.Z., Li Y.W., Li H., Cai Q.Y., Mo C.H., Wong M.H. Source, migration and toxicology of microplastics in soil. *Environmental International*. 2020; 137, 105263. DOI: https://doi.org/10.1016/j.envint.2019.105263

Han X., Lu X., Vogt R.D. An optimized density-based approach for extracting microplastics from soil and sediment samples. *Environmental Pollution*. 2019; 254, 113009. DOI: https://doi.org/10.1016/j.envpol.2019.113009

He D., Luo Y., Lu S., Liu M., Song Y., Lei L. Microplastics in soils: Analytical methods, pollution characteristics and ecological risks. *Trends in Analytical Chemistry*. 2018; 109, 163-172. DOI: https://doi.org/10.1016/j.trac.2018.10.006

Henry B., Laitala K., Klepp I.G. Microfibres from apparel and home textiles: Prospects for including microplastics in environmental sustainability assessment. *Science of the Total Environment*. 2019; 652, 483-494. DOI: https://doi.org/10.1016/j.scitotenv.2018.10.166

Hillier S., Hodson M.E. High-gradient magnetic separation applied to sand-size particles: An example of feldspar separation from mafic minerals. *Journal of Sedimentary Research*. 1997; 67: 975-977. DOI: http://dx.doi.org/10.2110/jsr.67.975

Huerta Lwanga E., Gertsen H., Gooren H., Peters P., Salánki T., van der Ploeg M., Besseling E., Koelmans A.A., Geissen V. Microplastics in the Terrestrial Ecosystem: Implications for *Lumbricus terrestris* (Oligochaeta, Lumbricidae). *Environmental Science and Technology*. 2016; 50, 2685-2691. DOI: https://doi.org/10.1021/acs.est.5b05478

Hurley R.R., Lusher A.L., Olsen M., Nizzetto L. Validation of a Method for Extracting Microplastics from Complex, Organic-Rich, Environmental Matrices. *Environmental Science & Technology*. 2018; 52, 7409-7417. DOI: https://doi.org/10.1021/acs.est.8b01517

Ignjatović M.R., Ćalić N., Marković Z.S., Ignjatović R. Development of a combined gravity-magnbetic separation process for magnetite ore using HGMS. *Magnetic and Electrical Separation*. 1995; 6, 161-170.

Keyser P.T., Jefferts S.R. Magnetic susceptibility of some materials used for apparatus construction (at 295 K). *Review of Scientific Instruments*. 1989; 60, 2711-2714. DOI: http://dx.doi.org/10.1063/1.1140646

Khalid N., Aqeel M., Noman A. Microplastics could be a threat to plants in terrestrial systems directly or indirectly. *Environmental Pollution*. 2020; 267, 115653. DOI: https://doi.org/10.1016/j.envpol.2020.115653

Li L., Luo Y., Li R., Zhou Q., Peijnenburg W.J.G.M., Yin N., Yang J., Tu C., Zhang Y. Effective uptake of submicrometre plastics by crop plants via a crack-entry mode. *Nature Sustainability*. 2020; 3, 929-937. DOI: https://doi.org/10.1038/s41893-020-0567-9

Liu M., Lu S., Song Y., Lei L., Hu J., Lv W., et al. Microplastic and mesoplastic pollution in farmland soils in suburbs of Shanghai, China. *Environmental Pollution*. 2018; 242, 855-862. DOI: https://doi.org/10.1016/j.envpol.2018.07.051

Liu M., Song Y., Lu S., Qiu R., Hu J., Li X., Bigalke M., Shi H., He D. A method for extracting soil microplastics through circulation of sodium bromide solutions. *Science of the Total Environment*. 2019; 691, 341-347. DOI: https://doi.org/10.1016/j.scitotenv.2019.07.144

Masura J., Baker J., Foster G., Arthur C., Herring C. 2015. Laboratory methods for the analysis of microplastics in the marine environment: recommendations for quantifying synthetic particles in waters and sediments. NOAA Technical Memorandum NOS-OR&R-48.

Mateos-Cárdenas A., van Pelt F.N.A.M., O'Halloran J., Jansen M.A.K. Adsorption, uptake and toxicity of micro- and nanoplastics: Effects on terrestrial plants and aquatic macrophytes. *Environmental Pollution*. 2021; 284, 117183. DOI: https://doi.org/10.1016/j.envpol.2021.117183

Mullins C.E. Magnetic Susceptibility of the Soil and its Significance in Soil Science – A Review. *Journal of Soil Science*. 1977; 28(2), 223-246. DOI: https://doi.org/10.1111/j.1365-2389.1977.tb02232.x

Ng E., Huerta Lwanga E., Eldridge S.M., Jonshton P., Hu H., Geissen V., Chen D. An overview of microplastic and nanoplastic pollution in agroecosystems. *Science of the Total Environment*. 2018; 627, 1377-1388. DOI: https://doi.org/10.1016/j.scitotenv.2018.01.341

Pathan S.I., Arfaioli P., Bardelli T., Ceccherini M.T, Nannipieri P., Pietramellara G. Soil Pollution from Micro- and Nanoplastic Debris: A Hidden and Unknown Biohazard. *Sustainability*. 2020; 12, 7255. DOI: https://doi.org/10.3390/su12187255

Pella E., Colombo B. Study of carbon, hydrogen and nitrogen by combustion gas-chromatography. *Mikrochim Acta*. 1973; 1973, 697-719. DOI: https://doi.org/10.1007/BF01218130

PlasticsEurope, 2019. Plastics – the Facts 2019. An Analysis of European Plastics Production, Demand and Waste Data. Association of Plastics Manufactures, Brussels. Plastics Europe. Available online at: https://www.plasticseurope.org/en/resources/publications/1804-plastics-facts-2019 (Accessed 02 February 2021).

Prata J.C., da Costa J.P., Girão A.V., Lopes I., Duarte A.C., Rocha-Santos T. Identifying a quick and efficient method of removing organic matter without damaging microplastic samples. *Science of the Total Environment*. 2019; 686, 131-139. DOI: https://doi.org/10.1016/j.scitotenv.2019.05.456

Prata J.C., da Costa J.P., Lopes I., Duarte A.C., Rocha-Santos T. Environmental exposure to microplastics: An overview on possible human health effects. *Science of the Total Environment*. 2020a; 702, 134455. DOI: https://doi.org/10.1016/j.scitotenv.2019.134455

Prata J.C., Alves J.R., da Costa J.P., Duarte A.C., Rocha-Santos T. Major factors influencing the quantification of Nile Red stained microplastics and improved automatic quantification (MP-VAT 2.0). *Science of The Total Environment*. 2020b; 719, 137498. DOI: https://doi.org/10.1016/j.scitotenv.2020.137498

Radford F., Zapata-Restrepo L.M., Horton A.A., Hudson M.D., Shaw P.J., Williams I.D. Developing a systematic method for extraction of microplastics in soils. Analytical Methods. 2021; 13, 1695-1705. DOI: https://doi.org/10.1039/D0AY02086A

Rikers R.A., Rem P., Dalmijn W.L., Honders A. Characterization of Heavy Metals in Soil by High Gradient Magnetic Separation. *Journal of Soil Contamination*. 1998; 7(2): 163-190. DOI: https://doi.org/10.5402/2011/402647

Rolsky C., Kelkar V., Driver E., Halden R.U. Municipal sewage sludge as a source of microplastics in the environment. *Current Opinion in Environmental Science & Health*. 2020; 14, 16-22. DOI: https://doi.org/10.1016/j.coesh.2019.12.001

Scheurer M., Bigalke M. Microplastics in Swiss Floodplain Soils. *Environmental Science & Technology*. 2018; 52, 3591-3598. DOI: https://doi.org/10.1021/acs.est.7b06003

Scopetani C., Chelazzi D., Mikola J., Leiniö V., Heikkinen R., Cincinelli A., Pellinen J. Olive oil-based method for the extraction, quantification and identification of microplastics in soil and compost samples. *Science of the Total Environment*. 2020; 733, 139338. DOI: https://doi.org/10.1016/j.scitotenv.2020.139338

Shah A.U.R., Lee D., Wang Y., Wasy A., Ham K.C., Jayaraman K., Kim B., Song J. Effect of concentration of ATH on mechanical properties of polypropylene/aluminium trihydrate (PP/ATH) composite. *Transactions of Nonferrous Metals Society of China*. 2014; 24, s81-s89. DOI: https://doi.org/10.1016/S1003-6326(14)63292-1

Shi X., Zhang X., Gao W., Zhang Y., He D. Removal of microplastics from water by magnetic nano-Fe_3O_4. *Science of the Total Environment*. 2022; 802, 149838. DOI: https://doi.org/10.1016/j.scitotenv.2021.149838

Sokolowska Z., Alekseev A., Skic K., Brzenzińska M. Impact of wastewater application on magnetic susceptibility in Terric Histosol soil. *International Agrophysics*. 2016; 30, 89-94. DOI: https://doi.org/10.1515/intag-2015-0064

Stanton T., Johnson M., Nathanail P., Gomes R.L., Needham T., Burson A. Exploring the Efficacy of Nile Red in Microplastic Quantification: A Costaining Approach. *Environmental Science and Technology Letters*. 2019; 10, 606-611. DOI: https://doi.org/10.1021/acs.estlett.9b00499

Sthle L., Wold S. Analysis of variance (ANOVA). *Chemometrics and Intelligent Laboratory Systems*. 1989; 6, 259-272. DOI: https://doi.org/10.1016/0169-7439(89)80095-4

Thomas D., Schütze B., Heinze W.M., Steinmetz Z. Sample Preparation Techniques for the Analysis of Microplastics in Soil—A Review. *Sustainability*. 2020; 12, 9074. DOI: https://doi.org/10.3390/su12219074

Vithanage M., Ramanayaka S., Hasinthara S., Navaratne A. Compost as a carrier for microplastics and plastic-bound toxic metals into agroecosystems. Current Opinion in Environmental Science & Health. 2021; 24, 100297. DOI: https://doi.org/10.1016/j.coesh.2021.100297

Wang Z., Taylor S.E., Sharma P., Flury M. Poor extraction efficiencies of polystyrene nano- and microplastics from biosolids and soil. *PLoS ONE*. 2018; 13, e0208009. DOI: https://doi.org/10.1371/journal.pone.0208009

Watson J.H.P. Magnetic filtration. *Journal of Applied Physics*. 1973; 44, 4209-4213. DOI: https://doi.org/10.1063/1.1662920

Welch B.L. The Significance of the Difference Between Two Means when the Population Variances are Unequal. *Biometrika*. 1938; 29, pp. 350–362. DOI: https://doi.org/10.1093/biomet/29.3-4.350

Yavuz C.T., Mayo J.T., Yu W.W., Prakash A., Falkner J.C., Yean S., Cong L., Shipley H.J., Kan A., Tomson M., Natelson D., Colvin V.L. Low-Field Magnetic Separation of Monodisperse Fe_3O_4 Nanocrystals. *Science*. 2006; 314, 964-967. DOI: https://doi.org/10.1126/science.1131475

Yavuz C.T., Prakash A., Mayo J.T., Colvin V.L. Magnetic separations: From steel plants to biotechnology. *Chemical Engineering Science*. 2009; 64, 2510-2521. DOI: https://doi.org/10.1016/J.CES.2008.11.018

Zhang G.S., Liu T.F. The distribution of microplastics in soil aggregate fractions in southwestern China. *Science of the Total Environment*. 2018; 642, 12-20. DOI: https://doi.org/10.1016/j.scitotenv.2018.06.004

Zhang S., Wang J., Liu X., Qu F., Wang X., Wang X., et al. Microplastics in the environment: A review of analytical methods, distribution, and biological effects. *Trends in Analytical Chemistry*. 2019; 111: 62-72. DOI: https://doi.org/10.1016/j.trac.2018.12.002

Zhang S., Yang X., Gertsen H., Peters P., Salánki T., Geissen V. A simple method for the extraction and identification of light density microplastics from soil. *Science of the Total Environment*. 2018; 616-617, 1056-1065. DOI: https://doi.org/10.1016/j.scitotenv.2017.10.213

3.6 Appendix: Publication

Rapid extraction of high- and low-density microplastics from soil using high-gradient magnetic separation

Stuart J.F.F. Ramage [a,b,*], Eulyn Pagaling [a], Reza K. Haghi [a], Lorna A. Dawson [a,b], Kyari Yates [b], Radhakrishna Prabhu [b], Stephen Hillier [a,c], Sandhya Devalla [a]

[a] The James Hutton Institute, Craigiebuckler Aberdeen AB15 8QH, United Kingdom
[b] Robert Gordon University, Aberdeen AB10 7GJ, United Kingdom
[c] Department of Soil and Environment, Swedish University of Agricultural Sciences (SLU), SE-75007 Uppsala, Sweden

HIGHLIGHTS

- Rapid High-Gradient Magnetic Separation method for microplastic extraction from soil
- The HGMS method performed significantly better than the density separation method.
- It was able to recover high- and low-density microplastics.
- Could recover microplastic particles and fibres 63 μm–15 mm in size ($\geq$ 87%)
- Avoided the use and disposal of hazardous salts associated with density separation

GRAPHICAL ABSTRACT
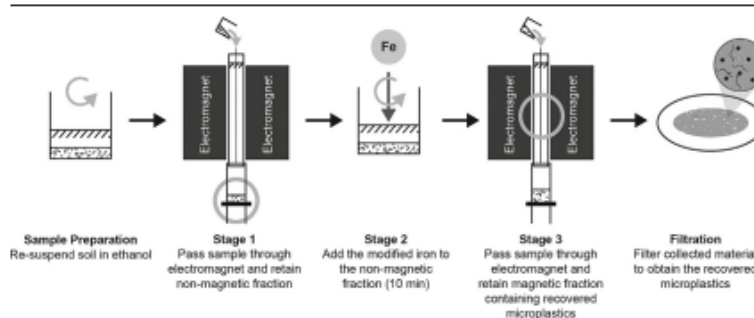
Sample Preparation — Re-suspend soil in ethanol
Stage 1 — Pass sample through electromagnet and retain non-magnetic fraction
Stage 2 — Add the modified iron to the non-magnetic fraction (10 min)
Stage 3 — Pass sample through electromagnet and retain magnetic fraction containing recovered microplastics
Filtration — Filter collected material to obtain the recovered microplastics

ARTICLE INFO

ABSTRACT

Microplastics (MPs) are present in all environments, and concerns over their possible detrimental effects on flora and fauna have arisen. Density separation (DS) is commonly used to separate MPs from soils to allow MP quantification; however, it frequently fails to extract high-density MPs sufficiently, resulting in under-estimation of MP abundances. In this proof-of-concept study, a novel three-stage extraction method was developed, involving high-gradient magnetic separation and removal of magnetic soil (Stage 1), magnetic tagging of MPs using surface modified iron nanoparticles (Stage 2), and high-gradient magnetic recovery of surface-modified MPs (Stage 3). The method was optimised for four different soil types (loam, high-carbon loamy sand, sandy loam and high-clay sandy loam) spiked with different MP types (polyethylene, polyethylene terephthalate, and polytetrafluoroethylene) of different particle sizes (63 μm to 2 mm) as well as polyethylene fibres (2–4 mm). The optimised method achieved average recoveries of 96% for fibres and 92% for particles in loam, 91% for fibres and 87% for particles in high-carbon loamy sand, 96% for fibres and 89% for particles in sandy loam, and 97% for fibres and 94% for particles in high-clay sandy loam. These were significantly higher than recoveries achieved by DS, particularly for fibres and high-density MPs ($p < 0.05$). To demonstrate the practical application of the HGMS method, it was applied to a farm soil sample, and high-density MP particles were only recovered by HGMS. Furthermore, this study showed that HGMS can recover fibre-aggregate complexes. This improved extraction method will provide better estimates of MP quantities in future studies focused on monitoring the prevalence of MPs in soils.

Chapter 4: The fate of microplastics over time in sewage sludge-treated soils

Sewage sludges applied to agricultural soils are sources of microplastic pollution, however, little is known about the accumulation, persistence, or degradation of these microplastics over time. In this long-term study (25 years), the abundance and degradation of microplastics was assessed in soils sampled biennially from an experimental field managed under an improved grassland regime following the application of five different sewage sludges. Microplastic abundance significantly increased by 1417-3700% following sewage sludge applications ($p < 0.05$) with abundance remaining relatively constant over time (22 years and possibly beyond) ($p > 0.05$). All sludges predominantly added microfibres to the soil, with the most abundant colour being white or transparent. Microfibres degraded the most significantly over time, showing the greatest reduction in size, highlighting the possibility that microfibres release detrimental secondary micro(nano)plastics. Microfilms were also highly susceptible to degradation whereby over time pits and cracks developed into tears and holes, while other microplastic morphologies were more resistant to degradation. Coloured fibres showed dye loss over time, which possibly leached into soil. The leaching of textile dyes into the soil environment may lead to unknown and potentially toxic effects on soil biota. The sludges contained different microplastic compositions (e.g., polyester, polyurethane), reflecting the different sources of the sludges. This evidence is useful in informing regulation on sewage sludge use and management, and in assessing the fate and impact of microplastics in soil.

4.1 Introduction

Microplastics are typically removed from wastewater at wastewater treatment works (WWTWs) and accumulate in the solid waste (sludge) (Carr et al., 2016; Murphy et al., 2016; Bayo et al., 2020) thus reducing microplastic output to receiving waters. Sewage sludge is commonly applied to agricultural soils worldwide as a fertiliser because it is rich in organic matter and macro- and micronutrients, which benefit soil fertility and function (Elmi et al., 2020), leading to the accumulation of microplastics in receiving soils. This practice is projected to continue, potentially resulting in the further accumulation of microplastics over time (Corradini et al., 2019). High-income countries (HICs) including the United Kingdom (UK), United States of America (USA), Japan, Australia, New Zealand, and the European Union (EU) have legislations and regulations on the use and management of sewage sludge applications (Jiminez et al., 2004; Christodoulou et al., 2016), however, microplastics are not currently regulated constituents in sludges.

The fate of microplastics in agricultural soils after sewage sludge applications is dependent on land management practices, soil attributes, and environmental and biological factors. Tillage causes mechanical fragmentation and degradation (Duan et al., 2021), and can incorporate microplastics to greater depths (Rillig et al., 2017a; Xu et al., 2020; Zhao et al., 2021), preventing photodegradation (Bonyadinejad et al., 2022). Microplastics can also be translocated to deeper layers of soil through bioturbation by earthworms and other soil biota (Huerta Lwanga et al., 2017; Maaß et al., 2017; Rillig et al., 2017b). Furthermore, smaller microplastics can be transported deeper into soil by vertical drainage of ground- and rainwater during wet-dry cycles (O'Connor et al., 2019), and the free movement of smaller microplastics into soil pores (Yang et al., 2021a). The incorporation of microplastics deeper in soil can increase their persistence.

To date, studies investigating the long-term fate of microplastics in soils have only been able to do so retrospectively (van der Berg et al., 2020; Yang et al., 2021b). As such, it is possible that important information may be missed in the fate of microplastics in soil long term. The information and data generated through a high temporal resolution, long-term study can help inform future studies on elucidating the fate and impact of microplastic pollution in soils.

The aim of this study was to quantify and assess the fate of microplastics in soil over a substantial period of time (25 years) following biosolid applications. It was hypothesised that sewage sludge contributes a significant amount of microplastics to soil and that the microplastics persist long-term and are subjected to minimal degradation. To address this, archived soil samples from a 25-year sewage sludge amendment experiment, maintained under improved grassland management, were analysed. The numbers, size, morphology, colour, composition, and weathering of microplastics were assessed to determine the accumulation, persistence, degradation, and potential sources of microplastics in soil. To the author's knowledge, this is the first study to provide long-term, quantitative evidence of microplastics in agricultural soils following biosolid application at a high temporal resolution. This provides a better understanding of the fate of microplastics in soil and the consequences of sewage sludge applications, which benefits and aids in informing the agricultural, food, and environmental sectors on future regulation of sewage sludge application to soil.

4.2 Materials and Methods

4.2.1 Experimental set-up and sampling

A field at Hartwood, North Lanarkshire (Scotland, UK) was included in a UK-wide sludge experiment from 1994 to 2019 investigating heavy metal toxicity and accumulation over time in the soil (a sandy clay loam) as a result of sewage sludge applications (refer to Gibbs et al. (2006) for detailed information regarding the original Hartwood experiment and initial outcomes).

In the first four years of the experiment, individual sludge cakes were applied annually. A plot that was not treated with any sludge was used as a negative control. Sludge D was an uncontaminated digested sludge (i.e., low metal concentrations) to match sludges A and C, while sludge E was an uncontaminated undigested sludge to match sludge B (Table 4.1). Plots treated with sludges A and C were supplemented with sludge D to maintain a constant organic matter content, while plots treated with sludge B were supplemented with sludge E (see Gibbs et al., 2006).

The treatments were replicated in three blocks of randomised plots. The plots were 8 x 4.5 m (36 m^2) and bordered by 2-3 m of permanent grassland to prevent soil movement during cultivations (Figure 4.1). Soil collected from plots treated with sludge D (plots 2 and 4), as well as the negative control plots (plots 7 and 8), were combined at time of sampling to make a composite soil sample. The sludge cakes were evenly spread over the surface of the plot manually then incorporated into the soil using a spading machine to a depth of 20-25 cm. The order of sludge incorporation using the spading machine was as follows: negative control → sludge D → sludge E → sludge A → sludge B → sludge C. Mixing of every plot of the same treatment were done across all three blocks before the blades of the spading machine and hand tools were cleaned ahead of mixing of the next treatment by running them several times through 'clean' soil at the edge of the field away from the plots to prevent cross-contamination between the treatments. Plots were maintained under an improved grassland regime. Ryegrass (*Lolium* spp.) seedlings were sown annually in all the treatment and control plots between July-August, and lime and inorganic fertiliser pellets were applied after sowing to maintain a constant pH of around 5.8 (the recommended pH level for Scottish grassland) to encourage plant growth. The pellets were applied to the plots by hand broadcasting. The plots were subjected to grassland cropping and cut regularly to deplete mineral nitrogen supply to the soil. The soil was tilled before every yearly cycle (June-July). Plots were sampled annually when the sludges were being applied, and then biennially thereafter.

Table 4.1: Types and sources of sludges applied to experimental plots.

Treatment Name	Type of Sludge	Source and Information
Sludge A	Digested	WWTW catchment area included a number of leather processing plants (tanneries). High in Zn.
Sludge B	Undigested	WWTW catchment area included a number of electronics factories. High in Cu.
Sludge C	Digested	Composite sludge. High in Cd.
Sludge D	Digested	Not recorded.
Sludge E	Undigested	Not recorded.
Negative control	N/A	N/A

Archived soil samples from each treatment all originated from one of the three blocks were used for this study. Original composite topsoil samples (0-25 cm) were collected from each plot using a 2.5 cm diameter auger in a 'W' pattern (15 cores) to produce a total of 2.5 kg soil per plot. Stones and plant material were removed using a sieve with a mesh size of 6.5 cm, before air-drying and sieving to 2 mm. The < 2 mm soils were then stored in paper bags and archived within The National Soil Archive of Scotland at the James Hutton Institute, Scotland, UK.

Several kilograms of the sludges were stored in large plastic bags at -20 °C. The archived sludges were partially thawed then subsampled for this study from the centre to avoid the outer layer which had been in contact with the plastic bag to minimise potential microplastic contamination. The subsampled sludges were left at room temperature to fully thaw and air-dry before sieving to 2 mm. Macroplastics were removed during sieving and large microplastics were removed by hand before microplastic extraction.
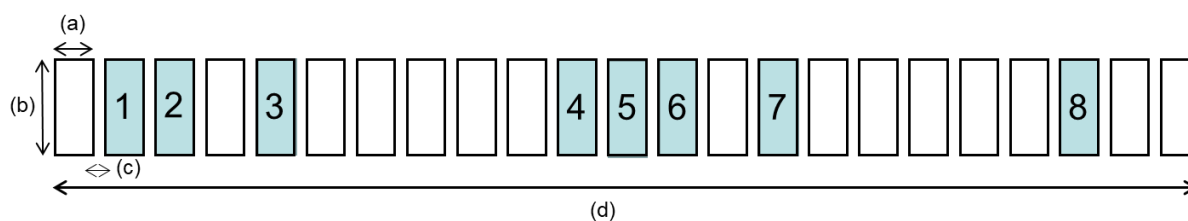
Figure 4.1: Layout and dimension of plots. Highlighted plots indicate those selected for microplastic analysis. Plot 1 – sludge E; Plots 2 and 4 – sludge D; Plot 3 – sludge C; Plot 5 – sludge B; Plot 6 – sludge A; Plots 7 and 8 – Negative Control. Unlabelled plots are other plots in the original experimental set-up that were not used in this study – data not shown. Dimensions of plots are: (a) 4.5 m, (b) 8 m, (c) 2-3 m, and (d) 164.4-204 m.

4.2.2 Microplastic extraction by high-gradient magnetic separation

After thorough mixing of the archived soil samples, 8 mL of the dried 2 mm sieved soil was subsampled using an 8 mL metal scoop in triplicate (average weight recorded) and subjected to high-gradient magnetic separation (HGMS), following the procedure outlined in Chapter 3 and Ramage et al. (2022) to recover microplastics. As the Hartwood soil was previously used as a test soil for HGMS method development in Chapter 3, the optimal magnetic flux densities for Stages 1 and 3 were already known. These were 0.16 and 0.39 Tesla, respectively. The material was vacuum filtered onto Whatman GF/C filter papers and stored in muffled glass petri dishes until further analysis. A blank measurement was taken after every 10 samples (8 in total). In order to ensure that a change in batches of modified iron nanoparticles did not affect microplastic recovery, the recovery of a spiked soil sample was checked with every new batch.

Sludges (dried) were treated similarly to peat samples due to their high organic matter content and similar texture. This was tested following the same protocol detailed in Chapter 3 and the performance was compared to that of density separation. It was confirmed that recovery was significantly better with the HGMS method ($p < 0.05$), and the magnetic flux densities prescribed to peat soils were optimal for microplastic extraction from dried sludges, i.e., 0.25 and 0.34 Tesla for Stages 1 and 3, respectively.

It was also assessed whether an initial organic matter digestion step before HGMS microplastic extraction would improve microplastic recovery from sewage sludge samples due to their high organic content. To test this, Sludge E (undigested) was spiked with microplastics as described in Chapter 3

section 3.2.2.1 (7 replicates), and then digested using Fenton's reagent (hydrogen peroxide with a Fe^{2+} catalyst) following the protocol detailed by Masura et al. (2015). Briefly, a 0.05 M Fe(II) solution was prepared by adding 7.5 g $Fe_2SO_4.7H_2O$ (Sigma-Aldrich) to 500 mL filtered Milli-Q water followed by 3 mL of 0.05M sulphuric acid (Fisher Scientific). Respectively, 20 mL of the 0.05 M Fe(II) solution and 30% (v/v) H_2O_2 were added to 8 mL spiked sludge samples, mixed thoroughly, and left at room temperature for 5 min before placing on a 60 °C hot plate for 1 h with regular stirring with a glass rod. A further 20 mL H_2O_2 was added once boiling subsided. The spiked sludge was then directly filtered onto filter papers (i.e., no HGMS extraction) and the spiked microplastics enumerated using the optical microscope (as outlined in section 3.2.4).

4.2.3 Categorisation and enumeration of microplastics

All filter papers were examined using a Nikon SMZ1500 stereomicroscope under 7.5-50x magnification. Microplastics were found by traversing the filter paper systematically. To store microplastics recovered from soil and sludge samples for further analysis, sterile tweezers were used to remove them from the filter papers and attach them to the adhesive side of transparent, colourless tape. The length of exposed tape on the tape dispenser was discarded before each use to minimise potential contamination from any microplastics present. The positions of the microplastics on the tape were immediately marked on the reverse side (the non-adhesive side) with a permanent marker pen to differentiate between microplastics from the laboratory environment that may have been accidentally trapped on the tape. After the filter paper had been completely searched, the tape was secured to an acetate sheet (backing material) so that the collected microplastics were trapped between the tape and the acetate. The collected microplastics were further circled so they could be located more easily, and the acetates stored prior to FTIR analysis. This is a common method of storing fibres in forensic science (Schotman and van der Weerd, 2015).

Microplastics were later removed from the tape by incising the tape in an L-shape using a scalpel dipped in xylene to dissolve the adhesive, making the tape easily retractable from the acetate using tweezers. While still held in the tweezers, the microplastic was shaken in Milli-Q water briefly then air dried before placing on a carbon adhesive pad mounted on a glass slide. To ensure that the use of xylene did not chemically alter the microplastics and affect their spectra, FTIR measurements of a test microplastic (polypropylene film) were taken before exposure to xylene, and 30 seconds, 1 minute and 2 minutes after continuous exposure.

When a microplastic was located, it was categorised based on its morphology using terminologies derived from Rochman et al. (2019) (see Chapter 2 section 2.1). The microplastic abundance (enumerated by each morphology) in soils prior to the addition of the sludges (i.e., the baseline number of microplastics) was subtracted from the results from all years following sewage sludge application. The average number of microplastics measured in HGMS blank controls was also subtracted from all final recorded abundances.

The colour of microplastics were recorded. Fibres that were predominantly transparent but with areas of colour were recorded as a separate colour category.

Due to the extremely high number of microplastics recovered from the soil samples (5745 in total), the sizes of microplastics (10% of fibres and total number of all other morphologies) were measured at three time points along their longest axes using the Leica Application Suite 4.13 software on a Leica DM5000B microscope. The time points were after the last addition of sludge (1997; n = 75), the middle of the time course (2009; n = 75), and the end of the experiment (2019; n = 73) (n is per treatment).

4.2.4 Spectroscopic analysis using Fourier-transform infrared (FTIR) microscopy

Microplastics that were $\geq$ 50 µm in size were subjected to FTIR analysis in reflectance mode using a Nicolet[TM] iN10 infrared microscope. Data points were recorded over 128 scans using a liquid nitrogen-cooled MCT detector in the range of 4000-650 cm^{-1} with a resolution of 8 cm^{-1}. Air blank spectra were recorded after each measurement (using the same number of scans and resolution). Some of the interpretation of the IR spectra was achieved using searchable in-house and commercial libraries of reference IR spectra. However, due to the level of weathering present in the spectra (i.e., additional bands), library matches often could not be made, so the majority of spectra were manually interpreted using spectral interpretation sheets and comparisons with published spectra of weathered microplastics (Fernández-González et al., 2021; Phan et al., 2022; Zvekic et al., 2022).

The carbonyl index (CI) of polyethylene films recovered from soil samples in 1997, 2001, 2005, 2009, and 2019, was calculated using the following equation from Syranidou et al. (2023):

$$CI = \frac{I_{1725}}{I_{1472}}.$$

I_{1725} refers to the area of the carbonyl band present at ~1725 cm^{-1} and I_{1472} refers to the area of the methylene band present at ~1472 cm^{-1}. The band areas were generated using the peak area function tool in the OMNIC software.

4.2.5 Scanning electron microscopy (SEM) imaging

Topographic images were taken of the surface of films recovered from soil samples in 1997, 2001, 2005, 2009, and 2019, using a Zeiss EVO LS10 SEM in variable pressure mode. The specimens were sputter coated in gold and imaged using a variable pressure secondary electron detector at a 6.0 mm working distance. The chamber pressure was set to 100 Pa with a beam current of 100 µA, probe current of 100 pA, and an accelerating potential of 25 kV.

4.2.6 Quality Control

To minimise potential contamination throughout the extraction and enumeration stages, the use of plastic utensils was avoided by using metal or glass alternatives. All glassware was muffled at 450 °C before use (Dris et al., 2018) and kept covered in aluminium foil prior to use. All reagents were filtered before use. Sample preparation and filtration was conducted in a clean environment within a HEPA filtered laminar flow hood (0.3 µm pore size) to minimise airborne contamination. To eliminate bias, all samples were anonymised using laboratory barcodes during processing.

4.2.7 Data Analysis

Recovered microplastics were recorded as macro- or microplastic number kg^{-1}, scaled up from the 8 mL soil and sludge subjected to HGMS extraction whereby the average weight of the 8 mL subsamples was taken for conversion from volume to weight. Statistical t-tests were performed to determine the significance of changes in microplastic abundance, microplastic size, and carbonyl indices of polyethylene films over time (Welch et al., 1938), with a significance level of $p < 0.05$ using R (version 4.3.1).

Primer v7 (PRIMER-e) was used to generate non-metric multidimensional scaling (nMDS) plots to evaluate the similarity in microplastic communities between the different treatments and sludges across the experimental timescale and assess factors driving dissimilarly. Data was square root transformed and subjected to a Bray-Curtis dissimilarity test. The similarity matrix was then used to draw the nMDS plots. Plots with a 2D stress value of < 0.2 were considered to have a good fit of the data points. Samples (microplastic communities) were grouped by year, treatment type, and sample type (soil or sludge) and the variation in microplastic community composition assessed against environmental data using Pearson's correlation. Pearson's correlations, where r < 0.5, were overlaid on the resulting nMDS plots. Environmental data included pH, lime and fertiliser quantities (total, N, P, and K values), %CN, total and extractable metals, biomass C, and microbial respiration available from the original Hartwood sludge experiment. The same was repeated with the post-sludge application (1997-2019) soil samples only to evaluate the similarity in microplastic communities between the different treatments across the experimental timescale and assess factors driving dissimilarity in the microplastic community in these soils. In this instance, Pearson's correlations, where r < 0.3, were overlaid on the resulting nMDS plots for morphology, and Pearson's correlations, where r < 0.5, were overlaid on the resulting nMDS plots for colour.

4.3 Results and Discussion

4.3.1 Sewage sludges contain macro- and microplastics

Sludge samples were subjected to microplastic extraction without the initial Fenton's reagent digestion step. This was because there was a loss of the smaller sized microplastics (polyethylene microbeads (63-75, 106-125, and 300-355 µm) and fibres) during the digestion process (30-55% loss). Since microplastics were lost at this stage, it was deemed unfavourable to proceed with digestion prior to microplastic extractions. Crucially, microplastic extraction from sewage sludge using HGMS without the use of organic matter digestion achieved high recovery rates (>95% for all microplastic types and sizes – see Chapter 3 section 3.2.2.1 for list of all microplastics tested).

All sludges were available for assessment, except Sludge E which could not be located in freezer storage at the time of analysis. Macroplastic abundance was highest in sludge A (5882 ± 0 macroplastics kg^{-1}), and lowest in sludge B (855 ± 740 macroplastics kg^{-1}) (Table 4.2). Films were the only macroplastic found except for a mass of fibres found in sludge B. At their longest edges, films were largest in sludge C (7.0 x 8.0 mm to 4.2 x 3.6 cm), and smallest in sludge B (1.2 x 0.6 cm) (Table 4.2). Macro-sized films

pose a threat to agricultural soils as they can negatively affect plant growth and reproduction (Qi et al., 2018), alter soil structure (Yuanqiao et al., 2020), and potentially release secondary micro- and nanoplastics into the soil along with their chemical additives as they degrade.

Microplastic abundance was highest in sludge B (41880 ± 2669 microplastics kg^{-1}) and lowest in sludge C (14035 ± 1149 microplastics kg^{-1}) (Table 4A.1). These abundances are comparable to sludge microplastic abundances in other high-income countries (HICs) (i.e., 7.91 to 495,000 particles kg^{-1} of dry weight sludge) (Mahon et al., 2017; El Hayany et al., 2022; Harley-Nyang et al., 2022). Sludges in low- and middle-income countries (LMICs), however, contain much lower microplastic abundances (830 microplastics kg^{-1}), but this probably reflects the fact that most wastewater in LMICs is directly discharged into water bodies, bypassing any treatment (Kamble et al., 2019). HICs have legislations and regulations on the use and management of sewage sludge applications (Jimenez et al., 2004; Christodoulou et al., 2016). Due to financial constraints and poor enforcement of environmental legislation, sludge treatment and management is inadequate, or in some cases, non-existent in LMICs (Jimenez et al., 2004).

Table 4.2: Numbers and dimensions of macroplastic morphologies detected in the sewage sludge. The average value across the replicates is shown, while the range of the values are given in brackets, those without brackets did not have a range due to the macroplastics measuring the same size across replicates.

Sewage sludge	Total no. macroplastics kg^{-1}	Dimensions (mm)
A	5882	Film: 16.8 x 7.4 (9.0 x 0.8 - 27.0 x 22.0)
B	855 (0-1282)	Film: 12.0 x 6.0
		Fibre bundle: 8.9 dia.
C	1253 (752-1504)	Film: 26.2 x 10.3 (8.0 x 7.0 - 42.0 x 36.0)
D	3101 (2326-3488)	Film: 24.0 x 20.25 (8.0 x 5.5 - 40.0 x 35.0)

Fibres were the predominant microplastic morphology within all the sewage sludges (> 65%) (Figure 4.2A and Table 4A.1), which is consistent with previous studies (Gies et al., 2018; Li et al., 2018; van der Berg et al., 2020; Yang et al., 2021b). On average, fibre lengths were longest in sludge A (3861.33 ± 2101.65 µm) and shortest in sludge B (3121.05 ± 2237.39 µm) (Table 4A.1). White, transparent, black,

and red were the most abundant fibre colours (Figure 4.2B), which is also consistent with another study (Li et al., 2018).
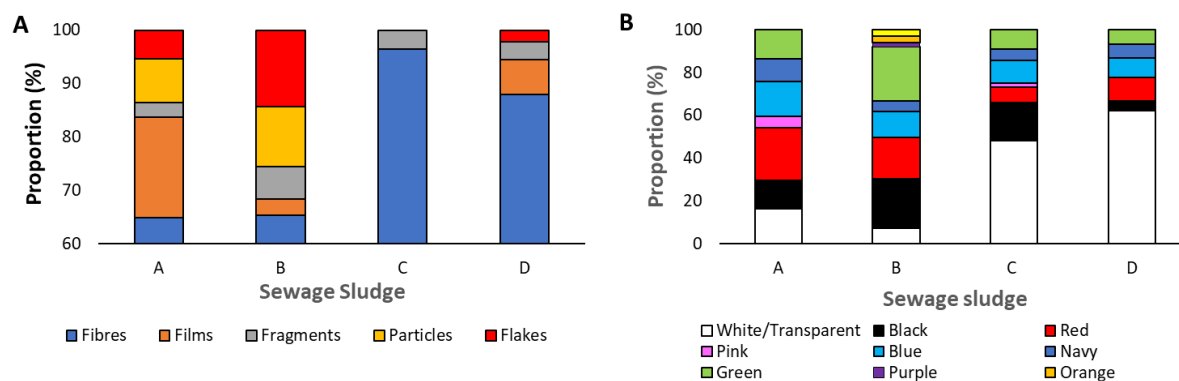
Figure 4.2: Proportions of (A) microplastic morphologies and (B) fibre colours recovered from the sewage sludges.

4.3.2 Microplastics from sewage sludges persist in soils

Microplastic abundance in soils prior to sewage sludge applications (1994) averaged 542 ± 292 microplastics kg^{-1} soil. After sludge applications (1994-1997), all plots significantly increased in microplastic abundance ($p < 0.05$) (Figure 4.3 and Table 4A.1), increasing by 3700% in the sludge E plot, 3367% in the sludge D plot, 1417% in the sludge C plot, 942% in the sludge B plot, and 1433% in the sludge A plot, indicating there was significant microplastic accumulation over the first 4 years. The differences in microplastic abundance between treatments are possibly due to the conditions of sludge production at the WWTWs because the servicing area, proportion of industrial waste and treatment processes, including secondary treatments and sludge dewatering, can affect the abundance of microplastics in sewage sludges (Harley-Nyang et al., 2022; Li et al., 2018). It may also be due to differences in sludge application rates (data not available).

The negative control plot also showed an increase in microplastic pollution by 1367% between 1994 to 1997, possibly from cross-contamination in the field from the treatment plots (Figure 4.1) through surface water runoff or atmospheric transportation or potentially from microplastics introduced by the inorganic fertiliser pellets, but this was not significant ($p > 0.05$). It is unlikely that there was much microplastic transfer between plots by the spading machine because the negative control plots were tilled before the treatment plots and the blades were cleaned between tillage of each plot. Therefore,

this demonstrates how a considerable amount of microplastics can disseminate away from the site of contamination, potentially through surface water run-off and atmospheric transportation (Allen et al., 2012; Zhang et al., 2022), to surrounding uncontaminated soil.

Overall, microplastic abundance remained relatively constant after cessation of sludge applications, with no significant change in abundance ($p > 0.05$; Figure 4.3 (A-D and negative control)), indicating that they persist in soil for over 25 years. The exception was the sludge E plot which significantly increased in abundance between 1997 and 2019 ($p < 0.05$; Figure 4.3), possibly due to the production of secondary microplastics. Fluctuations in the abundance of the different microplastic morphologies is due to the heterogenous nature of soil and the constant redistribution of microplastics from annual tillage. The relatively consistent within-treatment standard deviation in the HGMS extraction (Figure 4.3) gives confidence in the methodology and that deviations are attributed to heterogeneity within the soil.

Fibres were the dominant microplastic morphology found in all the treatment and negative control plots across all years, accounting for 81-99% (average 92%) of microplastics found (Figure 4.3). This is unsurprising given that the sewage sludges used in this study also predominantly contained fibres (see section 4.3.1). This also demonstrates that the contribution of microplastics from the inorganic fertiliser pellets was minimal. Fibres are the most abundant microplastic found in other sewage sludges (Liu et al., 2022; Yang et al., 2021b; Lares et al., 2018) and soils treated with sewage sludge (Liu et al., 2022; Yang et al., 2021b). These fibres are from clothing and textiles during commercial and industrial washing released into WWTWs (Hernandez et al., 2017). High concentrations of synthetic fibres in agricultural soils are indicative of sewage sludge applications (Piehl et al., 2018).

4.3.3 Size of microplastics decrease over time

The sizes of microplastics were assessed after the last addition of sludge (1997), halfway through the experiment (2009), and at the end of the experiment (2019) (Figure 4.4). Films were not detected in the 1997 soil samples for sludge A and sludge D plots, and particles were not detected in the sludge B-treated 1997 soil samples, therefore, the average sizes of those morphologies recovered from the respective sludges were used as time zero points instead (Figure 4.4). The size of microplastics recovered from the soil plots in the 1997 samples were not significantly different to the sizes of microplastics recovered from their respective sewage sludges (*t*-test; $p > 0.05$). Fibres displayed a wide

range in length (70-9000 μm), which all significantly decreased by the end of the experiment ($p < 0.05$) (Figure 4.4 and Table 4A.1). Fibres in the negative control plot showed no significant change in length ($p > 0.05$), possibly due to their smaller size.
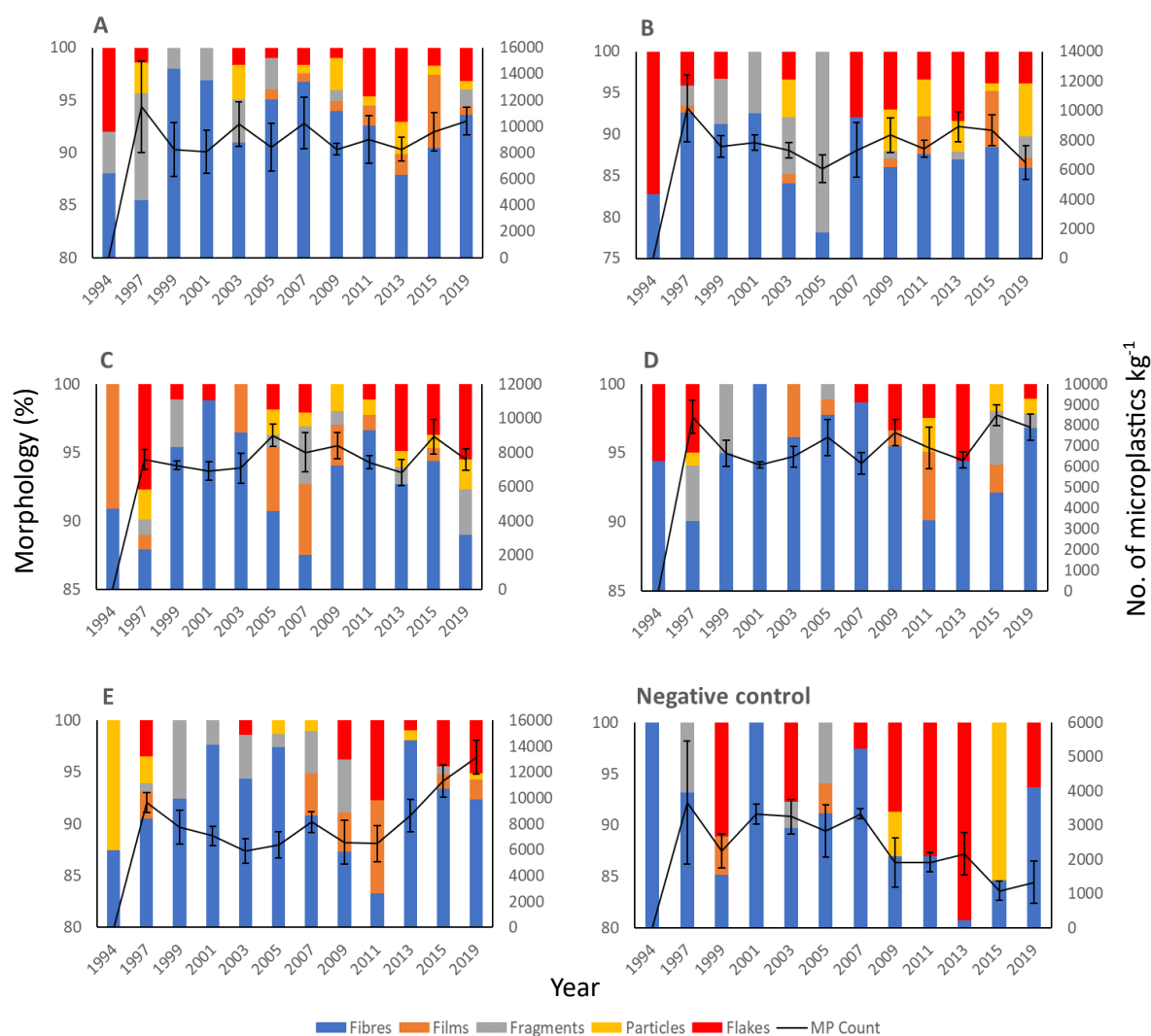
Figure 4.3: Numbers of microplastic kg⁻¹ soil over time (right axis) and proportions of microplastic morphologies over time (left axis). Graphs are labelled with their respective treatments. Error bars depict one standard deviation (n = 3).

All but one of the treatment plots (sludge C) showed a larger decrease in fibre length between 1997 and 2009 and then a smaller decrease from 2009 to 2019. This is possibly due to long fibres (approximately ≥ 3 mm) being more susceptible to mechanical fragmentation caused by tillage, and then as fibre lengths became shorter (approximately ≤ 1 mm), susceptibility to further mechanical
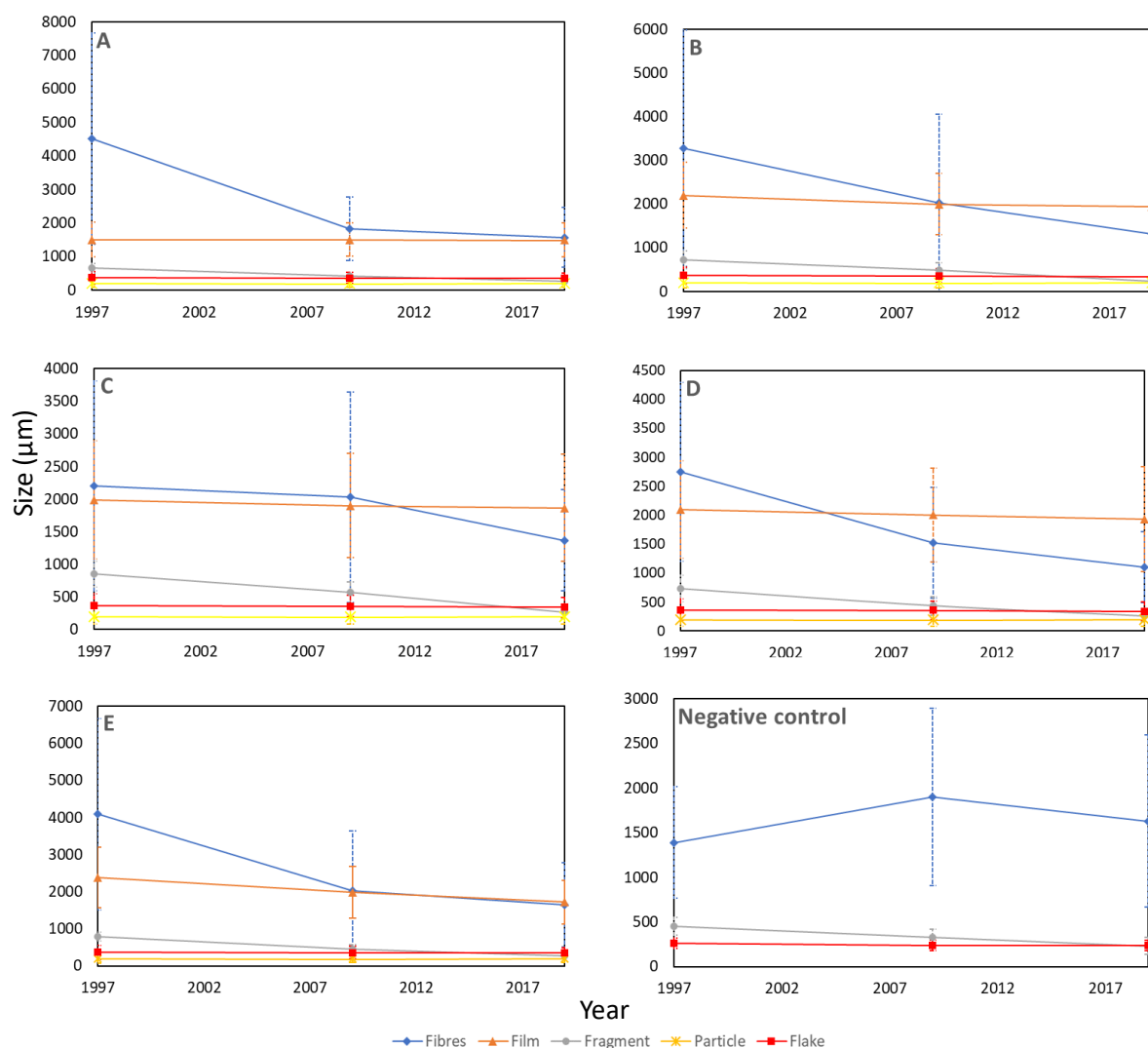
Figure 4.4: Microplastic sizes over time. Graphs are labelled with their respective treatments. Error bars depict one standard deviation (n was variable between treatments and years).

fragmentation decreased. The diameter of synthetic fibres is extremely small (13-25 μm), and they are, therefore, more susceptible to shearing. The exceptions to this trend were the fibres in the sludge C-treated and negative control plots, which might be because fibre lengths were already small (2202 ± 1604 μm and 1390 ± 625 μm, respectively). At smaller fibre lengths, further fragmentation could be through chemical weathering, which is a longer process and is dependent on soil depth, or biodegradation.

The other microplastics showed different susceptibilities to degradation. Flakes did not significantly decrease in size over time ($p > 0.05$) (Figure 4.4 and Table 4A.1), possibly because of their thick (250-

890 µm) but flexible morphology and their chemical composition. Particles remained at a constant size throughout (Figure 4.4 and Table 4A.1), possibly because of their very small sizes. Films also did not show a significant decrease in overall size ($p > 0.05$), possibly because they are thin (25-150 µm), soft, and pliable, and can easily stretch or form different shapes. However, these attributes made films susceptible to pitting, cracking, and tearing (see section 4.3.5). Fragments were the only other morphological category to significantly decrease in size over time ($p < 0.05$) because fragments are brittle.

It is possible that the reduction in microplastic size was also mediated by microbial degradation as, for example, fungi and bacteria can degrade polyethylene (Muhonja et al., 2018). However, microbial biodegradation may have been hindered in the plots treated with sludges containing the heavy metals due to metal toxicity causing cell injuries including oxidative stress, protein dysfunction or membrane damage (Lemire et al., 2013). In a previous study conducted on these Hartwood soils, biological functions were severely impaired in the sludge A- and sludge B-treated plots due to high levels of Zn and Cu, respectively (Campbell et al., 2009; Table 4.1). This suggests that microbial biodegradation of microplastics within these plots may have been hindered, contributing to microplastic persistence.

4.3.4 Microfibres potentially leach dyes

The colours of fibres were predominantly white or transparent in all treatment plots (> 67.8%) and in the control plot (61.7%), which is consistent with previous findings in soils (Figure 4.5) (Yang et al., 2021a). Several fibres were transparent with patches of blue or pink (Figure 4.6A-C). The coloured regions of the fibres were irregularly spaced along the fibres' length and were either coloured in blocks (striped) or speckled (dots), and their pigmentations were extremely faded and light in colour. By contrast, black, red, and dark blue/navy fibres had the boldest colouration (i.e., no signs of fading) (Figure 4.6D-H). The partially coloured fibres only appear in soil samples from 2001 onwards, significantly increased in 2003 ($p < 0.05$), and peaked in 2005 at 7.22 ± 0.76% (Figure 4.5). At the same time, transparent fibres increased over time in some of the treatment plots where there were slightly elevated (then decreasing) numbers of partially dyed fibres (sludge A-, B-, and E-treated soil – Figure 4.5). This may indicate that, as well as the fragmentation of white or colourless fragments giving rise to increased numbers over time, coloured fibres losing their dyes over time may contribute to the rising numbers of colourless fibres across the soil plots, indicating that these fibres had lost their dyes. Importantly, partially dyed fibres were not detected in any of the sludge samples.
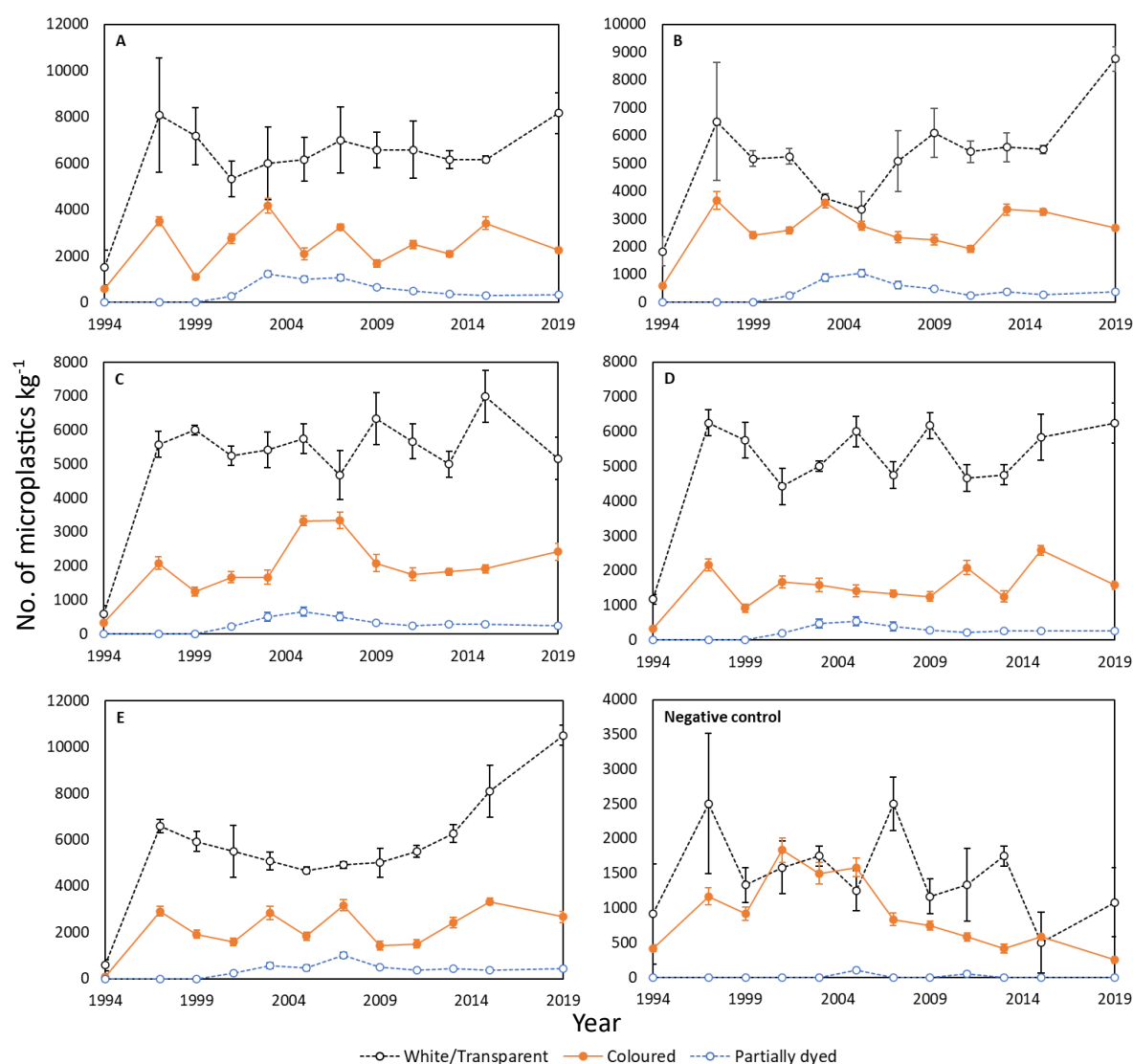
Figure 4.5: Number of microplastics by colour over time. Graphs are labelled with their respective treatments. Error bars depict one standard deviation (n = 3).

The absence of partially coloured fibres in the sewage sludges and soil samples pre-2001 suggests they were derived from coloured fibres that had been degraded and lost their dyes once in the soil. Textile dyes can persist in soils and have negative effects on soil microbial community composition and function (Imran et al., 2015; Lellis et al., 2019), and plant germination and growth (Çiçek et al., 2012). However, to the author's knowledge, there are no studies on the loss of dyes from microplastics or elucidating the effects of this dye loss on soil.
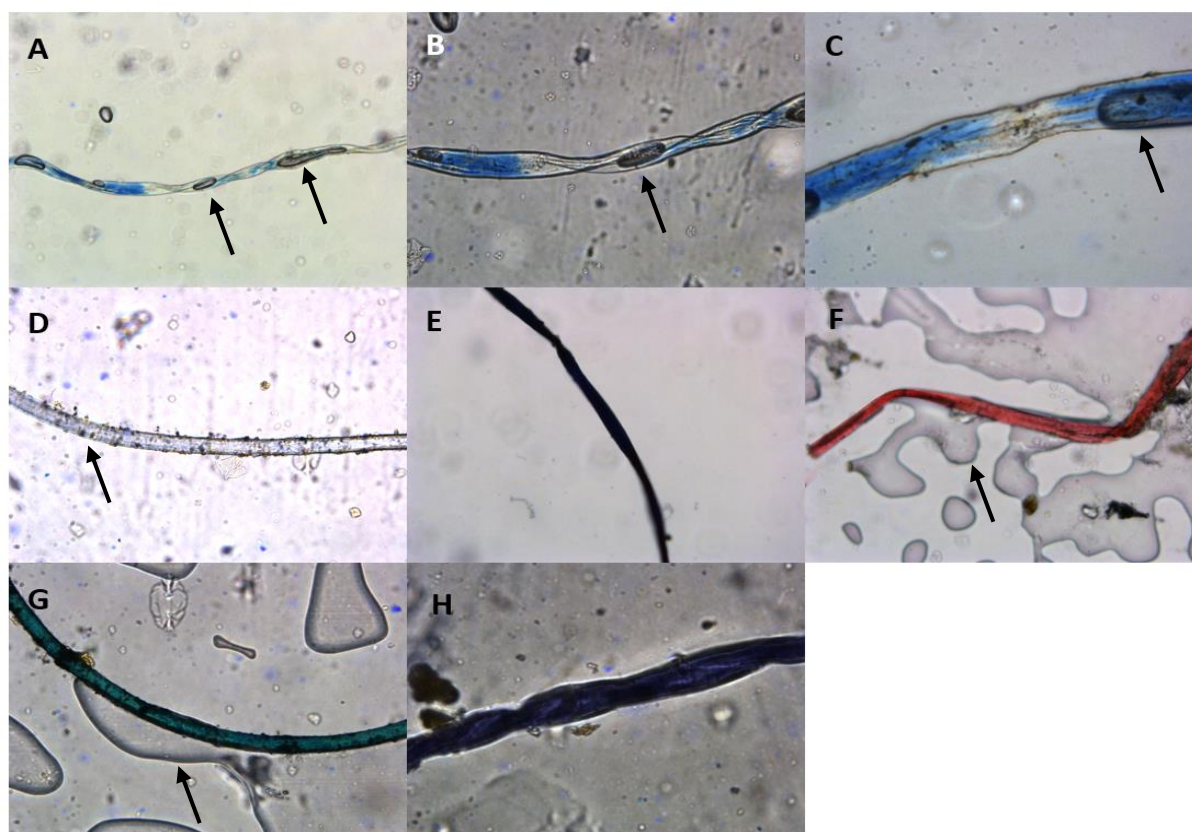
Figure 4.6: Images of (A-C) fibres that had leached their dyes, (D) a colourless, transparent fibre, and fibres where their dyes have not leached – (E) black, (F) red, (G) green, (H) and purple. Arrows indicate air bubbles trapped between the tape and the fibres.

The differences in dye loss could be due to the manufacturing and dyeing process or the molecular stability of the dye. Falk et al. (2001) attributed the loss of colour in natural fibre-thermoplastic composites over time to the susceptibility of the synthetic polymer component to UV exposure, chemical degradation, and environmental stresses such as thermal- and moisture-induced expansion. The rate of colour loss was dependent on the polymer's composition and whether any other additives were present in the polymeric fraction. Microorganisms can also biodegrade dyes, which may account for the loss of dyes (Patel et al., 2021), however, since a previous study showed that biological functions in these soils were severely impaired due to the high concentrations of heavy metals introduced through the sewage sludge (Campbell et al., 2009; Table 4.1), significant biodegradation of the dyes is unlikely. UV degradation would also be unlikely to significantly contribute to dye loss since microplastic exposure to UV light would be limited within the soil. Therefore, it is more likely that dyes leached into the surrounding soil. Further research is required to elucidate the fate of microplastic dyes in soils.

4.3.5 Micro-films weather over time

The degradation of polyethylene films (identified by FTIR) was assessed using SEM (Figure 4.7). Pristine polyethylene mulch film was obtained from a local farm and assessed in order to observe the surface of films before any degradation (Figure 4.7A). The films in soil samples after the final application of sludge (1997; n = 3) displayed little sign of ageing as they still had a smooth surface (Figure 4.7B). Over time, the surface of the films began to flake (2001; n = 1) (Figure 4.7C) before developing cracks and pitting (2005; n = 3) (Figure 4.7D). These became enlarged, forming holes or tears in the film while the edges also became more ragged (2009 and 2019; n = 2 and n = 2, respectively) (Figures 4.7E-F). The degree of degradation was visually similar across all treatment plots, therefore, it was independent of the sludge environment they originated from. Examples are displayed in Figure 4.7 (further micrographs of the other films observed are presented in Figure 4A.1).

While films were not significantly reduced in size, their surface displayed a higher degree of degradation compared to other microplastic morphologies because of their pliability and malleability (Yu et al., 2023). Films degrade faster at shallower soil depths (Huang et al., 2021), and since topsoils were used in this study, the microplastics within them would have been more susceptible to degradation. This could lead to the production of secondary micro- or nanoplastics, which have greater impacts on soil flora and fauna due to their smaller size (Pérez-Reverón et al., 2023). For example, microfilms are reported to negatively affect root biomass of plants by impeding root growth and also inhibit water flow within soils (Hu et al., 2022). Moreover, weathering changes the crystallinity, specific surface area, and oxygen functional groups, which increases sorption of other pollutants (Liu et al., 2020). The oxidation of the films' surfaces was assessed by calculating the carbonyl indices obtained from their FTIR spectra (collected before the SEM imaging process). The carbonyl index for polyethylene films recovered from the 1997 soils was 0.04 ± 0.04 (n = 3), 0.15 for 2001 (n = 1), 0.40 ± 0.15 for 2005 (n = 3), 1.28 ± 0.43, and 3.13 ± 0.86 for 2019 (n = 3). The carbonyl indices showed that oxidation increased over time, which corresponds to the visual degradation observed using SEM also increasing over time (Figure 4.7). The increase in carbonyl index observed between 1997 and 2019 was statistically significant (t-test; $p < 0.05$).
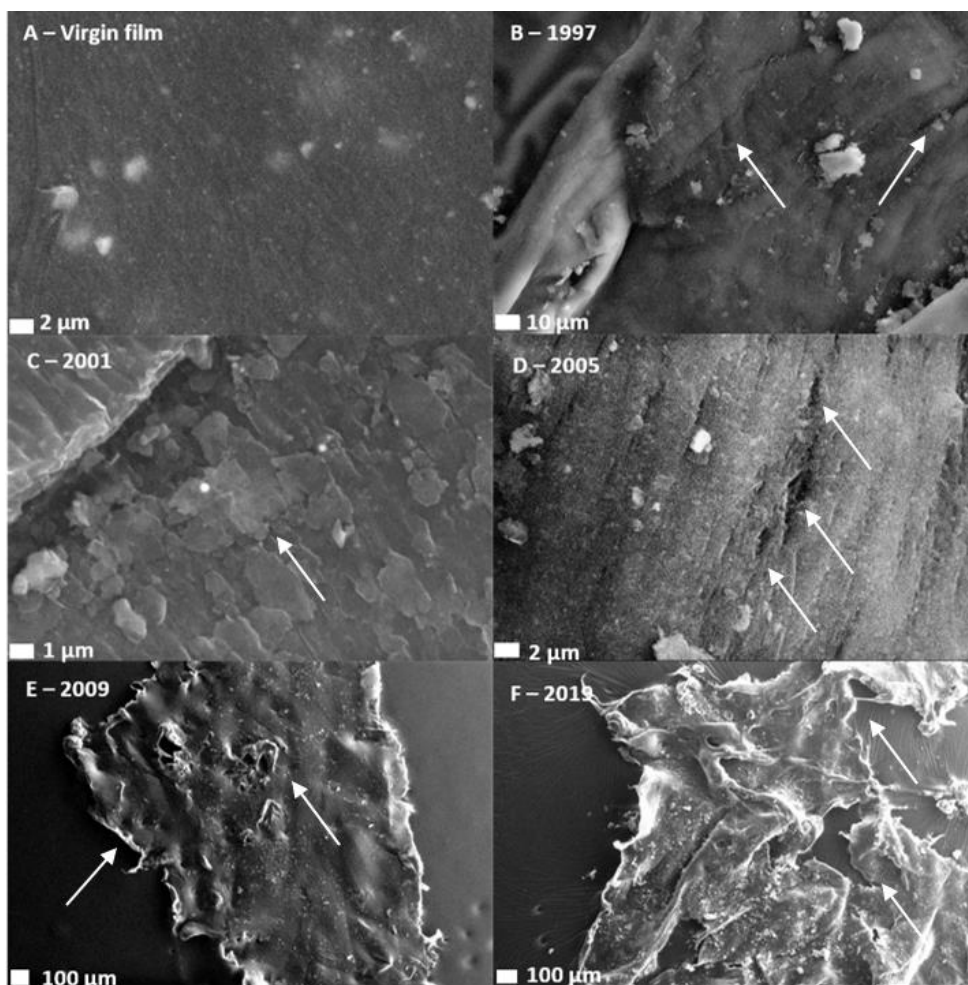
Figure 4.7: SEM micrographs of films displaying progressive weathered features. The panels show: virgin plastic film with a relatively smooth surface (A); early signs of degradation (B); surface flaking (C); cracks and pitting developing (D); holes/tears appearing with ragged edges (E-F). The panels are labelled with the year that the soil was sampled.

4.3.6 Microplastic composition can indicate source

Prior to FTIR analysis, the influence of xylene on microplastic spectra was investigated. FTIR spectra was obtained from polypropylene film at 0 s, 30 s, 1 min, and 2 min of continuous exposure to xylene (Figure 4.8). No changed occurred in the spectrum after 30 s, however, the band at ~1600 cm^{-1} showed an increase after 1 min of exposure, and a further increase after 2 min. The hydroxyl (OH) band between 3500-3000 cm^{-1} did not show any alteration until 2 min. The microplastics in this study were only exposed to xylene for a maximum of 10 s as part of the tape removal process before rinsing with Milli-Q water and air drying, therefore, the author is confident that the use of xylene to dissolve the tape adhesive did not affect the subsequent FTIR spectra generated. Furthermore, the long-established use

of this process in forensic science (Schotman and van der Weerd, 2015) also provides further confidence that this is an acceptable method to use.

Overall, the compositions of the microplastics recovered from soils corresponded to the compositions of the macro- and microplastics recovered from the sewage sludges (Table 4.3). In both the sludges and the soils, polyester was the most abundant microplastic polymer ($p < 0.05$) as this was the composition of the most abundant morphology (i.e., fibres). This is consistent with the findings of other published studies on sewage sludge and sludge-treated soils (Schell et al., 2022; El Hayany et al., 2022; Yang et al., 2021b).
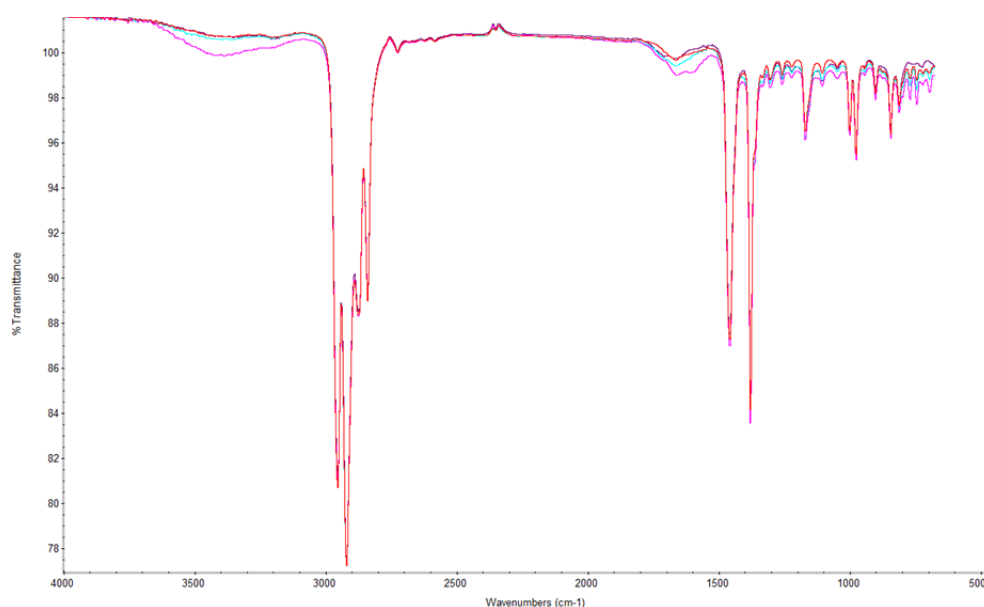
Figure 4.8: Composite FTIR spectrum of polypropylene exposed to xylene for 0 s (dark blue), 30 s (red), 1 min (light blue), and 2 min (pink).

Table 4.3: Compositions of microplastics recovered from sludge and soil samples after the application of sewage sludge.

Treatment	Microplastic composition												
	Fibres									Film	Fragment	Particle	Flake
	White and transparent	Black	Red	Pink	Blue	Navy	Green	Purple	Yellow				
A (sludge)	Polyester, PU	Acrylic	Polyester	Acrylic	Polyester	Polyester	PVC, Acrylic	-	-	PP, PVC	PE	PS, PE, PP	PET
A (soil)	Polyester, PU	Acrylic	Polyester, Acrylic	Acrylic	Polyester	Polyester	PVC	-	Polyester	PVC	PE	PS, PE	PET, PE
B (sludge)	Polyester	Acrylic, Nylon	Acrylic	-	Polyester	Polyester, Acrylic	Polyester, Acrylic	Acrylic	Nylon	PU	PMMA, PTFE	PMMA, PE	PMMA, PET
B (soil)	Polyester	Nylon	Acrylic	-	Polyester	Polyester	Polyester, Acrylic	Acrylic	Nylon	PU	PMMA, PTFE, PET	-	PMMA, PTFE, PET
C (sludge)	Polyester	Acrylic	Polyester, Acrylic	Acrylic	Polyester	Nylon	Polyester	-	-	-	PU	PS	PET
C (soil)	Polyester, PP	Acrylic	Polyester	Acrylic	Polyester, Acrylic	Nylon	Polyester, Acrylic	-	Nylon	PP	PU, PE	PS	PET
D (sludge)	Polyester	Acrylic	Acrylic	-	Polyester, Acrylic	Polyester, Acrylic	PVC	-	-	PE, PP	PTFE, PP	PE, PP	PET
D (soil)	Polyester	Acrylic	Acrylic	-	Polyester	Polyester	PVC	-	-	PE	PTFE	PE	PET
E (soil)	Polyester	Acrylic	Acrylic	Polyester	Acrylic	Nylon	PVC	-	Nylon	PE	-	PP, PE	PET, PE
Negative Control	Polyester	-	-	-	PE	-	Polyester	-	-	-	-	-	-

PU – polyurethane; PVC – polyvinyl chloride; PE – polyethylene; PP – polypropylene; PET – polyethylene terephthalate; PS – polystyrene; PMMA – polymethyl methacrylate; PTFE – polytetrafluoroethylene.
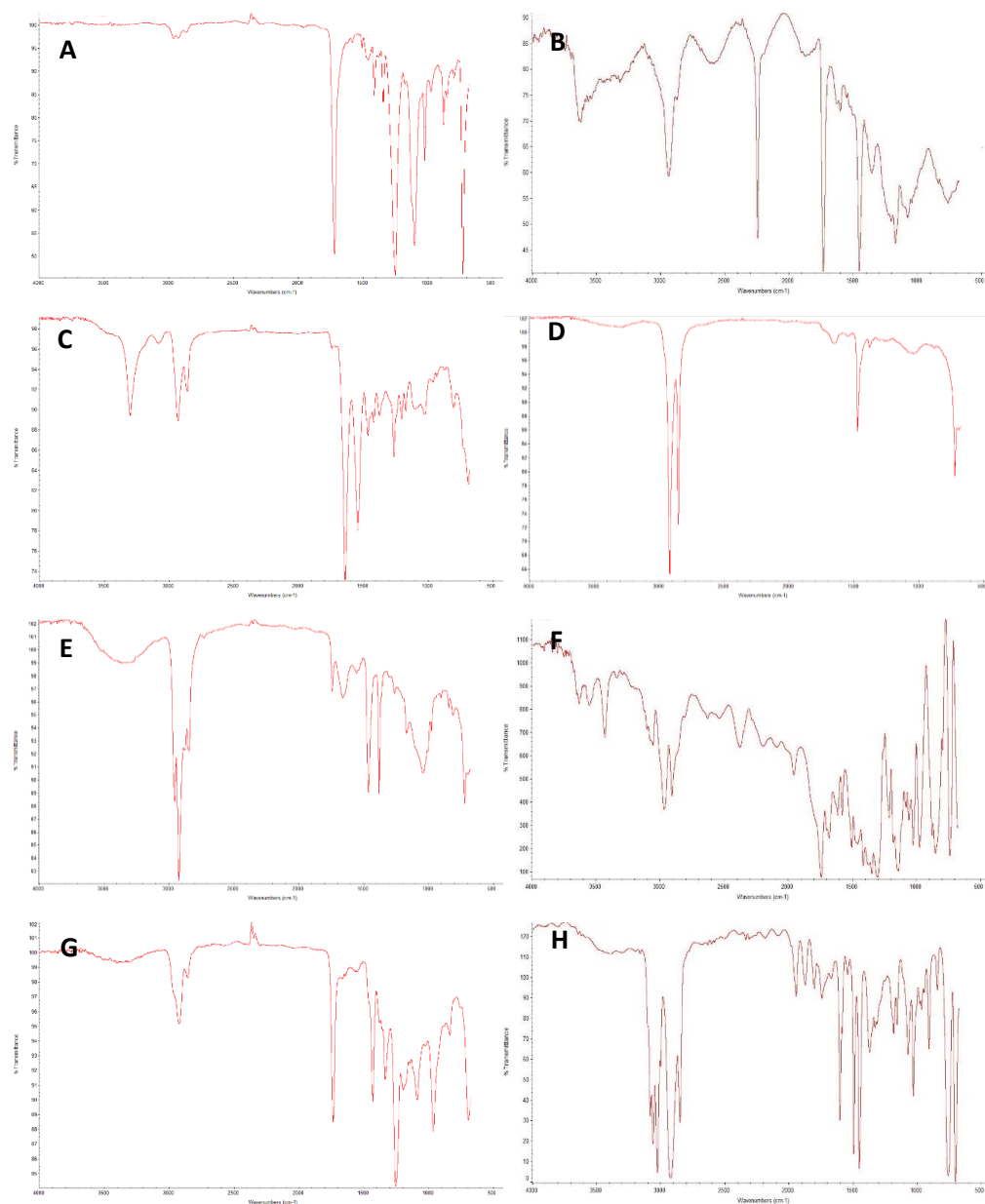
Figure 4.9: FTIR spectra of individual microplastics recovered from soil samples including: (A) polyester fibre, (B) acrylic fibre, (C) nylon fibre, (D) polyethylene film, (E) polypropylene fragment, (F) polyethylene terephthalate flake, (G) polyvinyl chloride film, and (H) polystyrene particle.
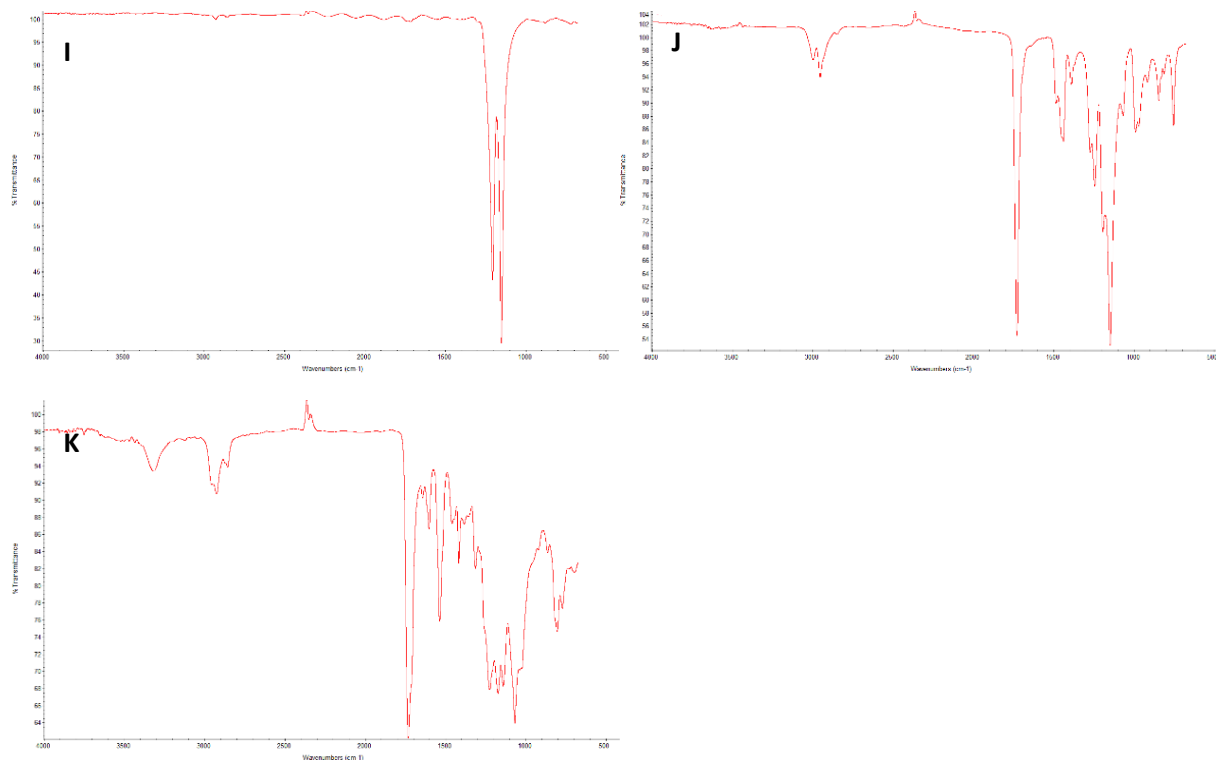
Figure 4.9 continued: FTIR spectra of individual microplastics recovered from soil samples including: (I) polytetrafluoroethylene fragment, (J) polymethyl methacrylate fragment, and (K) polyurethane fragment.

Of the five sludge treatments, rarely observed high-density microplastics (e.g., polymethyl methacrylate, polyurethane) were only identified in sludges A, B, and C, and their relative soil plots. These sludges originated from WWTWs servicing industrial wastes (Table 4.1), and the presence of these plastics indicates that the sludges they originated from are from industrial waste. Polyester and polyurethane fibres, which are commonly seen as co-polymers, are used as base materials in upholstery furnishings (Tables 4.1 and 4.3), specifically faux leather, were found in sludge A and its relative soil plot. Polymethyl methacrylate and polytetrafluoroethylene fragments, which are both commonly used polymers in electrical appliances (Tables 4.1 and 4.3), were identified in sludge B and its relative soil plot. Sludges A and B are known to originate from WWTWs servicing wastewater from the tannery and electronics industries, respectively (Tables 4.1 and 4.3). It is unknown where the waste in sludge C originated from. However, polyurethane was identified in sludge C and its relative soil plot, which strongly indicates that the WWTW which this sludge originated also from potentially served an industrial location (hence its high metal concentration (Table 4.1)). Sludges D and E, and their relative soil plots, did not contain any high-density or rarely observed polymers indicating that the associated

WWTWs served household waste rather than industrial waste (hence, the low metal concentrations (Table 4.1)). These results demonstrate that determination of the composition of microplastics in the environment is a useful tool for tracing potential sources of microplastic pollution. Exemplar FTIR spectra are presented in Figure 4.9.

4.3.7 Microplastic community varied in soil plots between control, sludges, and pre- and post-sludge applications

Non-metric multidimensional scaling (nMDS) plots were generated to evaluate the significance of patterns of microplastic communities within soil and sludge samples (Figure 4.10). The plots indicated that the microplastic community within samples from the control soil, soils before sludge applications (1994), all soil samples post-application (1997-2019), and the sludges were similar within each of these groupings (indicated by clustering which were circled manually and labelled in Figure 4.10). The control soils and 1994 untreated soils formed one cluster to the left of the plot. These points likely clustered together as their microplastic communities remained relatively unchanged throughout the experiment as microplastics were not introduced directly to these soils through sewage sludge additions. Sludges formed a distinct cluster to the right of the plot indicating the microplastic communities in the sludges were distinctly different to the control and 1994 soil samples. The third distinct cluster was formed by the 1997-2019 treated soil samples. This cluster appeared directly in between the sludge cluster and the control and 1994 soils cluster indicating the microplastic communities of the control and 1994 soil cluster and the sludge cluster were merged and mixed. These plots had 2D stress values of 0.12 and 0.11 for colour (Figure 4.10A) and morphology (Figure 4.10B), respectively, providing confidence in the fit of the data points in the plots. Total Mn, Cu, and Pb and most probable number per g, and total Mn, Cu, and Pb and %N, were found to significantly influence variation in microplastic community by colour (Figure 4.10A) and morphology (Figure 4.10B), respectively. These metals were likely significant in the nMDS plots as a reflection of the difference in the sludges added to the soils (i.e., each sludge contained high levels of selected heavy metals and different microplastic communities) and each of these respective sludges likely influence the microplastic community in the soil. The addition of these sewage sludges also influenced the %N levels in the soil and most probable number per g, again reflecting the addition of sewage sludge influencing the microplastic community.

The soils post-sludge application (1997-2019) were investigated separately (Figure 4.11). The disparity and spread of the samples in the plots indicated that the microplastic communities between each of

the sludge treatments were similar to one another, i.e., no separation or clustering of treatments and a high 2D stress value of 0.25 and 0.23 by colour (Figure 4.11A) and morphology (Figure 4.11B), respectively. This is likely because soils treated with sludges A and C, and sludge B, were supplemented with sludges D and E, respectively, meaning there was mixing of each of the sludges' microplastic communities during their applications to the soil plots.
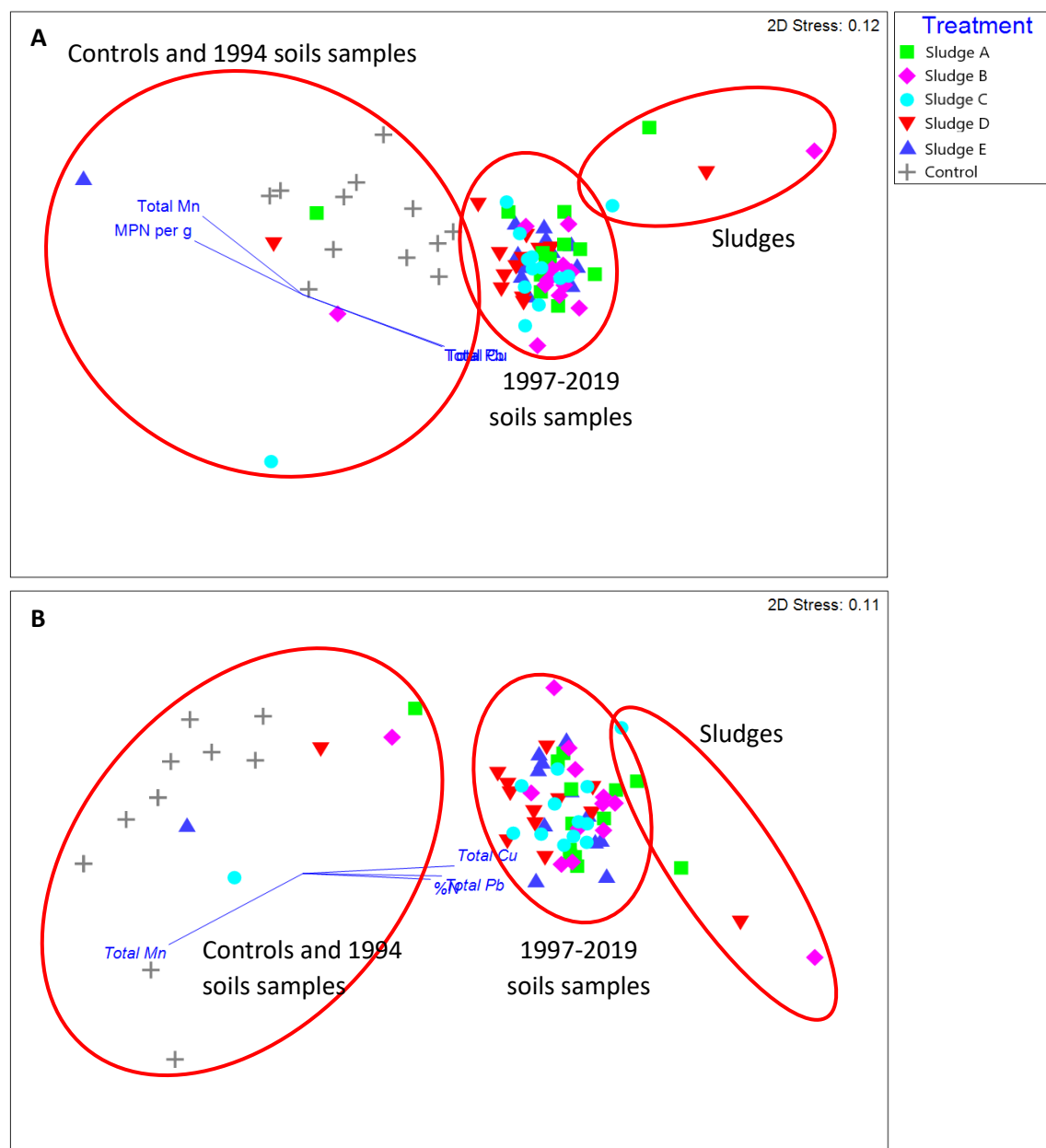
Figure 4.10: Non-metric multidimensional scaling plot (nMDS) of the microplastic communities within in all soil and sludge samples by (A) colour and (B) morphology with Pearson's correlations (r < 0.5) overlaid (total Mn, Cu, and Pb, most probable number per g, and %N). Data were square root transformed. Clusters are encircled in red (added manually) and annotated.
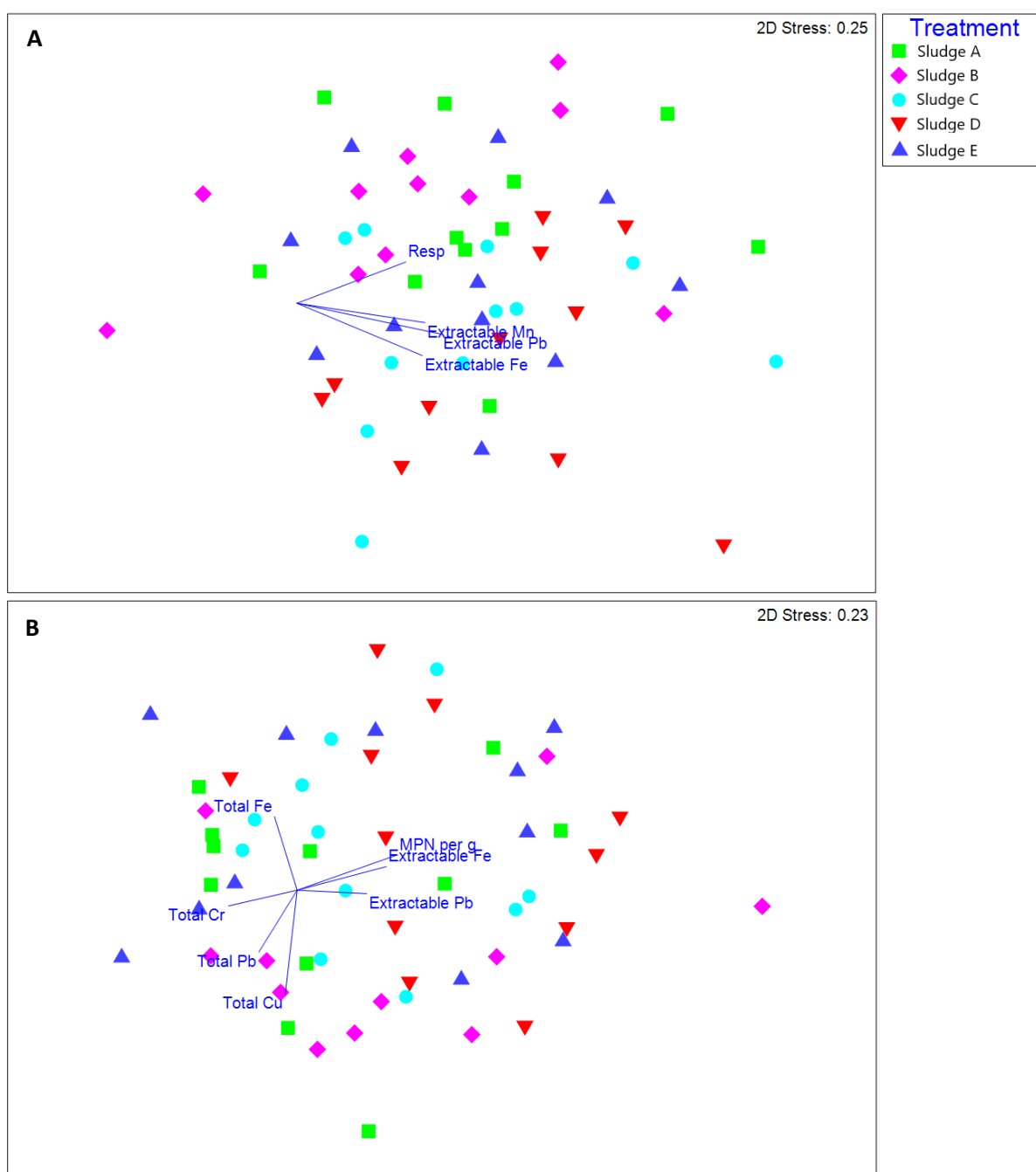
Figure 4.11: Non-metric multidimensional scaling (nMDS) plot of the microplastic communities within 1997-2019 soil samples by (A) colour and (B) morphology with Pearson's correlations (r > 0.3) overlaid (extractable Fe and Pb, biomass C, and %N). Data were square root transformed.

4.3.8 Limitations

Due to the experimental design of the original long-term sewage sludge experiment at Hartwood, the various treatment plots (sludges containing high concentrations of the three metals, respectively) were

supplemented with "uncontaminated" sludges to maintain constant carbon levels throughout the experiment (see Gibbs et al. (2006) for details on the experimental design). Because of this, it could not be explored in this study whether the fate of microplastics may differ under different soil conditions resulting from the sludge applications or which sludges may have contributed the highest number of microplastics. Similarly, establishing a mass balance was not possible because of the mixing of sludges but also because sludge E was not available for analysis.

Data analyses of microplastic abundance was conducted using three replicates and data was variable throughout. This is commonly observed due to the heterogeneity of microplastics in soils. Furthermore, the plots were rotavated annually meaning microplastics were continually redistributed throughout the plots potentially leading to some years of higher heterogeneity. The archived samples were mixed thoroughly prior to subsampling for this study to minimise this impact.

The sizes of microplastics were only monitored at three time periods, however, a high n value (> 70 per each treatment) was utilised for data analysis (see section 4.2.3), therefore, the author is confident in the use of these statistics for the purposes of this chapter. However, the number of replicates of microfilms that were observed under SEM was small (1-3 replicates) and varied between years and treatments. Further work would need to be done to further elucidate the degradation of microfilms and confirm the findings of this study.

Nonetheless, this is the first study to generate high temporal resolution data on the accumulation, persistence, and degradation of microplastics in soils over a substantial period of time. Other studies have only been able to look retrospectively at soils historically treated with sewage sludges (or mulching film) to confirm their presence but have not been able to offer information other than what microplastics are present and the state of their degradation through spectral and microscopic analyses (e.g., van der Berg et al., 2020; Yang et al., 2021b). Therefore, the work presented in this chapter will provide an exceptional contribution to the understanding of the fate of microplastics in soils over time.

4.4 Conclusions

To the author's knowledge, this study is the first to provide long-term data (25 years) on microplastics in agricultural soils following sewage sludge application in high temporal resolution. Quantitative data

showed that sewage sludge is a huge source and significant pathway of microplastics into soils, and that microplastics accumulate and persist at relatively constant levels across 25 years, and possibly beyond. Fibres, fragments, and films are more susceptible to degradation than other microplastic morphologies, and can release further micro- and nanoplastics into soil. Dye loss from fibres was evident, although, the fate of these dyes is unknown. Given the environmental toxicity of some dyes, this may be of concern and warrants further investigation. Furthermore, determining the composition of microplastics is a useful tool in tracing potential sources of the microplastics. For example, the presence of rarely observed high-density microplastics such as polymethyl methacrylate and polyurethane could be linked to industrial waste rather than typical municipal waste.

The findings of this study raise questions of the potential impact of the microplastics, secondary nanoplastics, and fibre dyes on soil ecosystem function, and whether these contaminants are able to be transported away from the site of contamination, leading to further effects in other locations. Of interest is the potential for these microplastics to act as vectors for other pollutants present in sewage sludge (e.g., organic pollutants, pathogens, and heavy metals), causing further effects on soil ecosystem functions (see Chapters 6 and 7), and potentially animal and human health. This study demonstrates that sewage sludge applications create long-term hot-spots of increased microplastic abundance, which have not yet been included in regulatory standards on sewage sludge use and management.

4.5 References

Allen S., Allen D., Phoenix V.R., Le Roux G., Jiménez P.D., Simonneau A., Binet S., Galop D. Atmospheric transport and deposition of microplastics in a remote mountain catchment. *Nature Geoscience*. 2012; 12, 339-344. DOI: https://doi.org/10.1038/s41561-019-0335-5

Bayo J., Olmos S., López-Castellanos J. Microplastics in an urban wastewater treatment plant: The influence of physicochemical parameters and environmental factors. *Chemosphere*. 2020; 238, 124593. DOI: https://doi.org/10.1016/j.chemosphere.2019.124593

Bonyadinejad G., Salehi M., Herath A. Investigating the sustainability of agricultural plastic products, combined influence of polymer characteristics and environmental conditions on microplastics aging. *Science of the Total Environment*. 2022; 15, 156385. DOI: https://doi.org/10.1016/j.scitotenv.2022.156385

Campbell C.D., Cooper P., Crooks W., Sinclair A., White D. 2009, *Impact of long term sludge additions to biological function in Scottish soils*, CR/2008/03, Scottish Government, Edinburgh.

Carr S.A., Lin J., Tesoro A.G. Transport and fate of microplastic particles in wastewater treatment plants. *Water Research*. 2016; 91, 174-182. DOI: https://doi.org/10.1016/j.watres.2016.01.002

Christodoulou A., Stamatelatou K. Overview of legislation on sewage sludge management in developed countries worldwide. *Water Science and Technology*. 2016; 73, 453-462. DOI: https://doi.org/10.2166/wst.2015.521

Çiçek N., Efeoğlu B., Tanyolaç D., Ekmekci Y., Strasser R.J. Growth and photochemical responses of three crop species treated with textile azo dyes. *Turkish Journal of Botany*. 2012; 36, 529-537. DOI: https://doi.org/10.3906/bot-1109-6

Corradini F., Meza P., Eguiluz R., Casado F., Huerta-Lwanga E., Geissen V. Evidence of microplastic accumulation in agricultural soils from sewage sludge disposal. *Science of The Total Environment*. 2019; 671, 411-420. DOI: https://doi.org/10.1016/j.scitotenv.2019.03.368

Duan J., Bolan N., Li Y., Ding S., Atugoda T., Vithanage M., Sarkar B., Tsang D.C.W., Kirkham M.B. Weathering of microplastics and interaction with other coexisting constituents in terrestrial and aquatic environments. *Water Research*. 2021; 1996, 117011. DOI: https://doi.org/10.1016/j.watres.2021.117011

Dris R., Gasperi J., Rocher V., Tassin B. Synthetic and non-synthetic anthropogenic fibers in a river under the impact of Paris megacity: sampling methodological aspects and flux estimations. *Science of the Total Environment*. 2018; 618, 157–164. DOI: https://doi.org/10.1016/j.scitotenv.2017.11.009

El Hayany B., Rumpel C., Hafidi M., El Fels L. Occurrence, analysis of microplastics in sewage sludge and their fate during composting: A literature review. *Journal of Environmental Management*. 2022; 317, 115364. DOI: https://doi.org/10.1016/j.jenvman.2022.115364

Elmi A., Al-Khaldy A., AlOlayan M. Sewage sludge land application: Balancing act between agronomic benefits and environmental concerns. *Journal of Cleaner Production*. 2020; 250, 119512. DOI: https://doi.org/10.1016/j.jclepro.2019.119512

Falk R.H., Felton C.C., & Lundin T. Effects of weathering on color loss of natural fiber thermoplastic composites. *Natural Polymers and Composites*. 2001; 382-385.

Fernández-González V., Andrade-Garda J.M., López-Mahía P., Muniategui-Lorenzo S. Impact of weathering on the chemical identification of microplastics from usual packaging polymers in the marine

environment. *Analytica Chimica Acta*. 2021; 1142, 179-188. DOI: https://doi.org/10.1016/j.aca.2020.11.002

Gibbs P.A., Chambers B.J., Chaudri A.M., McGrath S.P., Carlton-Smith C.H., Bacon J.R., Campbell C.D., Aitken M.N. Initial results from a long-term, multi-site field study of the effects on soil fertility and microbial activity of sludge cakes containing heavy metals. *Soil Use and Management*. 2006; 22, 11-21. DOI: https://doi.org/10.1111/j.1475-2743.2006.00003.x

Gies E.A., LeNoble J.L., Noël M., Etemadifar A., Bishay F., Hall E.R., Ross P.S. Retention of microplastics in a major secondary wastewater treatment plant in Vancouver, Canada. *Marine Pollution Bulletin*. 2018; 133, 553-561. DOI: https://doi.org/10.1016/j.marpolbul.2018.06.006

Harley-Nyang D., Memon F.A., Jones N., Galloway T. Investigation and analysis of microplastics in sewage sludge and biosolids: A case study from one wastewater treatment works in the UK. *Science of The Total Environment*. 2022; 823, 153735. DOI: https://doi.org/10.1016/j.scitotenv.2022.153735

Hernandez E., Nowack B., Mitrano D.M. Polyester Textiles as a Source of Microplastics from Households: A Mechanistic Study to Understand Microfiber Release During Washing. *Environmental Science and Technology*. 2017; 51, 7036-7046. DOI: http://dx.doi.org/10.1021/acs.est.7b01750

Hu J., He D., Zhang X., Li X., Chen Y., Gao W., Zhang Y., Ok Y.S., Luo Y. National-scale distribution of micro(meso)plastics in farmland soils across China: Implications for environmental impacts. *Journal of Hazardous Materials*. 2022; 424, 127283. DOI: https://doi.org/10.1016/j.jhazmat.2021.127283

Huang D., Xu Y., Lei F., Yu X., Ouyang Z., Chen Y., Jia h., Guo X. Degradation of polyethylene plastic in soil and effects on microbial community composition. *Journal of Hazardous Materials*. 2021; 416, 126173. DOI: https://doi.org/10.1016/j.jhazmat.2021.126173

Huerta Lwanga E., Gertsen H., Gooren H., Peters P., Salánki T., van der Ploeg M., Besseling E., Koelmans A.A., Geissen V. Incorporation of microplastics from litter into burrows of *Lumbricus terrestris*. *Environmental Pollution*. 2017; 220, 523-531. DOI: https://doi.org/10.1016/j.envpol.2016.09.096

Imran M., Shaharoona B., Crowley D.E. Khalid A., Hussain S., Arshad M. The stability of textile azo dyes in soil and their impact on microbial phospholipid fatty acid profiles. *Ecotoxicology and Environmental Safety*. 2015; 120, 163-168. DOI: https://doi.org/10.1016/j.ecoenv.2015.06.004

Jimenez B., Barrios J.A., Mendez J.M., Diaz J. Sustainable sludge management in developing countries. *Water Science and Technology*. 2004; 49, 251–258. DOI: https://doi.org/10.2166/wst.2004.0656

Kamble S., Singh A., Kazmi A., Starkl M. Environmental and economic performance evaluation of municipal wastewater treatment plants in India: a life cycle approach. *Water Science & Technology*. 2019; 79, 1102-1112. DOI: https://doi.org/10.2166/wst.2019.110

Lares M., Ncibi M.C., Sillanpää M., Sillanpää M. Occurrence, identification and removal of microplastic particles and fibers in conventional activated sludge process and advanced MBR technology. *Water Research*. 2018; 133, 236-246. DOI: https://doi.org/10.1016/j.watres.2018.01.049

Lellis B., Fávaro-Polonio C.Z., Pamphile J.A., Polonio J.C. Effects of textile dyes on health and the environment and bioremediation potential of living organisms. *Biotechnology Research and Innovation*. 2019; 3, 275-290. DOI: https://doi.org/10.1016/j.biori.2019.09.001

Lemire, J., Harrison, J. & Turner, R. Antimicrobial activity of metals: mechanisms, molecular targets and applications. *Nature Reviews Microbiology*. 2013; 11, 371–384. DOI: https://doi.org/10.1038/nrmicro3028

Li X., Chen L., Mei Q., Dong B., Dai X., Ding G., Zeng E.Y. Microplastics in sewage sludge from the wastewater treatment plants in China. *Water Research*. 2018; 142, 75-85. DOI: https://doi.org/10.1016/j.watres.2018.05.034

Liu P., Zhan X., Wu X., Li J., Wang H., Gao S. Effect of weathering on environmental behavior of microplastics: Properties, sorption and potential risks. *Chemosphere*. 2020; 242, 125193. DOI: https://doi.org/10.1016/j.chemosphere.2019.125193

Liu Z., Bai Y., Ma T., Liu X., Wei H., Meng H., Fu Y., Ma Z., Zhang L., Zhao J. Distribution and possible sources of atmospheric microplastic deposition in a valley basin city (Lanzhou, China). *Ecotoxicology and Environmental Safety*. 2022; 233, 113353. DOI: https://doi.org/10.1016/j.ecoenv.2022.113353

Maaß S., Daphi D., Lehmann A., Rillig M.C. Transport of microplastics by two collembolan species. *Environmental Pollution*. 2017; 225, 456-459. DOI: https://doi.org/10.1016/j.envpol.2017.03.009

Mahon A.M., O'Connell B., Healy M.G., O'Connor I., Officer R., Nash R., Morrison L. Microplastics in Sewage Sludge: Effects of Treatment. *Environmental Science and Technology*. 2017; 51, 810-818. DOI: https://doi.org/10.1021/acs.est.6b04048

Muhonja C.N., Makonde H., Magoma G., Imbuga M. Biodegradability of polyethylene by bacteria and fungi from Dandora dumpsite Nairobi-Kenya. *PLoS ONE*. 2018; 13, e0198446. DOI: www.doi.org/10.1371/journal.pone.0198446

Murphy F., Ewins C., Carbonnier F., Quinn B. Wastewater Treatment Works (WwTW) as a Source of Microplastics in the Aquatic Environment. *Environmental Science and Technology*. 2016; 50, 5800-5808. DOI: https://doi.org/10.1021/acs.est.5b05416

O'Connor D., Pan S., Shen Z., Song Y., Jin Y., Wu W.-M., Hou D. Microplastics undergo accelerated vertical migration in sand soil due to small size and wet-dry cycles. *Environmental Pollution*. 2019; 249, 527-534. DOI: https://doi.org/10.1016/j.envpol.2019.03.092

Patel Y., Chhaya U., Rudakiya D.M., Joshi S. (2021). Biological Decolorization and Degradation of Synthetic Dyes: A Green Step Toward Sustainable Environment. In: Panpatte, D.G., Jhala, Y.K. (eds) Microbial Rejuvenation of Polluted Environment. Microorganisms for Sustainability, vol 26. Springer, Singapore. https://doi.org/10.1007/978-981-15-7455-9_4

Pérez-Reverón R., Álvarez-Méndez S.J., González-Sálamo J., Socas-Hernández C., Díaz-Peña F.J., Hernández-Sánchez C., Hernández-Borges J. Nanoplastics in the soil environment: Analytical methods, occurrence, fate and ecological implications. *Environmental Pollution*. 2023; 317, 120788. DOI: https://doi.org/10.1016/j.envpol.2022.120788

Phan S., Padilla-Gamiño J.L., Luscombe C.K. The effect of weathering environments on microplastic chemical identification with Raman and IR spectroscopy: Part I. polyethylene and polypropylene. Polymer Testing. 2022; 116, 107752. DOI: https://doi.org/10.1016/j.polymertesting.2022.107752

Piehl S., Leibner A., Löder M.G.J., Dris R., Bogner C, Laforsch C. Identification and quantification of macro- and microplastics on an agricultural farmland. *Scientific Reports*. 2018; 8, 17950. DOI: https://doi.org/10.1038/s41598-018-36172-y

Qi Y., Yang X., Pelaez A.M., Huerta Lwanga E., Beriot N., Gertsen H., Garbeva P., Geissen V. Macro- and micro- plastics in soil-plant system: Effects of plastic mulch film residues on wheat (*Triticum aestivum*) growth. *Science of the Total Environment*. 2018; 645, 1048-1056. DOI: https://doi.org/10.1016/j.scitotenv.2018.07.229

Ramage S.J.F.F., Pagaling E., Haghi R.K., Dawson L.A., Yates K., Prabhu R., Hillier S., Devalla S. Rapid extraction of high- and low-density microplastics from soil using high-gradient magnetic separation. *Science of the Total Environment*. 2022; 831, 154912. DOI: https://doi.org/10.1016/j.scitotenv.2022.154912

Rillig M., Ingraffia R., de Souza Machado A.A. Microplastic Incorporation into Soil in Agroecosystems. *Frontiers in Plant Science*. 2017a; 8, 1805. DOI: https://doi.org/10.3389/fpls.2017.01805

Rillig M.C., Ziersch L., Hempel S. Microplastic transport in soil by earthworms. *Scientific Reports*. 2017b; 7, 1362. DOI: https://doi.org/10.1038/s41598-017-01594-7

Rochman C.M. *et al*. Rethinking microplastics as a diverse contaminant suite. *Environmental Toxicity and Chemistry*. 2019; 38, 703-711. DOI: https://doi.org/10.1002/etc.4371

Schell T., Hurley R., Buenaventura N.T., Mauri P.V., Nizzetto L., Rico A., Vighi M. Fate of microplastics in agricultural soils amended with sewage sludge: Is surface water runoff a relevant environmental pathway? *Environmental Pollution*. 2022; 293, 118520. DOI: https://doi.org/10.1016/j.envpol.2021.118520

Schotman T.G., van der Weerd J. On the recovery of fibres by tape lifts, tape scanning, and manual isolation. *Science & Justice*. 2015; 55, 415-421. DOI: https://doi.org/10.1016/j.scijus.2015.05.007

van den Berg P., Huerta-Lwanga E., Corradini F., Geissen V. Sewage sludge application as a vehicle for microplastics in eastern Spanish agricultural soils. *Environmental Pollution*. 2020; 261, 114198. DOI: https://doi.org/10.1016/j.envpol.2020.114198

Welch B.L. The significance of the difference between two means when the population variances are unequal. *Biometrika*. 1938; 29, 350-362. DOI: https://doi.org/10.1093/biomet/29.3-4.350

Xu B., Liu F., Cryder Z., Huang D., Lu Z., He Y., Wang H., Lu Z., Brookes P.C., Tang C., Gan J., Xu J. Microplastics in the soil environment: Occurrence, risks, interactions and fate – A review. *Critical Reviews in Environmental Science and Technology*. 2020; 50, 2175-2222. DOI: https://doi.org/10.1080/10643389.2019.1694822

Yang J., Zhang S., Kang S., Wang Z., Wu C. Microplastics in soil: A review on methods, occurrence, sources, and potential risk. *Science of the Total Environment*. 2021a; 780, 146546. DOI: https://doi.org/10.1016/j.scitotenv.2021.146546

Yang J., Li L., Li R., Xu L., Shen Y., Li S., Tu C., Wu L., Christie P., Luo Y. Microplastics in an agricultural soil following repeated application of three types of sewage sludge: A field study. *Environmental Pollution*. 2021b; 289, 117943. DOI: https://doi.org/10.1016/j.envpol.2021.117943

Yu Y., Zhang Z., Zhang Y., Jia H., Li Y., Yao H. Abundances of agricultural microplastics and their contribution to the soil organic carbon pool in plastic film mulching fields of Xinjiang, China. *Chemosphere*. 2023; 316, 137837. DOI: https://doi.org/10.1016/j.chemosphere.2023.137837

Yuanqiao L., Caixia Z., Changrong Y., Lili M., Qi L., Zhen L., Wenqing H. Effects of agricultural plastic film residues on transportation and distribution of water and nitrate in soil. *Chemosphere*. 2020; 242, 125131. DOI: https://doi.org/10.1016/j.chemosphere.2019.125131

Zhang Z., Wu X., Zhang J. Huang X. Distribution and migration characteristics of microplastics in farmland soils, surface water and sediments in Caohai Lake, southwestern plateau of China. *Journal of Cleaner Production*. 2022b; 366, 132912. DOI: https://doi.org/10.1016/j.jclepro.2022.132912

Zhao Z.-Y., Wang P.-Y., Wang Y.-B., Zhou R., Koshei K., Munyasya A.N., Liu S.-T., Wang W., Su Y.-Z., Xiong Y.-C. Fate of plastic film residues in agro-ecosystem and its effects on aggregate-associated soil carbon and nitrogen stocks. *Journal of Hazardous Materials*. 2021; 416, 125954. DOI: https://doi.org/10.1016/j.jhazmat.2021.125954

Zvekic M., Richards L.C., Tong C.C., Krogh E.T. Characterizing photochemical ageing processes of microplastic materials using multivariate analysis of infrared spectra. *Environmental Science: Processes Impact*. 2022; 24, 52-61. DOI: https://doi.org/10.1039/D1EM00392E

4.6 Appendix
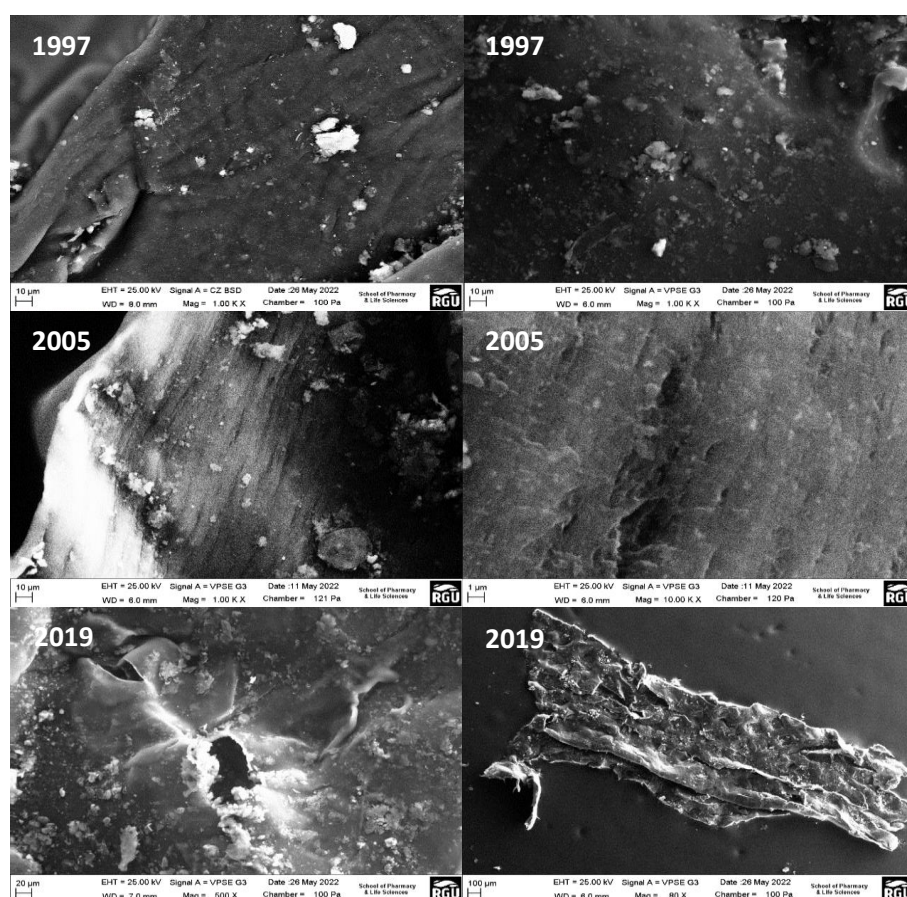
Figure 4A.1: Further SEM micrographs displaying progressive weathered features. The panels are labelled with the year that the soil was sampled. All films were identified as polyethylene through FTIR analysis.

Table 4A.1: Numbers and dimensions of different microplastic morphologies detected in the sewage sludge and the receiving soil plots. The average value across the replicates is shown, while the range of the values are given in brackets, those without did not have a range (i.e., were the same size). *N.D.* = Not detected.

| Sample | | No. of microplastics kg⁻¹ | | | | | | | Dimensions (µm) | | | | | |
Name	Type	Total kg⁻¹	no. Fibres	Fibre bundles	Films	Fragments	Particles	Flakes	Fibres	Fibre bundles	Films (longest edge)	Fragments	Particles	Flakes
A	Sludge	14510 (12941-16471)	9412 (8235-11765)	N.D.	2745 (2353-3529)	392 (0-1177)	1177 (0-2353)	784 (0-2353)	3861 (850-7520)	-	1506 (995-2100)	733 (520-840)	211 (80-260)	341 (195-460)
	Soil (1997)	11500 (9000-15500)	9833 (7500-13500)	N.D.	N.D.	1167 (750-1750)	333 (250-500)	167 (0-250)	4517 (600-9000)	-	-	654 (490-780)	220 (60-295)	341 (195-460)
	Soil (1999)	8250 (6500-10500)	7917 (6500-9750)	167 (0-250)	N.D.	167 (0-500)	167 (0-N.D.)	N.D.	-	-	-	-	-	-
	Soil (2001)	8083 (6500-9750)	7833 (5750-9750)	N.D.	N.D.	250 (0-750)	N.D.	N.D.	-	-	-	-	-	-
	Soil (2003)	10167 (8250-11500)	9000 (7500-10250)	250 (0-500)	N.D.	417 (250-500)	333 (250-500)	167 (0-250)	-	-	-	-	-	-
	Soil (2005)	8417 (7250-10500)	8000 (7250-9750)	N.D.	83 (0-250)	250 (0-500)	N.D.	83 (0-250)	-	-	-	-	-	-

Sample Name	Type	No. of microplastics kg⁻¹								Dimensions (μm)					
		Total kg⁻¹	no. Fibres	Fibre bundles	Films	Fragments	Particles	Flakes	Fibres	Fibre bundles	Films (longest edge)	Fragments	Particles	Flakes	
A (*continued*)	Soil (2007)	10250 (8000-11500)	9750 (7500-11500)	167 (100-250)	83 (0-250)	N.D.	83 (0-250)	167 (0-250)		-	-	-	-	-	-
	Soil (2009)	8250 (7750-8500)	7667 (7250-8000)	83 (0-250)	83 (0-250)	83 (0-250)	250	83 (0-250)	1828 (150-3760)	-	1502 (990-2000)	413 (300-525)	200 (100-270)	358 (160-475)	
	Soil (2011)	9000 (7000-10500)	8083 (6250-9750)	250 (0-500)	167 (0-250)	N.D.	83 (0-250)	417 (0-1000)		-	-	-	-	-	-
	Soil (2013)	8250 (7500-9250)	7167 (6750-7500)	83 (0-250)	167 (0-500)	N.D.	250	583 (250-1000)		-	-	-	-	-	-
	Soil (2015)	9583 (8500-11250)	8583 (8750-9250)	83 (0-250)	667 (250-1500)	N.D.	83 (0-250)	167 (0-250)		-	-	-	-	-	-
	Soil (2019)	10417 (9250-11250)	9750 (8250-10500)	N.D.	83 (0-250)	167 (0-250)	83 (0-250)	333 (0-750)	1575 (850-3400)	-	1502 (995-2010)	264 (150-360)	202 (105-275)	342 (170-445)	
B	Sludge	14035 (12782-15308)	27350 (24359-30769)	N.D.	1282	2564 (1282-3864)	4701 (3846-6410)	5983 (5128-6410)	3121 (250-7100)	-	2000 (1950-3700)	727 (500-890)	206 (60-270)	378 (20-495)	

Sample		No. of microplastics kg⁻¹							Dimensions (µm)					
Name	Type	Total kg⁻¹	no. Fibres	Fibre bundles	Films	Fragments	Particles	Flakes	Fibres	Fibre bundles	Films (longest edge)	Fragments	Particles	Flakes
B (continued)	Soil (1997)	10167 (8500-12750)	9417 (7500-12500)	N.D.	83 (0-250)	250 (0-500)	N.D.	417 (0-1250)	3277 (450-8600)	-	2201 (1800-3560)	725 (525-940)	-	350 (210-500)
	Soil (1999)	7583 (6750-8000)	6920 (6500-7500)	N.D.	N.D.	417 (0-1000)	N.D.	250 (0-750)	-	-	-	-	-	-
	Soil (2001)	7833 (7250-8250)	7167 (6750-7500)	83 (0-250)	N.D.	583 (250-1000)	N.D.	N.D.	-	-	-	-	-	-
	Soil (2003)	7333 (6750-7750)	6167 (5750-6500)	N.D.	83 (0-250)	500 (250-750)	333 (0-750)	250 (0-500)	-	-	-	-	-	-
	Soil (2005)	6333 (5000-7000)	4750 (3250-6000)	N.D.	83 (0-250)	1333 (500-1750)	83 (0-250)	83 (0-250)	-	-	-	-	-	-
	Soil (2007)	7333 (5250-8750)	6750 (4750-7750)	N.D.	N.D.	N.D.	N.D.	583 (250-1000)	-	-	-	-	-	-
	Soil (2009)	8333 (7000-9000)	7167 (5500-8750)	N.D.	83 (0-250)	83 (0-250)	417 (0-750)	583 (250-1000)	2030 (400-6300)	-	2000 (1800-3500)	490 (380-530)	200 (100-230)	358 (205-500)

Sample			No. of microplastics kg⁻¹							Dimensions (μm)					
Name	Type		Total kg⁻¹	no. Fibres	Fibre bundles	Films	Fragments	Particles	Flakes	Fibres	Fibre bundles (longest edge)	Films	Fragments	Particles	Flakes
B (*continued*)	Soil (2011)		7417 (6750-7750)	6500	N.D.	333 (0-750)	N.D.	333 (0-500)	250 (0-250)	-	-	-	-	-	-
	Soil (2013)		8916.67 (8000.00-10000.00)	7750 (6500-7750)	N.D.	N.D.	83 (0-250)	333 (0-750)	750 (500-1000)	-	-	-	-	-	-
	Soil (2015)		8667 (7500-9500)	7583 (7000-8000)	83 (0-250)	583 (500-750)	N.D.	83 (0-250)	333 (0-750)	-	-	-	-	-	-
	Soil (2019)		6500 (5250-7500)	5500 (4750-6250)	83 (0-250)	83 (0-250)	167 (0-250)	417 (250-500)	250 (0-500)	1315 (350-3100)	-	1943 (1750-3300)	242 (200-290)	202 (150-220)	342 (200-490)
C	Sludge		41880 (39744-44872)	13534 (12030-15037)	N.D.	N.D.	501 (0-752)	N.D.	N.D.	3716 (650-14000)	-	-	900 (600-1000)	-	-
	Soil (1997)		7583 (7250-8250)	6667 (5750-7750)	N.D.	83 (0-250)	83 (0-250)	167 (0-250)	583 (250-1000)	2219 (275-7300)	-	1984 (1000-2850)	850 (645-960)	206 (90-375)	345.26 (210.00-495.00)
	Soil (1999)		7250 (7000-7500)	6920 (5750-7750)	N.D.	N.D.	250 (0-250)	N.D.	83 (0-250)	-	-	-	-	-	-

Name	Type	Total no. kg⁻¹	Fibres	Fibre bundles	Films	Fragments	Particles	Flakes	Fibres	Fibre bundles	Films (longest edge)	Fragments	Particles	Flakes
					No. of microplastics kg⁻¹						Dimensions (µm)			
C (continued)	Soil (2001)	6917 (6500-7500)	6833 (6500-7250)	N.D.	N.D.	N.D.	N.D.	83 (0-250)	-	-	-	-	-	-
	Soil (2003)	7083 (6250-8000)	6833 (6000-7750)	N.D.	250	N.D.	N.D.	N.D.	-	-	-	-	-	-
	Soil (2005)	9000 (8500-9750)	8000 (7500-9000)	167 (0-250)	417 (250-500)	83 (0-250)	167 (0-500)	167 (0-500)	-	-	-	-	-	-
	Soil (2007)	8000 (7000-9250)	6920 (6750-7000)	83 (0-250)	417 (250-7500)	333 (0-1000)	83 (0-250)	167 (0-250)	-	-	-	-	-	-
	Soil (2009)	8500 (7750-9500)	7833 (7000-8750)	83 (0-250)	250 (0-250)	83 (0-250)	167 (0-250)	83 (0-250)	2027 (450-8000)	-	1898 (1100-2750)	566 (450-600)	200 (60-300)	358 (200-450)
	Soil (2011)	7417 (7000-7750)	7000 (6250-7500)	167 (0-250)	83 (0-250)	N.D.	83 (0-250)	83 (0-250)	-	-	-	-	-	-
	Soil (2013)	6833 (6000-7500)	6167 (5250-9250)	167 (0-250)	N.D.	83 (0-250)	83 (0-250)	333 (0-500)	-	-	-	-	-	-

Sample		No. of microplastics kg⁻¹							Dimensions (µm)					
Name	Type	Total kg⁻¹	no. Fibres	Fibre bundles	Films	Fragments	Particles	Flakes	Fibres	Fibre bundles	Films (longest edge)	Fragments	Particles	Flakes
C (*continued*)	Soil (2015)	8917 (8000-10000)	8250 (7500-9250)	167 (0-250)	83 (0-250)	N.D.	83 (0-250)	333 (0-750)	-	-	-	-	-	-
	Soil (2019)	7667 (7000-8500)	6750 (6000-7250)	N.D.	83 (0-250)	250 (0-500)	167 (0-250)	417 (250-750)	1370 (450-3000)	-	1876 (1000-2700)	268 (150-300)	202 (80-250)	342 (210-460)
D	Sludge	35271 (30232-39535)	30620 (24419-32558)	129 (0-388)	2326	1163 (0-2326)	N.D.	776 (0-1163)	3803 (450-7100)	-	2380 (1750-2975)	862 (630-970)	-	421 (240-460)
	Soil (1997)	8417 (7500-9000)	7583 (7000-8250)	N.D.	N.D.	333 (0-1000)	83 (0-250)	417 (0-750)	4087 (1100-8360)	-	-	792 (590-850)	201 (105-310)	369 (240-450)
	Soil (1999)	6667 (6000-7250)	6333 (6000-7000)	N.D.	N.D.	333 (0-1000)	N.D.	N.D.	-	-	-	-	-	-
	Soil (2001)	6083 (6000-6250)	6083 (6000-6250)	N.D.	N.D.	N.D.	N.D.	N.D.	-	-	-	-	-	-
	Soil (2003)	6500 (6000-7000)	6167 (5750-7000)	83 (0-250)	250 (0-500)	N.D.	N.D.	N.D.	-	-	-	-	-	-

| Sample | | | No. of microplastics kg⁻¹ | | | | | | Dimensions (µm) | | | | | |
Name	Type	Total kg⁻¹	no. Fibres	Fibre bundles	Films	Fragments	Particles	Flakes	Fibres	Fibre bundles	Films (longest edge)	Fragments	Particles	Flakes
D (continued)	Soil (2005)	7417 (6500-8250)	6917 (5750-6750)	333 (0-1000)	833 (0-250)	83 (0-250)	N.D.	N.D.	-	-	-	-	-	-
	Soil (2007)	6167 (5750-6750)	6000 (5750-6250)	N.D.	N.D.	N.D.	N.D.	83 (0.00-250)	-	-	-	-	-	-
	Soil (2009)	7833 (7000-8750)	7083 (6500-7750)	N.D.	83 (0-250)	83 (0-250)	83 (0-250)	250	2027 (760-5450)	-	1983 (1500-2250)	451 (400-590)	200 (125-290)	358 (100-550)
	Soil (2011)	6917 (5750-7500)	6000 (4500-7000)	83 (0-250)	333 (0-500)	N.D.	167 0-250)	167 (167 (0-250)	-	-	-	-	-	-
	Soil (2013)	6333 (6000-6750)	5667 (5500-5750)	N.D.	N.D.	N.D.	N.D.	333 (250-500)	-	-	-	-	-	-
	Soil (2015)	8500 (8000-9000)	7750 (7500-8000)	83 (0-250)	167 (0-500)	333 (250-500)	167 (0-500)	N.D.	-	-	-	-	-	-
	Soil (2019)	8000 (7250-8750)	7500 (7000-7750)	83 (0-250)	83	83 (0-250)	83 (0-250)	83 (0-250)	1643 (350-4700)	-	1724 (1300-1950)	270 (200-360)	202 (110-300)	342 (125-475)
E	Sludge	-	-	-	-	-	-	-	-	-	-	-	-	-

Sample		No. of microplastics kg⁻¹							Dimensions (µm)					
Name	Type	Total kg⁻¹	no. Fibres	Fibre bundles	Films	Fragments	Particles	Flakes	Fibres	Fibre bundles	Films (longest edge)	Fragments	Particles	Flakes
	Soil (1997)	9667 (8750-10750)	8583 (8000-9000.)	167 (0-250)	250 (0-500)	83	250 (0-500)	333 (0-500)	2749 (70-8600)	-	2102 (1750-3950)	735 (475-925)	201 (70-215)	367 (210-480)
E (continued)	Soil (1999)	7750 (6750-9250)	6916 (6250-8250)	250 (0-500)	N.D.	583 (0-1000)	N.D.	N.D.	-	-	-	-	-	-
	Soil (2001)	7083 (6250-7500)	6833 (6000-7250)	83 (0-250)	N.D.	167 (0-250)	N.D.	N.D.	-	-	-	-	-	-
	Soil (2003)	5917 (5250-7000)	5583 (4500-6750)	N.D.	N.D.	250 (0-500)	N.D.	83 (0-250)	-	-	-	-	-	-
	Soil (2005)	6417 (5500-7500)	6333 (5250-7500)	N.D.	N.D.	83 (0-250)	83 (0-250)	N.D.	-	-	-	-	-	-
	Soil (2007)	6583 (5250-8500)	5750 (4500-7250)	N.D.	250 (0-500)	333 (250-500)	N.D.	N.D.	-	-	-	-	-	-
	Soil (2009)	8250 (7250-9000)	7333 (6000-8250)	83 (0-250)	333 (0-750)	333 (250-500)	83 (0-250)	83 (0-250)	1527 (350-5600)	-	2005 (1600-3425)	436 (350-470)	200 (95-230)	358 (200-425)

| Sample | | | | No. of microplastics kg⁻¹ | | | | | | Dimensions (µm) | | | | | |
Name	Type	Total kg⁻¹	no. Fibres	Fibre bundles	Films	Fragments	Particles	Flakes	Fibres	Fibre bundles	Films (longest edge)	Fragments	Particles	Flakes
E (*continued*)	Soil (2011)	6500 (5250-8000)	5250 (4500-6750)	167 (0-500)	583 (500-750)	N.D.	N.D.	500 (250-1000)	-	-	-	-	-	-
	Soil (2013)	8667 (7500-10000)	8167 (7500-9750)	333 (250-500)	N.D.	N.D.	83.33 (0-250)	83 (0-250)	-	-	-	-	-	-
	Soil (2015)	11333 (10500-12750)	10500 (9750-11750)	83 (0-250)	167 (0-250)	83 (0-250)	N.D.	500 (250-750)	-	-	-	-	-	-
	Soil (2019)	13333 (11750-14500)	12167 (10250-13250)	83	250 (0-500)	83 (0-250)	83	667 (500-1000)	1104 (300-3000)	-	1934 (1550-2950)	254 (225-375)	202 (70-230)	342 (210-420)
Negative Control	Soil (1997)	4000 (2500-6000)	3417 (2000-5500)	N.D.	N.D.	250 (0-500)	N.D.	83 (0-250)	1390 (550-2100)	-	-	452 (350-495)	-	250 (210-300)
	Soil (1999)	2250 (1750-2750)	1917 (1250-2250)	N.D.	83 (0-250)	N.D.	N.D.	N.D.		-	-	-	-	-
	Soil (2001)	3333 (3000-3500)	3250 (2750-3500)	83 (0-250)	N.D.	N.D.	N.D.	N.D.		-	-	-	-	-

Sample			No. of microplastics kg⁻¹							Dimensions (µm)					
Name	Type	Total kg⁻¹	no. Fibres	Fibre bundles	Films	Fragments	Particles	Flakes	Fibres	Fibre bundles	Films (longest edge)	Fragments	Particles	Flakes
Negative Control (*continued*)														
	Soil (2003)	3250 (2750-3750)	2917 (2750-3000)	N.D.	N.D.	83 (0-250)	N.D.	250 (0-500)	-	-	-	-	-	-
	Soil (2005)	2833 (2000-3000)	2583 (1750-3000)	N.D.	83 (0-250)	167 (0-250)	N.D.	N.D.	-	-	-	-	-	-
	Soil (2007)	3333 (3250-3500)	3250 (3250-3500)	N.D.	N.D.	N.D.	N.D.	83 (0-250)	-	-	-	-	-	-
	Soil (2009)	1917 (1500-2750)	1667 (1250-2250)	N.D.	N.D.	N.D.	83 (0-250)	167 (0-250)	1900 (1100-3500)	-	-	326 (270-400)	-	237 (180-290)
	Soil (2011)	1917 (1750-2250)	1667 (1250-2000)	N.D.	N.D.	N.D.	N.D.	250 (0-500)	-	-	-	-	-	-
	Soil (2013)	2167 (1500-2750)	1750 (1500-2000)	N.D.	N.D.	N.D.	N.D.	417 (0-750)	-	-	-	-	-	-
	Soil (2015)	1083 (750-1250)	917 (500-1250)	N.D.	N.D.	N.D.	167 (0-250)	N.D.	-	-	-	-	-	-
	Soil (2019)	1417 (750-2250)	1250 (750-2000)	N.D.	N.D.	83	N.D.	83 (0-250)	1629 (300-4100)	-	-	230 (240-290)	-	235 (180-285)

Chapter 5: National scale distribution of microplastics in Scottish soils and factors influencing their distribution

To date, spatial distribution studies of microplastics in soils tend to focus on a single region or land use, creating a myopic view of the scale of the issue. National-scale studies will allow us to create a baseline that can be used to determine factors that influence microplastic prevalence. By utilising the National Soils Inventory of Scotland, 160 rural surface soil samples collected across the Scottish mainland and islands were used to generate the first national scale study on microplastic distribution. Results highlighted that microplastic 'hotspots' could be identified through distribution mapping which demonstrated that geography played a role in microplastic distribution. Fibres were the most abundant microplastic morphology ($\geq$ 88.91%). Land use was the most significant driver in the distribution of microplastics such that high-intensity land management resulted in higher microplastic pollution (average 3756 microplastics L^{-1} soil) compared to unmanaged soils (average 562 microplastics L^{-1} soil) ($p < 0.05$). Microplastic sizes were also larger in high-intensity land management compared to unmanaged soils ($p < 0.05$). Topographical features such as slope direction influenced microplastic distribution, e.g., slopes facing into the prevailing wind direction were more susceptible to atmospheric deposition of microplastics, while higher altitude soils container higher abundances of smaller sized microplastics. Other factors such as soil physicochemical and environmental properties were also found to be influential. Microplastic abundance had positive correlations with persistent organic pollutants, including plasticisers, and plastic additives, and degradation by-products, suggesting that microplastics may contribute to soil pollution of these contaminants through leaching or that they share a common anthropogenic source. The generation of this background microplastic data allows for the understanding and assessment of the scale of microplastic pollution in soils at a national scale, enabling the identification of potential mitigation strategies for preventing further significant terrestrial microplastic enrichment. Results reported in this study could also be used to compare microplastic abundance to corresponding soils in future studies both nationally and internationally.

5.1 Introduction

Every year, there is a significant input of plastic and microplastic pollution into the environment, particularly into soils (Horton et al., 2017), since its major introduction to domestic and industrial use in the 1950s. There are several mechanisms through which microplastics are generated such as littering, agricultural practices such as sewage sludge application and the use of plastic mulching film, vehicular tyre and brake wear, industrial processes, consumer products, and indoor particulate

emissions, which can be disseminated into the natural environment through surface run-off and atmospheric deposition (Bläsing and Amelung, 2018; Guo et al., 2020; Yang et al., 2021a). Therefore, microplastics have the potential to pollute urban, industrial, and agricultural soils (Kim et al., 2021; Nematollahi et al., 2022; Zhou et al., 2022). Microplastics can also pollute remote soils which are beyond most human presence and interference, primarily through processes such as atmospheric deposition (Scheurer and Bigalke, 2018; Wang et al., 2021a; Yang et al., 2022).

Recent research has highlighted that the accumulation and persistence of microplastics in the terrestrial environment change soil structure and have detrimental effects on soil fauna and flora, which, therefore, can disrupt soil function. De Souza Machado et al. (2018) reported that various types and shapes of microplastics could alter the water holding capacity and bulk density as well as decrease soil microbial activity, resulting in the soil structure and function being significantly altered. However, little is known on how soil physical parameters, such as soil drainage and root depth, can influence microplastic abundance in surface soils (and sublayers). Furthermore, soil topography has not largely been considered when investigating microplastic abundance and distribution except for a single location study by Rolf et al. (2022). Their study focused on an alluvial soil and its localised floodplain topography, whereby microplastic input and distribution was driven by flooding river water (Rolf et al., 2022).

Microplastics also have the potential to increase the bioavailability of some chemical pollutants to soil organisms through their ability to act as vectors (Heinrich and Braunbeck, 2019; Li et al., 2021a), while they may decrease the bioavailability of other persistent organic pollutants (POPs) due to strong intermolecular interactions (Yu et al., 2020; Zhu et al., 2022). Furthermore, adsorption of POPs to microplastics allows them to persist longer in the environment, prolonging their effects on the terrestrial environment. Similarly, POPs which are within microplastics (through manufacturing or chemical degradation of plastic additives) have the potential to leach out of the plastic matrix into the surrounding soil (Li et al., 2024). Despite the interaction of persistent organic pollutants with microplastics being well researched, little is known about the relationship between microplastic abundance and the concentration of persistent organic pollutants in soil, and what these potential relationships may imply (e.g., whether microplastics may contribute to soil POP concentrations through leaching).

Microplastics have also been found to affect soil macro-organisms such as earthworms (Prendergast-Miller et al., 2019; Chen et al., 2022) as well as being incorporated into crops and fruit/vegetables (Conti et al., 2020). This presents a major health concern, as evidence has been published demonstrating the potential for microplastic transfer along terrestrial food chains, e.g., from earthworms to chickens to humans (Huerta Lwanga et al., 2017), or through direct ingestion of crop products.

To date, there has been no national scale studies on the spatial distribution of microplastics in soil, and although microplastic pollution has been linked to land use (Corradini et al., 2021; Zhang et al., 2022a; Zhang et al., 2022b), these studies tend to only focus on one region, with the exception of Xue et al. (2023) whose study focused solely on agricultural soils in China. The James Hutton Institute (Aberdeen, Scotland, UK) curates the National Soils Archive of Scotland containing over 60,000 soil samples from over 15,000 locations. Included in this archive are around 200 rural soils samples that represent all the soil types across the Scottish mainland and islands collected between 2007 and 2009. This subset is called the National Soils Inventory of Scotland (NSIS), which is accompanied by large physical, chemical, and biological datasets. Included in the NSIS sampling programme are surface soils (0-5 cm) which were dried and stored in glass vials in the dark.

This work set out to be the first to undertake a study of this scale to elucidate the extent of microplastic pollution nationwide in order to generate background soil microplastic data for Scotland and inform and prioritise future mitigation and remediation strategies to reduce the input of plastic pollution to land. It also aimed to investigate which anthropogenic, topographical, soil physicochemical, and environmental factors may influence microplastic abundance, distribution, and size in Scottish soils. Furthermore, relationships between microplastics and selected persistent organic pollutants associated with plastic production or degradation were also investigated.

5.2 Materials and Methods

5.2.1 Sample collection, metadata analyses, and sample categorisation

Surface soil samples (0-5 cm) were obtained from the National Soils Inventory of Scotland (NSIS) at the James Hutton Institute, Aberdeen, UK. Soils were collected between 2007 and 2009 from rural locations in a 20 km grid sampling framework across the Scottish mainland and islands totalling 195 sites (12 sites were classed as non-soils) to generate the second NSIS (Lilly et al., 2011). The land area of Scotland

is approximately 78,789 km^2 including its islands. The main NSIS samples were collected and stored in plastic, hence could not be used to evaluate microplastic abundance since it is not known how storage in plastic bags could contribute to microplastics present in the soil samples. However, a subset was specially collected avoiding plastic throughout the whole process for the initial purpose of organic contaminant analysis (polycyclic aromatic hydrocarbons (PAHs), polychlorinated biphenyls (PCBs), and polybrominated diphenyl ethers (PBDEs) (Rhind et al., 2013)) which were used in this study for microplastic analysis. Representative soil samples were collected using a soil corer (7.5 cm diameter × 5 cm depth) and stored directly in glass jars with aluminium foil isolating the plastic lid from the glass jar and soil. The soils were air-dried and sieved to < 2 mm and re-stored in glass jars. Of the 195 soil samples, 160 were available for microplastic analysis (Figure 5.1). The quantities of the remaining 35 samples were insufficient to subsample for this project while preserving some of the samples for future work. Soils were categorised when the NSIS database was generated by various parameters including soil type, land use, vegetation at time of sampling, soil drainage – Tables 5A.1-5A.7. An additional two composite samples from Hirta in the highly remote archipelago, *St. Kilda*, collected in 2013 using the same sampling protocol, were also subjected to microplastic assessment due to its extremely remote location but high yearly tourist footfall and military occupancy.

Concentrations of persistent organic pollutants (di (2-phenylhexyl) phthalate (DEHP), PAHs, PCBs, and PBDEs) were measured at the time of the NSIS database generation using gas chromatography – mass spectrometry (GC-MS) (Rhind et al., 2013). Elemental analysis was performed using inductively coupled plasma – mass spectrometry (ICP-MS) using the method described by Shand et al. (2012). Soil pH (in water) was measured using the method described by McLean (1982). Total soil carbon and total organic carbon (loss on ignition) were measured using a Flash EA 1112 Elemental Analyser (Pella and Colombo, 1973).

Soils were categorised based on various parameters, defined below:

- Regions – Scottish region where soil sample was collected (Figure 5.1);
- Land use – type of land management i.e., *arable farmland, managed grassland, forestry/woodland, and minimally managed* or *unmanaged semi-natural* soils (Figure 5.2);
- Slope form – the profile of a slope i.e., *straight, convex*, or *concave* (Table 5A.1);
- Slope type – defined as *simple* if the slope only had one form along its length or *complex* if the slope had multiple slope forms along its length (Table 5A.1);

- Soil drainage – natural drainage of soil profile assessed from profile morphology alone, categorised as *excessive, free, moderate, imperfect, poor*, or *very poor* (Table 5A.2);

- Soil phase – terminology used for mapping purposes to define the state of the soil at time of sampling e.g., *cultivated, hagged/severely eroded peat* or *neither* (Table 5A.3);

- Peatland type – classification for type of peat i.e., *hill and blanket peat* or *basin peat* (Table 5A.4);

- Soil group – soil group based on Scottish Soil Classification (Table 5A.5);

- Parent material – underlying material from which the overlying soils develops from (Table 5A.6), and;

- Vegetation – type of vegetation present at time of sampling (Table 5A.7).

5.2.2 Microplastic extraction

Each soil sample was mixed thoroughly on an end-over-end shaker, and 8 mL was subsampled in triplicate for microplastic extraction using the high-gradient magnetic separation method (Chapter 3 and Ramage et al., 2022). Magnetic flux densities (MFDs) for each sample were ascribed to each soil based on the parameters prescribed in Chapter 3 for each soil texture and carbon content. Briefly, soils classed as peat were assigned MFDs of 0.25 and 0.34 T for Stages 1 and 3, respectively, 0.29 and 0.39 T for loam, 0.53 and 0.53 T for loamy sand, 0.34 and 0.39 T for high-carbon loamy sand (> 7%C), 0.53 and 0.53 T for low-carbon sand (< 7%C), 0.25 and 0.34 T for high-carbon sand (> 7%C), 0.53 and 0.53 T for sandy loam, 0.16 and 0.39 T for high-clay sandy loam (> 10%), and 0.34 and 0.40 T for silt loam. No further testing for MFD determination was required as Chapter 3 covered the broad range of soil types in this study.

A blank measurement was taken after every 10 samples (16 in total). In order to ensure that a change in batches of modified iron nanoparticles did not affect microplastic recovery, the recovery of a spiked soil sample was checked with every new batch.

5.2.3 Microplastic enumeration, categorisation, measurement, and identification

Recovered microplastics were enumerated on the filter papers using a Nikon SMZ1500 stereomicroscope between 7.5 to 50 x magnification. The suspected microplastics were categorised based on their shape and colour, removed from the filter papers using tweezers, and stored on adhesive

tape secured to acetate sheets for further analysis, both as described in Chapter 4 (section 4.2.3). The average number of microplastics measured in HGMS blank controls was also subtracted from all final recorded abundances. Microplastic abundance was reported as microplastic number L^{-1} soil to prevent potential skewing of results due to the large variation in soil densities. Spatial distribution maps were generated using ArcGIS Pro 3.1.

The size of a random 10% subsample of each microplastic morphology per land use, as well as a 10% random subsample of all arable microplastics, were measured with an Olympus BX53M microscope fitted with a YenCam HD camera using the YenCam imaging software.

The composition of a random 10% subsample of microplastics ($\geq$ 50 µm) for each region and land use, respectively, were determined using an iN10 Fourier-transform infrared (FTIR) microscope. Fibres were analysed in reflectance mode, while all other microplastic types were analysed using a Ge tip ATR (attenuated total reflectance) attachment. Spectra were obtained using a liquid nitrogen-cooled MCT detector in the range of 4000-650 cm^{-1} at a resolution of 4 cm^{-1} with an average of 128 scans. Air blank spectra were recorded after each measurement with the same number of scans and resolution.

5.2.4 Quality control

Soils were kept away from plastic materials during sampling and throughout all analyses through the use of glass or metal utensils (sterilised prior to use). All glassware was heated in a muffle oven to 450 °C before use to eliminate any potential microplastic contamination (Dris et al., 2018) and kept covered in aluminium foil throughout. Sample preparation and filtration was conducted in a clean environment within a HEPA filtered fume hood (0.3 µm pore size) to minimise airborne contamination. To eliminate bias, all samples were anonymised using laboratory barcodes during processing.
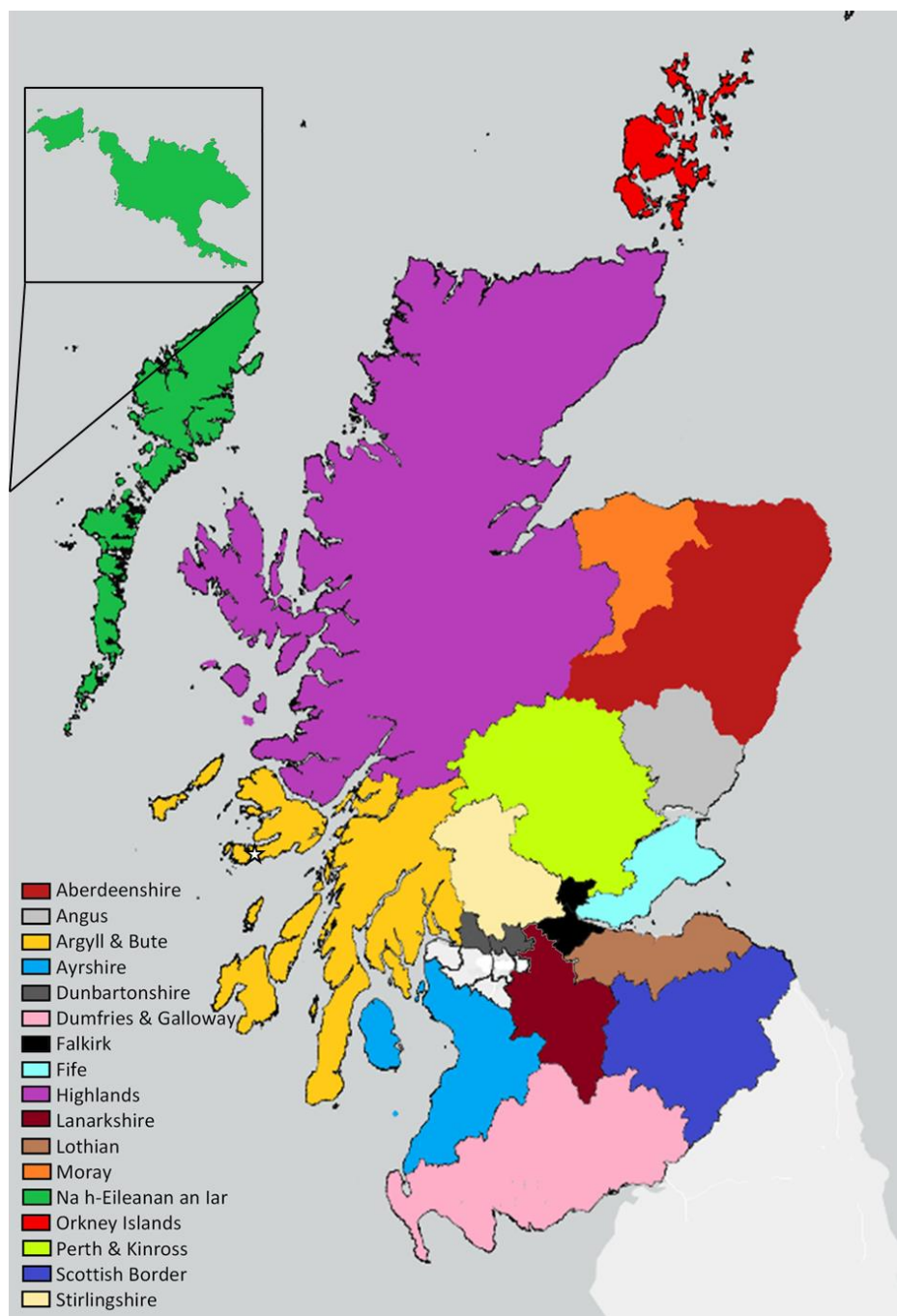
Figure 5.1: Map displaying the regions of Scotland. Soil samples from areas in white (central Scotland) were not available for analysis from these areas. Shetland Islands (northeast of Orkney Islands) have also been omitted as no samples were available for analysis from this area. *St. Kilda* appears in the top left box.
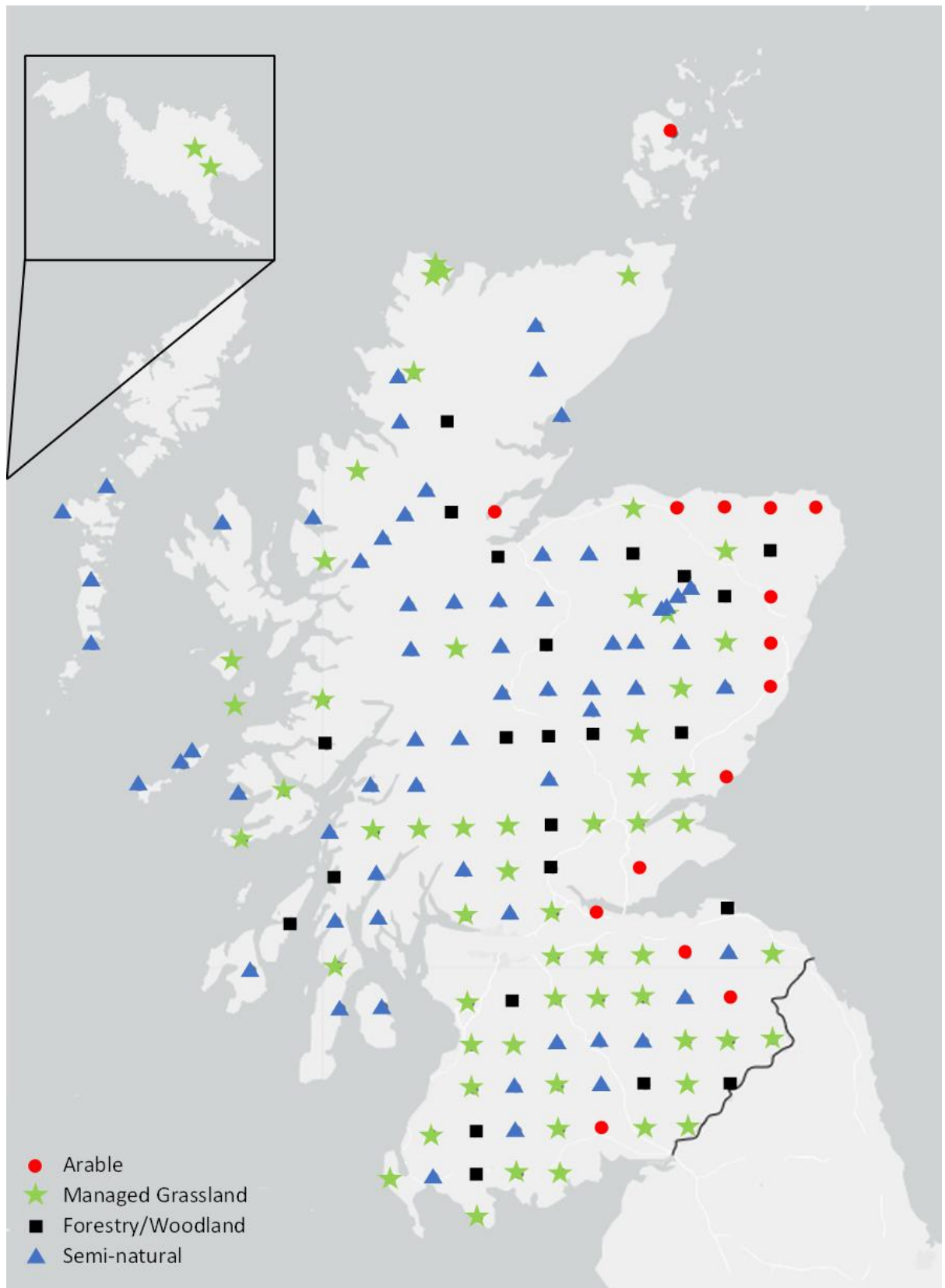
Figure 5.2: Map displaying the distribution of the land use categories investigated in this study (arable, managed grassland, forestry/woodland, and semi-natural).

5.2.5 Statistical Evaluation

Spearman's rank correlation and Kruskal-Wallis tests have previously been used to statistically assess relationships between microplastic abundance and environmental, region, and land use data (Wang et al., 2023). Spearman's rank correlation tests were, therefore, performed in R (version 4.3.1) to determine the strength of association between microplastic abundance and geographical data (northing and easting, latitude and longitude, and distance from roads), topographical data (altitude, slope gradient, and slope bearing), soil physicochemical data (root depth, soil texture (sand, silt, clay), pH, total carbon, total organic carbon, and soil bulk density), environmental data (rainfall), and persistent organic pollutant data (plasticisers (DEHP), PAHs, PCBs, and PBDEs). When assessing the relationship between rainfall and microplastics, rainfall data for all sampling locations was assessed as well as those from semi-natural soils only in order to eliminate any bias introduced by land use type. For determining correlations with soil texture, peat samples (which do not have soil texture data) were removed from the test. For organic pollutant data, the total sum of all the organic pollutant types was assessed as well as all the individual congeners for which data was available. The same as repeated for microplastic size and geographical, topographical, soil physicochemical, and environmental data. All correlations with a $p < 0.05$ value were considered significant.

Kruskal-Wallis H tests (*K-W*) were performed in IBM SPSS Statistics (version 22) to determine the strength of association of microplastic abundance with discrete NSIS metadata (region, land use, slope type and form, vegetation, soil drainage, soil phase, soil group, peatland type, and parent material). Land use was further grouped into 4 broader categories to reflect management intensity for statistical comparisons: arable, managed grassland, forestry/woodland, and semi-natural (in order of decreasing management intensity). Forestry/woodland included broadleaf and coniferous woodlands and plantations, and semi-natural included bog, dune, heath, mire wetland, moorland, and scrub. The same was also repeated for microplastic size. *K-W* test was also used to determine the significance in the difference between microplastic abundance in *St. Kilda* compared to the island samples within the NSIS dataset (one grouping consisted of the *St. Kilda* soil samples while the other grouping consisted of all the NSIS island samples). All correlations with a $p < 0.05$ value were considered significant.

The four land uses categories were used in *K-W* tests to group the broad land uses when evaluating the relationship between all land uses and microplastic size. The differences in microplastic size and the different arable land uses alone (based on vegetation) were also assessed by *K-W* test. For further

assessing the relationship between altitude and microplastic size, altitude was split into three groups (0-300, 301-600, and 601-900+ m) to establish the significance of the microplastic size ranges within these altitudes.

Primer v7 (PRIMER-e) was used to generate non-metric multidimensional scaling (nMDS) plots to evaluate the similarity in microplastic community composition between land uses and assess factors driving dissimilarly. Data was square root transformed and subjected to a Bray-Curtis dissimilarity test. The similarity matrix was then used to draw the nMDS plots. Plots with a 2D stress value of < 0.2 were considered to have a good fit of the data points. Samples (microplastic community compositions) were grouped by land use and the variation in microplastic community composition was assessed against location, topographic, soil physicochemical, environmental, and pollutant data (outlined above) using Pearson's correlation. Pearson's correlations, where r < 0.4, were overlaid on the resulting nMDS plots.

As the *St. Kilda* soil samples were not part of the NSIS dataset and were collected 6 years after the start of the NSIS sample collection, it was deemed it would not be appropriate to include these results in the statistical tests on the NSIS samples outlined above. Therefore, they were not included in any of those statistical tests. However, for comparison purposes, microplastic abundance data from the *St. Kilda* samples were compared to microplastic abundances in NSIS island samples using the *K-W* test.

5.3 Results and Discussion

5.3.1 Microplastic abundance across Scotland

The abundance of microplastics varied greatly across Scottish soils from different regions and land uses (Figure 5.3). Abundance was also greatly variable within all regions, likely due to the variety and different proportions of land uses present within each region as well as other influencing factors. Microplastic abundance ranged from 83 to 8500 microplastics L^{-1} soil (average of 1199 microplastics L^{-1} soil). Two samples did not contain any detectable microplastics, one was a forestry/woodland soil sample (coniferous plantation), and the other was a semi-natural soil sample (peat bog). The highest microplastic abundance (8500 microplastics L^{-1} soil) was observed in a soil sample from an arable farm while the lowest detectable abundance (83 microplastics L^{-1} soil) was observed at 6 different sampling locations: three were rough grassland, two were bogs, and one was moorland. Average microplastic abundance per region and land use are presented in Tables 5.1 and 5.2, respectively.

There was a significant difference in microplastic abundance between region (*K-W* test, p < 0.05). On average, *Na h-Eileanan an Iar* (Western Isles) (n = 4) had the lowest microplastic abundance (396 ± 105 microplastics L^{-1} soil) while *Fife* (n = 1) had the highest abundance (3833 ± 0 microplastics L^{-1} soil) (Table 5.1). All samples were purposefully collected from rural locations. Soils collected from sampling locations in the mountainous regions, *Highlands* (n = 40) and *Argyll and Bute* (n = 20), are the most remote samples on mainland Scotland, therefore, these areas are sparsely populated. Much of the soils from these two regions are classed as semi-natural (Figures 5.1 and 5.2). As such, microplastic abundance was expected to be lower in these samples than those from areas which are highly or more densely populated on mainland Scotland and subject to higher land management intensity (Allen et al., 2019). Average microplastic abundances measured in these mainland soils confirmed that this was true, with *Argyll and Bute* measuring the lowest microplastic abundance (500 ± 309 microplastics L^{-1} soil) and *Highlands* accounting for the second lowest (644 ± 550 microplastics L^{-1} soil).

Table 5.1: Microplastic abundance per region. The average value across the samples is shown, while the range of the values are given in brackets.

Region	Number of samples	Average no. of microplastics L^{-1} soil
Fife	1	3833
St. Kilda	2	3167 (2167 - 4167)
Moray	7	2798 (417 - 6333)
Aberdeenshire	21	2325 (0 - 8500)
Stirlingshire	4	1938 (333 - 5583)
Angus	5	1850 (750 - 4750)
Lothian	5	1517 (917 - 2167)
Orkney Islands	1	1500
Falkirk	2	1375 (667 - 2083)
Perth & Kinross	11	977 (333 - 4000)
Ayrshire	7	964 (583 - 1500)
Dumfries & Galloway	15	961 (167 - 4333)
Dunbartonshire	2	917 (250 - 1583)
Scottish Border	11	902 (0 - 2167)
Lanarkshire	4	750 (500 - 1250)
Highlands	40	644 (83 - 2583)
Argyll & Bute	20	500 (83 - 1167)
Na h-Eileanan an Iar	4	396 (250 - 417)
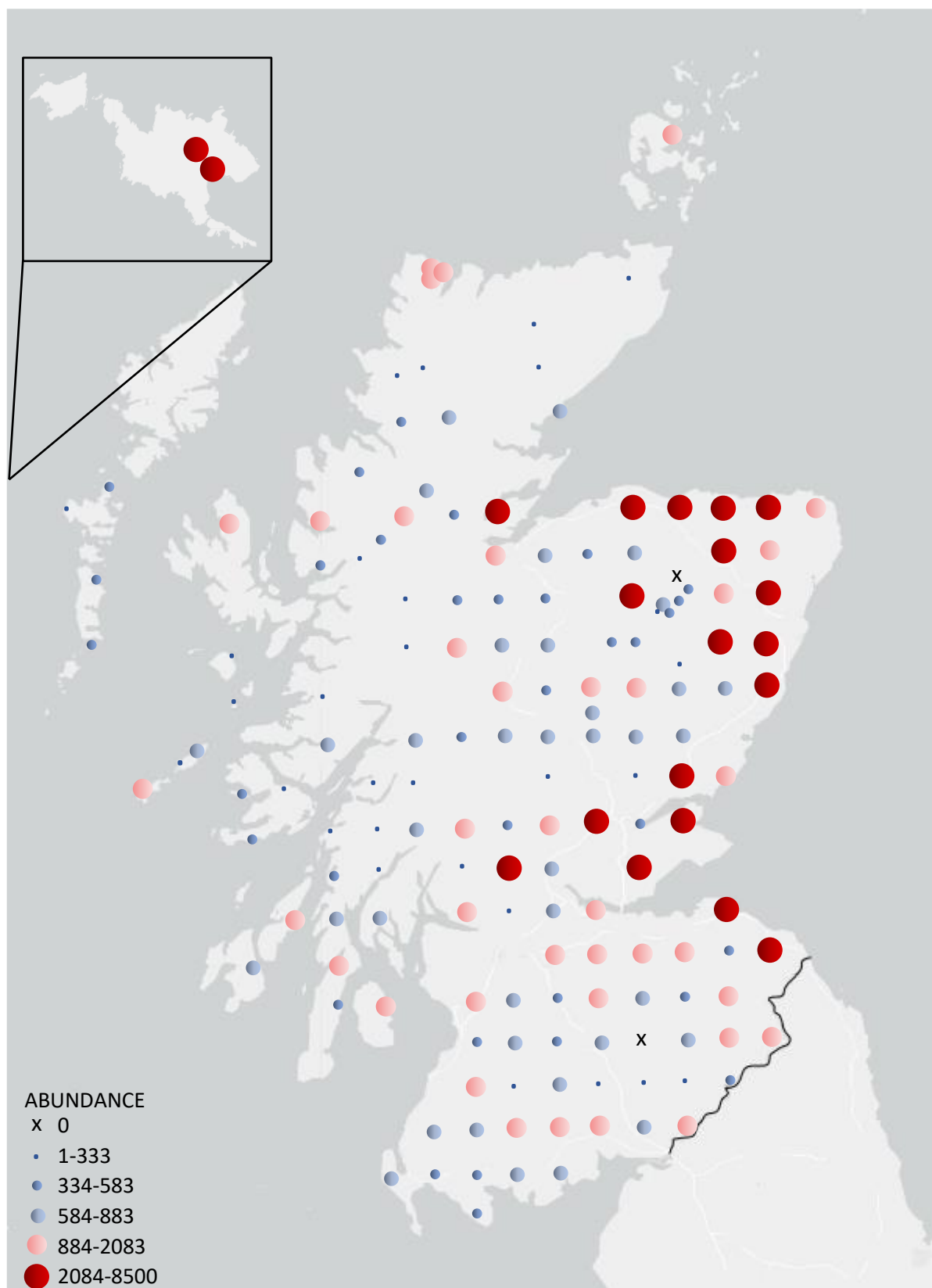
Figure 5.3: Map of microplastic abundance across Scottish soils. Abundance is expressed as number of microplastics L^{-1} soil.

Similarly, samples obtained from *Na h-Eileanan an Iar* (n = 4) were expected to be low in microplastic abundance due to their low and sparse populations, minimal land management (all soils were semi-natural – bog (n = 1) and dunes (n = 3)), and their separation from mainland Scotland. As such, microplastic abundance was almost half of that measured in the sparsely populated mainland regions of *Argyll and Bute* and *Highlands* (Table 5.1). However, some regions and land uses have as few as one to three samples for representation (Tables 5.1 and 5.2) – refer to section 5.4.

Samples from dune habitats were taken from machairs in close proximity to the sea. Marine-based microplastics from aquaculture/fishing industries and leisure activities may be deposited on dunes and machair land through airborne sea spray or atmospheric deposition (Allen et al., 2020). Furthermore, breeding seabirds on machairs may introduce microplastics to coastal soils through their excrement (Bourdages et al., 2021). However, the transference of microplastics from the marine environment to land is a largely under-researched area, with research predominantly focusing on their exportation from land to sea.

Table 5.2: Microplastic abundance per land use type. The average values across the samples are shown, while the range of the values are given in brackets.

Land use category	Land use	Number of samples	Average no. of microplastics L^{-1} soil
Arable	Arable	17	3756 (1500 - 7917)
Managed grassland	Improved	27	1931 (333 - 6333)
	Rough	30	991 (83 - 4167)
Woodland/forestry	Broadleaf	3	1000 (500 - 1917)
	Coniferous	19	842 (167 - 2167)
	Plantation	1	*Not detected*
Semi-natural	Scrub	2	792 (667 - 917)
	Heath	5	633 (417 - 833)
	Dune	7	552 (250 - 1167)
	Bog	17	543 (0 - 1000)
	Moorland	32	516 (83 - 917)
	Mire wetland	1	333

5.3.2 Microplastic characterisation

5.3.2.1 Morphology and colour

Microplastics were categorised based on their morphology and colour during enumeration, and the morphologies were divided into fibres, fibre bundles, films, fragments, particles, and flakes (definitions are provided in Chapter 2, Section 2.1 (Figure 2.1)). Fibres were the predominant microplastic morphology found in all soil samples, accounting for ≥ 88.91% of the microplastics recovered across all four broad land use categories (Figure 5.4A). This is consistent with other studies reporting fibres to be the most abundant morphology in soils (Yang et al., 2021b; Liu et al., 2022). In addition, fibres were identified as one of the predominant factors in influencing variation of microplastic community compositions when generating nMDS plots in accordance with land use (Figure 5.5A) (r < 0.4). Arable soils contained a lower proportion of fibres (88.91 ± 13.36%) compared to the other land uses (e.g., 92.58 ± 1.90% for semi-natural soils). This is likely due to higher proportions of other morphologies, however, it may also be possible that agricultural activities may lead to fragmentation of fibres (see Chapter 4) which may impede their recovery. Nevertheless, fibres still contributed the greatest overall number compared to other microplastic morphologies. The processes involved in this high intensity land management, such as sewage sludge amendments (see Chapter 4; Elmi et al., 2020; Xu et al., 2020) and the use of mulching film (see Chapter 6; Tian et al. 2022), are likely to account for the greater variety in microplastic morphologies in these soils (see Chapter 4). Despite this fact, the morphologies making up the microplastic community compositions were not significantly different when grouped according to land use, i.e., there was no meaningful separation of the data points in the nMDS plot (Figure 5.5A), whereby all the points, except for a single semi-natural soil sample, were clustered together. This indicates that the microplastic community composition of this semi-natural soil sample (based on morphology) was significantly different to all other soil samples, with this separation driven by the presence of films. This sample had a higher proportion of both fibres and films compared to all other semi-natural soils (16667 and 2083 L^{-1} soil, respectively) and was located on a remote hilltop (547 m). Farmland was located at the base of the hill to the west which may be the potential source of the higher abundance of microplastics and microfilms in particular (i.e., atmospheric transport and deposition). Figure 5.5A had a 2D stress value of 0.14 providing confidence in the fit of the data points in the plot.
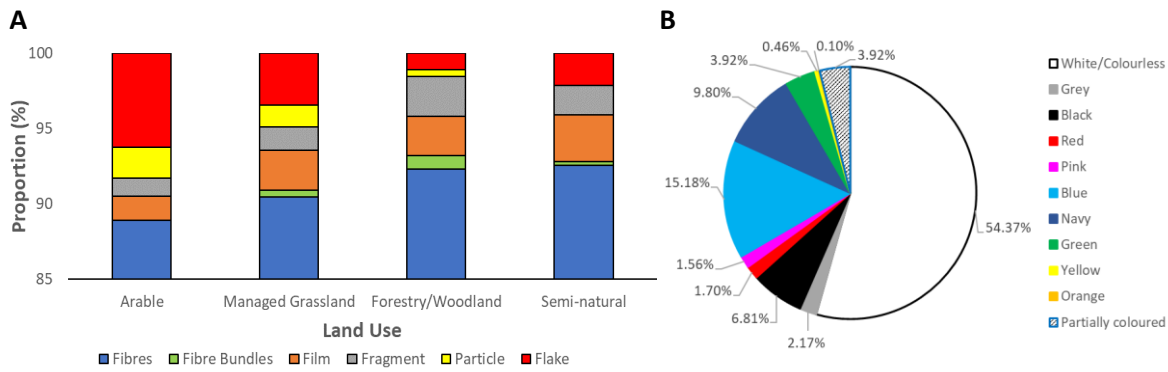
Figure 5.4: Proportion of (A) microplastic morphologies per land use and (B) total microplastics based on colours across Scottish soils.
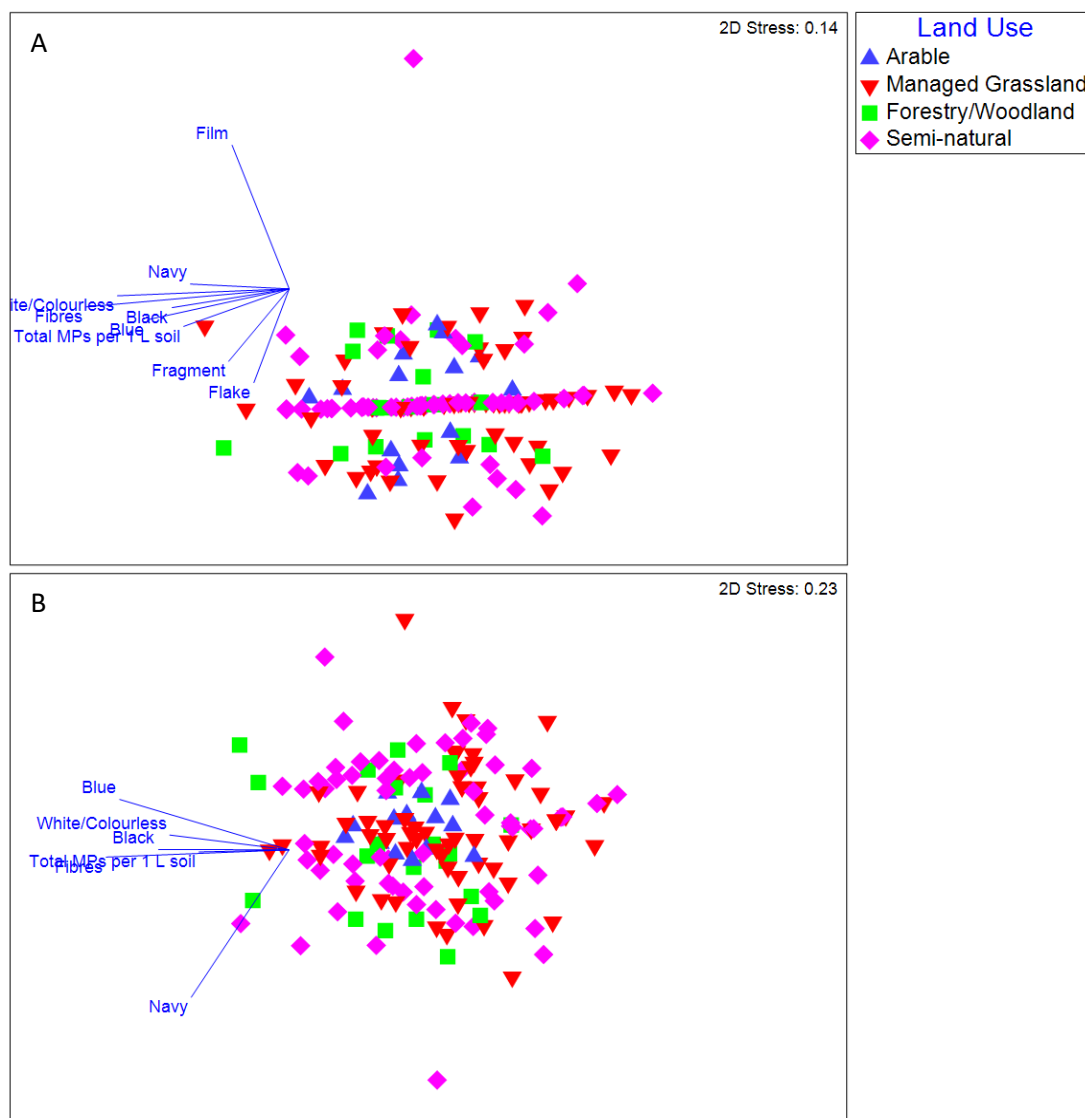
Figure 5.5: Non-metric multidimensional scaling plot (nMDS) of microplastic community composition within all soil samples by (A) morphology and (B) colour, in accordance with land use. Pearson's correlations (r < 0.4) are overlaid (abundance, morphologies, and colours).

A total of 10 colours of microplastics (all morphologies) were detected (Figure 5.4B), amongst which, the largest proportion were white or colourless (54.37%). This is consistent with previous studies where soils were treated with sewage sludges (e.g., Yang et al., 2021b). Blue was the second most abundant colour (15.18%), followed by navy (9.80%), black (6.81%), green (3.92%), grey (2.17%), red (1.70%), pink (1.56%), yellow (0.46%), and orange (0.10%). Partially dyed fibres alone accounted for the remaining 3.92%. These fibres were also detected and discussed in Chapter 4. However, their detection at a substantial abundance on a national scale across all regions and land uses indicates that their presence, and the loss of textile dyes, may pose an unknown, significant threat to Scotland's terrestrial environment nationwide. An nMDS plot was generated to evaluate the similarity in microplastic community compositions based on microplastic colour within soils in accordance with land use (Figure 5.5B). Figure 5.5B indicated that the microplastic community composition within these land use samples had a high level of similarity, resulting in the data points clustering together. Figure 5.5B also had a high 2D stress value of 0.23. The nMDS plot indicated that white or colourless, blue, black, and navy were the predominant microplastic colours influencing the variation in microplastic community composition (Figure 5.5B). Colour likely does not significantly differ within microplastic community compositions between land uses as microplastic colour is an arbitrary feature and not likely to be significantly influenced by land use.

5.3.2.2 Composition

Polyester was the most abundant microplastic composition recovered from soils across all land use categories (average of 24.53%; Figure 5.6) which has been identified as the most common polymer detected in soils in previous studies (Yang et al., 2021a; Schell et al., 2022), followed by nylon (16.13%) and acrylic (13.95%). This is due to the much higher proportion of fibres present in the soil samples. Polyester, nylon, and acrylic account for the majority of all synthetic textile materials (El Hayany et al., 2022). Polypropylene accounted for the highest proportion of microplastic compositions in forestry/woodland (28.57%; Figure 5.6) identified from films, flakes, and fragments. These microplastics may have originated from plastic tree guards (commonly composed of polypropylene) which are widely used to protect young trees from herbivores in forestry and woodland management (Wilson et al., 2015). Table 1.1 in Chapter 1 displays common uses for various plastic compositions.
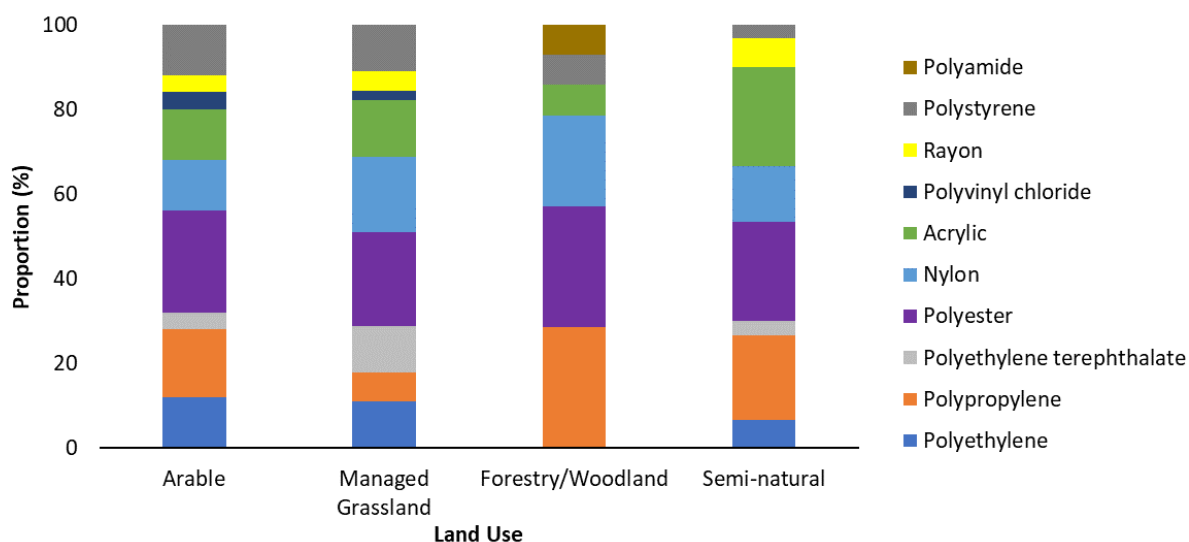
Figure 5.6: Proportion of microplastic compositions per land use.

Examples of microplastic spectra generated by FTIR are presented in Figure 5.7. Microplastics recovered from soil samples exhibited varying levels of weathering, most notable in polyethylene (Figure 5.7F), polypropylene (Figure 5.7G), and polyvinyl chloride microplastics (Figure 5.7I). Oxidation of polyolefins, such as polyethylene and polypropylene, leads to chemical changes in their simple C and H structures, whereby carbonyl groups (C=O) can form (Almond et al., 2020; Zvekic et al., 2022). As such, the appearance of carbonyl (C=O) bands (~1725 cm^{-1}) in IR spectra can indicate the level of weathering (oxidation) and they can be used as a method of monitoring oxidation over time by calculating the carbonyl index (the ratio of the area of the carbonyl band relative to the area of a reference peak which does not change over time) (Almond et al., 2020). The carbonyl index ranges were 0 to 3.64 and 0 to 4.34 for polyethylene and polypropylene, respectively, indicating there is a wide range of microplastic degradation across Scottish soils. Microplastics with carbonyl indices < 2.0 were comparable to other microplastics recovered from surface soils (Wahl et al., 2024), however, the few which were > 2.0 indicates that these microplastics were in an advanced weathering state. The carbonyl indices of the examples shown in Figure 5.7F (polyethylene) and Figure 5.7G (polypropylene) are 2.13 and 0.16, respectively. The appearance of broad hydroxyl (O-H) bands in their spectra (3500-3000 cm^{-1}) also indicates these microplastics are severely weathered (Zvekic et al., 2022). Arrows in Figure 5.7 indicate non-standard peaks in the IR spectra emerged due to weathering (oxidation). The weathering of other microplastic compositions have not been researched fully. Alterations in the chemical structures of polyethylene and polypropylene microplastics through oxidative degradation results in increased crystallinity, which weakens their structural integrity, leading to the production of secondary microplastics (Zvekic et al., 2022), as well as increased polarity allowing for elevated interactions with
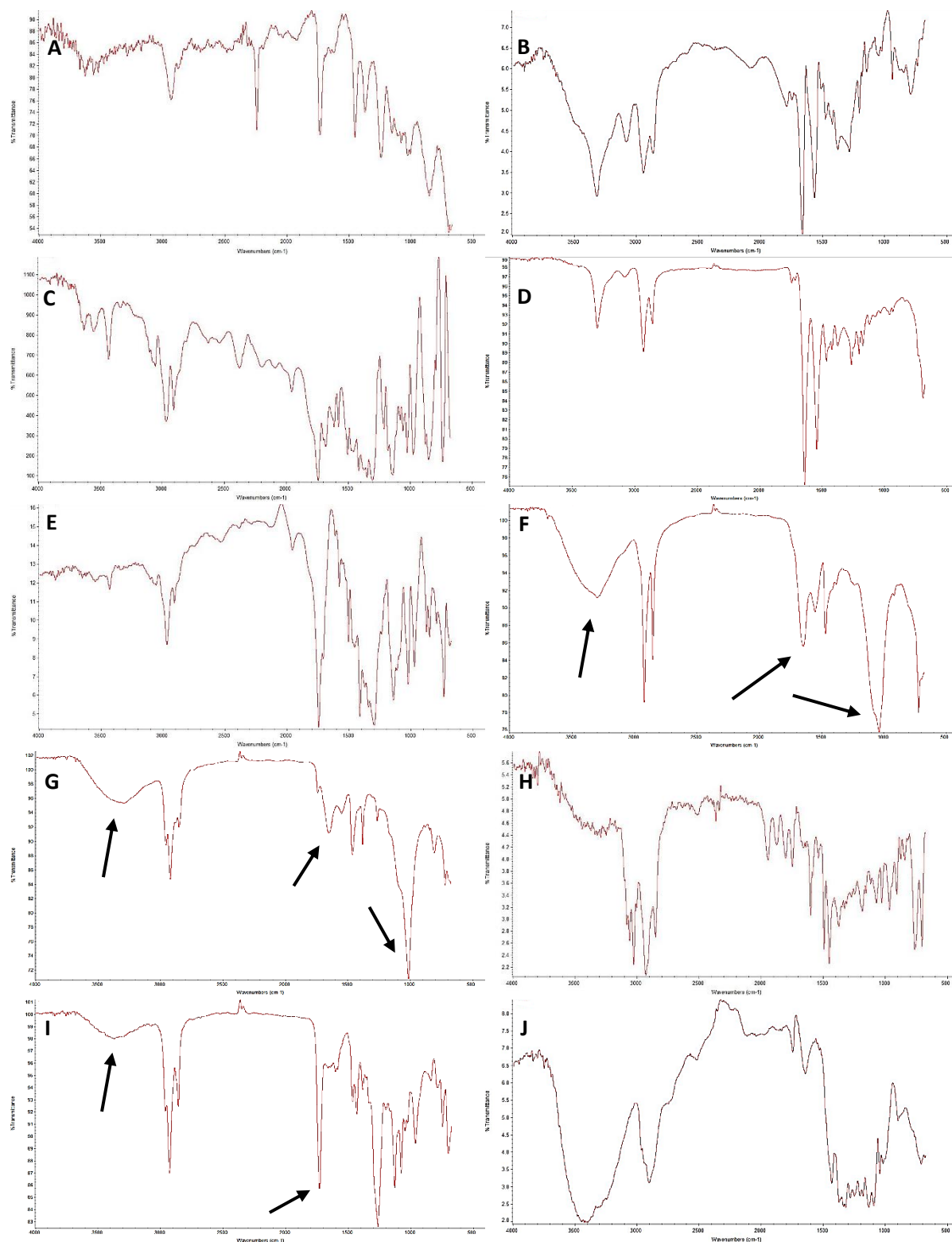
Figure 5.7: IR spectra of individual microplastics recovered from soil samples including: (A) acrylic fibre, (B) nylon fibre, (C) polyethylene terephthalate, (D) polyacrylic, (E) polyester fibre, (F) polyethylene, (G) polypropylene, (H) polystyrene, (I) polyvinyl chloride, and (J) rayon fibre. Arrows highlight additional peaks present in spectra most likely due to oxidation (weathering).

hydrophilic soil pollutants (Duan et al., 2021). The leaching of polymer additives toxic to soil microorganisms is also promoted through this weathering process (Bridson et al., 2023). The presence of weathered polyethylene and polypropylene microplastics in soils of all land use types with a high carbonyl index range raises concerns regarding their potential to accelerate the production of smaller, more hazardous micro- and nanoplastics, leaching of toxic additives into the surrounding soil, and potentially increased adverse interactions with other environmental pollutants in soils across Scotland through structural changes at their surface (see Chapter 6).

5.3.3 Factors influencing microplastic distribution

5.3.3.1 Geography, topography, and climate

The spatial distribution and abundance of microplastics was statistically significant between regions (*K-W* test, $p < 0.05$) and had a geographical relationship with easting ($r_S = 0.32$) and longitude ($r_S = 0.36$) showing greater microplastic abundances on the east of Scotland (Table 5.3 and Figure 5.3; Spearman correlations, $p < 0.05$), but not with northing or latitude (Spearman correlations, $p > 0.05$). This may be explained by the spatial distribution of land uses throughout Scotland, whereby arable soils are almost solely concentrated to the east of the country, managed grassland soils evenly spread across the western and eastern areas, forestry/woodland soils sparsely spread over the country, and semi-natural soils dominating the west of Scotland (Figure 5.2). Since arable soils contribute the highest microplastic abundances (see section 5.3.3.2), it is likely that this explains why eastern Scotland is more polluted with microplastics compared to the west.

This study considered topographical features including altitude, slope gradient, slope form and type, and slope bearing. Slope form and type (see section 5.2.1 for definitions) did not have a significant relationship with microplastic abundance (*K-W* test, $p > 0.05$). Abundance was negatively correlated with altitude (Spearman correlations, $r_S = -0.27$; $p < 0.05$), likely due to less human presence and activity at high altitude areas (Feng et al., 2023). As such, correlations were negative with slope gradient (Spearman correlations, $r_S = -0.28$; $p < 0.05$). The *Highlands* and *Argyll and Bute* are the hilliest areas of Scotland, and these areas were reported to have the lowest microplastic contamination (Table 5.1). This correlation between slope gradient may be a contributing factor to low microplastic levels in these soils in combination with other factors such as land use. Zhang et al. (2022c) previously reported that an increase in slope gradient promoted greater horizontal transport of microplastics through surface run-off which may also help explain the findings in this study. This could potentially lead to the

accumulation of microplastics at flatter, lower altitude areas below the slopes. The relationship between microplastics and the bearing of the slope was positive (Spearman correlations, r_S = 0.19; p < 0.05) indicating that slopes facing south to west had a higher microplastic abundance than those facing north to east. This is likely caused by prevailing winds in Scotland coming from the south-west (Turrell, 2019), which would promote atmospheric transportation and subsequent deposition to slopes facing into the prevailing winds (south through west). This is the first study to the author's knowledge to consider soil topography and, importantly, the significance of slope bearing and prevailing wind direction on microplastic distribution in soils.

Higher rainfall had a negative correlation with microplastic abundance across all soil samples (Spearman correlations, r_S = -0.47, p < 0.05). Semi-natural soils were also analysed by themselves so that land management did not confound any effects of precipitation. However, Spearman's correlation showed there was no significant relationship when assessing the semi-natural soils alone (p > 0.05). In a study by Abbasi and Turner (2021), it was reported that atmospheric microplastic deposition was greater during dry cycles compared to wet cycles, which supports the findings in this study. The wetter climate in Scotland may impede atmospheric fallout, leading to the negative correlation between rainfall and microplastics observed here. This indicates rainfall is not a prominent factor in microplastic pollution in Scottish soils or perhaps that higher rainfall causes the horizontal translocation of surface soil microplastics through surface run-off (Zhang et al., 2022c; Huerta Lwanga et al., 2023) or vertical translocation to subsoil layers through soil drainage (see Section 5.3.3.3). It is also important to consider that this may be a reflection of the fact that the west of Scotland has a wetter climate (Brown, 2017), whereby semi-natural soils dominate the west where less microplastics were found compared to the east which has more higher land management soil samples (i.e., arable and managed grassland) (Figures 5.2 and 5.3).

The final consideration for microplastic abundance and location was the distance of sampling locations to roads. The wearing of tyres and brakes of vehicles are known to be a significant pathway for microplastic pollution in the soil environment (Evangeliou et al., 2020; Myszka et al., 2023). Spearman's rank results showed that this was a negative relationship (r_S = -0.37, p < 0.05) indicating that the further the sampling location was from roadways, the lower the microplastic abundance. As well as tyre and brake wear microplastic particulates, locations nearer to roadways are subject to higher human activity and are more accessible to human presence than locations a greater distance away.

Table 5.3: Significant correlations between microplastic abundance and geographical, topographical, environmental, soil physicochemical, and pollutant data using Spearman's rank correlation test ($p < 0.05$). Values of r_s are presented in brackets. Positive correlations are in green and negative correlations in red.

Geographical, topographical, and environmental	Soil physico-chemical	DEHP	PBDE	PCB	PAH	PAH (continued)
Easting (0.35)	pH (0.32)	0.37	47 (2,2',4,4'-tetra-BDE) (0.42)	28 (2,4,4'-tri-CB) (0.46)	Naphthalene (0.37)	Chrysene (0.32)
Longitude (0.36)	Total carbon (-0.42)		99 (2,2',4,4',5-penta-BDE) (0.39)	52 (2,2',5,5'-tetra-CB) (0.41)	Acenaphthylene (0.22)	Benzo[b]fluoranthene (0.38)
Altitude (-0.27)	Organic carbon (-0.44)		100 (2,2',4,4',6-penta-BDE) (0.27)	101 (2,2',4,5,5'-penta-CB) (0.36)	Acenaphthene (0.26)	Benzo[k]fluoranthene (0.35)
Slope gradient (-0.28)	Bulk density (0.43)		153 (2,2',4,4',5,5'-hexa-BDE) (0.33)	118 (2,3',4,4',5-penta-CB) (0.32)	Fluorene (0.19)	Benzo[a]pyrene (0.25)
Slope bearing (0.19)			154 (2,2',4,4',5,6'-hexa-BDE) (0.25)	138 (2,2',3,4,4',5'-hexa-CB) (0.32)	Phenanthrene (0.18)	Indeno[1,2,3-cd]pyrene (0.34)
Rainfall (-0.47)			183 (2,2',3,4,4',5',6-hepta-BDE) (0.23)	153 (2,2',4,4',5,5'-hexa-CB) (0.34)	Fluoranthene (0.21)	Dibenzo[a,h]anthracene (0.34)
Distance from road (-0.37)			ΣPBDE (0.42)	180 (2,2',3,4,4',5,5'-heptaCB) (0.31) ΣPCB (0.42)	Pyrene (0.18) Benzo[a]anthracene (0.20)	Benzo[g,h,i]perylene (0.23) ΣPAH (0.33)

5.3.3.2 Land use

K-W test showed that land use had a significantly strong relationship with microplastic abundance (Table 5.3; $p < 0.05$). Notably, highly managed soils (i.e., arable soils) presented the highest microplastic abundances (average of 3756 ± 2259 microplastics L^{-1} soil), followed by managed grassland (1448 ± 1404 microplastics L^{-1} soil), forestry/woodland (827 ± 477 microplastics L^{-1} soil), and finally, minimally managed semi-natural soils (535 ± 295 microplastics L^{-1} soil). While variation is large within land use types, there is a clear, positive trend between the intensity of land management with microplastic pollution. This was anticipated since agricultural soils are more susceptible to microplastic pollution through well documented pathways (see Chapter 4; Yang et al., 2021a; Yang et al., 2021b) while semi-natural soils were anticipated to be less polluted due to their remote locations, sparse populations, generally poorer soil quality, and reduced levels of cultivation (see Section 5.3.3.3).

5.3.3.3 Soil physicochemical properties

Microplastics are known to affect the physicochemical properties of soil which can have negative implications on soil health and function (de Souza Machado et al., 2018; de Souza Machado et al., 2019). Soil texture did not show any significant relationship with microplastic abundance and neither did root depth of the vegetation present at the time of sampling (Table 5.3; Spearman correlations, $p > 0.05$). Li et al. (2021b) similarly reported that crops had no effect on the vertical migration of microplastics present in the topsoil layer (0-5 cm), however, significant relationships were observed with root depth of different crops and microplastic abundance and migration in subsoils (below 5 cm). Future studies would need to be conducted to determine the relationship between topsoil and subsoil microplastic abundances and influencing factors such as root type and depth, as this study examined the surface soil (0-5 cm) only.

It was revealed that microplastic abundance in topsoils (0-5 cm) was influenced by soil drainage (*K-W* test, $p < 0.05$). For example, soils with imperfect drainage had high abundance of microplastics (2301 ± 2289 microplastics L^{-1} soil), whereas soils that were freely drained had a lower abundance (607 ± 252 microplastics L^{-1} soil), which implies that the drainage of water may facilitate the vertical movement of microplastics from the topsoil horizon to deeper layers, particularly smaller-sized microplastics (e.g., those < 200 μm) (Ren et al., 2021). However, the leaching of microplastics through soil is limited by several factors including microplastic size and shape as well as soil pore size distribution and the presence of macro-pores (Huerta Lwanga et al., 2022). The findings in this study suggest it would be

advantageous for further research to establish the scale of microplastic pollution in Scottish subsoils (> 5 cm) and the influence of soil drainage on vertical microplastic translocation.

Microplastic abundances were positively correlated with soil pH (Spearman correlations, r_S = 0.32; p < 0.05) which is likely to be associated with the higher pHs found in arable soils (where soil pH is often maintained through liming). These soils were the most contaminated, while acidic semi-natural soils contained less microplastics (see section 5.3.3.2). However, the presence of microplastics has been shown to increase soil pH depending on the polymer type and morphology (Zhao et al., 2021).

Carbon content (both total and organic (loss on ignition)) had negative correlations with microplastic abundance (Spearman correlations, r_S = -0.42 and -0.44, respectively; p < 0.05). Semi-natural soils (e.g., peat soils) contained a significantly higher carbon content than soils classed under arable land management, thereby explaining why microplastics are negatively correlated with C content.

Soil bulk density also shared a positive relationship with microplastic abundance (Spearman correlations, r_S = 0.43; p < 0.05), again, likely due to the higher bulk density of arable soils compared to semi-natural soils. Microplastics can negatively affect bulk soil density, potentially because microplastics are less dense than soil minerals and because they can affect soil structure, pore spacing, and particle interactions within soil (de Souza Machado et al., 2018). Therefore, their high prevalence in dense arable soils may induce decreases in bulk density over time, decreasing the soil quality for arable use.

5.3.3.4 Soil type and vegetation

Soil group, parent material, and soil phase all had significant correlations with microplastic abundance (*K-W* test, p < 0.05) – definitions provided in section 5.2.1. Peatland type (basin or hill and blanket peat) did not have a significant relationship with microplastic abundance (*K-W* test, p > 0.05). The correlation of microplastics with soil group and its parent material reflect the variation in land use dependent on the properties of the soil. For example, peats provide low quality soils for grazing and have little other agricultural value (whereby levels of microplastic pollution are likely not to be significant – see section 5.3.3.2), whereas brown soils offer high fertility and widespread uses for agriculture/cultivation where

greater microplastic abundance is expected. This further reflects soil phase, whereby the soil group can suggest the likely land use (e.g., cultivation) or the degradative state of peatland soils.

K-W test showed that microplastic abundance also had significant relationship with vegetation ($p < 0.05$). Vegetation can also be an indication of land use, whereby cereals (e.g., barley, wheat, oilseed rape) are associated with soils managed under arable conditions, while heathers, brackens, and heaths are associated with semi-natural soils. Tree types and related vegetation are associated with forestry/woodland. Various grasses are associated with managed grassland. As such, microplastic correlations with, for example, cereals are likely a result of the agricultural land management practices involved in these soils rather than due to the vegetation directly. Soils with cereal crops contained a higher abundance of microplastics (3655 ± 2456 microplastics L^{-1} soil), while semi-natural soils containing vegetation such as blanket bog contained a lower abundance (403 ± 339 microplastics L^{-1} soil). Semi-natural soil vegetation may directly influence microplastic abundance in soil. Semi-natural vegetation, such as heather, thickly cover the surface of soils which may physically impede any microplastics reaching the topsoil, but rather entrap them unless perturbed. Little is known of the role that vegetation cover has on microplastic pollution of the underlying soil, although, Helcoski et al. (2020) also previously reported that microplastics were negatively correlated with vegetation cover in wetland soils. Further research would need to be conducted to assess the specific role that different vegetation has on microplastic distribution in the terrestrial environment.

5.3.3.5 Microplastic community composition is not influenced by land use

Non-metric multidimensional scaling (nMDS) plots were generated to evaluate the significance of patterns of microplastic community compositions (according to morphologies and colours) within soil samples classified by land use (Figure 5.8). The disparity of the samples when considering colour in the plots indicated that the microplastic community compositions between each of the land uses were similar, i.e., there was no clear separation or clustering of the data points. As such, Figure 5.8A had a high 2D stress value of 0.23. Colour likely does not differ within microplastic community compositions between land uses as microplastic colour is an arbitrary feature and not likely to be significantly influenced by land use. On the other hand, it was anticipated that the morphologies within microplastic community compositions would be significantly different between different land uses and result in separation and clustering of the data points in the nMDS plot based on the land use categories. For example, the use of mulching film and addition of sewage sludge within arable land would diversify the

microplastic community composition to include many microplastic morphologies including fibres, films, fragments, particles, and flakes (see Chapter 4), whereas the lack of human presence or direct use of plastics within locations of semi-natural soils would mean that their microplastic community compositions may be less diverse and restricted to only small, lightweight microplastics such as fibres which are more susceptible to atmospheric transport and deposition in remote areas. However, this was not the case as there was no separation of the data points in the nMDS plot (Figure 5.8B), whereby all the points, with the exception of a single semi-natural soil sample, were closely clustered together. This indicates that the morphological microplastic community composition of this sample was significantly different to all other soil samples (see section 5.3.2.1; Figure 5.5). This plot had a 2D stress value of 0.14 providing confidence in the fit of the data points in the plot. Soil physicochemical properties (pH, total C, and organic C) and PCB data (total and 2,4,4'-trichlorobiphenyl (PCB-28)) were the predominant factors influencing variation in the plot. Total and organic C, as well as pH, PCB-28, and ΣPCB, are likely influencing factors as a reflection of the soil's land use, e.g., semi-natural soils such as peat have significantly higher C contents, are more acidic than arable soils, and are less polluted with organic contaminants than highly managed soils.

5.3.4 The relationship between microplastic abundance and persistent organic pollutants

The abundance and spatial distribution of persistent organic pollutants (POPs) in Scottish topsoils have previously been reported by Rhind et al. (2013) using the same soil samples used in this study. POPs reported were DEHP, PBDEs, PCBs, and PAHs. DEHP is a common plasticiser added to plastics during manufacturing to increase their flexibility (Pivnenko et al., 2016), while PBDEs are a form of brominated flame retardant often found in plastic materials (Wu et al., 2019). PCBs can be present in plastics as a by-product of the manufacturing process (Yeo et al., 2020), whereas PAHs are present in plastics due to the decomposition of additives such as carbon black or extender oils (Alassali et al., 2020). As reported in Chapters 2, 6, and 7, microplastics act as vectors for these organic pollutants in the natural environment. Because of their association with plastics, potential correlations between microplastic abundance and distribution with these organic contaminants were investigated.

Spearman's rank showed there were positive correlations between microplastic abundance and the concentration of all total sums of each of the organic contaminant classes as well as individual congeners (Table 5.3; $p < 0.05$) with the exception of PBDE-28 (*2,4,4'-tribromodiphenyl ether*) and anthracene ($p > 0.05$). Significant correlations were observed with all PBDEs in this study (except PBDE-
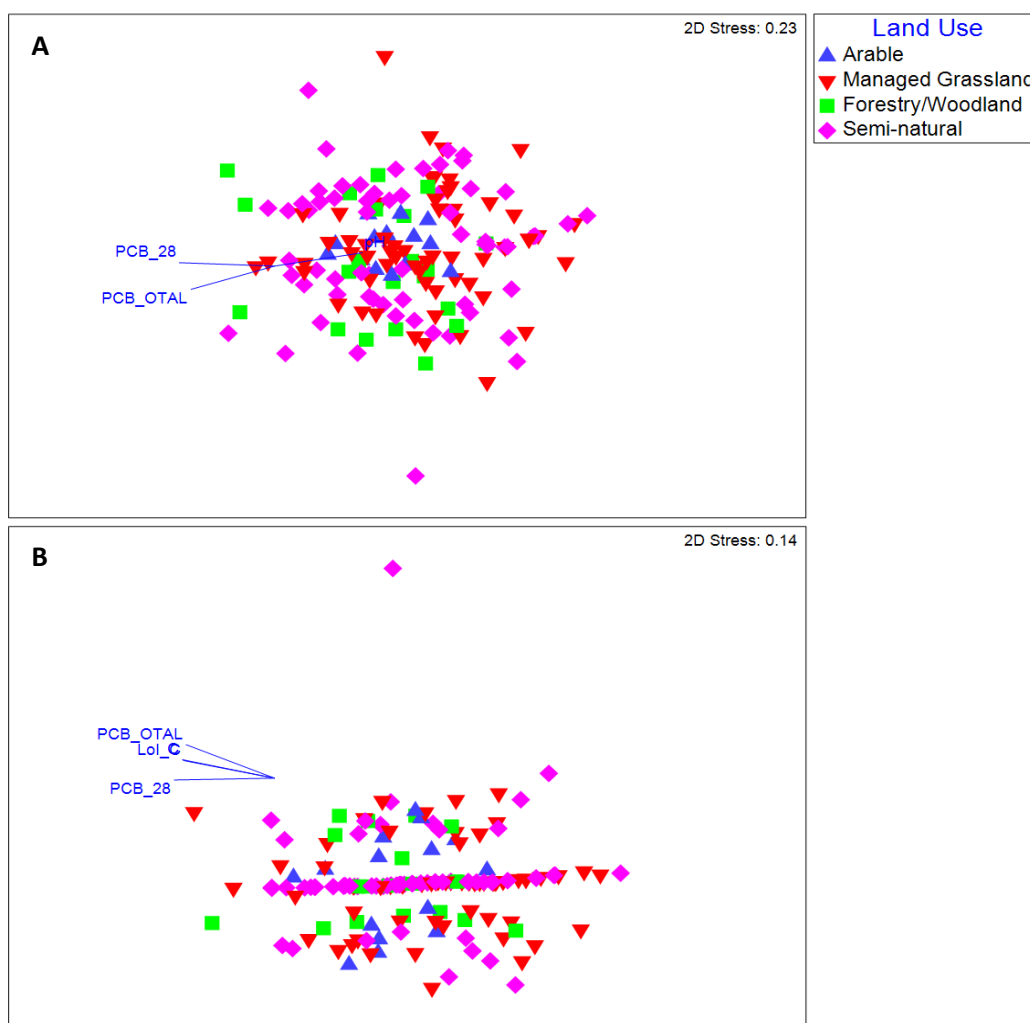
Figure 5.8: Non-metric multidimensional scaling plot (nMDS) of microplastic community composition within all soil samples by (A) colour and (B) morphology, in accordance with land use. Pearson's correlations (r < 0.4) are overlaid (pH, total C, organic C, ΣPCB, and 2,4,4'-trichlorobiphenyl).

28; $p > 0.05$) and microplastics (Spearman correlations, r_S = 0.23-0.42; $p < 0.05$; Table 5.3). Mixtures of penta- and hexa-BDEs (amongst other PBDEs) are commonly added to plastics as flame retardants (Tanaka et al., 2015), and all PBDE congeners measured as part of the NSIS dataset have previously been individually detected in environmentally retrieved microplastics (Tanaka et al., 2013; Tanaka et al., 2015). Significant correlations were also observed with all PAHs in this study (except anthracene; $p > 0.05$) and microplastics (Spearman correlations, r_S = 0.18-0.38; $p < 0.05$; Table 5.3). Anthracene is susceptible to photo-oxidation (Runberg and Majestic, 2022) which may explain the lack of correlation with microplastics. Similarly, all 16 PAH congeners recorded in the NSIS dataset have previously been detected in plastic products (Lassen et al., 2012; Weidmer et al., 2019) due to the use of petrochemical oils such as extender oils and carbon black (Alassali et al., 2020). PCBs, which have also been detected

in plastics (Li et al., 2012), also had a significant relationship with microplastics (Spearman correlations, r_S = 0.31-0.46; p < 0.05). Total PCB and PCB-28 (*2,4,4'-trichlorobiphenyl*) were also significant factors driving variation in the nMDS plot (see section 5.3.3.5; Figure 5.8). The common plasticiser, DEHP, also exhibited a significant relationship with microplastics (Spearman correlations, r_S = 0.37; p < 0.05).

These plastic additives and degradation products are commonly observed POPs in soils (Rhind et al., 2013), and some share common sources with plastics, e.g., petrochemicals. While the correlation of microplastics and POPs is significant, it is likely the spatial distribution and abundance of these contaminants is due to factors such as land use and atmospheric deposition amongst other influencing factors (Rhind et al., 2013). Nonetheless, their significant relationship with microplastics may indicate that microplastics could potentially contribute to organic contaminant pollution concentrations in soils through degradation and leaching or concentrate and spatially translocate these contaminants in soils through vectoring.

5.3.5 Microplastic sizes across Scotland

5.3.5.1 Geographical

Fibre lengths greatly varied across all soil samples with a range of 60 to 17000 µm. The longest average fibre lengths were from soils in *Falkirk* (3726.92 ± 3707.52 µm), whereas the shortest average fibre lengths were from soils in *Highlands* (912.50 ± 372.15 µm). Fibres can enter the terrestrial environment through a number of ways. Primary routes include the physical abrasion and shedding of fibres from synthetic clothing and secondary sources include household waste, utilisation of wastewater treatment products in soil management (sewage sludge (see Chapter 4) or repurposed wastewater effluent), atmospheric deposition, and surface water run-off (Zhou et al., 2020). Of all the fibres measured, 30.92% accounted for fibres ≤ 1000 µm, 31.58% for 1001-2000 µm, 18.42% for 2001-3000 µm, 7.89% for 3001-4000 µm, and 11.18% for fibres > 4000 µm. Fibre lengths reported in this study are within a similar range to previous publications regarding fibres in soils (He et al., 2018; Frost et al., 2022). The high proportion of small-sized microplastic fibres (< 1000 µm) increases the potential for increased soil stress as small microplastics are well established as being more toxic to soil biota compared to larger microplastics (Kim et al., 2023). All other morphologies displayed less variation in size across all soil samples: films (1075.00 ± 440.17 µm on the longest edge (100-2000 µm)), flakes (582.92 ± 279.58 µm (100-1200 µm)), particles (324.00 ± 168.34 µm (50-650 µm)), and fragments (468.18 ± 184.76 µm (250-

900 μm)). The size ranges reported in this study are also within a similar range to those reported in a previous soil-based study (Corradini et al., 2021).

Similarly with abundance (see section 5.3.3.1), microplastic size significantly varied geographically between regions (*K-W* test, p < 0.05) and had positive relationships with easting (r_S = 0.16) and longitude (r_S = 0.19) (Table 5.4; Spearman correlations, p < 0.05). Again, no relationships were observed between northing or latitude (Spearman correlations, p > 0.05). As discussed with microplastic abundance in section 5.3.3.1, this is likely a reflection of the spatial distribution of land uses throughout Scotland, whereby land use was also observed to have significant differences in microplastic size (*K-W* test, p < 0.05). Microplastics extracted from arable soils were observed to have the largest sizes (3071.35 ± 3186.88 μm), likely due to the direct use of plastic in these soils (e.g., mulch film) or the application of amendments containing microplastics (see Chapter 4; Elmi et al., 2020; Xu et al., 2020). Microplastic sizes then decreased in order of decreasing land management intensity: managed grassland (2775.96 ± 2285.04 μm), forestry/woodland (1073.33 ± 651.20 μm), and semi-natural (973.43 ± 564.11 μm). Wang et al. (2021b) previously reported that different managed land uses (arable and forestry/woodland) contributed different size ranges of microplastics, stating that cereal farm soils were more likely to contain large microplastics in the 1-5 mm size range, whereas orchard soils were likely to contain small microplastics (20-200 μm). The likely presence of microplastics in semi-natural soils is through atmospheric deposition (amongst other influencing factors such as tourism in certain locations), therefore, it was expected that microplastic sizes are smaller in these locations as atmospheric transportation and deposition favours smaller microplastic sizes (Zhang et al., 2020). The influence of different arable land uses (i.e., different crop types – see Table 5A.7) on microplastic size was further assessed, however, there was no statistical significance between microplastic size across the different arable land use samples (*K-W*, p > 0.05).

Another geographical feature assessed was the distance of the sampling location from the nearest road. Microplastic size was negatively correlated with distance from roadways (Spearman correlations, r_S = -0.29; p < 0.05) indicating that the further the sampling location was from roadways, the smaller the microplastics were. As with abundance, this is likely due to higher human presence and activity near roadways compared to locations further away. Microplastics in remote areas away from roads are likely to be present through atmospheric transportation and deposition which, as previously discussed, preferentially acts on smaller sized microplastics (Zhang et al., 2020).

Table 5.4: Significant correlations between microplastic sizes and geographical, topographical, environmental, and soil physicochemical data using Spearman's rank correlation test ($p < 0.05$). Values of r_S are presented in brackets. Positive correlations are in green and negative correlations are in red.

Geographical, environmental, and topographical data	Soil physicochemical data
Easting (0.16)	pH (0.35)
Longitude (0.19)	Total carbon (-0.30)
Distance from road (-0.29)	Organic carbon (-0.30)
Rainfall (-0.24)	Total nitrogen (-0.34)
Altitude (-0.26)	Bulk density (0.37)
Slope gradient (-0.21)	Root depth (-0.18)
Slope bearing (0.28)	%Clay (0.24)
	%Silt (0.27)
	%Sand (0.20)

5.3.5.2 Topographical and environmental

Topographical features (altitude, slope gradient, slope form and type, and slope bearing) were assessed. Contrary to microplastic abundance, slope form was found to have a significant relationship with microplastic size (*K-W*, $p < 0.05$). Slope form did not have a significant relationship with microplastic size (*K-W*, $p > 0.05$). The influence of altitude on microplastic size was investigated as microplastics are likely to be present at high altitudes due to atmospheric fallout which favours the transportation and deposition of smaller microplastic sizes (Feng et al., 2021). However, microplastic pollution in high altitude soil samples may also be present through tourism in some locations with easily accessible walking routes. Considering these points, it was anticipated smaller sized microplastics were present at higher altitudes. Microplastic size had negative relationships with altitude ($r_S = -0.26$) as well as slope gradient ($r_S = -0.21$) (Spearman correlations, $p < 0.05$) (Table 5.4), likely due to less human presence and activity at high altitude areas (Feng et al., 2023), increased surface run-off (Zhang et al., 2022c), and the preferential transport and deposition of smaller sized microplastics through the wind (Zhang et al., 2020). Altitude was split into three ranges (0-300, 301-600, and 601-900+ m) and the relationship between microplastic size range and altitude was assessed using the *K-W* test to establish where the microplastic size ranges observed in each altitude range were significantly different. There was a significant correlation between microplastic size and altitude (*K-W* test, $p < 0.05$),

whereby smaller microplastic sizes (60-1300 μm) were present in the highest altitude range (600-900+ m) and larger microplastic sizes (400-17000 μm) were present in the lower altitude range (0-100 m). This confirmed that remote, high-altitude soils are likely to be susceptible to smaller sized microplastic pollution due to the preferential atmospheric deposition of smaller sized microplastics. In relation to microplastic abundance, Spearman correlations revealed that the bearing of slopes had a positive relationship with microplastic size (r_S = 0.28; p < 0.05), indicating that slopes facing south through west were susceptible to higher microplastic abundances and larger microplastic sizes due to the prevailing wind direction (Turrell, 2019).

Higher rainfall had a negative correlation with microplastic size (Spearman correlations, r_S = -0.24; p < 0.05). This finding suggests that higher rainfall may cause the deposition of smaller sized microplastics. A study characterising microplastics in rainwater samples found that in wetter climates (i.e., higher rainfall), microplastics that were <100 μm dominated in the rainwater samples followed by 100-250 μm (Abbasi and Turner, 2021) suggesting that these smaller sized microplastics are more readily entrapped in rainwater and deposited in surface soils and water environments. Despite this, higher rainfall would cause more surface run-off which could wash away microplastics from higher altitudes, therefore, further studies monitoring the deposition of microplastics in rainwater to surface soils should be further investigated. As similarly described with abundance (see section 5.3.3.1), it is important to consider that western Scotland has a wetter climate in relation to eastern Scotland (Brown, 2017) which may explain this relationship. Furthermore, as reported, semi-natural soils (which dominate western Scotland – Figure 5.2) have smaller microplastic sizes compared to highly managed soils such as arable and managed grassland which are prevalent in the east (Figure 5.2).

5.3.5.3 Soil physicochemical properties

The relationships between microplastic size and soil physicochemical properties were also assessed. Microplastic size had positive relationships with soil pH (r_S = 0.35) and bulk density (r_S = 0.37), and negative relationships with total carbon (r_S = -0.30) and organic carbon (r_S = -0.30) (Spearman correlations, p < 0.05) (Table 5.4). As discussed in section 5.3.3.3, these correlations are likely to be associated with land use (i.e., higher pH, higher bulk density soils with low carbon levels are more suitable for arable use whereby larger microplastic sizes have been reported and discussed in section 5.3.5.1). However, considering this reasoning, it was anticipated that microplastic size would have a

positive relationship with total nitrogen, however, Spearman correlations revealed that this was a negative relationship (r_S = -0.34; p < 0.05) (Table 5.4).

Root depth had a negative relationship with microplastic size (Spearman correlations, r_S = -0.18; p < 0.05) (Table 5.4). This may indicate that smaller microplastics may more readily be translocated vertically downward during root growth through crack-entry pathways leaving larger sized fibres/microplastics in the surface soil (0-5 cm) (Li et al., 2020). There is limited research on the role of plant roots have on the movement of microplastics through soil in relation to their size, and these findings highlight the necessity for further research into the factors influencing the distribution of different microplastic sizes between different soil layers.

K-W test revealed that soil drainage also influenced microplastic size in topsoils (p < 0.05). Similarly with abundance, microplastic sizes were largest in soils with imperfect drainage (2971 ± 2909 µm), whereas soils with free drainage had the smallest microplastic size range (1045 ± 608 µm). This implies that the movement of water through soils with free drainage (suggesting larger soil pore sizes) promotes the vertical movement of smaller sized microplastics as well as potentially some larger sized microplastics to deeper soil layers. This finding, again, suggests it would be advantageous for further research to establish the abundance and size of microplastic pollution in Scottish subsoils (> 5 cm) and the influence of soil drainage on vertical microplastic translocation.

Soil texture of non-peat soil samples was assessed for relationships with microplastic size. Spearman correlation test revealed there were positive correlations with microplastic size (Table 5.4) – clay (r_S = 0.24), silt (r_S = 0.27), and sand (r_S = 0.20) (p < 0.05). These correlations may be linked to both land use and soil drainage whereby soil texture influences both of these parameters.

5.3.5.4 Soil type and vegetation

Soil group, parent material, and soil phase all had significant correlations with microplastic size (Table 5.3; *K-W* test, p < 0.05). As discussed in section 5.3.3.4, these relationships are likely reflections of land use.

Microplastic size also had a relationship with vegetation (*K-W* test, p < 0.05), another indicator of land use. Larger microplastics were observed in arable soils planted with cereal crops (3292 ± 378 µm) while semi-natural soils with vegetation such as blanket bog had the smallest microplastic sizes (450 ± 71 µm). It was considered in section 5.3.3.4 that dense semi-natural vegetation may physically impede microplastics reaching the topsoil through entrapment. Further to this, these findings suggest that larger microplastics are more likely to become entangled in this dense vegetation, allowing smaller sized microplastics to reach the surface soil underneath.

5.3.6 Microplastic pollution in the isolated archipelago of St. Kilda

Two soil samples collected from the largest island of the *St. Kilda* archipelago, *Hirta* (6.5 km^2), were assessed for microplastic pollution as the archipelago is highly remote, situated 55 km west of North Uist in *Na h-Eileanan an Iar* and 160 km west of mainland Scotland, and has not been permanently populated since the islanders were evacuated in 1930 (Donaldson et al., 2009). However, a small military base has been in operation there since 1957, whereby a small number of military (and National Trust for Scotland) employees are temporarily based on the island at various stages throughout the year. *Hirta* also receives a high yearly footfall of tourists visiting the island in the summer months. Therefore, it was of interest to investigate the effects of tourist and construction activities on soil microplastic pollution in a remote, uninhabited area. One sample was collected from *Am Baile*, the remains of the 19th Century village, and the other was collected at around 200 m on the slope of *Conachair* situated directly behind *Am Baile* to the northwest (Figure 5.3). *Am Baile* provides a high thoroughfare for tourists as it is the main historical attraction on the island, so it was anticipated that microplastic pollution would be higher here ("hotspot") compared to the *Conachair* soil sample which was anticipated to receive less footfall as it is further away from the tourist hotspot.

The abundance of microplastics was indeed greater in the soil sample from *Am Baile,* containing 4167 ± 520 microplastics L^{-1} soil, while *Conachair* measured nearly half of that in *Am Baile* (2167 ± 289 microplastics L^{-1} soil). This supports that *Am Baile* is a hotspot for microplastic pollution. The microplastic abundance of both *St. Kilda* samples were significantly higher than any other island soil sample in the NSIS dataset (n = 18) (*K-W* test, p < 0.05). Microplastic abundance for NSIS island samples ranged between 83 and 1167 microplastics L^{-1} soil. Fibres accounted for 96.0% of microplastics detected in the *Am Baile* sample, with fibre bundles and particles accounting for 2.0% each. Fibres accounted for 96.2% in the *Conachair* sample with flakes accounting for the remaining 3.9%. The average

proportion of microplastic morphologies for island samples from the NSIS dataset are as follows: 91.4% for fibres, 3.4% for films, 1.4% for fragments, 0.5% for particles, and 3.4% for flakes. It is appreciated that the *St. Kilda* samples (collected in 2013) and the NSIS island samples (2007-2009) may not be directly comparable (see Section 5.4). Nonetheless, the results here highlight that, despite *St. Kilda*'s remote, temporary and lowly inhabited nature, it is highly polluted compared to other islands with sparse but permanent populations, likely due to highly-concentrated, high-intensity tourism.

The predominant microplastic colour in the *St. Kilda* samples was white or colourless (Figure 5.9), accounting for 40.68% and 43.75% of microplastics in the *Am Baile* and *Conachair* samples, respectively. As discussed in Chapter 4 and in section 5.3.2.1, the high abundance of partially dyed fibres may be of environmental concern, which accounted for > 15% of all microplastic colours in both *St. Kilda* samples, the second highest proportion in both samples.
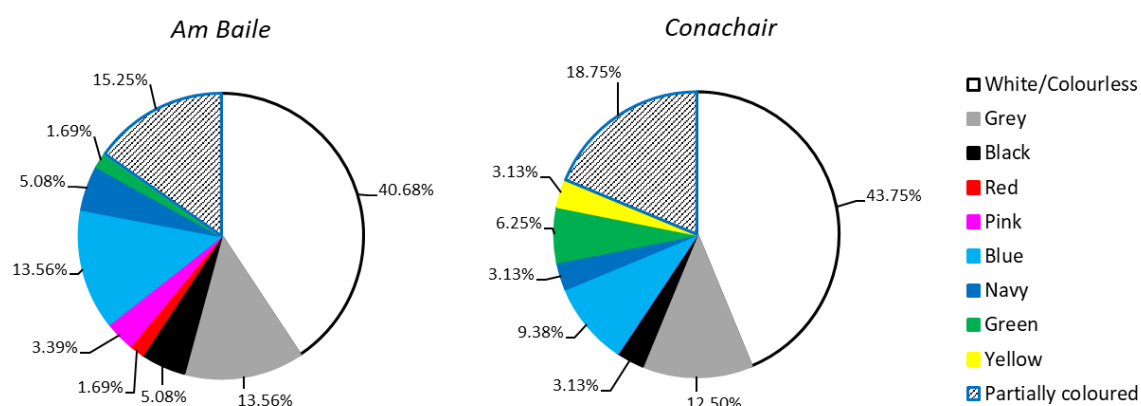
Figure 5.9: Pie charts of the proportion of microplastic colours in the *St. Kilda* soil samples.

Differences in microplastic composition were observed between the two samples (Figure 5.10). Polyester accounted for the highest proportion of microplastics in *Am Baile* (41.18%), while polyester and polyethylene both accounted for the highest proportion in *Conachair* (22.22% each). Polyester was also the most common polymer type identified in the NSIS samples (see Section 5.3.2.1 and Figure 5.5B). Polyethylene terephthalate was only found in the *Conachair* sample. Fibres identified as polyurethane were recovered from both soil samples (Figure 5.11A), which is an uncommonly recovered polymer type from soil samples. Polyurethane is commonly applied to fabrics as a waterproof coating (Joshi et al., 2023), therefore, it is possible these fibres may have originated from

waterproof clothing worn by tourists as well as resident military and National Trust for Scotland employees. Polyurethane is also a commonly used material in construction (Xing et al., 2023), therefore, these fibres may also be present in soil samples as a result of previous restoration works of the houses in the village (*Am Baile*) and other past modern construction works (e.g., military base).

Spectra generated from FTIR analysis of the microplastics indicated there was weathering present on all polyethylene microplastics, with a carbonyl index range of 0.02-2.13. The spectrum of polyethylene displayed as an example in Figure 5.11B had a carbonyl index of 0.29. There was a smaller carbonyl index range for these polyethylene microplastics compared to those in the NSIS dataset (0-3.64 – see section 5.3.2.2). This indicates that the polyethylene microplastics recovered from *St. Kilda* have been subjected to less weathering, suggesting that these microplastics may have been exposed to the environment for a shorter period of time. These samples were collected during the tourist season when footfall was high and the likelihood of direct microplastic deposition was higher.
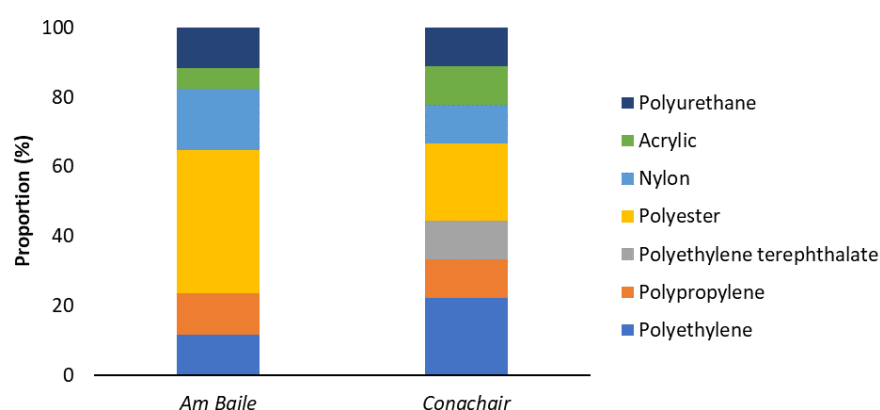
Figure 5.10: Proportion of microplastic compositions from two areas of *St. Kilda*.
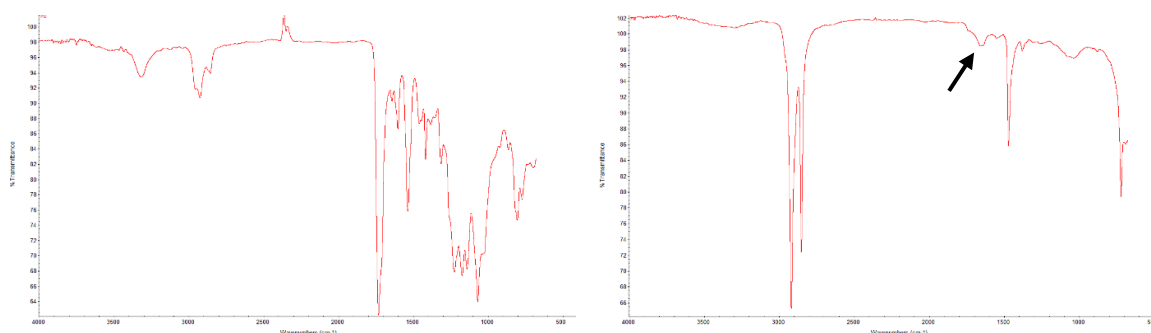
Figure 5.11: FTIR spectra of (A) polyurethane and (B) polyethylene. Arrow indicates the carbonyl band.

5.4 Limitations

Due to the scale of the sampling regime for the NSIS dataset, it was logistically implausible to collect all samples within a single year and, as such, the soil sampling took place over a three-year period. The significance of temporal changes in microplastic abundance is currently not known, particularly in minimally managed areas such as semi-natural soils, although microplastic abundance is more likely to change over time in highly managed soils (i.e., arable and some managed grassland areas) as observed in Chapter 4. Thus, there may be some temporal variation in microplastic abundances between samples of the same land use from each sampling year, however, samples were treated on the assumption no significant changes occurred throughout the three-year sampling period.

Some areas and land uses may have as few as one or two soil samples to represent that area or land use due to either the availability of samples or the size of the geographical area and the land uses represented in the 20 km grid points (Tables 5.1 and 5.2). Furthermore, the soil samples collected were obtained from a single soil core (7.5 x 5 cm) rather than a composite topsoil sample generated from multiple core samples across a designated area at the sampling location so may not be fully representative. Additionally, some soil samples were not available for this project due to the quantity of these samples being too low to allow for microplastic analysis, resulting in some sparsity in sample numbers in some regions (particularly the north/north-west of Scotland) (Figures 5.2 and 5.3).

The microplastic abundances in the *St. Kilda* samples were compared to the microplastic abundances reported from island samples as part of the NSIS dataset. A true comparison cannot be made as the NSIS dataset and the St. Kilda samples were collected a substantial period of time apart (2007-2009 and 2013, respectively). It is anticipated there may have been temporal changes in the microplastic abundances in soils from the NSIS island sampling locations between their time of sampling and 2013.

Nonetheless, the data generated provides important national background data on the environmental concentrations of microplastics in soils across Scotland and raises many issues for further investigation.

5.5 Conclusions and future perspectives

This is the first national scale study to assess microplastic pollution in soils. Microplastics in Scottish soils were dominated by synthetic fibres which were predominantly white or colourless, however,

there was also a high proportion of partially dyed fibres whereby the loss of their dyes (potentially into the surrounding soil) may have an unknown impact on the soil environment. Microplastics recovered from all regions and land uses displayed spectral signs of weathering (high carbonyl indices), also indicating potentially severe consequences for soil health and function. Through statistical evaluations (Spearman's and *K-W* test), it was concluded that the geographical, topographical, soil physicochemical, environmental, and persistent organic pollutant parameters have an influence on microplastic abundance in Scottish soils.

Arable and cultivated soils were founded to be the most polluted with microplastics and are larger sized likely due to the high intensity of land management and the use of plastics directly on the land or the introduction of microplastics through agricultural practices such as sewage sludge amendments (see Chapter 4). However, microplastic community compositions were not different between land uses. Similarly, sampling locations in close proximity to roadways and in areas of higher population densities (e.g., *Falkirk, Lothian*) had higher microplastic abundances and larger sizes compared to soils which were collected a greater distance away from roadways or in areas of low population densities (e.g., *Argyll & Bute, Na h-Eileanan an Iar*). This likely a result of human presence and interaction with the land being higher or lower in these areas.

This is the first study, to the author's knowledge, to investigate soil topography in relation to microplastic distribution in soils. Of significance, evaluation of the data indicated that slope bearing at sampling locations influenced microplastic abundance and size. Areas facing into the direction of prevailing winds were more susceptible to atmospheric deposition of microplastics than areas that were sheltered or faced away from the direction of prevailing winds. Furthermore, slope gradient also had a significant negative relationship with microplastic abundance, indicating that microplastics may be potentially translocated through processes such as horizontal surface run-off which may lead to accumulation at flatter, lower altitude areas. Microplastic size and abundance had a significant relationship with altitude, with smaller microplastic sizes being present at high altitudes due to the preferential atmospheric transportation and deposition of these smaller microplastics.

Significant relationships with soil bulk density, pH, total and organic C, soil group, and parent material were observed. These are likely explained due to these attributed relating to land use (e.g., acidic soils associated with peat (semi-natural) while more neutral, richer soils are associated with arable land).

Relationships with soil texture (and the differences in pore sizes associated with these soil texture) was only observed for microplastic size. Of interest, microplastics are known to affect the soil physicochemical parameters that microplastics were statistically related to. Furthermore, evidence from this study suggested that the vegetation present significantly influenced microplastic abundance and size. For example, dense semi-natural vegetation (e.g., heather) may physically impede microplastics reaching the surface of soils, particularly larger microplastics, and warrants further investigation.

There were significant correlations with persistent organic pollutants, including plasticisers, additives, and by-products, which each have links to plastic manufacturing and degradation, suggesting that microplastics may contribute to soil pollution of these contaminants through leaching or that they share a common anthropogenic source.

This study only assessed microplastics in the surface soils (0-5 cm) and the findings suggest that future work would be beneficial in measuring and assessing microplastic pollution in the lower soil horizons, and the factors which affect their distribution such as root depth and soil drainage, in which, results for this study suggest these factors may play an important role. Samples were also collected between 2007 and 2009 which are now over a decade old and may not accurately represent the current day level of microplastic pollution in Scotland. It is recommended that a new sampling and evaluation scheme is carried out in the future to compare with the results of this study.

Nonetheless, the generation of this background microplastic data allows the understanding and assessment of the scale of microplastic pollution in soils at a national scale, enabling the identification of potential mitigation strategies for preventing further significant terrestrial microplastic enrichment. Results reported in this study could be used to compare microplastic abundance to corresponding soils in future studies both nationally and internationally. Microplastics could also potentially be extracted from the first NSIS collection (1978-1987) to assess the changes in microplastic abundance over a substantial period of time at a national level. However, the influence of long-term storage of soil samples in plastic bags would need to be assessed first. Results could also be applied to modelling approaches to estimate microplastic abundance in samples from locations unavailable for assessment in this study. The potential effects that microplastics have on soil structure and function is well documented, and this study enables a better understanding of the potential consequences that may

occur through the physical and chemical presence of microplastics. Chapters 6 and 7 assess the chemical interactions and biological consequences of microplastic interactions with organic contaminants (specifically PAHs) which were found to have significant correlations with microplastic abundance in this study.

This work identified and highlighted several novel and important factors which influence microplastic distribution in Scottish soils, ranging from direct anthropogenic influences to natural and topographical features. However, this work also raises further important questions outlined above. This study provides precedence for future national scale studies on microplastics in soils both within and out with Scotland.

5.6 References

Abbasi S., Turner A. Dry and wet deposition of microplastics in a semi-arid region (Shiraz, Iran). *Science of the Total Environment*. 2021; 786, 147358. DOI: https://doi.org/10.1016/j.scitotenv.2021.147358

Alassali A., Calmano W., Gidarakos E., Kutcha K. The degree and source of plastic recyclates contamination with polycyclic aromatic hydrocarbons. *RSC Advances*. 2020; 10, 44989-44996. DOI: https://doi.org/10.1039/D0RA08554E

Allen S., Allen D., Phoenix V.R., Le Roux G., Jiménez P.D., Simonneau A., Binet S., Galop D. Atmospheric transport and deposition of microplastics in a remote mountain catchment. Nature geoscience. 2019; 12, 339-344. DOI: https://doi.org/10.1038/s41561-019-0335-5

Allen S., Allen D., Moss K., Le Roux G., Phoenix V.R., Sonke J.E. Examination of the ocean as a source for atmospheric microplastics. *PLoSONE*. 2020; 15, e0232746. DOI: https://doi.org/10.1371/journal.pone.0232746

Almond J., Sugumaar P., Wenzel M.N., Hill G., Wallis C. Determination of the carbonyl index of polyethylene and polypropylene using specified area under band methodology with ATR-FTIR spectroscopy. *E-Polymers*. 20, 369-381. DOI: http://dx.doi.org/10.1515/epoly-2020-0041

Bläsing M., Amelung W. Plastics in soil: analytical methods and possible sources. *Science of the Total Environment*. 2018; 612, 422–435. DOI: https://doi.org/10.1016/j.scitotenv.2017.08.086

Bourdages M.P.T., Provencher J.F., Baak J.E., Mallory M.L., Vermaire J.C. Breeding seabirds as vectors of microplastics from sea to land: Evidence from colonies in Arctic Canada. *Science of the Total Environment*. 2021; 764, 142808. DOI: https://doi.org/10.1016/j.scitotenv.2020.142808

Bridson J.H., Abbel R., Smith D.A., Northcott G.L., Gaw S. Impact of accelerated weathering on the leaching kinetics of stabiliser additives from microplastics. *Journal of Hazardous Materials*. 2023; 459, 132303. DOI: https://doi.org/10.1016/j.jhazmat.2023.132303

Brown I. Climate change and soil wetness limitations for agriculture: Spatial risk assessment framework with application to Scotland. *Geoderma*. 2017; 285, 173-184. DOI: http://dx.doi.org/10.1016/j.geoderma.2016.09.023

Chen K., Tang R., Luo Y., Chen Y., El-Nagga A., Du J., Bu A., Yan Y., Lu X., Cai Y., Chang S.X. Transcriptomic and metabolic responses of earthworms to contaminated soil with polypropylene and polyethylene microplastics at environmentally relevant concentrations. *Journal of Hazardous Materials*. 2022; 427, 128176. DOI: https://doi.org/10.1016/j.jhazmat.2021.128176

Conti G.O., Ferrante M., Banni M., Favara C., Nicolosi I., Cristaldi A., Fiore M., Zuccarello P. Micro- and nano-plastics in edible fruit and vegetables. The first diet risks assessment for the general population. *Environmental Research*. 2020; 187, 109677. DOI: https://doi.org/10.1016/j.envres.2020.109677

Corradini F., Casado F., Leiva V., Huerta-Lwanga E., Geissen V. Microplastics occurrence and frequency in soils under different land uses on a regional scale. *Science of the Total Environment*. 2021; 752, 141917. DOI: https://doi.org/10.1016/j.scitotenv.2020.141917

de Souza Machado A.A, Lau C.W., Till J., Kloas W., Lehmann A., Becker R., Rillig M.C. Impacts of Microplastics on the Soil Biophysical Environment. *Environmental Science and Technology*. 2018; 52, 9656-9665. DOI: http://dx.doi.org/10.1021/acs.est.8b02212

de Souza Machado A.A., Lau C.W., Kloas W., Bergmann J., Bachelier J.B., Faltin E., Becker R., Görlich A.S., Rillig M.C. Microplastics Can Change Soil Properties and Affect Plant Performance. *Environmental Science and Technology*. 2019; 53, 6044-6052. DOI: https://doi.org/10.1021/acs.est.9b01339

Donaldson M.P., Edwards K.J., Meharg A.A., Deacon C., Davidson D.A. Land use history of Village Bay, Hirta, St Kilda World Heritage Site: A palynological investigation of plaggen soils. *Review of Palaeobotany and Palynology*. 2009; 153, 46-61. DOI: http://dx.doi.org/10.1016/j.revpalbo.2008.06.005

Dris R., Gasperi J., Rocher V., Tassin B. Synthetic and non-synthetic anthropogenic fibers in a river under the impact of Paris megacity: sampling methodological aspects and flux estimations. *Science of the Total Environment*. 2018; 618, 157–164. DOI: https://doi.org/10.1016/j.scitotenv.2017.11.009

Duan J., Bolan N., Li Y., Ding S., Atugoda T., Vithanage M., Sarkar B., Tsang D.C.W., Kirkham M.B. Weathering of microplastics and interaction with other coexisting constituents in terrestrial and aquatic environments. *Water Research*. 2021; 196, 117011. DOI: https://doi.org/10.1016/j.watres.2021.117011

El Hayany B., Rumpel C., Hafidi M., El Fels L. Occurrence, analysis of microplastics in sewage sludge and their fate during composting: A literature review. *Journal of Environmental Management*. 2022; 317, 115364. DOI: https://doi.org/10.1016/j.jenvman.2022.115364

Elmi A., Al-Khaldy A., AlOlayan M. Sewage sludge land application: Balancing act between agronomic benefits and environmental concerns. *Journal of Cleaner Production*. 2020; 250, 119512. DOI: https://doi.org/10.1016/j.jclepro.2019.119512

Evangeliou N., Grythe H., Klimont Z., Heyes C., Eckhardt S., Lopez-Aparicio S., Stohl A. Atmospheric transport is a major pathway of microplastics to remote regions. *Nature Communications*. 2020; 11, 3381. https://doi.org/10.1038/s41467-020-17201-9

Feng S., Lu H., Yao T., Xue Y., Yin C., Tang M. Spatial characteristics of microplastics in the high-altitude area on the Tibetan Plateau. Journal of Hazardous Materials. 2021; 417, 126034. DOI: https://doi.org/10.1016/j.jhazmat.2021.126034

Feng S., Lu H., Yao T., Tang M., Yin C. Analysis of microplastics in soils on the high-altitude area of the Tibetan Plateau: Multiple environmental factors. *Science of the Total Environment*. 2023; 857, 159399. DOI: https://doi.org/10.1016/j.scitotenv.2022.159399

Frost H., Bond T., Sizmur T., Felipe-Sotelo M. A review of microplastic fibres: generation, transport, and vectors for metal(loid)s in terrestrial environments. *Environmental Science: Processes and Impacts*. 2022; 24, 504-524. DOI: https://doi.org/10.1039/D1EM00541C

Guo J.-J., Huang X.P., Xiang L., Wang Y.-Z., Li Y.-W., Li H., Cai Q.-Y., Mo C.-H., Wong M.-H. Source, migration and toxicology of microplastics in soil. *Environment International*. 2020; 137, 105263. DOI: https://doi.org/10.1016/j.envint.2019.105263

He D., Luo Y., Lu S., Liu M., Song Y., Lei L. Microplastics in soils: Analytical methods, pollution characteristics and ecological risks. *TrAC Trends in Analytical Chemistry*. 2018; 109, 163-172. DOI: https://doi.org/10.1016/j.trac.2018.10.006

Heinrich P., Braunbeck T. Bioavailability of microplastic-bound pollutants *in vitro*: The role of adsorbate lipophilicity and surfactants. *Comparative Biochemistry and Physiology, Part C.* 2019; 221, 59-67. DOI: https://doi.org/10.1016/j.cbpc.2019.03.012

Helcoski R., Yonkos L.T., Sanchez A., Baldwin A.H. Wetland soil microplastics are negatively related to vegetation cover and stem density. *Environmental Pollution*. 2020; 256, 113391. DOI: https://doi.org/10.1016/j.envpol.2019.113391

Horton A.A., Walton A., Spurgeon D.J., Lahive E., Svendson C. Microplastics in freshwater and terrestrial environments: Evaluating the current understanding to identify the knowledge gaps and future research priorities. *Science of the Total Environment*. 2017; 586, 127-141. DOI: https://doi.org/10.1016/j.scitotenv.2017.01.190

Huerta Lwanga E., Vega J.M., Quej V.K, de los Angeles Chi J., del Cid L.S., Chi C., Segura G.E., Gertsen H., Salánki T., van der Ploeg M., Koelmans A.A., Geissen V. Field evidence for transfer of plastic debris along a terrestrial food chain. *Scientific Reports*. 2017; 7, 14071. DOI: https://doi.org/10.1038/s41598-017-14588-2

Huerta Lwanga E., Beriot N., Corradini F., Silva V., Yang X., Baartman J., Rezaei M., van Schaik L., Riksen M., Geissen V. Review of microplastic sources, transport pathways and correlations with other soil stressors: a journey from agricultural sites into the environment. *Chemical and Biological Technologies in Agriculture*. 2022; 9, 20. DOI: https://doi.org/10.1186/s40538-021-00278-9

Huerta Lwanga E., van Roshum I., Munhoz D.R., Meng K., Rezaei M., Goossens D., Bijsterbosch J., Alexandre N., Oosterwijk J., Krol M., Peters P., Geissen V., Ritsema C. Microplastic appraisal of soil, water, ditch sediment and airborne dust: The case of agricultural systems. *Environmental Pollution*. 2023; 316, 120513. DOI: https://doi.org/10.1016/j.envpol.2022.120513

Joshi S., Midha V., Rajendran S. Multifunctional waterproof breathable coating on polyester-based woven protective clothing for healthcare application. *Progress in Organic Coatings*. 2023; 178, 107482. DOI: https://doi.org/10.1016/j.porgcoat.2023.107482

Kim S.-K., Kim J.-S., Lee H., Lee H.-J. Abundance and characteristics of microplastics in soils with different agricultural practices: Importance of sources with internal origin and environmental fate. *Journal of Hazardous Materials*. 2021; 403, 123997. DOI: https://doi.org/10.1016/j.jhazmat.2020.123997

Kim D., Kim H., An Y.J. Species sensitivity distribution of micro- and nanoplastics in soil based on particle characteristics. *Journal of Hazardous Materials*. 2023; 452, 131229. DOI: https://doi.org/10.1016/j.jhazmat.2023.131229

Lassen P., Hoffmann L., Thomsen M. (2012) *PAHs in toys and childcare products. Survey of Chemical Substances in Consumer Products No. 114 2011*. Danish Ministry of the Environment – Environmental Protection Agency.

Li Z., Li D., Ren J., Wang L., Yuan L., Lui Y. Optimization and application of accelerated solvent extraction for rapid quantification of PCBs in food packaging materials using GC-ECD. *Food Control*. 2012; 27, 300-306. DOI: http://dx.doi.org/10.1016/j.foodcont.2012.04.006

Li M., Liu Y., Xu G., Wang Y., Yu Y. Impacts of polyethylene microplastics on bioavailability and toxicity of metals in soil. *Science of the Total Environment*. 2021a; 760, 144037. DOI: https://doi.org/10.1016/j.scitotenv.2020.144037

Li H., Lu X., Wang S., Zheng B., Xu Y. Vertical migration of microplastics along soil profile under different crop root systems. *Environmental Pollution*. 2021b; 278, 116833. DOI: https://doi.org/10.1016/j.envpol.2021.116833

Li Y., Liu C., Yang H., He W., Li B., Zhu X., Liu S., Jia S., Li R., Tang K.H.D. Leaching of chemicals from microplastics: A review of chemical types, leaching mechanisms and influencing factors. *Science of the Total Environment*. 2024; 906, 167666. DOI: https://doi.org/10.1016/j.scitotenv.2023.167666

Lilly A., Bell J.S., Hudson G., Nolan A.J., Towers W. 2011. National Soil Inventory of Scotland 2007-2009: Profile description and soil sampling protocols. (NSIS_2). Technical Bulletin, James Hutton Institute.

Liu Z., Bai Y., Ma T., Liu X., Wei H., Meng H., Fu Y., Ma Z., Zhang L., Zhao J. Distribution and possible sources of atmospheric microplastic deposition in a valley basin city (Lanzhou, China). *Ecotoxicology and Environmental Safety*. 2022; 233, 113353. DOI: https://doi.org/10.1016/j.ecoenv.2022.113353

McLean E.O., 1982. Soil pH and Lime Requirement. In: A.L. Page, R.H. Miller, D.R. Keeney, eds. *Methods of Soil Analysis: Part 2 Chemical and Microbiological Properties*. 2nd edition. Wisconsin: American Society of Agronomy, Inc., Soil Science Society of America, Inc. pp 225-246.

Myszka R., Enfrin M., Giustozzi F. Microplastics in road dust: A practical guide for identification and characterisation. *Chemosphere*. 2023; 315, 137757. DOI: https://doi.org/10.1016/j.chemosphere.2023.137757

Nematollahi M.J., Keshavarzi B., Mohit F., Moore F., Busquets R. Microplastic occurrence in urban and industrial soils of Ahvaz metropolis: A city with a sustained record of air pollution. *Science of the Total Environment*. 2022; 819, 152051. DOI: http://dx.doi.org/10.1016/j.scitotenv.2021.152051

Panno S.V., Kelly W.R., Scott J., Zheng W., McNeish R.E., Holm N., Hoellein T.J., Baranski E.L. Microplastic Contamination in Karst Groundwater Systems. Groundwater. 2019; 57, 189-196. DOI: https://doi.org/10.1111/gwat.12862

Pella E., Colombo B. Study of carbon, hydrogen and nitrogen by combustion gas-chromatography. *Mikrochimica Acta*. 1973, 697-719. DOI: https://doi.org/10.1007/BF01218130

Pivnenko K., Eriksen M.K., Martín-Fernández J.A., Eriksson E., Astrup T.F. Recycling of plastic waste: Presence of phthalates in plastics from households and industry. *Waste Management*. 2016; 54, 44-52. DOI: https://doi.org/10.1016/j.wasman.2016.05.014

Prendergast-Miller M.T., Katsiamides A., Abbass M., Sturzenbaum S.R., Thorpe K.L., Hodson M.E. Polyester-derived microfibre impacts on the soil-dwelling earthworm *Lumbricus terrestris*. *Environmental Pollution*. 2019; 251, 453-459. DOI: https://doi.org/10.1016/j.envpol.2019.05.037

Ramage S.J.F.F., Pagaling E., Haghi R.K., Dawson L.A., Yates K., Prabhu R., Hillier S., Devalla S. Rapid extraction of high- and low-density microplastics from soil using high-gradient magnetic separation. *Science of the Total Environment*. 2022; 831, 154912. DOI: https://doi.org/10.1016/j.scitotenv.2022.154912

Ren Z., Gui X., Xu X., Zhao L., Qiu H., Cao X. Microplastics in the soil-groundwater environment: Aging, migration, and co-transport of contaminants – A critical review. *Journal of Hazardous Materials*. 2021; 419, 126455. DOI: https://doi.org/10.1016/j.jhazmat.2021.126455

Rhind S.M., Kyle C.E., Kerr C., Osprey M., Zhang Z.L., Duff E.I., Lilly A., Nolan A., Hudson G., Tower W., Bell J., Coull M., McKenzie C. Concentrations and geographic distribution of selected organic pollutants in Scottish surface soils. *Environmental Pollution*. 2013; 182, 182, 15-27. DOI: https://doi.org/10.1016/j.envpol.2013.06.041

Rolf M., Laermanns H., Kienzler L., Pohl C., Möller J.N., Laforsch C., Löder M.G.J., Bogner C. Flooding frequency and floodplain topography determine abundance of microplastics in an alluvial Rhine soil. *Science of the Total Environment*. 2022; 836, 155141. DOI: https://doi.org/10.1016/j.scitotenv.2022.155141

Runberg H.L., Majestic B.J. Hydroxyl radical (OH) formation during the photooxidation of anthracene and its oxidized derivatives. *Atmospheric Environment*. 2022; 286, 119214. DOI: https://doi.org/10.1016/j.atmosenv.2022.119214

Schell T., Hurley R., Buenaventura N.T., Mauri P.V., Nizzetto L., Rico A., Vighi M. Fate of microplastics in agricultural soils amended with sewage sludge: Is surface water runoff a relevant environmental

pathway? *Environmental Pollution*. 2022; 293, 118520. DOI: https://doi.org/10.1016/j.envpol.2021.118520

Scheurer M., Bigalke M. Microplastics in Swiss Floodplain Soils. *Environmental Science and Technology*. 2018; 52, 3591-3598. DOI: https://doi.org/10.1021/acs.est.7b06003

Shand C.A., Eriksson J., Dahlin A.S., Lumsdon D.G. Selenium concentrations in national inventory soils from Scotland and Sweden and their relationship with geochemical factors. Journal of Geochemical Exploration. 2012; 121, 4-14. DOI: http://dx.doi.org/10.1016/j.gexplo.2012.06.001

Tanaka K., Takada H., Yamashita R., Mizukawa K., Fukuwaka M., Watanuki Y. Accumulation of plastic-derived chemicals in tissues of seabirds ingesting marine plastics. *Marine Pollution Bulletin*. 2013; 69, 219-222. DOI: https://doi.org/10.1016/j.marpolbul.2012.12.010

Tanaka K., Takada H., Yamashita R., Mizukawa K., Fukuwaka M., Watanuki Y. Facilitated Leaching of Additive-Derived PBDEs from Plastic by Seabirds' Stomach Oil and Accumulation in Tissues. *Environmental Science and Technology*. 2015; 49, 11799-11807. DOI: https://doi.org/10.1021/acs.est.5b01376

Tian X., Yang M., Guo Z., Chang C., Li J., Guo Z., Wang R., Li Q., Zou X. Plastic mulch film induced soil microplastic enrichment and its impact on wind-blown sand and dust. *Science of the Total Environment*. 2022; 813, 152490. DOI: https://doi.org/10.1016/j.scitotenv.2021.152490

Turrell W.R. Spatial distribution of foreshore litter on the northwest European continental shelf. *Marine Pollution Bulletin*. 2019; 142, 583-594. DOI: https://doi.org/10.1016/j.marpolbul.2019.04.009

Wahl A., Davranche M., Rabiller-Baudry M., Pédrot M., Khatib I., Labonne F., Canté M., Cuisinier C., Gigault. J. Condition of composted microplastics after they have been buried for 30 years: Vertical distribution in the soil and degree of degradation. *Journal of Hazardous Materials*. 2024; 462, 132686. DOI: https://doi.org/10.1016/j.jhazmat.2023.132686

Wang F., Lai Z., Peng G., Luo L., Liu K., Huang X., Xu Y., Shen Q., Li D. Microplastic abundance and distribution in a Central Asian desert. *Science of the Total Environment*. 2021a; 800, 149529. DOI: https://doi.org/10.1016/j.scitotenv.2021.149529

Wang J., Li J., Liu S., Li H., Chen X., Peng C., Zhang P., Liu X. Distinct microplastic distributions in soils of different land-use types: A case study of Chinese farmlands. *Environmental Pollution*. 2021b; 269, 116199. DOI: https://doi.org/10.1016/j.envpol.2020.116199

Wang B., Chen X., Xiong X., Wu W., He Q., Hu H., Wu C. Spatial analysis of the influence on "microplastic communities" in the water at a medium scale. *Science of the Total Environment*. 2023; 885, 163788. DOI: https://doi.org/10.1016/j.scitotenv.2023.163788

Weidmer C., Velasco-Schön C., Buettner A. Toy swords revisited: identification of additional odour-active contaminants. *Journal of Consumer Protection and Food Safety*. 2019; 14, 415-419. DOI: https://doi.org/10.1007/s00003-019-01253-1

Wilson M.D., Menary R.C., Close D.C. Effects of tree guards and mulching on plantation establishment of 'Tasmanian Native Pepper' (*Tasmannia lanceolata* (Poir.) A.C. Smith). *Journal of Applied Research on Medicinal and Aromatic Plants*. 2015; 2, 154-159. DOI: http://dx.doi.org/10.1016/j.jarmap.2015.07.004

Wu Z., Han W., Yang X., Ki Y., Wang Y. The occurrence of polybrominated diphenyl ether (PBDE) contamination in soil, water/sediment, and air. *Environmental Science and Pollution Research*. 2019; 26, 23219-23241. DOI: https://doi.org/10.1007/s11356-019-05768-w

Xing W., Xi J., Qi L., Hai Z., Cai W., Zhang W., Wang B., Chen L., Hu Y. Construction of a flame retardant polyurethane elastomer with degradability, high mechanical strength and shape memory. *Composites Part A*. 2023; 169, 107512. DOI: https://doi.org/10.1016/j.compositesa.2023.107512

Xu B., Liu F., Cryder Z., Huang D., Lu Z., He Y., Wang H., Lu Z., Brookes P.C., Tang C., Gan J., Xu J. Microplastics in the soil environment: occurrence, risks, interactions and fate – a review. *Critical Reviews in Environmental Science and Technology*. 2020; 50, 2175-2222. DOI: https://doi.org/10.1080/10643389.2019.1694822

Xue Y., Li J., Jin T., Liu D., Zou G., Li F., Wang K., Xu L. Meso- and microplastic contamination in mulching cultivated soil at a national scale, China. *Journal of Cleaner Production*. 2023; 418, 138215. DOI: https://doi.org/10.1016/j.jclepro.2023.138215

Yang L., Zhang Y., Kang S., Wang Z., Wu C. Microplastics in soil: A review on methods, occurrence, sources, and potential risk. *Science of the Total Environment*. 2021a; 780, 146546. DOI: https://doi.org/10.1016/j.scitotenv.2021.146546

Yang J., Li L., Li R., Xu L., Shen Y., Li S., Tu C., Wu L., Christie P., Luo Y. Microplastics in an agricultural soil following repeated application of three types of sewage sludge: A field study. *Environmental Pollution*. 2021b; 289, 117943. DOI: https://doi.org/10.1016/j.envpol.2021.117943

Yang L., Kang S., Wang Z., Luo X., Guo J., Gao T., Chen P., Yang C., Zhang Y. Microplastic characteristic in the soil across the Tibetan Plateau. *Science of the Total Environment*. 2022; 828, 154518. DOI: http://dx.doi.org/10.1016/j.scitotenv.2022.154518

Yeo B.G., Takada H., Yamashita R., Okazaki Y., Uchida K., Tokai T., Tanaka K., Trenholm N. PCBs and PBDEs in microplastic particles and zooplankton in open water in the Pacific Ocean and around the coast of Japan. *Marine Pollution Bulletin*. 2020; 151, 110806. DOI: https://doi.org/10.1016/j.marpolbul.2019.110806

Yu H., Hou J., Dang Q., Cui D., Xi B., Tan W. Decrease in bioavailability of soil heavy metals caused by the presence of microplastics varies across aggregate levels. *Journal of Hazardous Materials*. 2020; 395, 122690. DOI: https://doi.org/10.1016/j.jhazmat.2020.122690

Zhang Y., Kang S., Allen S., Allen D., Gao T., Sillanpää M. Atmospheric microplastics: A review on current status and perspectives. *Earth-Science Reviews*. 2020; 203, 103118. DOI: https://doi.org/10.1016/j.earscirev.2020.103118

Zhang Y., Wang K., Chen W., Ba Y., Khan K., Chen W., Tu C., Chen C., Xu L. Effects of land use and landscape on the occurrence and distribution of microplastics in soil, China. *Science of the Total Environment*. 2022a; 847, 157598. DOI: http://dx.doi.org/10.1016/j.scitotenv.2022.157598

Zhang H., Yimel H., Shaoshan A., Haohao L., Xiaoqian D., Pan W., Mengyuan F. Land-use patterns determine the distribution of soil microplastics in typical agricultural areas on the eastern Qinghai-Tibetan Plateau. *Journal of Hazardous Materials*. 2022b; 426, 127806. DOI: https://doi.org/10.1016/j.jhazmat.2021.127806

Zhang X., Chen Y., Li X., Zhang Y., Gao W., Jiang J., Mo A., He D. Size/shape-dependent migration of microplastics in agricultural soil under simulative and natural rainfall. *Science of the Total Environment*. 2022c; 815, 152507. DOI: https://doi.org/10.1016/j.scitotenv.2021.152507

Zhao T., Lozano Y.M., Rillig M.C. Microplastics Increase Soil pH and Decrease Microbial Activities as a Function of Microplastic Shape, Polymer Type, and Exposure Time. *Frontiers in Environmental Science*. 2021; 9, 675803. DOI: https://doi.org/10.3389/fenvs.2021.675803

Zhou Y., Wang J., Zou M., Jia Z., Zhou S., Li Y. Microplastics in soils: A review of methods, occurrence, fate, transport, ecological and environmental risks. *Science of the Total Environment*. 2020; 748, 141368. DOI: https://doi.org/10.1016/j.scitotenv.2020.141368

Zhou Y., Wang J., Zou M., Yin Q., Qiu Y., Li C., Ye B., Guo T., Jia Z., Li Y., Wang C., Zhou S. Microplastics in urban soils of Nanjing in eastern China: Occurrence, relationships, and sources. *Chemosphere*. 2022; 303, 134999. DOI: https://doi.org/10.1016/j.chemosphere.2022.134999

Zhu J., Liu S., Shen Y., Wang J., Wang H., Zhan X. Microplastics lag the leaching of phenanthrene in soil and reduce its bioavailability to wheat. *Environmental Pollution*. 2022; 292, 118472. DOI: https://doi.org/10.1016/j.envpol.2021.118472

Zvekic M., Richards L.C., Tong C.C., Krogh E.T. Characterizing photochemical ageing processes of microplastic materials using multivariate analysis of infrared spectra. *Environmental Science: Processes Impacts*. 2022; 24,52-61. DOI: https://doi.org/10.1039/D1EM00392E

5.7 Appendix

Table 5A.1: Slope form and type.

Slope form	Number of samples	Slope type	Number of samples
Concave	18	Complex	55
Convex	34	Simple	89
Straight	92		

Table 5A.2: Soil drainage.

Drainage	Number of samples
Excessive	2
Free	44
Moderate	24
Poor	38
Very poor	23
Imperfect	27

Table 5A.3: Soil phase.

Soil phase	Number of samples
Cultivated	28
Hagged/severely eroded peat	2
Not classified	131

Table 5A.4: Peatland type.

Peatland type	Number of samples
Basin peat	6
Hill and blanket peat	20

Table 5A.5: Soil group.

Soil group	Number of samples	Soil group	Number of samples
Alpine podzol	5	Humic ranker	1
Brown calcareous soil	3	Humus-iron podzol	17
Brown forest soil	13	Iron podzol	2
Brown forest soil with gleying	13	Mesotrophic peat	2
Brown magnesian soil	5	Mineral alluvial soil	5
Brown podzolic soil	6	Non-calcareous gley	11
Brown ranker	5	Peaty gley	15
Brown rendzina	4	Peaty podzol	6
Calcareous regosol	4	Peaty podzol with gleying	5
Dystrophic peat	24	Peaty ranker	3
Gleyed ranker	1	Subalpine gley	1
Humic gley	6	Subalpine podzol	1

Table 5A.6: Parent material.

Parent material	Number of samples
Aeolian	7
Alluvium	4
Colluvium	20
Cryogenic	5
Fluvioglacial	9
Moraine	9
Organic	29
Raised beach	4
Residual	17
Scree	1
Till	43
Undefined	1
Water-modified till	9

Table 5A.7: Vegetation.

Vegetation	Number of samples	Vegetation	Number of samples
Alpine azalea - lichen heath	1	Flying bent - bracken grassland	1
Arable	3	Flying bent (Molinia) grassland	3
Brassicas - Oil seed rape	3	Heath grass - white bent grassland	2
Brassicas - Swedes/turnips	1	Larch plantation	2
Base-rich bracken scrub	1	Lichen-rich boreal heather moor	2
Bell-heather - Scots pine plantations	2	Lodgepole pine plantations	2
Bent - fescue grassland with bracken	1	Moist Atlantic heather moor	8
Blanket bog - terminal phase	1	Mountain blanket bog	6
Bog moss water track	1	Mountain blaeberry heath	1
Bog whortleberry heath	2	Northern Atlantic heather moor	5
Cereals - Barley (spring)	4	Northern bog heather moor	1
Cereals - Barley (winter)	3	Northern mossy dune	1
Cereals - Oats (spring)	1	Permanent & old ley pastures of rye-grass and crested dogs-tail	5
Cereals - Wheat (winter)	2	Rotational ley pastures of rye-grass and crested dogs-tail	24
Common bent - fescue grassland	4	Scots pine plantation	2
Common bog heather moor	3	Silver pine plantation	1
Common (lowland) blanket bog	6	Sitka spruce plantation	7
Common cotton-grass bog	1	Soft rush pasture	4
Coniferous plantation	3	Southern oakwood with bluebell	1
Cotton-grass bog	1	Species-poor sharp-flowered rush pasture	1
Dry Atlantic heather moor	4	Species-rich sharp-flowered rush pasture	3
Dry boreal heather moor	7	Spruce plantation	2
Eastern highland birchwood	1	Upland bent - fescue grassland	1
Eyebright - red fescue dune pasture (N and W fixed dune)	4	Upland blanket bog	1
Fescue - woolly fringe-moss heath	1	White bent (Nardus) grassland	2
Flying bent bog	2	White bent - tussock-grass grassland	1

Chapter 6: Sorption kinetics of polycyclic aromatic hydrocarbons on polyethylene microfilms in soil

Agricultural soils are more at risk of pollution from microfilms compared to other soils due to mulch film degradation and organic pollutants are also prevalent in these soils through other agricultural practices. The role of microplastics sequestering organic pollutants in soil is still relatively unclear. Furthermore, studies investigating these interactions soil suspensions which do not mimic the natural soil environment. Therefore, the sorption and desorption kinetics of 16 priority polycyclic aromatic hydrocarbons (PAHs) on two different sizes of polyethylene microfilms (2 x 2 and 5 x 1 mm) was investigated using a true agricultural soil matrix over a 30-day period. Sorption data fitted a first order equilibrium model while desorption data fitted an exponential decay model. All PAHs except 6-fused ring PAHs in the 2 x 2 mm microfilms and 4-6-fused ring PAHs in the 5 x 1 mm microfilms reached equilibrium in the 30-day period. Additionally, the rates of sorption and desorption for ≤3-fused ring PAHs were two-fold faster than 4-6-fused ring PAHs ($p < 0.05$), indicating that sorption and desorption kinetics were influenced by the molecular weight, water solubility, and logK_{ow} values of PAHs. No significant differences between corresponding rates of sorption or desorption were observed. Decreases in soil organic matter indicated that the smaller-sized microfilms sequestered a higher amount of PAHs (3.36% decrease compared to 2.93%). Soils undergoing sorption underwent significant acidification throughout the 30-day period, possibly due to the production of acidic degradation products through microbial degradation. This suggests that PAH sorption to microfilms decreases their availability for degradation, thereby alleviating the soil from acidification which would negatively impact crop production. However, the interaction of these toxic PAHs with microfilms in agricultural soils may lead to prolonged exposure of PAHs to the soil environment, crops intended for human consumption, livestock, and humans.

6.1 Introduction

Agriculture has been identified as a potentially significant source of plastic waste and their soils a sink for microplastic pollution, with annual global plastic use in agricultural production estimated at 12.5 million tonnes (FAO, 2021). Films (mulching or silage wrap) are the highest used plastic in crop and livestock production, accounting for an estimated 75% of European Union agricultural plastic (FAO, 2021), while China is recorded as the highest consumers of plastic films worldwide (Liu et al., 2014). Mulching films, predominantly composed of polyethylene, are widely used due to their benefits in improving crop production and health by protecting crops from harsh environmental conditions by

modifying soil temperature, reducing evapotranspiration, and suppressing weed growth (Ng et al., 2018). As such, their use in agricultural crop production has dramatically increased over time and is expected to rise over the coming years due to higher global demand in crop yields (Kasirajan and Ngouajio, 2012). Due to their prevalence in agronomy worldwide, plastic films pose a substantial threat to agroecosystems through the direct release of microplastics as a result of their degradation or mismanagement. Mulching and silage films throughout their operational life cycle are subjected to UV, chemical, biological, and mechanical degradation processes (Astner et al., 2019; Wang et al., 2021a) causing the production of film-derived macro- and microplastics which leak into the surrounding soil. Furthermore, the labour intensiveness of mulching film retrieval and disposal may lead to the abandonment or deposition of the films in agricultural fields, further facilitating the release of microplastics (Huang et al., 2020).
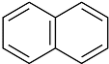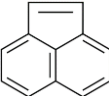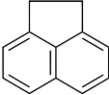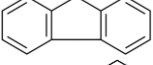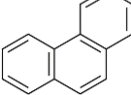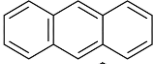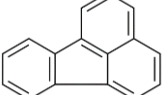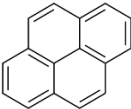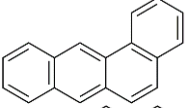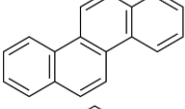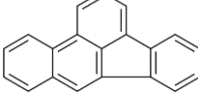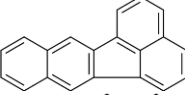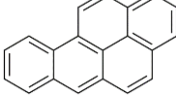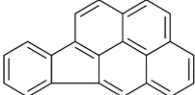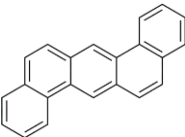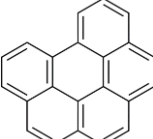
Microplastics may also be introduced to agricultural environments through indirect pathways, such as the applications of sewage sludge or other organic composts (see Chapter 4). These soil amendments are one of the principal source of microplastic pollution within the agriculture industry. In addition to microplastics, sewage sludges are also significant sources of biological (e.g., pathogens) (Gholipour et al., 2022), inorganic (e.g., heavy metals) (Gibbs et al., 2006), and organic contaminants (e.g., polycyclic aromatic hydrocarbons (PAHs)) (Suciu et al., 2015). PAHs are ubiquitous in the environment and can originate from both natural and anthropogenic activities. PAHs can also be produced in agricultural soils during the burning of crop residues and other wood-based materials in farms (Yadav et al., 2022). PAHs can also be found in agricultural soils where no amendment or burning practices have been used as well as non-agricultural soils (Rhind et al., 2013). Soil microbes can be susceptible to high concentrations of PAHs which can negatively affect microbial populations, metabolic process, and enzyme activities (Picariello et al., 2020). PAHs can also adversely affect growth and inhibit physiological processes such as photosynthesis in crops, thus reducing crop yields (Jajoo et al., 2014). Crops may also uptake PAHs from contaminated soils (Wang et al., 2017) which can potentially lead to a critical pathway for human exposure of these toxic, mutagenic, and carcinogenic contaminants.

While microplastics and PAHs can independently induce negative impacts on the soil environment, the sorption of PAHs to microplastics may pose a greater, long-term risk. Microplastics can act as vectors for chemical pollutants and biological agents in both marine and soil environments (Tumwesigye et al., 2023). Due to the large surface area and hydrophobicity, microplastics are capable of sorbing a large range of different organic contaminants through various sorption mechanisms including partitioning,

surface sorption (hydrogen bonding, π-π and electrostatic interactions, and van der Waals force), and pore filling (Wang et al., 2020). Several factors affect the sorption of organic contaminants including environmental factors (e.g., temperature, pH, dissolved organic matter), microplastic physicochemical characteristics (e.g., chemical composition, particle size, degree of aging, additives), and organic contaminant properties (e.g., polarity, molecular weight and structure, hydrophobicity, functional groups) (Xia et al., 2023). Although more work has been carried out in the marine environment (Amelia et al., 2021), the ecological impact of organic contaminant-sorbed microplastics in the soil environment is largely under researched and currently poorly understood. However, the sorption of organic contaminants may prolong their environmental exposure and limit their bioavailability for microbial degradation. To the author's knowledge, very few studies have investigated the sorption and desorption of PAHs to microplastic sized films (microfilms) derived from mulching film, despite agricultural film representing the largest use of plastic across all agricultural practices (FAO, 2021). Furthermore, no studies to the author's knowledge have investigated the sorption and desorption behaviour of PAHs to microplastics in a true soil matrix as soil-based studies typically employ a soil suspension approach for sorption experiments which are not always environmentally realistic (e.g., Zhang et al., 2021; Li et al., 2022; Sahai et al., 2023; Yu et al., 2023) and often promote chemical interactions through sample agitation which rarely occurs frequently in short periods of time in an agricultural setting. The significant correlations reported in Chapter 5 between microplastics and PAHs across Scotland raises concerns to the magnitude of the unknown consequences of their potential interactions in soils.

It was the aim of this study to investigate the simultaneous sorption and desorption behaviour of sixteen (16) priority PAHs (Table 6.1) to microfilms derived from mulching film in a true soil matrix obtained from an agricultural field under environmentally realistic conditions. These PAHs (as listed by the United States Environmental Protection Agency) were selected for this study as they are recognised worldwide as representative PAHs for chemical analyses associated with their toxicity and potential for human exposure, persistence, as well as their frequency in hazardous wastes.

Table 6.1: Physicochemical properties of polycyclic aromatic hydrocarbons (Yates et al., 2007; Patel et al., 2020). Structures were created using ChemDraw.

Name	Structure	Formula	Molecular weight (g/mol)	Solubility in water (mg/L)	$\log K_{ow}$
Naphthalene (Nap)		$C_{10}H_8$	128.17	31	3.35
Acenaphthylene (Acy)		$C_{12}H_8$	152.20	16.1	3.61
Acenaphthene (Ace)		$C_{12}H_{10}$	154.21	3.8	3.92
Fluorene (Flu)		$C_{13}H_{10}$	166.22	1.9	4.18
Phenanthrene (Phe)		$C_{14}H_{10}$	178.23	1.1	4.52
Anthracene (Ant)		$C_{14}H_{10}$	178.23	0.045	4.50
Fluoranthene (Fluo)		$C_{16}H_{10}$	202.26	0.26	5.20
Pyrene (Pyr)		$C_{16}H_{10}$	202.26	0.132	5.00
Benz[a]anthracene (BaA)		$C_{20}H_{12}$	228.29	0.011	5.91
Chrysene (Chr)		$C_{18}H_{12}$	228.29	0.0015	5.86
Benzo[b]fluoranthene (BbF)		$C_{20}H_{12}$	252.32	0.0015	5.78
Benzo[k]fluoranthene (BkF)		$C_{20}H_{12}$	252.32	0.0008	6.11
Benzo[a]pyrene (BaP)		$C_{20}H_{12}$	252.32	0.0038	6.35
Indeno[1,2,3-cd]pyrene (IcdP)		$C_{22}H_{12}$	276.34	0.062	7.66
Dibenz[a,h]anthracene (DahA)		$C_{22}H_{14}$	278.35	0.0005	6.75
Benzo[g,h,i]perylene (BghiP)		$C_{22}H_{12}$	276.34	0.00026	6.90

6.2 Materials and Methods

6.2.1 Chemicals and materials

All solvents were of analytical grade and 18 MΩ Milli-Q water was used throughout. Dichloromethane, *iso*-hexane, and methanol were supplied by Rathburn Chemicals. A standard mixture of 16 PAH including naphthalene (Nap), acenaphthylene (Acy), acenaphthene (Ace), fluorene (Flu), phenanthrene (Phe), anthracene (Ant), fluoranthene (Fluo), pyrene (Pyr), benz[*a*]anthracene (BaA), chrysene (Chr), benzo[*b*]fluoranthene (BbF), benzo[*k*]fluoranthene (BkF), benzo[*a*]pyrene (BaP), indeno[1,2,3-*cd*]pyrene (IcdP), dibenz[*a,h*]anthracene (DahA), and benzo[*g,h,i*]perylene (BghiP) prepared in dichloromethane (DCM) was supplied by Restek (approximately 2000 µg/mL of each standard and >98% purity). Internal standards (naphthalene-*d*8, acenaphthene-*d*10, fluorene-*d*10, phenanthrene-*d*10, anthracene-*d*10, pyrene-*d*10, and chrysene-*d*12) were prepared in-house using solid standards to a concentration of 2 µg/mL in methanol. Sodium sulphate (analytical grade) was purchased from Honeywell Fluka® and muffled at 450 °C before use.

A sheet of pristine polyethylene mulching film (thickness = 0.065 mm) was obtained from a local farmer and was cut by hand into approximately 2 x 2 and 5 x 1 mm microfilms using a scalpel. The scalpel blade was sequentially rinsed with acetone, DCM, and *iso*-hexane to remove any potential organic contaminants, and the microplastics were subsequently rinsed with deionised water to remove potential adhered contaminants and dirt. FTIR analysis was employed to confirm the composition of the mulching film and to assess the degree of weathering using a Nicolet™ iN10 infrared microscope with Ge ATR (attenuated total reflectance) attachment. Spectra were obtained using a liquid nitrogen-cooled MCT detector in the range of 4000-650 cm^{-1} at a resolution of 4 cm^{-1} with an average of 128 scans. Air blank spectra were recorded after each measurement with the same number of scans and resolution. The average carbonyl index (CI) of the microfilms (n = 7) at the start of the experiment was calculated using equation 6.1 to assess the level of weathering (oxidation) on the microfilm's surface using the areas of the carbonyl (I_{1725}) and the methylene (I_{1472}) bands (Syranidou et al., 2023). The band areas were generated using the peak area function tool in the OMNIC software.

$$CI = \frac{I_{1725}}{I_{1472}}$$
(6.1)

The surface texture (topography) of the mulching film was assessed using a Zeiss EVO LS10 SEM in variable pressure mode. The film was sputter coated in gold and imaged using a variable pressure secondary electron detector at a 6.0 mm working distance. The chamber pressure was set to 100 Pa with a beam current of 100 μA, probe current of 100 pA, and an accelerating potential of 25 kV.

Surface soil (0-10 cm), characterised as a sandy loam through particle size distribution analysis, was obtained from improved grassland in Collieston, Aberdeenshire (Scotland, UK). Stones and plant material were removed while the soil remained wet using a sieve with a mesh size of 6.5 cm, before final wet sieving to 2 mm. The soil was stored at 4 °C from time of collection until the start of the experiment. Particle size distribution was determined by laser diffraction (British Standards Institution, 2009) using a Mastersizer 3000 particle analyser with Hydro LV sample dispersion unit (Malvern Panalytical). The soil's maximum water holding capacity was determined gravimetrically using the method described by Voroney (2019).

All glassware used was machine-washed and muffled at 450 °C for 12 h to eliminate the potential for any organic contamination. All work was conducted in a fume hood to minimise contamination.

6.2.2 Kinetics studies

Individual jars containing 20 g soil were set up in triplicate for sacrificial sampling on days 0, 1, 3, 5, 7, 14, and 30. The treatments were as follows: *soil only, soil + PAH, soil + 5 x 1 mm microfilm, soil + 2 x 2 mm microfilm*, *5 x 1 mm desorption*, *5 x 1 mm adsorption*, *2 x 2 mm desorption*, and *2 x 2 mm adsorption* (Figure 6.1) (see section 6.3.2.1 for discussion on microfilm sizes). All soils were spiked with their respective microfilms at an environmentally relevant concentration of 1% (w/w) (de Souza Machado et al., 2018) and were mixed for 2 h on an end-over-end shaker to evenly distribute the microfilms throughout the soil. To mimic the behaviour of soil in the environment, once the treatments were set up, the soil was left undisturbed (i.e., not shaken or stirred) for the remainder of the experiment. The tops of the jars were covered in perforated aluminium foil to prevent the surface of the soil drying out quickly and minimising any potential interferences contaminating the soils. The soils were also maintained at 60% of their maximum water holding capacity (WHC_{max}) throughout the experiment. The weight of each jar was recorded at the beginning of the experiment and the $WHC_{60\%}$ was maintained by adjusting the weight lost through soil evapotranspiration by evenly distributing droplets of Milli-Q water over the surface of the soil using a Pasteur pipette until the soil reached their respective start

weights. Soil moisture was adjusted as necessary. All jars were kept in the dark to prevent photodegradation of the PAHs in an environmentally controlled room with a temperature of 20 ± 0.5 °C and a humidity of 70 ± 1.0 %.
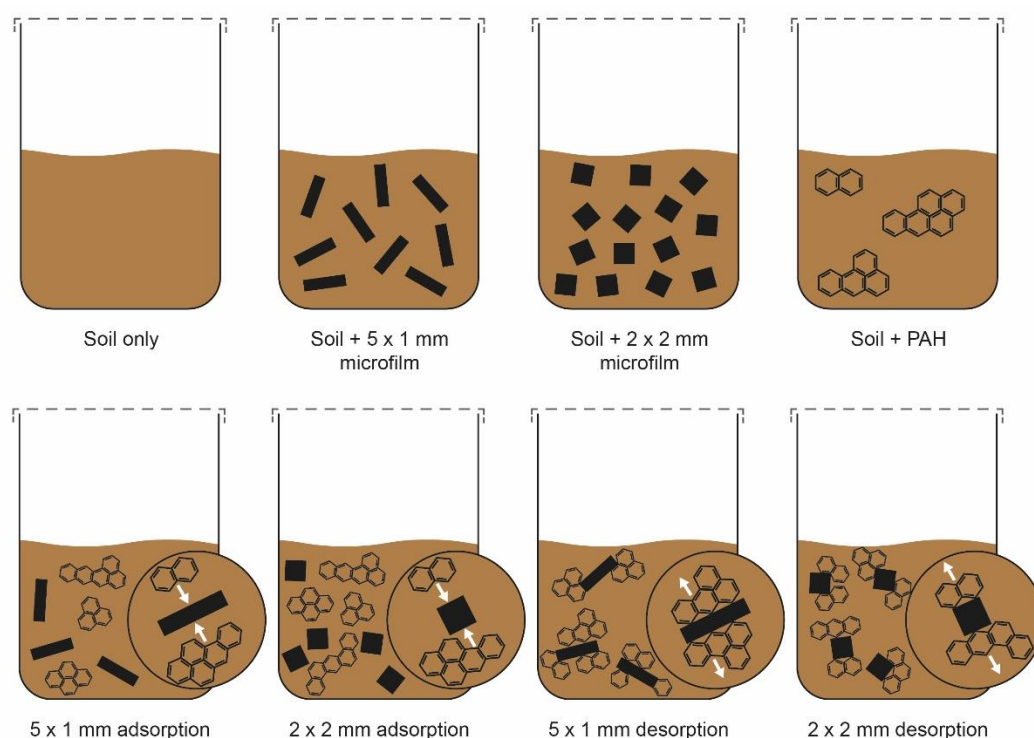
Figure 6.1: Schematic of the experimental set-up. There were three individual replicates per treatment.

6.2.2.1 Sorption experiment

Soils were spiked with the prepared PAH solution to obtain a concentration of 500 ng/g-soil, which is of environmental relevance (Cui et al., 2020). All PAH-spiked soil was prepared in bulk by laying the total quantity of soil required out in a thin layer and covering the total soil surface evenly in the PAH solution. This was done in several stages in order to mix the soil by hand and allowing the DCM to evaporate quickly. The bulk soil was then mixed for 12 h on an end-over-end shaker before dividing up the spiked soil into jars and mixing in pristine 5 x 1 and 2 x 2 mm microfilms, respectively.

6.2.2.2 Desorption experiment

Both sizes of microfilm were separately spiked with PAHs following the equation outlined by Booij et al. (2002):

$$N_t = N_m \frac{V_s + n m_m K_{ms}}{m_m K_{ms}},\tag{6.2}$$

Where N_t is the amount of PAHs to be added to the system, N_m is the target amount of PAHs per microfilm, V_s is the solvent volume, n is the number of microfilms, m_m is the mass of microfilms, and K_{ms} is the membrane-solution partition coefficient of the PAHs.

The equation was used as a means of estimating the required amount of PAHs, thereby the K_{ms} values reported by Booij et al. (2002) were used to represent all PAHs. A total mass of 30 g of each microfilm (equating to 60000 and 75000 individual pieces of 5 x 1 and 2 x 2 mm, respectively) were separately added to 800 mL of MeOH:H$_2$O (80:20 v/v) with a target of obtaining 7500 ng/g-microfilm (3.75 and 3 ng per individual piece of 5 x 1 and 2 x 2 mm microfilm, respectively). Therefore, 225 µg PAHs were added to each incubation solution. The MeOH:H$_2$O solutions individually containing both sizes of microfilm were incubated at room temperature for 12 h and continuously mixed using an end-over-end shaker.

The microfilms were then transferred to a clean fine mesh sieve, lightly rinsed with Milli-Q water, then allowed to air dry (maximum of 2 h) while covered with perforated aluminium foil. Final PAH concentrations were measured by gas chromatography – mass spectrometry (GC-MS) (see section 6.2.3). Pristine soils were then spiked with the PAH-spiked microfilms, respectively, at 1% (w/w) in 20 g soil and sampled as outlined in section 6.2.2.

6.2.3 Extraction of PAHs from microfilms and GC-MS analysis

Approximately 0.5 g of microfilms were recovered from each jar using tweezers and rinsed lightly with Milli-Q water to remove adhering soil particles. The 0.5 g microfilms were then shaken in 3 x 50 mL DCM for 1 min each at room temperature to extract the PAHs. Internal standards (0.2 µg) and 5 g of anhydrous Na$_2$SO$_4$ were added to the 150 mL DCM extract and left overnight. The DCM extract was then decanted into a clean round bottom flask and rotary evaporated to 2-3 mL, and finally solvent exchanged to *iso*-hexane which was then concentrated by rotary evaporation for analysis by GC-MS.

A Perkin-Elmer Clarus® 690 GC with autosampler fitted with a HP-5MS column (5%-phenyl)-methylpolysiloxane phase; 30 m length, 0.25 mm i.d., 0.25 µm film thickness) linked to a Clarus® SQ8T MS was used for analysing the PAH extracts. The carrier gas was helium with a constant flow rate of 1 mL min^{-1}. Samples (1 µL) were auto-injected in splitless mode at 275 °C. The oven temperature programme began at 80 °C (1 min), ramped to 240 °C at 15 °C min^{-1}, then subsequently ramped to 325 °C at 5 °C min^{-1} and held for 2 min. The MS was kept at 200 °C with an electron impact energy of 70 eV and operated in selected ion monitoring mode.

6.2.3.1 Quality control

Reference standard mixtures, a spiked quality control (QC) sample, and a blank were run with each batch of samples to assess contamination, instrumental performance, peak identification, and quantification. Spiked QC samples were prepared by adding 1 mL of a 100 ppb PAH standard mix to DCM and subjected to the same PAH extraction procedure outlined above in section 5.2.3. The method limits of detection for PAHs were 1.0-5.0 ng/g. Results were reported as ng/g-microfilm.

6.2.4 pH measurements

Soil pH was measured using the method by McLean (1982). Approximately 10 g soil was removed from each jar (triplicate per treatment) at each time point to assess soil pH and microfilms were completely removed by hand. The sample was suspended in 25 mL deionised water and thoroughly mixed for 30 min on a roller. The supernatant was allowed to settle, and the pH of the solution was measured using a Hach® HQ430d flexi pH meter.

6.2.5 Soil organic carbon content

The remainder of the soil was freeze dried and a portion from the desorption samples was ball-milled for soil organic carbon (%OC) content analysis (triplicate per treatment). All microfilms were removed manually using tweezers. Organic carbon (loss on ignition) was measured using an automated Duma combustion procedure using a Flash EA 1112 Elemental Analyser (Pella and Colombo, 1973).

6.2.6 Data analysis

Sorption data was fitted to a first-order kinetics equilibrium model (equation 6.3) and desorption data was fitted to an exponential decay model (equation 6.4) (Rochman et al., 2013a). Experimental data were fitted onto the kinetic models using the Microsoft Excel Solver tool to achieve the optimal model fit (i.e., where the sum of square residuals was the lowest) (Sahai et al., 2023).

$$C_t = C_{eq}(1 - e^{-kt}) \qquad\qquad (6.3)$$

$$C_t = \left(C_0 - C_{eq}\right)e^{-k't} + C_{eq} \qquad\qquad (6.4)$$

Where C_t is concentration (ng/g-microfilm) at time t (day), C_{eq} is the predicted equilibrium concentration (ng/g-microfilm), C_0 is the initial concentration (ng/g-microfilm), and k is the sorption rate constant and k' is the desorption rate constant.

Spearman's rank correlation tests were performed in R (version 4.3.1) to determine the strength of association between the rate constants, solubility, octanol-water partition coefficient values ($\log K_{ow}$) and molecular weights of the PAHs, respectively, as physicochemical properties have been suggested to influence the sorption of pollutants to plastics (Xia et al., 2023). The non-parametric Kruskal-Wallis H tests (K-W) were performed in IBM SPSS Statistics (version 22) to determine the strength of association between rate constants of fused-ring number between microfilm sizes, rate constants between sorption and desorption experiments, predicted equilibrium concentration values between sizes for sorption and desorption experiments, pH values between sorption and desorption experiments, and between the controls, and %OC values between control and sorption experiments, and between the controls.

6.3 Results and Discussion

6.3.1 Microfilm characterisation

FTIR analysis of the pristine mulching film (as received from the farmer) confirmed it was composed of polyethylene (Figure 6.2A). The spectrum displayed a small (weak) band appearing at ~1725 cm^{-1}

(indicated by an arrow in Figure 6.2A) which corresponds to carbonyl (C=O) stretching but lacks a broad OH stretching band above 3000 cm^{-1}. The appearance of bands at ~1350 cm^{-1} and between 1190-1080 cm^{-1} also correspond to OH bending and C-O stretching, respectively. The CI was calculated to be 0.08 ± 0.01 indicating the surface of the polyethylene had been slightly oxidised, a process which occurs naturally through photo-oxidation (Almond et al., 2020; Zvekic et al., 2022). Oxidation affects the sorption of PAHs and other hydrophobic organic contaminants due to the increased polarity of the polymer structure, thereby decreasing sorption capacity (Yu et al., 2020; Duan et al., 2021). However, the increased crystallinity of the polymer leads to microcracking or fragmentation which increases specific surface area. In turn, this can increase the sorption capacity of organic contaminants through sorption mechanisms such as pore filling (Tourinho et al., 2019). SEM micrographs of the mulching film topography (Figure 6.2B) showed that the film surface was relatively smooth with early signs of physical weathering (i.e., pitting). Given these characterisations, it was anticipated that the microfilms would sorb the PAHs with little or no chemical hinderances by the polymer. However, future work would need to be conducted to assess the kinetics of PAHs with weathered microfilms which are likely to be present in higher abundances in the environment.
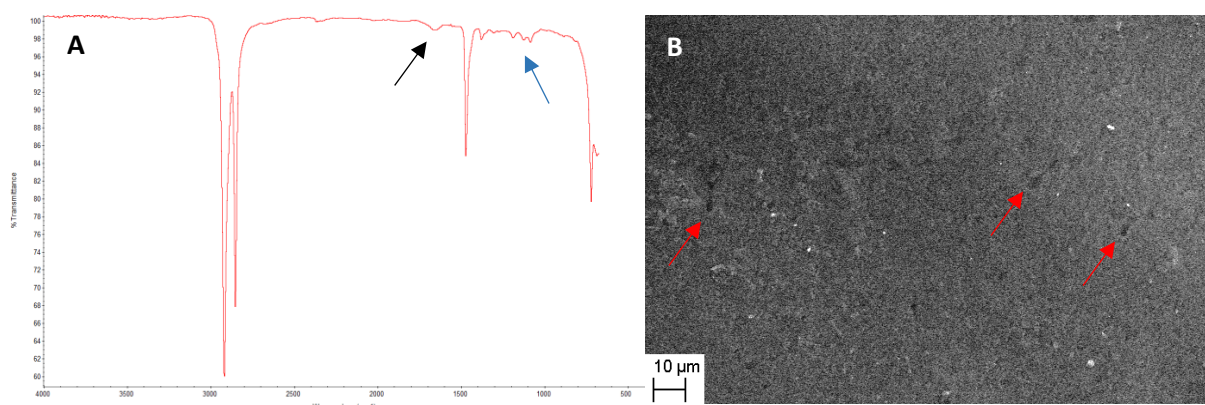
Figure 6.2: Mulching film characterisation: spectrum generated by ATR-FTIR (A) and SEM micrograph of the surface of mulching film (B). The black arrow indicates the carbonyl (C=O) band, the blue arrow indicates C-O bands, and red arrows indicate pitting in the microfilm surface.

6.3.2 Sorption kinetics

6.3.2.1 Sorption

No microplastic films were observed in the control soil samples, therefore, any microfilms subsequently recovered for analysis were from what was added. Figure 6.3 displays the sorption kinetics for the 16

PAHs by both sizes of microfilm (2 x 2 and 5 x 1 mm), and the k and C_{eq} values are presented in Table 6.2. These two sizes of microfilm were selected to assess sorption on two different sizes and shapes. Square and rectangular-shaped microfilms were the most observed shapes of films recovered from soil samples in Chapters 4 and 5. These film sizes were also selected so that microfilms could be removed from the soil without the need of chemicals, such as salts which are commonly used to separate microplastics from soil through floatation, which can influence the sorption of PAHs (Sahai et al., 2023). Equilibrium was reached for all PAHs during the 30-day sorption period for 2 x 2 mm, with the exception of IcdP, DahA, and BghiP for 2 x 2 mm microfilms. Fewer PAHs reached equilibrium in the 30-day period with the 5 x 1 mm microfilms. Those that did not reach equilibrium for the larger microfilm size included BbF, BkF, BaP, IcdP, DahA, and BghiP. Furthermore, the sorption rates were around two-fold higher for 4-ring (Fluo, Pyr, BaA, and Chr), 5-ring (BbF, BkF, BaP, and DahA), and 6-ring structures (IcdP and BghiP) in the 2 x 2 mm microfilms compared with 5 x 1 mm microfilms. As such, there was a statistical difference between the rate constants for sorption between the two sizes of microfilm for PAHs with 4-6 fused rings in their structures (*K-W* test, $p < 0.05$), but not for PAHs with 2 and 3 fused rings (*K-W* test, $p > 0.05$). The number of days it took for each PAH to reach their predicted equilibrium concentrations (C_{eq}) for both 2 x 2 and 5 x 1 mm microfilms, respectively, are presented in Table 6.2.

Spearman's rank showed there was significantly strong correlations between the rate constants (k) for sorption and physicochemical properties of PAHs including their molecular weight ($p < 0.05$, $r_S = -0.96$), solubility ($p < 0.05$, $r_S = 0.87$), and logK_{ow} values ($p < 0.05$, $r_S = -0.95$) (see Table 6.1). Low molecular weight PAHs are classed as those with 3 fused rings in their structure or less, while high molecular weight PAHs are those with 4 or more fused rings. Higher molecular weight PAHs were slower to sorb to the microfilms (Figure 6.3 and Table 6.2). This could be explained based on octanol-water partition coefficients influencing interactions with soil organic matter and solubilities in interstitial water. The logK_{ow} values increase with molecular weight (Table 6.2), and organic compounds with high octanol-water partition coefficients have significant correlations with soil organic matter as they have a tendency to absorb more readily leading to higher recalcitrance of high molecular weight PAHs in soil (Wang et al., 2021b). On the other hand, low molecular weight PAHs have higher solubilities (low logK_{ow} values, lower hydrophobicity) (Table 6.1) compared to high molecular weight PAHs (high logK_{ow} values, higher hydrophobicity), hence, high molecular weight PAHs associate strongly with soil organic matter

Figure 6.3: Sorption data of PAHs to 2 x 2 mm (circles) and 5 x 1 mm (triangles) microfilms fitted to a first order equilibrium model using equation (6.3).

(Kariyawasam et al., 2022; Vijayanand et al., 2023). In order for PAHs to sorb to the microfilms, they must first be free in the soil matrix (i.e., suspended in the interstitial water, unbound to soil organic matter), explaining why the low molecular weight (low $\log K_{ow}$ value) PAHs were faster at sorbing to the microfilms. Higher molecular weight PAHs were likely hindered by soil organic matter interactions, limiting their rate of sorption over time. In the study by Rochman et al. (2013b) and Li et al. (2022), it was similarly observed that high molecular weight PAHs with high $\log K_{ow}$ values sorbed at a slower rate to microplastics in seawater and soil solutions, respectively, compared to low molecular weight and $\log K_{ow}$ PAHs. It was anticipated that 2 x 2 mm microfilms would facilitate higher C_{eq} values due to their higher surface area. Despite all PAHs sorbing to 2 x 2 mm microfilms exhibiting C_{eq} values which were approximately equal to or higher than their respective C_{eq} values for 5 x 1 mm sorption (with the exception of Ace, Flu, BaP, IcdP, and BghiP), there was no significant difference between the two sizes of microfilm (K-W test, p > 0.05; Table 6.2).

Table 6.2: Calculated values for first order equilibrium (equation (6.3) – $C_t = C_{eq}(1-e^{-kt})$) and exponential decay (equation (6.4) – $C_t = (C_0 - C_{eq})\,e^{-k't} + C_{eq}$) model equations.

PAH	Sorption				Desorption					
	2 x 2 mm		5 x 1 mm		2 x 2 mm			5 x 1 mm		
	C_{eq}	k	C_{eq}	k	C_0-C_{eq}	C_{eq}	k'	C_0-C_{eq}	C_{eq}	k'
Nap	1047	1.95	1050	1.78	4874	663	1.72	6087	548	1.56
Acy	1200	1.91	1200	1.68	5066	917	1.71	6276	525	1.44
Ace	960	1.82	1087	1.63	6316	1081	1.74	6036	818	1.38
Flu	840	1.73	941	1.57	5733	882	1.63	5924	852	1.35
Phe	958	1.48	901	1.28	6358	540	1.33	6698	561	1.11
Ant	1256	1.46	1007	1.22	6596	786	1.21	6904	626	0.99
Fluo	1154	0.91	1056	0.55	4211	1849	0.71	5622	709	0.32
Pyr	1293	0.83	1164	0.43	4412	1704	0.67	5710	608	0.32
BaA	1007	0.64	972	0.34	6736	828	0.46	5801	1023	0.32
Chr	1129	0.60	1003	0.31	5771	1475	0.37	5108	1435	0.21
BbF	1818	0.32	1445	0.20	6116	1500	0.24	6159	1000	0.15
BkF	1298	0.31	1287	0.19	6567	1182	0.20	6542	971	0.11
BaP	947	0.30	1441	0.13	5599	1581	0.20	5367	1344	0.10
IcdP	944	0.20	1196	0.12	5956	1415	0.18	6932	878	0.10
DahA	1026	0.18	957	0.12	6132	1444	0.17	5890	1274	0.08
BghiP	801	0.17	997	0.10	6151	1157	0.16	6317	766	0.09

Since polyethylene is a non-aromatic polymer, it cannot undergo strong π-π interactions with PAHs like with polymers such as polystyrene (Rochman et al., 2013a). Rather, polyethylene can only undergo

hydrophobic and non-specific van der Waals interactions with PAHs (Hüffer and Hofmann, 2016; Mei et al., 2020). Hüffer and Hofmann (2016) reported that non-specific van der Waals interactions were the dominant intermolecular forces driving the sorption of non-polar organic compounds by polyethylene. Furthermore, the presence of proton acceptor groups (i.e., C=O carbonyl groups) on the surface of the polyethylene (see section 5.3.1 and Figure 6.3) gives rise to hydrogen bonding, strengthening the sorption interactions with PAHs (Mei et al., 2020). The point of zero charge for polyethylene (pH_{PZC}) is achieved at pH 4.96 (Li et al., 2022). Since the pH of soil through the experiment was between 5.56-5.86, it suggests that the sorbate surface of the polyethylene microfilms was near to polyethylene's pH_{PZC} (slight negative charge) and, therefore, close to the optimal conditions of PAH sorption (i.e., minimum electrostatic repulsion), further promoting PAH sorption. If the soil's pH was above or below the pH_{PZC} value for polyethylene, the microfilms would be negatively and positively charged, respectively, which may result in opposing electrostatic forces with the PAHs, decreasing their sorption rate.

6.3.2.2 Desorption

To the author's knowledge, this is the first study to report the desorption of PAHs from microplastics in a soil matrix, whereas other studies employed soil suspensions in water and salts (e.g., Zhang et al., 2021; Li et al., 2022; Sahai et al., 2023; Yu et al., 2023). A starting concentration of 7500 ng/g-microfilm for each PAH was targeted. Actual concentrations ranged from 6497.6-7937.4 (average = 7014.9) and 5538.7-7706.1 (average = 7067.1) ng/g-microfilm for 5 x 1 and 2 x 2 mm, respectively. Figure 6.4 displays the desorption kinetics for the 16 PAHs by both sizes of microfilm (2 x 2 and 5 x 1 mm), and the k', C_0-C_{eq}, and C_{eq} values are presented in Table 6.2. There was no statistical difference in the rates of sorption and desorption for each size of microfilm (K-W test, p > 0.05) indicating that both sorption and desorption occur at a similar rate to one another to reach the respective equilibria of each PAH (C_{eq}). Similarly with sorption, Spearman's rank showed there was significantly strong correlations between the rate constants for desorption (k') and physicochemical properties of PAHs including their molecular weight (p < 0.05, r_S = -0.94), solubility (p < 0.05, r_S = 0.86), and logK_{ow} values (p < 0.05, r_S = -0.92) (Table 6.1). Unlike for sorption, there was a significant difference in C_{eq} values between the two sizes of microfilm (K-W test, p < 0.05), with 2 x 2 mm microfilms overall possessing higher C_{eq} values. This was expected as the total amount of 2 x 2 mm microfilms had a higher surface area for PAHs to interact with.
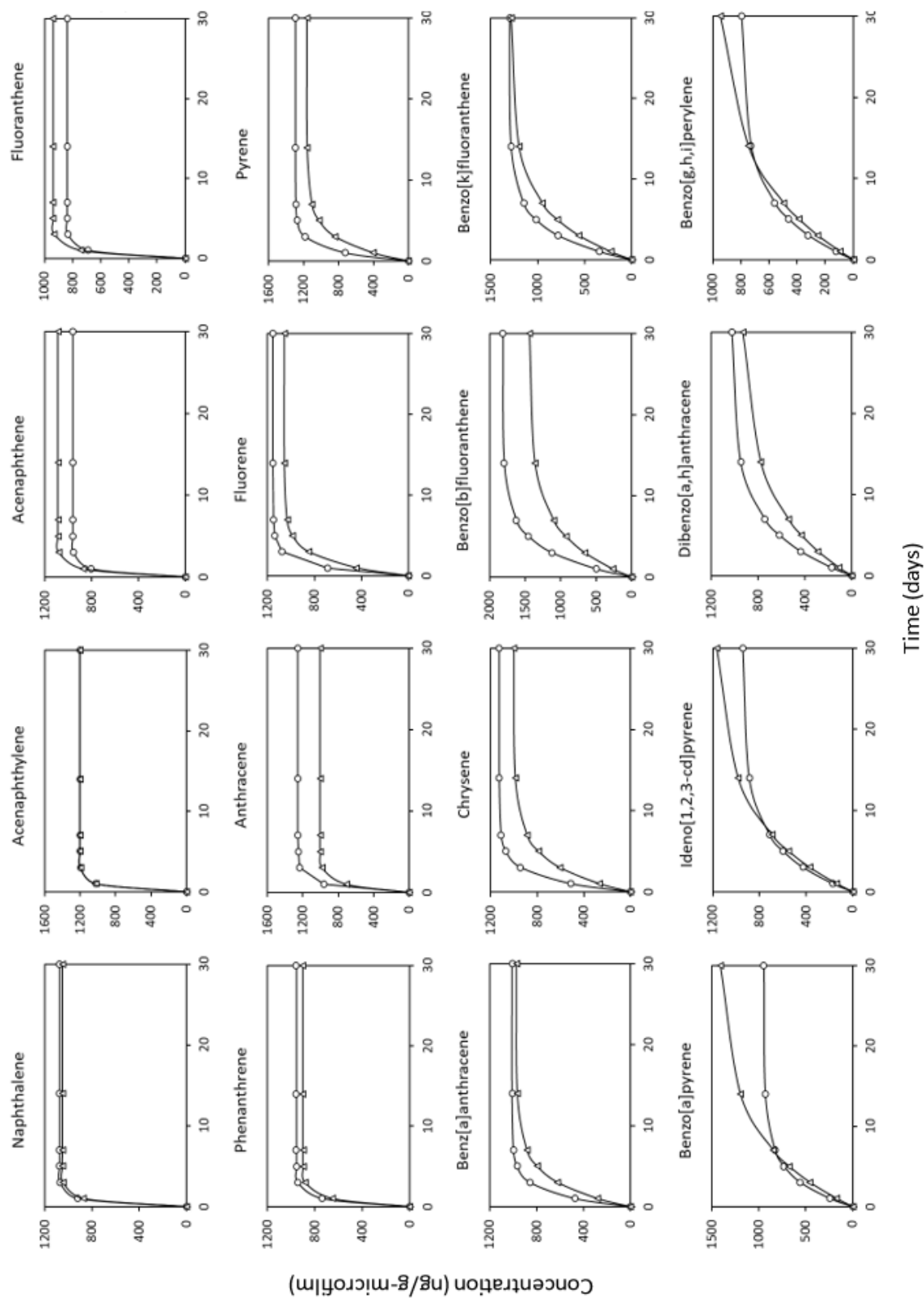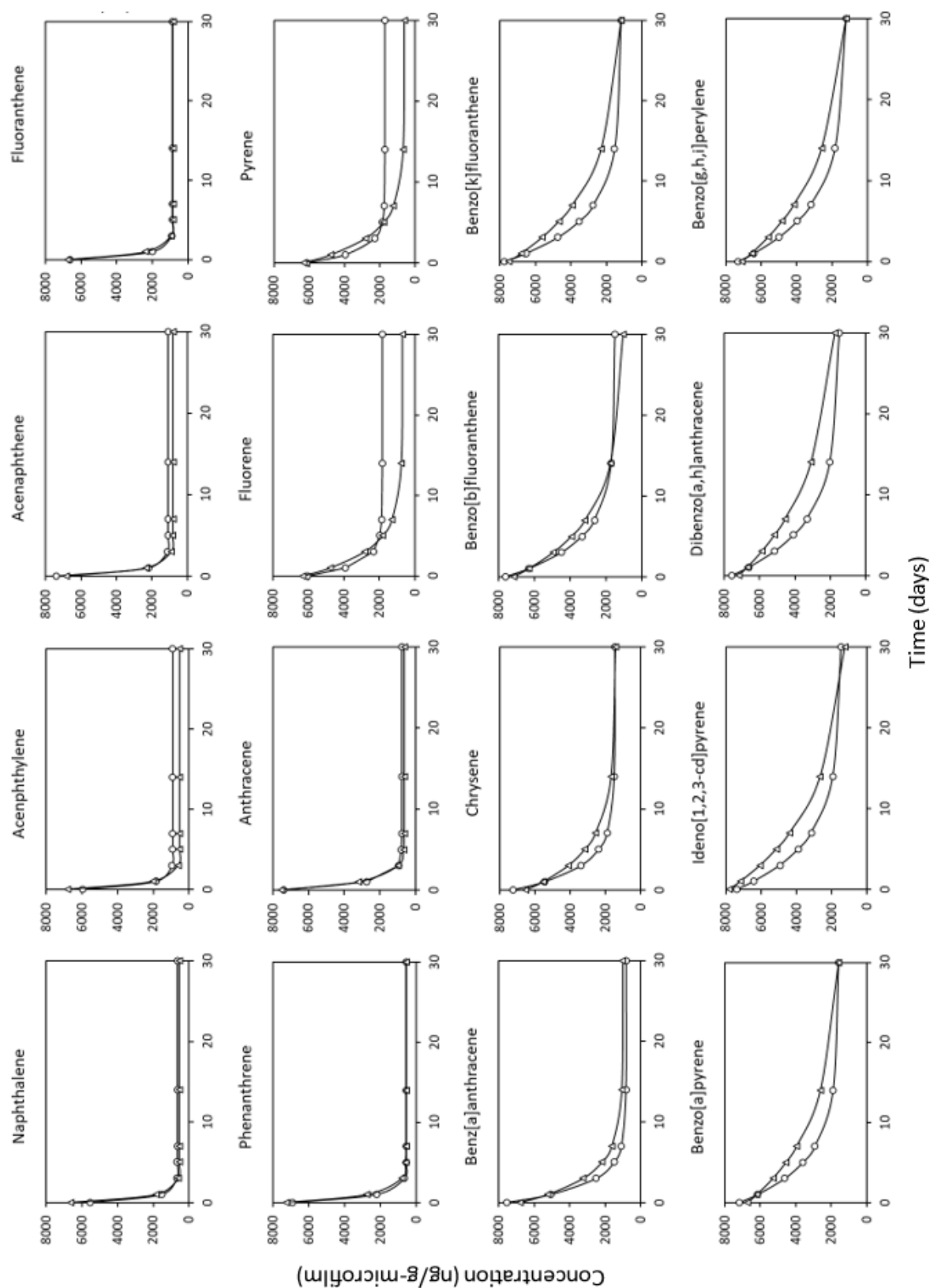
Figure 6.4: Desorption data of PAHs to 2 x 2 mm (circles) and 5 x 1 mm (triangles) microfilms fitted to an exponential decay model using equation (6.4).

Similar to sorption, the desorption rate constants (k') for 4-6 fused ring PAHs were around two-fold higher from the 2 x 2 mm microfilms compared to 5 x 1 mm (Table 6.2), and showed significant differences (*K-W* test, p < 0.05). High molecular weight PAHs desorbed at a slower rate to low molecular weight PAHs (Table 6.2 and Figure 6.4) likely due to their increased hydrophobicity (high logK_{ow} values) repelling them away from the surrounding soil environment (interstitial water) leading to stronger associations with the polyethylene microfilms. This was similarly observed by Sahai et al. (2023) whereby other organic contaminants (e.g., pesticides) with low logK_{ow} values rapidly desorbed from polyethylene microplastics in soil. Low molecular weight PAHs are considered to be acutely toxic while high molecular weight PAHs are considered to be genotoxic (Ghosal et al., 2016). As such, the strong interaction between highly toxic high molecular weight PAHs and polyethylene microfilms raises concerns regarding their slow release in the soil environment over an extended period of time, leading to their chronic exposure to soil (micro)organisms, agricultural plants and crops, and even humans.

6.3.3 Alterations to soil parameters

Over the 30-day exposure period, soil pH and organic C were monitored to investigate the effects of PAH sorption and desorption on the soil environment. Temporal trends for pH and C content are presented in Figure 6.5. Measurements from a soil only control sample were used to compare temporal changes in soil chemical properties.

The addition of PAHs to soil (for the sorption study) resulted in a 3.4% increase in soil organic carbon (Figure 6.5A). Over time it was observed that the %OC remained relatively constant in the soil control (1.1% decrease), however, the 2 x 2 mm and 5 x 1 mm sorption soils showed a bigger decrease (average of 3.2%) which indicates that this larger decrease was due to the removal of PAHs from soil through sorption to the polyethylene microfilms. The differences in %OC between the control and sorption soils, however, were not significant (*K-W* test, p > 0.05). The decrease in %OC observed with the 2 x 2 mm microfilm indicates that a greater amount of PAHs were sorbed, which is corroborated by the respective C_{eq} values (see section 5.3.2.1), however, the difference in %OC between the soils for the two microfilm sizes were not significant (*K-W* test, p > 0.05).

Soil pH also displayed a universal decrease over the 30-day period with a starting range of pH 5.76-5.86 (Figure 6.5B). All treatment soils and control soil followed the same decrease until day 7 where the pH diverged, with the soil + microfilm control and desorption treatments grouping together around pH

5.65 and the sorption soils grouping together at a lower pH around pH 5.58 (Figure 6.5B). This divergence was statistically significant (K-W test, $p < 0.05$). Microbial degradation of PAHs (as well as other soil organic matter) may account for the slightly more acidic condition in the sorption treatments. This may be explained due to the aerobic metabolism of PAHs leading to the production of free H^+ protons or the transformation of PAHs to acidic degradation products (Zhang et al., 2006), thereby decreasing soil pH. The extent of microbial degradation of PAHs also increases in acidic soils (Wu et al., 2017). Since PAHs are sorbed (concentrated) to the microfilms in the desorption treatments and are not readily available for microbial degradation (i.e., freely available throughout the total volume of soil), their soil pH follows the same trend as the *soil + microfilm* control.
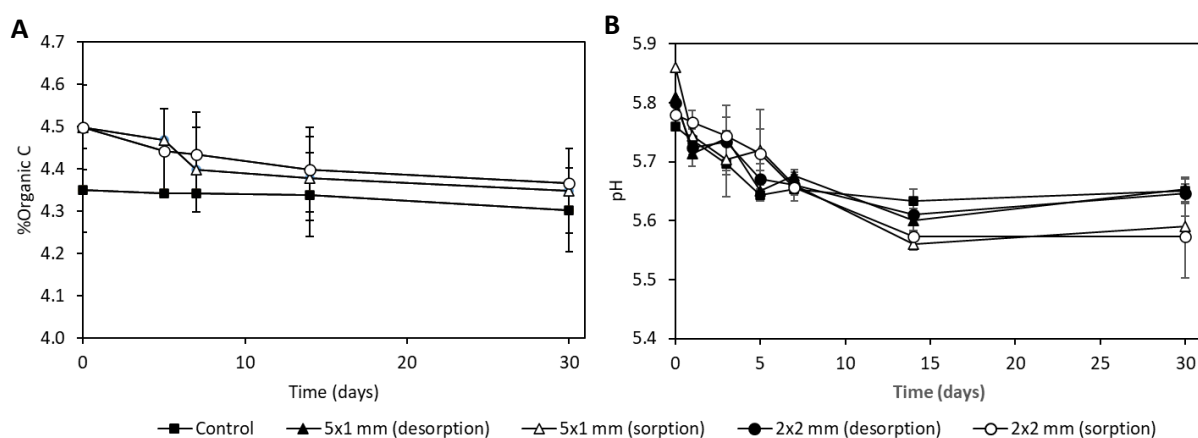
Figure 6.5: Temporal trends in soil organic carbon content (A) and pH (B). Control sample is the average of soil + microfilms only (*soil + 5 x 1 mm microfilm* and *soil + 2 x 2 mm microfilm*). The average control pH and %OC values of both sizes were plotted as no significant difference was found between them (*K-W* test; $p > 0.05$). Error bars indicate standard deviations (n = 3 for %OC and soil pH, respectively).

6.3.4 Impact of interactions between PAHs and microfilms in agricultural soils

The sorption and desorption of PAHs to and from microfilms derived from mulching or silage film may have potentially long-term impacts on the agricultural soil environment. The sorption of PAHs to microfilms alleviates the direct exposure and impact of PAHs to the soil environment, crops, livestock, and humans. Crops exposed to contaminated soils have been reported to contain PAHs (Wang et al., 2017) which, as a primary food source, can lead to the transfer of PAHs through the food chain, both to livestock (through grazing or grain feed) and humans (Kobayashi et al., 2008; Bortey-Sam et al., 2016). The sorption and retention of PAHs to microfilms may, therefore, limit the exposure of PAHs to

crops directly. However, small micro- and nanoplastics can enter crop vascular systems through crack-entry pathways in crop roots, whereby micro- and nanoplastics can enter the root vascular system (xylem) and be transported from the roots via transpiration into the shoots (Li et al., 2020). These micro- and nanoplastics, which concentrate and retain PAHs, could then potentially act as vectors for PAH contamination to crops. Similarly, PAH sorption to microfilms may reduce the amount of PAHs free to directly enter surface water and contaminate water systems repurposed for irrigation (Zhao et al., 2018). However, their slow desorption over time could lead to chronic exposure at low levels over time, particularly low molecular weight PAHs with higher water solubilities which also had higher desorption rates in this study. The concentrating of PAHs on microfilms (particularly larger-sized microfilms like those used in this study) may pose a significant risk to human and livestock exposure. PAH uptake to larger-sized microfilms may increase the likelihood of ingestion during grazing by livestock or dermal contact to humans through occupational exposure (Sun et al. 2021; Ramachandraiah et al., 2022). Results from this study suggest that microfilms decrease the exposure of PAHs to the wider soil microbial community through sorption (i.e., those not directly near or colonising the microfilms). The microbial degradation through aerobic pathways produces acidic degradation products such as naphthoic acid and salicylic acid leading to acidification of the soil (Zhang et al., 2006). The acidification of soil leads to low yield, poor quality cereal crops due to the increased availability of toxic heavy metals such as Al, Mn, and Fe, and, conversely, the reduced availability of nutrients for plant uptake (Jordan-Meille et al., 2021). The sorption of PAHs by microfilms reduces the decrease in soil pH and may alleviate the need for liming to increase soil pH to optimal cereal crop production. Further research would be required to elucidate these hypotheses.

6.4 Conclusions

The sorption and desorption of PAHs to and from different sizes of polyethylene microfilms were investigated in this study. This is the first study to investigate the interaction of PAHs with microfilms in a true soil matrix (i.e., not a soil suspension) and also the first to report the PAH desorption behaviour from microplastics in soil. Sorption data fitted a first order equilibrium model while desorption data fitted an exponential decay model. Equilibrium was reached for all PAHs in the 30-day period with exception of 6-fused ring PAHs in the 2 x 2 mm microfilms and 4-6-fused ring PAHs in the 5 x 1 mm microfilms. Sorption and desorption rates were two-fold faster for ≤3-fused ring PAHs compared to 4-6-fused ring PAHs. Results indicated that sorption and desorption kinetics were influenced by the molecular weight, water solubility, and logK_{ow} values of PAHs, and there were no significant differences between the rate of sorption or desorption observed. Smaller microfilm sizes (2 x 2 mm) reached higher

estimated equilibrium concentrations during desorption but no significant difference between the different microfilm sizes was observed during sorption. The addition of PAHs to soil increased the %OC, and the subsequent sorption of PAHs resulted in a decrease in %OC, with 2 x 2 mm reducing the %OC more than 5 x 1 mm indicating the smaller microfilm size sorbed a greater amount of PAHs, however, the difference was not significant. The insignificant differences between sorption/desorption rates and %OC levels between microfilm sizes are likely because there was not a substantial difference between the surface areas of a single 2 x 2 mm and 5 x 1 mm microfilm, therefore, future studies should compare a wider range of microfilm sizes to establish the effect of microfilm size on sorption and desorption of PAHs. Soils undergoing sorption underwent significant acidification throughout the 30-day period likely due to the production of acidic degradation products (e.g., naphthoic acid) through microbial degradation. This suggests that PAH sorption to microfilms decreases their availability for degradation thereby alleviating the soil from acidification which would negatively impact on crop production. The interaction of PAHs with microfilms in agricultural soils may lead to prolonged exposure of PAHs to the soil environment, crops intended for human consumption, livestock, and humans. Additional experiments will be required to understand the isotherms and thermodynamics of the PAHs tested. Further studies are needed to investigate the environmental effect of microfilm interactions with PAHs in different agricultural soils and with films of different compositions and states of weathering. Additionally, smaller sized microfilms (< 2 mm) should also be studied due to their higher abundance in the environment and their increased risk of exposure to humans, animals, and plants. However, a method of recovering these smaller sized microfilms from soils without the use of chemicals which may have implications on subsequent analyses must first be established.

6.5 References

Almond J., Sugumaar P., Wenzel M.N., Hill G., Wallis C. Determination of the carbonyl index of polyethylene and polypropylene using specified area under band methodology with ATR-FTIR spectroscopy. *E-Polymers*. 20, 369-381. DOI: http://dx.doi.org/10.1515/epoly-2020-0041

Amelia T.S.M., Khaid W.M.A.W.M., Ong M.C., Shao Y.T., Pan H.J., Bhubalan K. Marine microplastics as vectors of major ocean pollutants and its hazards to the marine ecosystem and humans. *Progress in Earth and Planetary Science*.2021; 8. DOI: https://doi.org/10.1186/s40645-020-00405-4

Astner A.F., Hyaes D.G., O'Neill H., Evans B.R., Pingali S.V., Urban V.S., Young T.M. Mechanical formation of micro- and nano-plastic materials for environmental studies in agricultural ecosystems. *Science of The Total Environment*. 2019; 685, 1097-1106. DOI: https://doi.org/10.1016/j.scitotenv.2019.06.241

Booij K., Smedes F., van Weerlee E.M. Spiking of performance reference compounds in low density polyethylene and silicone passive water samplers. *Chemosphere*. 2002; 46, 1157-1161. DOI: https://doi.org/10.1016/S0045-6535(01)00200-4

Bortey-Sam N., Ikenaka Y., Akoto O., Nakayama S.M.M., Marfo J., Saengtienchai A., Mizukawa H., Ishizuka M. Excretion of polycyclic aromatic hydrocarbon metabolites (OH-PAHs) in cattle urine in Ghana. *Environmental Pollution*. 2016; 218, 331-337. DOI: https://doi.org/10.1016/j.envpol.2016.07.008

British Standards Institution (2009) BS EN ISO 13320:2009: Particle size analysis – laser diffraction methods. Available at: https://www.iso.org/standard/44929.html (Accessed: 02 February 2021).

Cui S., Zhang Z., Fu Q., HoughR., Yates K., Osprey M., Yakowa G., Coull M. Long-term spatial and temporal patterns of polycyclic aromatic hydrocarbons (PAHs) in Scottish soils over 20 years (1990–2009): A national picture. *Geoderma*. 2022; 361, 114135. DOI: https://doi.org/10.1016/j.geoderma.2019.114135

de Souza Machado A.A., Lau C.W., Till J., Kloas W., Lehmann A., Becker R., Rillig M.C. Impacts of microplastics on the soil biophysical environment. *Environmental Science and Technology*. 2018; 52, 9656-9665. DOI: https://doi.org/10.1021/acs.est.8b02212

Duan J., Bolan N., Li Y., Ding S., Atugoda T., Vinthanage M., Sarkar B., Tsang D.C.W., Kirkham M.B. Weathering of microplastics and interaction with other coexisting constituents in terrestrial and aquatic environments. *Water Research*. 2021; 196, 117011. DOI: https://doi.org/10.1016/j.watres.2021.117011

FAO. 2021. *Assessment of agricultural plastics and their sustainability. A call for acti*on. Rome. https://doi.org/10.4060/cb7856en

Gholipour S., Ghalhari M.R., Nikaeen M., Rabbani D., Pakzad P., Miranzadeh M.B. Occurrence of viruses in sewage sludge: A systematic review. *Science of The Total Environment*. 2022; 824, 153886. DOI: https://doi.org/10.1016/j.scitotenv.2022.153886

Ghosal D., Ghosh S., Dutta T.K., Ahn Y. Current State of Knowledge in Microbial Degradation of Polycyclic Aromatic Hydrocarbons (PAHs): A Review. *Frontiers in Microbiology*. 2016; 7, 1369. DOI: https://doi.org/10.3389/fmicb.2016.01369

Gibbs P.A., Chambers B.J., Chaudri A.M., McGrath S.P., Carlton-Smith C.H., Bacon J.R., Campbell C.D., Aitken M.N. Initial results from a long-term, multi-site field study of the effects on soil fertility and

microbial activity of sludge cakes containing heavy metals. *Soil Use and Management*. 2006; 22, 11-21. DOI: https://doi.org/10.1111/j.1475-2743.2006.00003.x

Huang Y., Liu Q., Jia W., Yan C., Wang J. Agricultural plastic mulching as a source of microplastics in the terrestrial environment. *Environmental Pollution*. 2020; 260, 114096. DOI: https://doi.org/10.1016/j.envpol.2020.114096

Hüffer T., Hofmann T. Sorption of non-polar organic compounds by micro-sized plastic particles in aqueous solution. *Environmental Pollution*. 2016; 214, 194-201. DOI: https://doi.org/10.1016/j.envpol.2016.04.018

Jajoo A., Mekala N.R., Tomar R.S., Grieco M., Tikkanen M., Aro E.M. Inhibitory effects of polycyclic aromatic hydrocarbons (PAHs) on photosynthetic performance are not related to their aromaticity. *Journal of Photochemistry and Photobiology B: Biology*. 2014; 137, 151-155. DOI: https://doi.org/10.1016/j.jphotobiol.2014.03.011

Jordan-Meille L., Holland J.E., McGrath S.P., Glendining M.J., Thomas C.L., Haefele S.M. The grain mineral composition of barley, oat and wheat on soils with pH and soil phosphorus gradients. *European Journal of Agronomy*. 2021; 126, 126281. DOI: https://doi.org/10.1016/j.eja.2021.126281

Kariyawasam T., Doran G.S., Howitt J.A., Prenzler P.D. Polycyclic aromatic hydrocarbon contamination in soils and sediments: Sustainable approaches for extraction and remediation. *Chemosphere*. 2022; 291, 132981. DOI: https://doi.org/10.1016/j.chemosphere.2021.132981

Kasirajan S., Ngouajio M. Polyethylene and biodegradable mulches for agricultural applications: a review. *Agronomy for Sustainable Development*. 2012; 32, 501-529. DOI: https://doi.org/10.1007/s13593-011-0068-3

Kobayashi R., Okamoto R.A., Maddalena R.L., Kado N.Y. Polycyclic aromatic hydrocarbons in edible grain: a pilot study of agricultural crops as a human exposure pathway for environmental contaminants using wheat as a model crop. *Environmental Research*. 2008; 107, 145-151. DOI: https://doi.org/10.1016/j.envres.2007.11.002

Li L., Luo Y., Li R., Zhou Q., Peijnenburg W.J.G.M., Yin N., Yang J., Tu C., Zhang Y. Effective uptake of submicrometre plastics by crop plants via a crack-entry mode. *Nature Sustainability*. 2020; 3, 927-937. DOI: https://doi.org/10.1038/s41893-020-0567-9

Li Z., Sun L., Wang H. Adsorption behaviour and mechanism of polycyclic aromatic hydrocarbons onto typical microplastics in a soil solution. *International Journal of Environmental Analytical Chemistry*. 2022. DOI: https://doi.org/10.1080/03067319.2022.2128791

Liu E.K., He W.Q., Yan C.R. 'White revolution' to 'white pollution'—agricultural plastic film mulch in China. *Environmental Research Letters*. 2014; 9, 091001. DOI: https://doi.org/10.1088/1748-9326/9/9/091001

McLean E.O., 1982. Soil pH and Lime Requirement. In: A.L. Page, R.H. Miller, D.R. Keeney, eds. *Methods of Soil Analysis: Part 2 Chemical and Microbiological Properties*. 2nd edition. Wisconsin: American Society of Agronomy, Inc., Soil Science Society of America, Inc. pp 225-246.

Mei W., Chen G., Bao J., Song M., Li Y., Luo C. Interactions between microplastics and organic compounds in aquatic environments: A mini review. *Science of The Total Environment*. 2020; 736, 139472. DOI: https://doi.org/10.1016/j.scitotenv.2020.139472

Ng E.L., Huerta Lwanga E., Eldridge S.M., Johnston P., Hu H.W., Geissen V., Chen D. An overview of microplastic and nanoplastic pollution in agroecosystems. *Science of The Total Environment*. 2018; 627, 1377-1388. DOI: https://doi.org/10.1016/j.scitotenv.2018.01.341

Patel A.B., Shaikh S., Jain K.R., Desai C., Madamwar D. Polycyclic Aromatic Hydrocarbons: Sources, Toxicity, and Remediation Approaches. *Frontiers in Microbiology*. 2020; 11, 562813. DOI: https://doi.org/10.3389%2Ffmicb.2020.562813

Pella E., Colombo B. Study of carbon, hydrogen and nitrogen by combustion gas-chromatography. *Mikrochimica Acta*. 1973, 697-719. DOI: https://doi.org/10.1007/BF01218130

Picariello E., Baldantoni D., De Nicola F. Acute effects of PAH contamination on microbial community of different forest soils. *Environmental Pollution*. 2020; 262, 114378. DOI: https://doi.org/10.1016/j.envpol.2020.114378

Ramachandraiah K., Ameer K., Jiang G., Hong G.P. Micro- and nanoplastic contamination in livestock production: Entry pathways, potential effects and analytical challenges. *Science of The Total Environment*. 2022; 844, 157234. DOI: https://doi.org/10.1016/j.scitotenv.2022.157234

Rhind S.M., Kyle C.E., Kerr C., Osprey M., Zhang Z.L., Duff E.I., Lilly A., Nolan A., Hudson G., Towers W., Bell J., Coull M., McKenzie C. Concentrations and geographic distribution of selected organic pollutants in Scottish surface soils. *Environmental Pollution*. 2013; 182, 15-27. DOI: https://doi.org/10.1016/j.envpol.2013.06.041

Rochman C.M., Manzano C., Hentschel B.T., Massey Simonich S.L., Hoh E. Polystyrene plastic: A source and sink for polycyclic aromatic hydrocarbons in the marine environment. *Environmental Science and Technology*. 2013a; 47, 13976-13984. DOI: https://dx.doi.org/10.1021/es403605f

Rochman C.M., Hoh E., Hentschel B.T., Kaye S. Long-Term Field Measurement of Sorption of Organic Contaminants to Five Types of Plastic Pellets: Implications for Plastic Marine Debris. *Environmental Science and Technology*. 2013b; 47, 1646-1654. DOI: https://doi.org/10.1021/es303700s

Sahai H., Valverde M.G., Morales M.M., Hernando M.D., del Real A.M.A., Fernández-Alba A.R. Exploring sorption of pesticides and PAHs in microplastics derived from plastic mulch films used in modern agriculture. *Chemosphere*. 2023; 333, 138959. DOI: https://doi.org/10.1016/j.chemosphere.2023.138959

Suciu N.A, Lamastra L., Trevisan M. PAHs content of sewage sludge in Europe and its use as soil fertilizer. *Waste Management*. 2015; 41, 119-127. DOI: https://doi.org/10.1016/j.wasman.2015.03.018

Sun K., Song Y., He F., Jing M., Tang J., Liu R. A review of human and animals exposure to polycyclic aromatic hydrocarbons: Health risk and adverse effects, photo-induced toxicity and regulating effect of microplastics. *Science of The Total Environment*. 2021; 773, 145403. DOI: https://doi.org/10.1016/j.scitotenv.2021.145403

Syranidou E., Karkanorachaki K., Barouta D., Papadaki E., Moschovas D., Avgeropoulos A., Kalogerakis N. Relationship between the Carbonyl Index (CI) and Fragmentation of Polyolefin Plastics during Aging. *Environmental Science and Technology*. 2023; 57, 8130-8138. DOI: https://doi.org/10.1021/acs.est.3c01430

Tourinho P.S., Kočí V., Loureiro S., van Gastel C.A.M. Partitioning of chemical contaminants to microplastics: Sorption mechanisms, environmental distribution and effects on toxicity and bioaccumulation. *Environmental Pollution*. 2019; 252, 1246-1256. DOI: https://doi.org/10.1016/j.envpol.2019.06.030

Tumwesigye E., Nnadozie C.F., Akamagwuna F.C., Noundou X.S., Nyakairu G.W., Odume O.N. Microplastics as vectors of chemical contaminants and biological agents in freshwater ecosystems: Current knowledge status and future perspectives. *Environmental Pollution*. 2023; 330, 121829. DOI: https://doi.org/10.1016/j.envpol.2023.121829

Vijayanand M., Ramakrishnan A., Subramanian R., Issac P.K., Nasr M., Khoo K.S., Rajagopal R., Greff B., Azelee N.I.W., Jeon B.H., Chang S.W., Ravindran B. Polyaromatic hydrocarbons (PAHs) in the water environment: A review on toxicity, microbial biodegradation, systematic biological advancements, and environmental fate. *Environmental Research*. 2023; 227, 115716. DOI: https://doi.org/10.1016/j.envres.2023.115716

Voroney P., 2019. Soils for Horse Pasture Management. In: P. Sharpe, ed. *Horse Pasture Management*. Massachusetts: Academic Press. pp 65-79.

Wang J., Zhang X., Ling W., Liu R., Liu J., Kang F., Gao Y. Contamination and health risk assessment of PAHs in soils and crops in industrial areas of the Yangtze River Delta region, China. *Chemosphere*. 2017; 168, 976-987. DOI: http://dx.doi.org/10.1016/j.chemosphere.2016.10.113

Wang F., Zhang M., Sha W., Wang Y., Hao H., Dou Y., Li Y. Sorption Behavior and Mechanisms of Organic Contaminants to Nano and Microplastics. *Molecules*. 2020; 25, 1827. DOI: https://doi.org/10.3390/molecules25081827

Wang T., Ma Y., Ji R. Aging Processes of Polyethylene Mulch Films and Preparation of Microplastics with Environmental Characteristics. *Bulletin of Environmental Contamination and Toxicology*. 2021a; 107, 736-740. DOI: https://doi.org/10.1007/s00128-020-02975-x

Wang W., Qu X., Lin D., Yang K. Octanol-water partition coefficient (logKow) dependent movement and time lagging of polycyclic aromatic hydrocarbons (PAHs) from emission sources to lake sediments: A case study of Taihu Lake, China. *Environmental Pollution*. 2021b; 288, 117709. DOI: https://doi.org/10.1016/j.envpol.2021.117709

Wu Y., Zeng J., Zhu Q., Zhang Z., Lin X. pH is the primary determinant of the bacterial community structure in agricultural soils impacted by polycyclic aromatic hydrocarbon pollution. *Scientific Reports*. 2017; 7, 40093. DOI: https://doi.org/10.1038/srep40093

Xia Y., Niu S., Yuu J. Microplastics as vectors of organic pollutants in aquatic environment: A review on mechanisms, numerical models, and influencing factors. *Science of the Total Environment*. 2023; 887, 164008. DOI: http://dx.doi.org/10.1016/j.scitotenv.2023.164008

Yadav D.K., Kumar A.R., Jayaraman S., Lenka S., Gurjar S., Sarkar A., Saha J.K., Patra A.K. Polycyclic aromatic hydrocarbons in diverse agricultural soils of central India: occurrence, sources, and potential risks. *International Journal of Environmental Analytical Chemistry*. 2022. DOI: https://doi.org/10.1080/03067319.2022.2125307

Yates K., Davies I., Webster L., Pollard P., Lawton L., Moffat C. Passive sampling: partition coefficients for a silicone rubber reference phase. *Journal of Environmental Monitoring*. 2007; 9, 1116-1121. DOI: https://doi.org/10.1039/B706716J

Yu H., Yang B., Waigi M.G., Peng F., Li Z., Hu X. The effects of functional groups on the sorption of naphthalene on microplastics. *Chemosphere*. 2020; 261, 127592. DOI: https://doi.org/10.1016/j.chemosphere.2020.127592

Yu B., Zhao T., Gustave W., Li B., Cai Y., Ouyang D., Guo T., Zhang H. Do microplastics affect sulfamethoxazole sorption in soil? Experiments on polymers, ionic strength and fulvic acid. *Science of the Total Environment*. 2023; 860, 160221. DOI: http://dx.doi.org/10.1016/j.scitotenv.2022.160221

Zhang X.X., Cheng S.P., Zhu C.J., Sun S.L. Microbial PAH-Degradation in Soil: Degradation Pathways and Contributing Factors. *Pedosphere*. 2006; 16, 555-565. DOI: https://doi.org/10.1016/S1002-0160(06)60088-X

Zhang C., Lei Y., Qian Y., Qiao J., Liu J., Li S., Dai L., Sun K., Guo H., Sui G., Jing W. Sorption of organochlorine pesticides on polyethylene microplastics in soil suspension. *Ecotoxicology and Environmental Safety*. 2021; 223, 112591. DOI: https://doi.org/10.1016/j.ecoenv.2021.112591

Zhao Z., Xia L., Jiang X., Gao Y. Effects of water-saving irrigation on the residues and risk of polycyclic aromatic hydrocarbon in paddy field. *Science of The Total Environment*. 2018; 618, 736-745. DOI: https://doi.org/10.1016/j.scitotenv.2017.08.096

Zvekic M., Richards L.C., Tong C.C., Krogh E.T. Characterizing photochemical ageing processes of microplastic materials using multivariate analysis of infrared spectra. *Environmental Science: Processes Impacts*. 2022; 24,52-61. DOI: https://doi.org/10.1039/D1EM00392E

Chapter 7: The combined effect of microfilms and chrysene on soil ecosystem function and microbial community composition

Both microplastics and polycyclic aromatic hydrocarbons (PAHs) are well recorded soil pollutants globally, and previous research has reported the ability of microplastics to act as vectors for these organic pollutants. This research aimed to elucidate the impact of the combined impact of these pollutants on soil health, with chrysene used as a model PAH. Microcosms were set up and spiked with three different concentrations of chrysene-sorbed microfilms (4500, 23,000, and 50,000 ng/g-microfilm) and soil respiration and substrate-induced respiration were measured at 7 timepoints over a 57-day period (0, 2, 7, 14, 21, 30, and 57 days) to assess microbial activity. 16S rRNA gene sequencing was also performed on days 0, 2, 14, and 30 to assess the impact on bacterial community composition. Soil respiration measurements indicated that ecosystem function was significantly decreased in chrysene treatments (p < 0.05) and slightly elevated in microfilm treatments (p > 0.05), however, the presence of microfilms in the chrysene-bound microfilm treatment alleviated the negative impact of chrysene. Further exploration using substrate-induced respiration supported these findings and glucose-induced respiration indicated that the increases and decreases in soil respiration measurements reflected changes in biomass, with chrysene reducing biomass and microfilms increasing biomass. Bacterial 16S rRNA gene sequencing revealed that each treatment had effects on alpha and beta diversity (p < 0.05) and as well as microbial community composition, particularly at lower taxonomic levels (i.e., family). An increase in rarer taxa associated with PAH degradation was observed in the chrysene and chrysene-bound microfilm treatments. These changes in microbial community composition for chrysene-treated soil may reflect functional redundancy in the microbial population to allow ecosystem function to continue or resilience of the population to recover from disturbance in the form of added pollutants. A non-metric multidimensional scaling plot further indicated that microbial community compositions between treatments were dissimilar by the end of the time course. While this study highlights the ability of polyethylene microplastic to negate the effects of chrysene, the sorption of these contaminants to microplastics may further prolonged their exposure to the terrestrial environment.

7.1 Introduction

Microplastics are ubiquitous in agricultural soils due to various land management practices including the application of soil amendments and mulch film (Xu et al., 2020). The impact of microplastic pollution in agricultural soils has been well documented, with studies reporting the alteration of water

holding capacity, bulk density, and soil structure (de Souza Machado et al., 2018; de Souza Machado et al., 2019), all of which subsequently have negative implications for soil flora and fauna (see Chapter 2, section 2.4). However, the interactions of microplastics with other chemical contaminants, particularly persistent organic contaminants, may pose greater risk to soil health and function long-term as microplastics concentrate these organic pollutants (Cui et al., 2023). It is also anticipated that, since sorption is a dynamic interaction (Chapter 6), the organic pollutants may slowly be released into the soil environment over a prolonged period of time.

Polycyclic aromatic hydrocarbon (PAH)-contaminated soils can induce stress on soil microbial communities, resulting in decreases in microbial abundance and community diversity (Cao et al., 2008; Ling et al., 2015; Picariello et al., 2020; Liu et al., 2022). PAHs are also mutagenic agents which induce genetic changes in bacterial and mammalian DNA, possibly rendering genes responsible for metabolic processes and enzymatic activities inactive (Bonin et al., 1989). However, soil microbes have the potential to utilise "fresh" mineralised PAHs (e.g., PAHs newly entered in the soil environment through wet-dry cycle deposition) as a carbon source which can stimulate short-term activity (Li et al., 2019; Picariello et al., 2020). PAHs have been found in a wide range of concentrations in soils across Scotland with high molecular weight PAHs (such as chrysene, benzo[b]fluoranthene, and benzo[a]pyrene) contributing the highest abundances due to their greater chemical stability and persistence (Rhind et al., 2013).

As discussed in Chapter 6, polycyclic aromatic hydrocarbons (PAHs) are found at considerable levels in agricultural soils and sorb to microplastic-sized mulch films (polyethylene), whereby they can remain bound to PE microplastics for 30 days, and potentially beyond that. The impact of microplastics bound with organic contaminants on soil biota is currently relatively under-researched (Wang et al., 2020). Additionally, a review by Burns and Boxall (2018) evaluating the evidence for the ingestion and subsequent desorption of organic pollutants from microplastics as an exposure pathway highlighted that the outcome of the majority of studies were often inconclusive. However, previous studies which have investigated the effects of combined exposure of microplastics and organic contaminants (e.g., antibiotics) to soils and sediments have reported that the presence of microplastics alleviated the independent detrimental effects of both the unbound contaminant and the microplastics (Xu et al., 2021; Hedfi et al., 2022). This is likely due to the reduced bioavailability of the contaminants through bonding with microplastics.

This study aimed to elucidate the combined effect of microplastics and the PAH, chrysene, on soil microbial community composition and their activity. Chrysene was selected as a representative PAH in this study due to its high abundance in Scottish soils (Rhind et al., 2013) and because its molecular weight and ring number lies in the middle of the PAH size and weight range.

7.2 Materials and Methods

7.2.1 Field sampling and soil characterisation

Surface soil (0-10 cm) was collected from an improved grassland field in Collieston, Aberdeenshire (Scotland, UK) in January 2022 (NK 06504 31919). The soil was characterised as a sandy loam through particle size distribution analysis using laser diffraction (British Standards Institution, 2009) with a Mastersizer 3000 particle analyser and Hydro LV sample dispersion unit (Malvern Panalytical). Total carbon and nitrogen content (6.68% and 0.43%, respectively) was determined by an automated Dumas combustion procedure (Pella and Colombo, 1973) using a Flash 2000 Elemental Analyser. Soil pH was 5.86, determined through the water method (McLean, 1982) using a Hach® HQ430d flexi pH meter. Stones and plant material were removed while the soil remained wet using a sieve with a mesh size of 6.5 cm, before final wet sieving through a 2 mm sieve. The soil was stored at 4 °C from time of collection until the start of the experiment.

7.2.2 Microplastics

A sheet of pristine polyethylene (PE) mulching film was obtained from a local farmer and characterised using Fourier-transform infrared analysis and scanning electron microscopy (see Chapter 6). The film had a thickness of 0.065 mm. The different sizes of microplastics were prepared by cutting the film by hand into approximately 5 x 5 and 1 x 1 mm individual microfilms using an ethanol-sterilised scalpel. A separate portion of polyethylene film was cryo-milled using a SPEX 6775 Freezer/Mill® to generate microplastics < 1 mm in size. The cryo-mill was operated under the following parameters: 3 cycles with a run time of 45 s at a rate of 5 cycles per second. Microplastics > 1 mm were removed through sieving.

A subset of each size of microfilm were spiked with chrysene (CHR) at three different concentrations, respectively. The target concentrations were 4500 ng/g-microfilm (PE-CHR1), 23000 ng/g-microfilm

(PE-CHR2), and 50000 ng/g-microfilm (PE-CHR3). Chrysene (analytical grade) was obtained from Sigma-Aldrich. Microfilms were spiked following the procedure outlined in Chapter 6, section 6.2.2.2).

7.2.3 Experimental set-up

Soil microcosms were spiked with different concentrations of polyethylene microfilms and chrysene to test these pollutants' effects on soil microbial community and function. The soil microcosms were set up in a climate-controlled room (20 °C in the dark with a relative humidity of 70%) for a 57-day period. Polypropylene pots (18.8 cm diameter, 15.5 cm height, 3.5 L volume) were used in the study. Three replicate pots were prepared containing 3 kg of soil in each. Three sets of pots were prepared containing microplastics spiked with three different concentrations of chrysene – 4500, 23000, and 50000 ng/g-microfilm (PE-CHR1, PE-CHR2, and PE-CHR3, respectively). Additional pots were also set up as controls. These were soil only (SOIL), autoclaved soil (AC), soil + ampicillin (200 mg/kg-soil) (AMP), soil + microplastics (not spiked with chrysene) (PE), and soils containing 4500, 23000, and 50000 ng/g-soil of chrysene (CHR1, CHR2, and CHR3, respectively) (Figure 7.1). The broad-spectrum antibiotic, ampicillin, was used to as a positive control as antibiotics are known to negatively affect the function and community structure of soil microbes (Unger et al., 2013). Microplastics were incorporated into the respective soils at a 1% (w/w) concentration, which is considered to be an environmentally relevant concentration (Sun et al. 2022), and equal proportions of all three size ranges were added. This was done to simulate an environmental soil where a range of microplastic sizes would be expected.

Microplastics were added to each 3 kg of soil individually and mixed manually using a sterilised metal scoop before potting to ensure each pot received the correct microplastic concentration and a homogeneous distribution of microplastics throughout the soil volume.
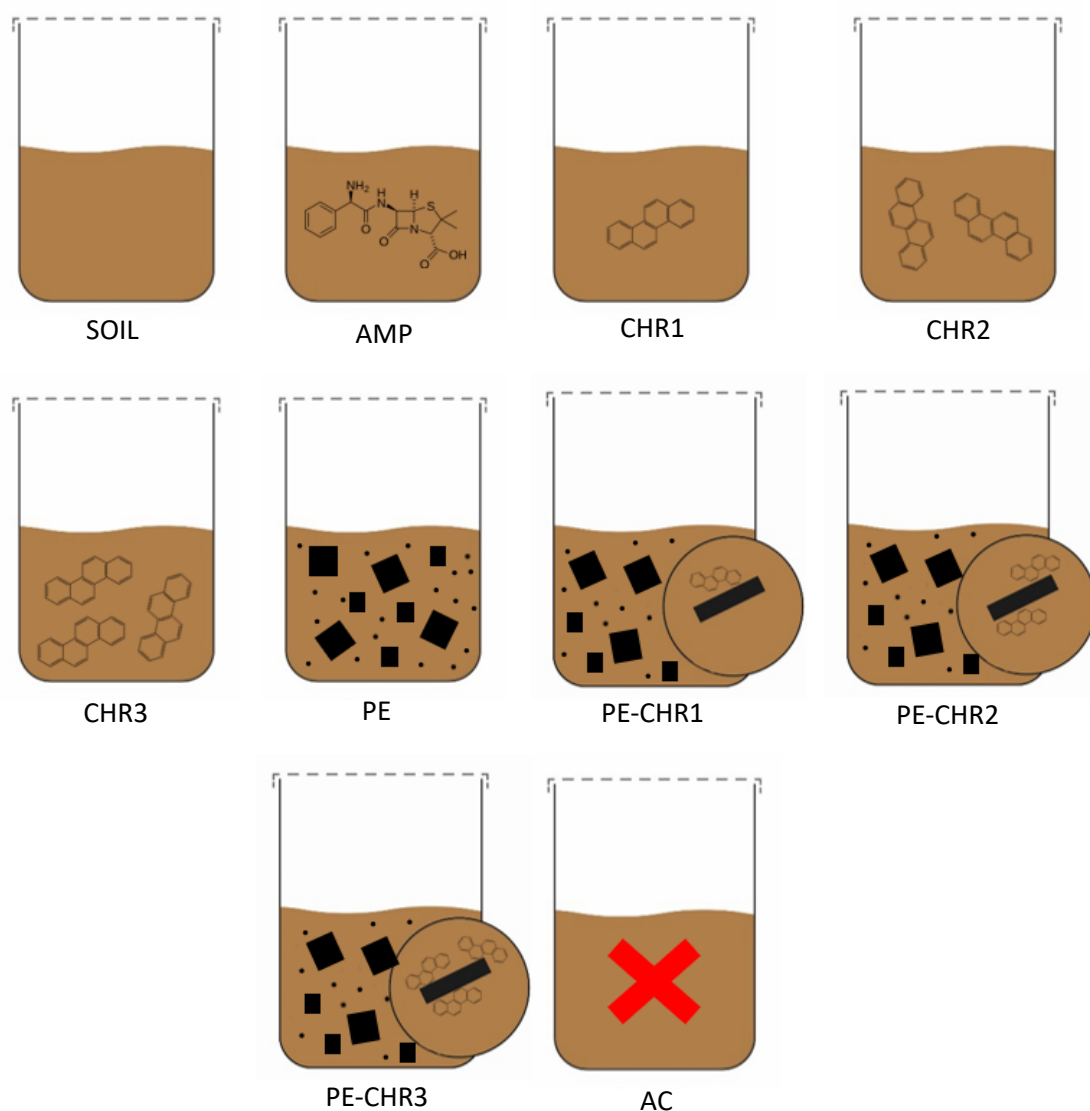
Figure 7.1: Schematic of experimental set up. SOIL = soil only; AMP = ampicillin control (200 mg/kg-soil); CHR1 = 4500 ng/g-soil; CHR2 = 23000 ng/g-soil; CHR3 = 50000 ng/g-soil; PE = microfilms (1% w/w); PE-CHR1 = 4500 ng/g-microfilm; PE-CHR2 = 23000 ng/g-microfilm; PE-CHR3 = 50000 ng/g-microfilm; AC = autoclaved control. Each treatment had three individual replicate pots.

Soils to be treated with chrysene were spiked using individual solutions of chrysene prepared in dichloromethane (DCM) to reach the three target soil concentrations (CHR1, CHR2, and CHR3), respectively. Each 3 kg of soil was laid out in a thin layer and evenly covered in the chrysene solutions, respectively, and mixed manually to provide a homogeneous distribution of chrysene throughout the soil. This was repeated until all the chrysene solution was added. The soil was air dried for several

minutes to allow the DCM to evaporate before potting. The soil + ampicillin control soil (AMP) was similarly prepared. Ampicillin sodium salt was obtained from Sigma-Aldrich, UK.

The autoclaved soil (AC) was prepared by subjecting the soil to three sequential cycles at 123 °C for 60 min each using a Systec VX-120 autoclave. This was an additional control. Autoclaving soil has been shown to be an effective method of soil sterilisation (Querejeta, 2023).

All soils were mixed manually to by a single operator to ensure all received the same level of disturbance. Soil moistures were subsequently adjusted using ultrapure 18.2 MΩ cm^{-1} water (Milli-Q) to achieve 60% of their maximum water holding capacity, weighed, and maintained throughout every 3 days thereafter. Pots were covered with perforated aluminium foil to prevent contamination from external sources and minimise the rate of water loss.

Incubated soils were subsampled at seven separate time intervals (0, 2, 7, 14, 21, 30, and 57 days) using a sterilised 1.5 cm *dia*. x 10 cm soil corer (total of 7 cores collected evenly across each pot). Soil subsamples were thoroughly mixed, and aliquots were removed for subsequent analysis (soil respiration, microbial activity, and 16S rRNA gene sequencing). Microplastics were not removed from their respective soil samples to ensure that any potential micro-organisms colonising directly on the microplastics were included in all analyses.

7.2.4 Soil respiration

Soil respiration was used as a proxy for ecosystem function. Soil aliquots (5 g) were placed in sterilised 20 mL glass vials, left for 1 h, and then sealed with crimp-seal caps with self-sealing silicone/PTFE septa. Subsamples of 5 g soil have previously been used to measure soil respiration (e.g., Evans and Wallenstein, 2012; Mingorance and Peña, 2016). The vials were then purged using CO_2-free air for 5 min (when the CO_2 concentration in the vial reached zero) then left to incubate for 1 h. The CO_2 evolution in the headspace was measured by extracting 7 mL headspace using an airtight syringe and injected into a PP Systems EGM-4 CO_2 infrared analyser. Results were reported as parts per million (ppm) and convert to CO_2 production rate (μg CO_2-C g^{-1}-soil h^{-1}) using equation (3) (see section 7.2.5). Respiration data throughout the time course were normalised (following equation (1) (see section 7.2.5), using respiration measurements (μg CO_2-C g^{-1}-soil h^{-1}) instead of absorbance values).

7.2.5 Substrate-induced respiration for microbial activity assessment

Microbial activity was assessed using MicroResp™, a colorimetric microplate-based respiration system whereby pH indicator set in agar gel undergoes a colour change upon exposure to CO_2 released from soil micro-organisms (Campbell et al., 2003).

The following carbon substrates were used for MicroResp™ (all obtained from Sigma-Aldrich): citric acid (99%), *N*-acetyl-glucosamine (≥ 95%), D-(+)-trehalose (≥ 99%), 3,4-dihydroxybenzoic acid (≥ 97%), α-cyclodextrin (≥ 98%), lignin alkali, *p*-coumaric acid, salicylic acid (≥ 99%), oxalic acid dihydrate (≥ 99%), L-arginine (≥ 98%), D-(+)-glucose (≥ 99.5%), γ-amino butyric acid (≥ 99%), L-cysteine hydrochloride (≥ 98%), lysine monohydrochloride (≥ 98%), D-(-)-fructose (≥ 99%). Cresol red, potassium chloride (≥99%), and sodium bicarbonate (≥ 99%) were also obtained from Sigma-Aldrich. Purified agar was obtained from Oxoid. Microplates (96-well) and 96-well deep-well plates (1.2 mL) were obtained from ThermoScientific and FisherScientific, respectively. MicroResp™ apparatus was obtained from The James Hutton Institute, Aberdeen.

Detection plates were prepared by adding 150 μL of 1% agar containing 12.5 ppm cresol red, 150 mM potassium chloride, and 2.5 mM sodium bicarbonate to 96-well microplates. Once the agar was set, the detection plates were placed in a desiccator in the dark at room temperature. Each soil sample was added to one half of a deep-well plate (48 wells) using the provided filling device and the weight of each sample was recorded. Deep-well plates containing the soil sample were covered in Parafilm and stored in the dark at 4 °C until ready for analysis. Soils were removed from cold storage and incubated at 25 °C for 4 days in the dark (still covered) to allow microbial activity to stabilise. The moisture content of each sample was determined using a 5 g subsample in order to calculate the required concentrations of the carbon substrate solutions. Citric acid, D-(+)-glucose, γ-amino butyric acid, *N*-acetyl-glucosamine, D-(+)-trehalose, L-cysteine hydrochloride, D-(-)-fructose, oxalic acid dihydrate, and lysine monohydrochloride were prepared individually to a concentration of 30.0 mg g^{-1} H$_2$O in 25 μL aliquots, L-arginine and α-cyclodextrin were prepared individually to a concentration of 7.5 mg g^{-1} H$_2$O in 25 μL aliquots, and 3,4-dihydroxybenzoic acid was prepared to a concentration of 3.0 mg g^{-1} H$_2$O in 25 μL aliquots, as per manufacturer's instructions. Carbon substrates plus an ultrapure water control (25 μL) were added to the soil samples in their corresponding wells as per the manufacturer's instructions. Lignin alkali, *p*-coumaric acid, and salicylic acid (average of 2.2, 5.5, and 5.5 mg, respectively) were added to their corresponding wells in solid form using a levelled microspatula with 25 μL ultrapure

water added immediately after. Each detection plate was placed in a Tecan Infinite® absorbance reader (with Magellan software) to measure the plates' initial absorbance values in each well at 570 nm. The deep-well plate and detection plate were assembled using the provided clamp whereby an airtight silicone seal with interconnecting holes sealed the two plates together. The samples were incubated in the dark at 25 °C for 6 h, then the detection plates were re-read to measure the wells' absorbance values. Absorbance data were normalised (Ai) using equation (1):

$$Ai = \left(\frac{At6}{At0}\right) x \; Mean(At0) \tag{1}$$

Where $At6$ is the absorbance values at 6 h and $At0$ is the absorbance values at 0 h.

The normalised 6 h data (Ai) was then converted into %CO$_2$ using the following linear-to-linear (rectangular hyperbola) standard curve equation (2):

$$\%CO_2 = \frac{A + B}{(1 + D \; x \; Ai)} \tag{2}$$

Where A = -0.2265, B = -1.6060, and D = -6.7710. Values used in this equation are from a calibration curve previously established within the laboratory under the same conditions and instrumentation as used in this experiment.

Finally, the CO$_2$ production rate was calculated using equation (3) (results were expressed as μg CO$_2$-C g^{-1}-soil h^{-1}):

$$\frac{\frac{\left(\frac{\%CO_2}{100}\right) x \; vol \; x \left(\frac{44}{22.4}\right) x \left(\frac{12}{44}\right) x \left(\frac{273}{(273+T)}\right)}{soil \; fwt \; x \left(\frac{soil \; \% \; dwt}{100}\right)}}{incubation \; time} \tag{3}$$

Where T is incubation temperature (°C), vol is the headspace volume of well (945 μL), $\frac{44}{22.4}$ is the molecular weight of CO₂ in 22.4 L air at normal temperature and pressure (1 atmosphere and 20 °C), $\frac{12}{44}$ is the proportion of C in CO₂ by molecular weight, $soil\ fwt$ is the fresh weight of soil per well (g), $soil\ \%\ dwt$ is the percentage of soil sample dry weight, and $incubation\ time$ (h).

7.2.6 DNA extraction and sequencing

Soil samples from days 0, 2, 14, and 30 intended for 16S rRNA gene sequencing were immediately stored at -80 °C until processing. DNA was extracted from triplicate 250 mg soil samples using the DNeasy® PowerSoil® Pro Kit (Qiagen) according to the manufacturer's instructions. The DNA extracts were then cleaned using the NuceloSpin® Gel and PCR Clean-up kit (Macherey-Nagel) following the manufacturer's instructions. The quality and quantity of the isolated DNA extracts were determined using a NanoDrop® ND-1000 spectrophotometer and a Qubit™ Flex fluorometer (ThermoFisher), respectively. For pure DNA, a 260/280 absorbance ratio should be 1.8. DNA integrity was assessed visually using 1.0% agarose gel electrophoresis. Once all samples passed quality checking, the three replicate DNA extractions per treatment were pooled and stored at -20 °C until sequencing.

DNA extracts were submitted to Novogene (Cambridge, United Kingdom) for bacterial 16S rRNA gene sequencing using the Illumina NovaSeq™ paired-end sequencing platform. The V3-V4 hypervariable regions of the bacterial 16S rRNA gene were amplified by the primer pair, 341F (5'-CCTAYGGGRBGCASCAG-3') and 806R (5'-GGACTACNNGGGTATCTAAT-3').

7.2.7 Data processing and analysis

Raw data sequences were analysed using QIIME2 (version 2023.9) (Bolyen et al., 2019) supported by the UK Crop Diversity Bioinformatics HPC Resource (The James Hutton Institute, 2024). The DADA2 plugin was used to denoise the raw FASTQ files by using cutadapt to remove the primer sequences and Illumina barcode sequences and truncating to remove lower quality sequence bases, followed by dereplication, merging, and removal of chimeric reads. Operational taxonomic units (OTUs) were clustered at a 97.5% threshold using the vsearch plug-in. Taxonomic assignment of the sequences was performed using the Naive Bayes classifier in QIIME2, trained using the 16S rRNA Greengenes database. The OTU abundance table was transformed into the BIOM format and extracted as a tab separated file for downstream analysis.

7.2.8 Statistical analysis

Respiration data were normalised in order that the Day 0 values started from the same value to ensure differences in soil respiration over the time course were due to treatment effects. Initial respiration measurements (ppm) were converted to CO_2 production rate (μg CO_2-C g^{-1}-soil h^{-1}) using equation (3) (headspace volume was 21 mL). Measurements from the final soil respiration timepoint (day 57) were subjected to the Kruskal-Wallis (*K-W*) test to determine the strength of association between the treatment groups and CO_2 efflux using IBM SPSS Statistics (version 22). Significant differences between treatment groups were further explored by performing *t*-tests on these values using R 4.3.1. Differences were considered significant where $p < 0.05$. Day 57 results were plotted in box plots with *t*-test results represented on the plot as a series of letters where shared letters indicated where there was no statistically significant difference between the treatments ($p > 0.1$).

Substrate-induced respiration (MicroResp™) data were similarly normalised and analysed by *K-W* test and *t*-tests. Differences were considered significant where $p < 0.05$. Principal components analysis (PCA) plots were generated using PRIMER-e (v7.0.13). A PCA plot was generated to evaluate the dissimilarity in spatial variation for the comparison of how individual carbon substrates are utilised by the microbial communities of each treatment over time. A further PCA plot was generated for the comparison of the ability of the microbial communities to utilise the full suite of carbon substrates at day 57.

Various downstream analyses of the OTU table were performed. Stacked bar plots at the class and family level were generated using QIIME2. PRIMER-e v7.0.13 was used to generate diversity indices including Margalef richness, Pielou's evenness, and Shannon-Weiner (diversity) index. *t*-Tests were performed on the day 30 values to evaluate beta diversity across the treatment groups. Differences were considered significant where $p < 0.1$. Day 30 results were plotted in box plots with *t*-test results represented on the plot as a series of letters where shared letters indicated where there was no statistically significant difference between the treatments ($p > 0.1$). PRIMER-e was also used to generate a non-metric multidimensional scaling (nMDS) plot to evaluate the similarity in microbial community composition between treatments for the day 30 samples and assess factors driving dissimilarly. Data were square root transformed and subjected to a Bray-Curtis dissimilarity test. The similarity matrix was then used to draw the nMDS plots, whereby microbial community compositions which were similar were orientated close to each other, while those which were dissimilar were plotted

away from each other. A 2D stress value of < 0.2 was considered to be an accurate representation. Samples were grouped by treatment type and the variation in the microbial community composition was assessed against the communities' ability to respire and utilise the various carbon substrates using Pearson's correlation, where substrates with an r > 0.5, were overlaid on the resulting nMDS plot. One-way ANOSIM (analysis of similarities) tests were performed on the nMDS plot data and pairwise tests were performed to evaluate the significance in similarity between the treatments. Differences were considered significant where p < 0.1 for assessment of the day 30 samples. R values close to 1 indicated complete dissimilarity between the treatments.

7.3 Results and Discussion

7.3.1 Microfilms and chrysene affect soil respiration

Soil respiration was used as a proxy for ecosystem function. It is appreciated that small subsamples of 5 g soil were used to measure soil respiration, however, samples as low as 5 g have been used successfully in previous studies (Evans and Wallenstein, 2012; Mingorance and Peña, 2016). Furthermore, disturbance to the soil can lead to spikes in CO_2 efflux (Mayer et al., 2017), therefore, the subsamples were left for 1 h after transferring into the glass vials to allow some time for this elevated level of CO_2 to be emitted. Additionally, all samples were treated the same, therefore, it was anticipated that any treatment effects on soil respiration would still be observed. Indeed, analysis of the normalised soil respiration measurements indicated that the different treatments affected soil respiration (Figure 7.2).

Figure 7.2 shows a drop in respiration between day 0 and 21 in all treatments, indicating the initial set-up of the experiment (i.e., mixing of the soil) caused a spike in CO_2 efflux which settled over this initial period of time. Following that, there was little or no change in respiration between days 21 and 57, indicating that respiration had stabilised. By day 57, treatment groups were relatively distinct from one another. The AC control showed low levels of CO_2 throughout the time course (0.02-1.27 µg CO_2-C g^{-1}-soil h^{-1}). It would be anticipated that respiration would increase over time if these CO_2 levels were a result of a biological source (i.e., micro-organisms surviving the autoclaving process and respiration increasing over time as microbial biomass increased). However, since this level of respiration remained relatively constant throughout (Figure 7.2), these CO_2 measurements can be attributed to methodical issues such as a CO_2 leakage in the respiration apparatus system, potentially through the pierced vial septa post-CO_2 purging, or through residual CO_2 present in the gas syringe. Additionally, since this was

constant throughout, it indicates this anomaly would have been uniform across all samples, therefore, differences in soil respiration are still attributed to treatment effects.
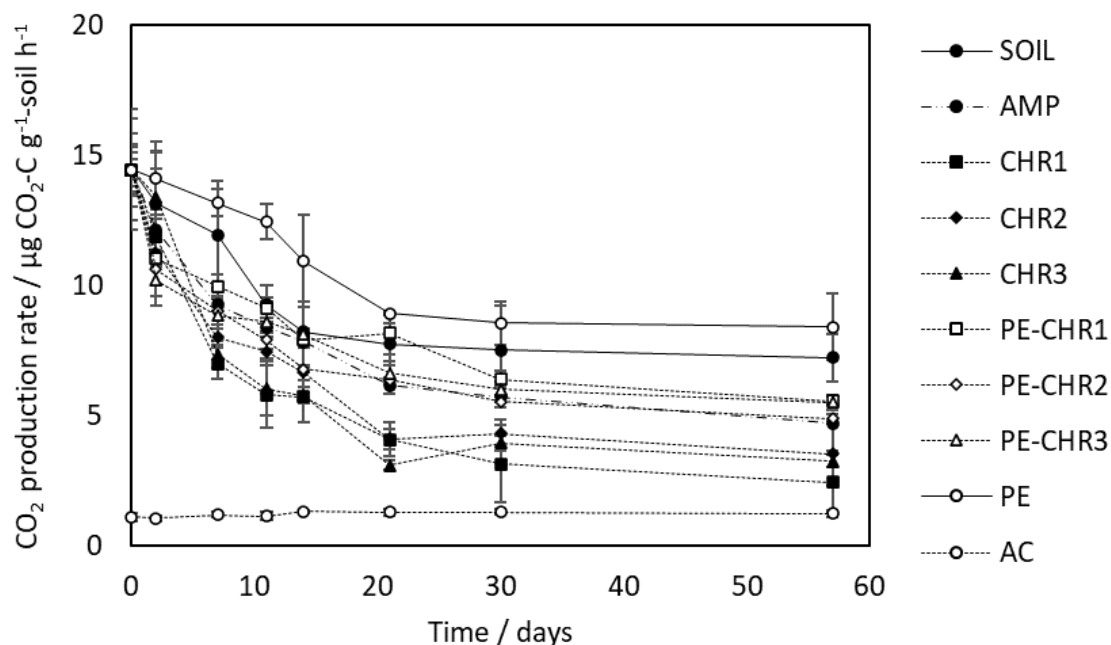
Figure 7.2: Rate of soil respiration over time. Error bars depict one standard deviation (n = 3).

Since there was no significant change over day 21 to 57 ($p > 0.05$), the respiration values at day 57 were used for analysis. *K-W* test was used to assess whether there was a statistical difference between the treatment groups at the end of the time course (day 57) which revealed that there was a statistical difference between the treatments ($p < 0.05$). *t*-Tests were used to further explore which treatments induced significant differences in soil respiration (Figure 7.3). The AMP positive control showed a significant decrease in respiration (4.70 ± 0.02 µg CO_2-C g^{-1}-soil h^{-1}) compared to SOIL, used as a baseline (7.22 ± 0.92 µg CO_2-C g^{-1}-soil h^{-1}) ($p < 0.05$). Ampicillin is a broad-spectrum, bactericidal antibiotic, killing any susceptible soil bacteria. Ampicillin is ineffective against fungi (Nurjanah et al., 2015), therefore, fungi as well as resistant bacteria may be accountable for some remaining CO_2 emissions in the AMP positive control. Nonetheless, the decrease in soil respiration suggested that the AMP positive control was effective at reducing microbial biomass and, therefore, soil respiration. However, further analyses, such as qPCR, would need to be conducted to confirm the microbial biomass present in all samples.
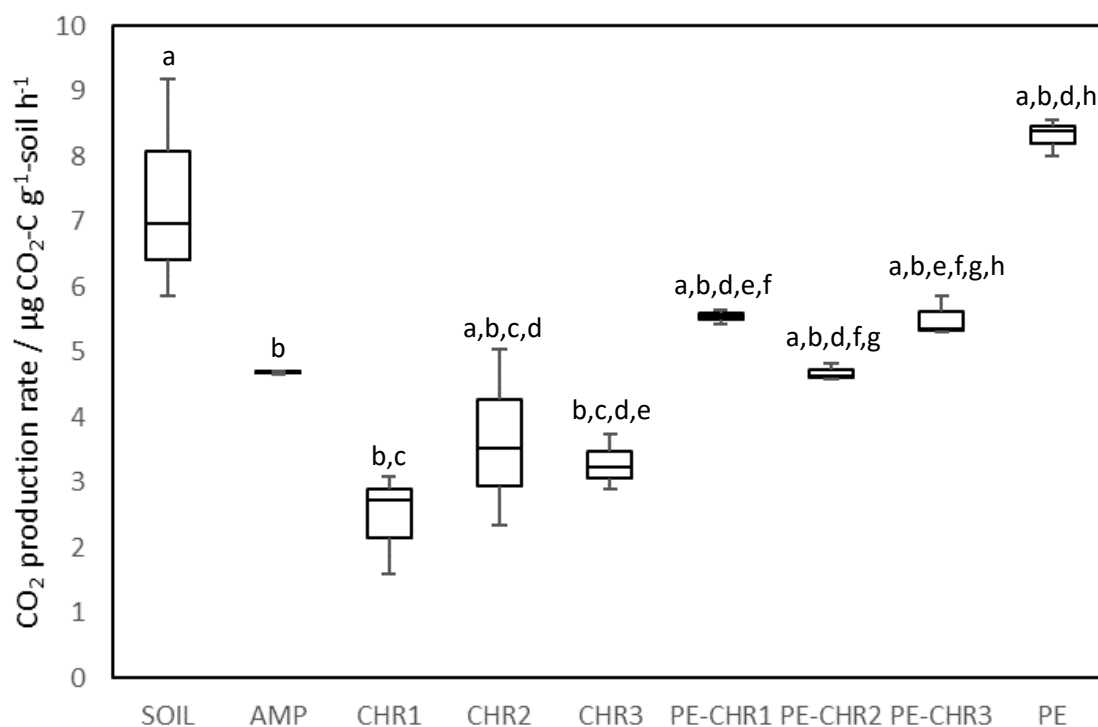
Figure 7.3: Box plots of the day 57 soil respiration values per treatment. *t*-Test results were represented on the box plots as a series of letters where shared letters indicated where there was no statistically significant difference between the treatments.

7.3.1.1 Chrysene significantly reduced soil respiration

PAH contamination in soil was observed to result in altered soil properties such as pH in Chapter 6, which can affect soil respiration. Indeed, the addition of chrysene to soils (CHR1, CHR2, and CHR3) showed the largest drop in respiration (2.45-3.52 µg CO_2-C g^{-1}-soil h^{-1}), collectively and individually, compared to the SOIL control ($p < 0.05$), indicating that CHR was the greater inhibitor of microbial respiration (Figure 7.2). There were no statistically significant differences in soil respiration between the three concentrations of chrysene ($p > 0.05$). The effect of PAH contamination in soils on microbial activity (particularly soil respiration) is highly variable due to factors such as microbial community composition, soil pH, and organic carbon content (Maliszewska-Kordybach and Smreczak, 2003a). In one study by Maliszewska-Kordybach and Smreczak (2003a) investigating the changes in soil microbial properties induced by PAH contamination (100,000 ng/g-soil), it was reported that PAH contamination in acidic soils stimulated microbial activity resulting in increased soil respiration. Meanwhile, in other studies, respiration in PAH contaminated soils (100,000 ng/g-soil) and sediments (20,000 ng/g-sediment) was lower than the controls (Maliszewska-Kordybach and Smreczak; 2003b; Zoppini et al.,

2016) as observed in this study. The AMP positive control produced the same effect on soil respiration as CHR, and since ampicillin is known to reduce microbial biomass (Unger et al., 2013), chrysene may potentially have the same effect on soil microbial biomass and soil respiration.

7.3.1.2 Microfilms increased soil respiration

Soil respiration is sensitive to environmental factors such as pH, soil moisture, and porosity (Lou and Zhou, 2006), and the addition of microplastics have a demonstrated capability of altering these soil properties (de Souza Machado et al, 2019; Lozano et al., 2021).

Figure 7.2 shows that PE increased soil respiration, resulting in elevated CO_2 levels (8.40 ± 1.27 µg CO_2-C g^{-1}-soil h^{-1}) compared to SOIL, however, this elevation was not significant (p > 0.05). Previous studies investigating the effect of polyethylene microfilms on soil respiration using similar soil and land use types reported that soil respiration was also elevated compared to uncontaminated control soils (Kim et al., 2021; Zhao et al., 2021), however, as observed in this experiment, the elevated soil respiration levels were not significant. This may be due to micro-organisms utilising the microplastics as a complex carbon substrate promoting increased microbial biomass resulting in increased respiration. On the other hand, if biomass had in fact stayed the same or decreased, the higher soil respiration may be due to a stress response (Schindlbacher et al., 2011). Further analyses would need to be performed to confirm whether the result is due to increased biomass or stress, however, see section 7.3.2 for further discussion on indicating biomass changes using MicroResp^{TM}.

7.3.1.3 Microfilms alleviated the impact of chrysene on soil respiration

The respiration measurements illustrated that when PE-CHR was compared with SOIL, measurements were lower but not significantly different (p > 0.05). This suggests that PE alleviated the effect of chrysene (Figure 7.2). Compared to CHR, PE-CHR exhibited significantly higher respiration measurements (185.95-212.27 µg CO_2-C g^{-1}-soil h^{-1}; p < 0.05). Similar to CHR, there were no significant differences between the three concentrations (PE-CHR1, PE-CHR2, and PE-CHR3). These results are consistent with previous studies investigating the combined effects of microplastics and organic contaminants (e.g., Xu et al., 2021). A possible reason for this may be because polyethylene microplastics are highly efficient in the sorption of chrysene (see Chapter 6) through non-specific van der Waals interactions (Hüffer and Hofmann, 2016), which may limit its bioavailability to soil micro-

organisms. Additionally, microplastics can act as a substrate for the development of biofilms through microbial colonisation, whereby the microbial community composition of the biofilms may be distinct from the microbial community structure of the surrounding soil and act as a barrier in protecting the surrounding soil micro-organisms from the effects of the microplastic bound-chrysene (Miao et al., 2019; Xu et al., 2021). Despite the positive effect observed here, the presence of chrysene-bound microplastics in the environment may pose a greater risk to soil health and function in the long-term since the sorption of chrysene to polyethylene is a dynamic interaction (see Chapter 6) and may allow chrysene to be slowly released into the soil environment and persist over a prolonged period of time.

Taken together, chrysene (CHR) caused significant decreases in soil respiration ($p < 0.05$), likely due to a reduction in microbial biomass, while polyethylene microfilms (PE) caused a non-significant increase in respiration ($p > 0.05$). The sorption of chrysene to polyethylene microfilms (PE-CHR) resulted in an alleviation of the detrimental impact of chrysene ($p < 0.05$) such that no significant difference in respiration between the PE-CHR treatments and SOIL were observed ($p > 0.05$). The presence of polyethylene microfilms in chrysene contaminated soils likely alleviated reduction in soil respiration by effective sorption of the chrysene to the microplastics.

7.3.2 Substrate-induced respiration confirms findings from soil respiration

MicroResp^{TM} was used as a proxy to measure microbial activity through substrate-induced respiration, using a variety of carbon substrates (see section 7.2.5) – substrate-induced respiration rates are presented in Figure 7.4. These tests provide an indication of the microbial community's ability to respire during utilisation of each substrate and differences in the ability to utilise the same substrate may indicate changes have occurred to the microbial communities as a result of the treatment. The level of substrate-induced respiration similarly reflected that of the soil respiration test (section 7.3.1). Overall, both PE and PE-CHR resulted in the highest activity, followed by SOIL, CHR, AMP, and AC, respectively. *K-W* test was used to assess whether there was a statistical difference between the treatment groups at the end of the time course investigated (day 57). This revealed that there were statistical differences between the treatments for all carbon substrates ($p < 0.05$), except for water, citric acid, α-cyclodextrin, and oxalic acid ($p > 0.05$). These differences were further explored using *t*-tests. In all cases where *K-W* test was significant ($p < 0.05$), the microbial respiration of both CHR and AMP treatments were statistically lower than SOIL ($p < 0.05$), again suggesting that chrysene behaved similarly to ampicillin in inhibiting microbial activity (see section 7.3.1). The higher activities observed of PE and PE-CHR were

not statistically different to SOIL ($p > 0.05$). PE-CHR was significantly higher than CHR ($p < 0.05$), which further indicates that the sorption of chrysene to polyethylene microfilms significantly alleviated the inhibitory effects of chrysene. MicroResp[TM] was used in a previous study by Lozano et al. (2021) to investigate the effect of various microplastics compositions and morphologies on soil microbial activity. It was reported that polyethylene microfilms resulted in a decrease in microbial activity, however, only large-sized microfilms were used in their study (5 x 5 mm) and incorporated into soil at a lower concentration ($\leq 0.4\%$ w/w) compared to this study (1% w/w). Microplastic size greatly influences the effects caused to soil micro-organisms (Li et al., 2023), therefore, it is possible that the smaller sized microplastics used in this study (1 x 1 mm and < 1 mm) could induce a different microbial response compared to that observed by Lozano et al. (2021). Similarly to soil respiration, no significant differences were observed between the three concentrations of CHR and PE-CHR, respectively ($p > 0.05$).
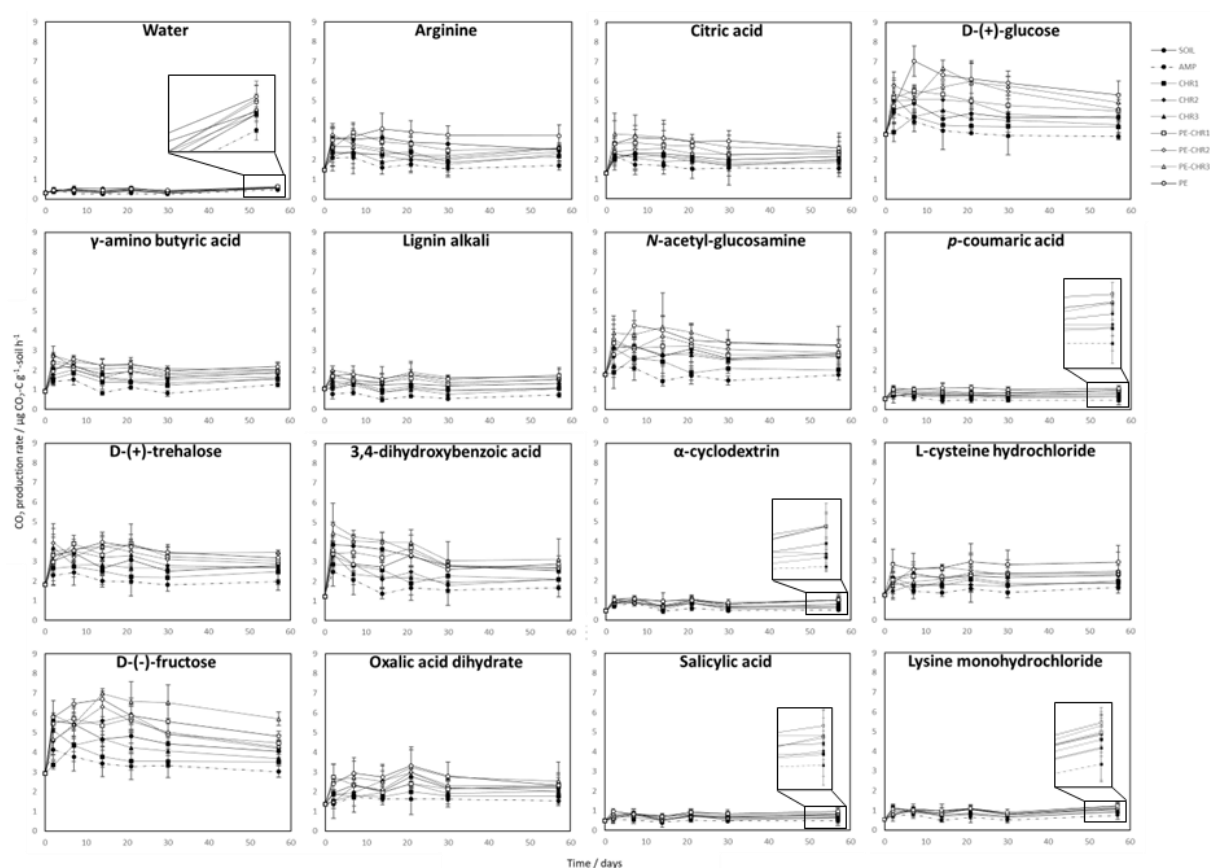
Figure 7.4: Graphs displaying the substrate-induced respiration values over the time course for each substrate and treatment. Error bars depict one standard deviation (n = 3).

A principal components analysis (PCA) plot was generated using the average respiration values for each substrate over the time course to evaluate the dissimilarity in how individual carbon substrates were utilised by the microbial communities of each treatment (Figure 7.5A). PCO1 accounted for the majority of the variation within the plot (96.0%). This indicated that D-(+)-glucose and D-(-)-fructose produced the biggest difference in respiration as they clustered the furthest from the water control. This is likely because these are simple sugars which are easily utilised as a carbon source for microbes universally (Chen et al., 2023). It was also observed that substrates such as lysine monohydrochloride, *p*-coumaric acid, salicylic acid, and α-cyclodextrin had the smallest impact on substrate-induced respiration as they were not much different to the water control, likely since these are chemically complex and harder for micro-organisms to readily utilise (Evans et al., 2017).

A PCA plot exploring the variation of the microbial communities' ability to utilise the carbon substrates within each of the treatments was also assessed (Figure 7.5B). All showed the same pattern, whereby AMP and CHR were clustered to the left while SOIL, PE, and PE-CHR were clustered to the right. This indicates that microbial communities' ability to utilise individual substrates in the AMP and CHR treatments was different the communities' abilities in the SOIL, PE, and PE-CHR treatments. This complements the results from the *t*-tests outlined above, i.e., that AMP and CHR displayed significantly lower microbial activity than SOIL ($p < 0.05$) while PE and PE-CHR displayed higher microbial activity, but not significantly ($p > 0.05$). The clustering of AMP and CHR towards the water control (compared to PE and PE-CHR) may also suggest that the microbial communities of these treatments struggled to utilise individual substrates as reflected in the MicroResp™ measurements (Figure 7.4).

A further PCA plot was generated to evaluate how the treatments affected their microbial communities' ability to utilise the full suite of carbon substrates at day 57 (Figure 7.6). This plot showed there was separation of AMP to the right of the plot with CHR overlapping with SOIL towards the right. There was separation of PE to the left of the plot while PE-CHR overlapped with SOIL with some separation to the left. The spatial separation of the treatments in Figure 7.6 aligns with the results observed with both soil respiration and substrate-induced respiration. AMP resulted in a significant decrease in soil respiration, while CHR1-3 also lead to significant reductions in soil respiration ($p < 0.05$; see section 7.3.1). Opposingly, PE resulted in an increase in soil respiration (but not significantly ($p > 0.05$)), while PE-CHR showed no significant change in soil respiration compared to SOIL. Similar results were observed for substrate-induced respiration.
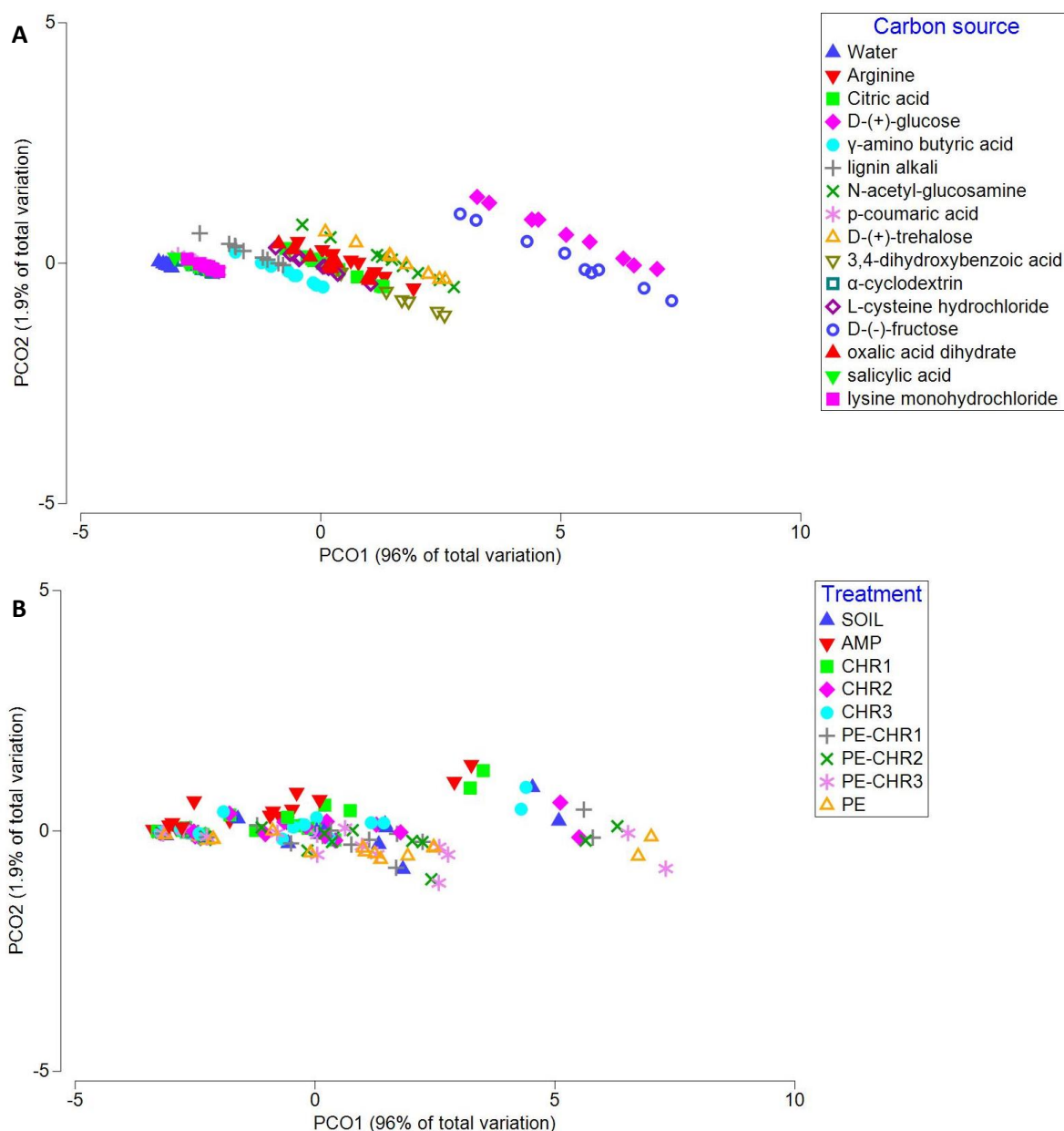
Figure 7.5: PCA plot showing the variation in (A) individual carbon substrates utilisation by the microbial communities of each treatment over time and (B) how each treatment can utilise individual substrates.

Factors driving separation of the groups were overlaid on the plot (r > 0.85) (Figure 7.6A) and further examination of the component loading values informed which substrate utilisations drove spatial variation for PCO1 and PCO2 (Figure 7.6B). PCO1 accounted for most of the variation (59.4%). D-(+)-trehalose (r = 0.861), D-(-)-fructose (r = 0.842), and α-cyclodextrin (r = 0.819) were the three strongest component loadings for driving separation along PCO1. PCO2 only accounted for 9.1% of the variation. *N*-acetyl-glucosamine (r = 0.541), D-(+)-glucose (r = 0.503), and γ-amino butyric acid (r = 0.453) in each of the treatments were the three strongest component loadings for driving separation along PCO2.

Taken together, the effects of the treatments on their microbial communities' potential to respire a suite of carbon substrates aligns with the spatial variation of the treatments within the PCA plot. The lack of considerable spatial separation of the treatments may indicate that, overall, the treatments did not substantially affect microbial function. However, assessment of the microbial community structures within the treatments should be assessed.

Substrate	PCO1	PCO2
Water	-0.796	0.174
Arginine	-0.732	0.071
Citric acid	-0.757	0.016
D-(+)-glucose	-0.760	-0.503
γ-amino butyric acid	-0.801	-0.453
lignin alkali	-0.773	-0.305
N-acetyl-glucosamine	-0.789	-0.541
p-coumaric acid	-0.701	-0.141
D-(+)-trehalose	-0.861	0.241
3,4-dihydroxybenzoic acid	-0.814	0.249
α-cyclodextrin	-0.819	0.152
L-cysteine hydrochloride	-0.785	0.319
D-(-)-fructose	-0.842	0.249
oxalic acid dihydrate	-0.707	0.439
salicylic acid	-0.551	0.187
lysine monohydrochloride	-0.795	-0.129

Figure 7.6: (A) PCA plot showing the variation in the microbial communities' ability to utilise all the carbon substrates between treatments at day 57 with Pearson's correlations overlaid (where r > 0.85). (B) Component loadings are tabulated below the graph, with the three highest loadings highlighted in red for PCO1 and PCO2, respectively.

7.3.2.1 Substrate-induced respiration indicates changes to microbial biomass between treatments

Glucose is a readily decomposable respiratory substrate in soil and has previously been used as an indicator for microbial biomass (Anderson and Domsch, 1973; Nakamoto and Wakahara, 2004; Bérard et al., 2014). Assessments of the day 57 values for microbial activity in response to glucose-induced respiration showed that AMP was significantly lower than SOIL ($p < 0.05$). As discussed in section 7.3.1, ampicillin is a broad-spectrum, bactericidal antibiotic, therefore, should decrease microbial biomass. Since microbial activity was significantly lower in AMP, this indicates that microbial biomass was indeed reduced, which confirms that the lower soil respiration was a result of this reduction in microbial biomass (Figure 7.2).

CHR displayed a similar response to AMP. Since CHR resulted in a significant decrease in glucose-induced respiration ($p < 0.05$), this indicates that CHR reduced microbial biomass, explaining the decrease observed in soil respiration (Figure 7.2). PAHs can potentially induce toxic effects to soil micro-organisms by inhibiting metabolic and enzymatic activities, e.g., oxidative phosphorylation processes (Zoppini et al., 2016) and decreased secretion of enzymes such as β-1,4-glucosidase, β-1,4-*N*-acetyl-glucosaminidase, and alkaline phosphatase (Pérez-Leblic et al., 2012) used in carbon, nitrogen, and phosphorus cycling, respectively. The disruption to these microbial functions can lead to reduced microbial biomass, limited nutrient availability, and reduced biodiversity in affected soils (Feyissa et al., 2023).

PE displayed an increase in microbial activity in glucose-induced respiration, but not significantly ($p > 0.05$). This indicates that the presence of polyethylene microplastics resulted in a slight increase in microbial biomass. PE similarly displayed a slight increase in soil respiration (Figure 7.2). These results suggest that the increase in soil respiration was a result of increased biomass, rather than due to a stress response (Schindlbacher et al., 2011). Substrate-induced respiration in microplastic contaminated soils has resulted in varied microbial responses, whereby some studies report a decrease in respiration indicating reduced biomass (e.g., Li et al., 2023) while other studies reported increased respiration indicating elevated microbial biomass (e.g., Chen, 2016). Further analyses to determine microbial biomass would need to be conducted to confirm these inferences based on soil respiration and MicroResp™ (glucose-induced respiration).

Similar to PE, PE-CHR displayed an increase in microbial activity in glucose-induced respiration. However, soil respiration for PE-CHR was slightly lower than SOIL (Figure 7.2). A possible reason for this could be that the polyethylene microfilms promoted an increase in microbial biomass, however, the presence of chrysene sorbed to their surface may have inhibited microbial activity/respiration.

Microplastics have been described as a potential carbon source for microbial metabolism (Cao et al., 2023). Carbon priming involves the addition of a new carbon substrate which affects the microbial community's ability to mineralise native carbon sources, and this can both be positive priming (i.e., stimulates native carbon mineralisation) or negative priming (i.e., hinders native carbon mineralisation) (Rillig et al., 2021). Positive priming may occur as a result of co-metabolism of the microplastics (or it's additives) and native carbon substrates, while negative priming could occur as a result of adsorption of soil dissolved carbon to the microplastic surface or a switch in metabolism to mineralise easily mineralisable carbon in microplastics (Rillig et al., 2021; Yao et al, 2021; Cao et al., 2023; Ma et al., 2023). The same can be said for the introduction of chrysene as a new carbon source to soils. The potential for carbon priming induced by microplastics or chrysene may explain the differences in the metabolism of the different carbon substrates. Further work would need to be conducted to determine the potential for microplastic- and chrysene-induced priming through isotopic analysis to distinguish between depletion of microplastic carbon relative to soil organic carbon.

Overall, substrate-induced respiration confirmed the findings observed with soil respiration and, specifically, glucose-induced respiration further indicated that the treatments affected microbial biomass, which in turn affected soil respiration. Results suggested that amendment of soil with chrysene and ampicillin resulted in decreased biomass (leading to a decrease in soil respiration was), while amendment with polyethylene microfilms increased microbial biomass, leading to an increase in soil respiration. The addition of chrysene-bound microfilms increased biomass, however, soil respiration was lowered indicating that the presence of chrysene on the microfilms may have induced a stress effect on the soil micro-organisms.

7.3.3 Microfilms and chrysene alter soil microbial diversity

The bacterial 16S rRNA gene sequences for each treatment were investigated to determine whether the incorporation of microplastics, chrysene, or both influenced soil microbial community composition, particularly given the effects observed with microbial activity (see sections 7.3.1 and 7.3.2). Following

the bioinformatics pipeline, samples with read counts < 40,000 were removed from downstream analyses. These number of reads is slightly lower than the recommended threshold, however, significantly lower thresholds have been used previously for low biomass samples (Bender et al., 2018).

Alpha diversity (within sample diversity) was assessed by comparing the OTUs at day 2 and day 30 using *t*-tests. CHR1, PE-CHR2, and PE-CHR3 significantly increased in richness (Margalef index; $p < 0.05$), CHR1, AMP, PE, and PE-CHR1-3 increased in species evenness (Pielou's evenness; $p < 0.05$), and all treatments except PE increased in species diversity (Shannon-Weiner index; $p < 0.05$). These changes within treatments may suggest that rarer members of the microbial community proliferated over time (see section 7.3.3.2).

7.3.3.1 Effect of microfilms and chrysene on microbial diversity

Beta diversity was assessed on OTUs from day 30. This was acceptable to use as the data from the soil respiration (section 7.3.1) and substrate-induced respiration data (section 7.3.2) indicated that communities appeared to be stable. Compared to SOIL, AMP and CHR slightly decreased in species richness, however, these were not significant ($p > 0.1$), while PE and PE-CHR significantly increased in species richness, ($p < 0.1$). All treatments led to a slight increase in both species evenness and diversity compared to SOIL, however, only AMP and PE-CHR1-3 for species richness, and AMP, PE-CHR2, and PE-CHR3 for species diversity exhibited significant increases ($p < 0.1$). Figure 7.7 displays the results for species richness, Pielou's evenness, and Shannon diversity index, with *t*-test results represented on the box plots as a series of letters where shared letters indicated there was no statistically significant difference between the treatments.

Chrysene contamination in soils has been reported to reduce bacterial richness (Shen et al., 2023), which was observed in this study, albeit not significantly ($p > 0.05$). Other studies investigating the influence of polyethylene microplastic addition to soils on microbial communities similarly reported that no meaningful change in richness, evenness, or diversity occurred compared to control soils (e.g., Huang et al., 2019). However, Huang et al. (2019) reported that the community structure of the microbes on the microplastics was significantly altered. As previously mentioned, microplastics can act as a substrate for the development of biofilms through microbial colonisation, whereby the microbial community composition of the biofilms may be distinct from the microbial community structure of the surrounding soil and act as a barrier in protecting the surrounding soil micro-organisms from the effects
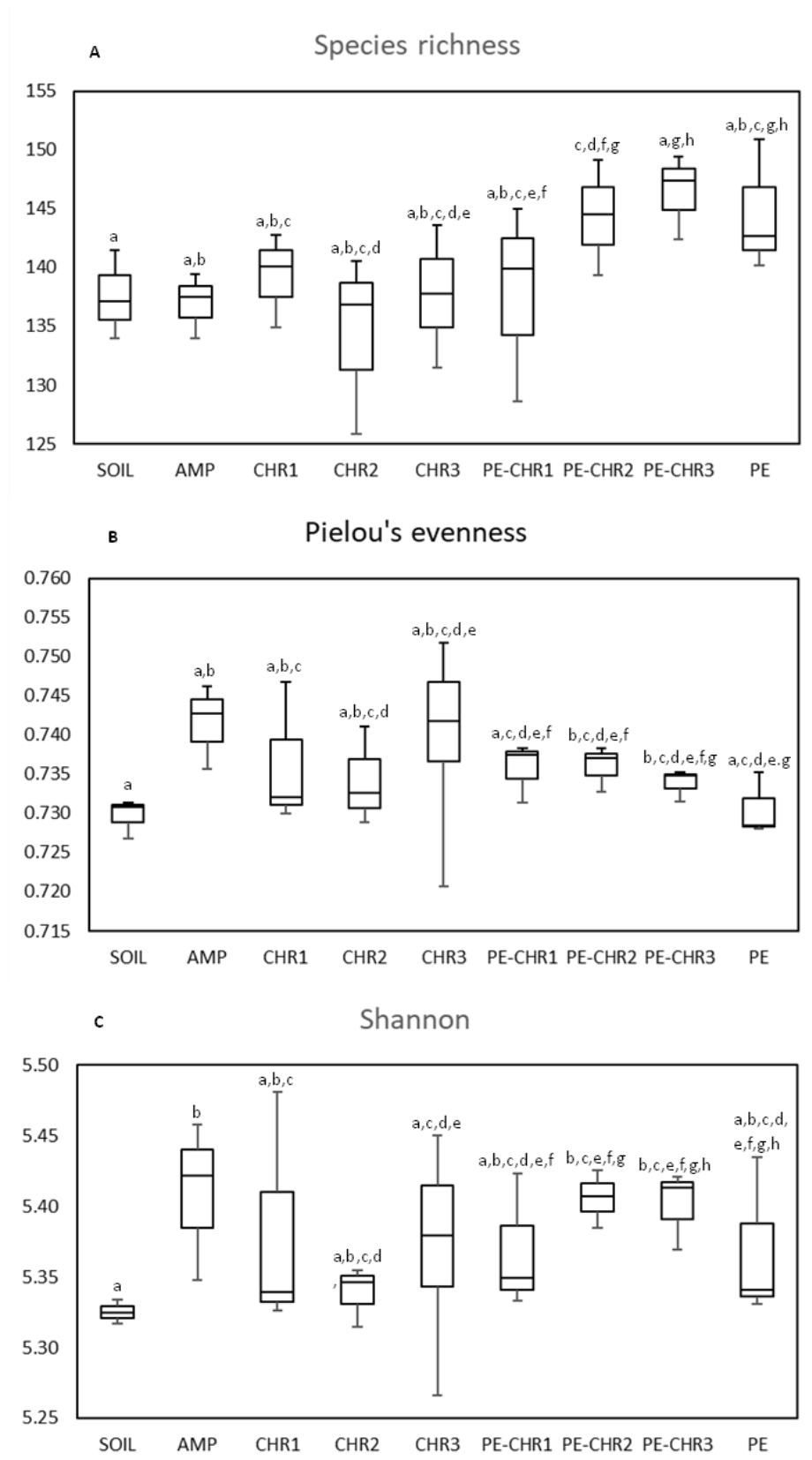
Figure 7.7: Box plots displaying (A) species richness (Margalef), (B) Pielou's evenness, and (C) Shannon diversity index for each treatment. *t*-Test results were represented on the box plots as a series of letters where shared letters indicated there was no statistically significant difference between the treatments.

of the microplastic bound-chrysene (Miao et al., 2019; Xu et al., 2021). While the impact on micro-organisms potentially colonising the microfilms was attempted to be included in all analyses by ensuring that the microfilms remained in the soil for all tests (soil respiration, MicroResp™, and 16S sequencing), any effects may potentially have been confounded by the microbes in the surrounding soil which were in greater abundance. Therefore, future studies would aim to investigate the impact of microbial communities attached to microfilms and those within the bulk soil separately.

Overall, results from beta diversity analysis did not align with what was anticipated (i.e., that CHR would significantly alter the microbial community structure compared to the control (SOIL) as the results from soil and substrate-induced respiration potentially indicated – section 7.3.1 and 7.3.2, respectively). However, assessment of the community composition revealed significant changes between treatment groups at a finer level (see section 7.3.3.2).

7.3.3.2 Chrysene-bound microfilms and chrysene affected soil microbial community structure

Differences in the species relative abundance in the soil microcosms for each treatment at the class and family levels are displayed in Figure 7.8. At the class level, the three most abundant classes were *Bacilli* (15.0-25.1% in relative abundance), *Alphaproteobacteria* (15.3-21.8%), and *Actinomycetia* (12.2-16.1%), and were represented across all the treatment groups and time points (Figure 7.8A). *Firmicutes*, *Proteobacteria*, and *Actinobacteria* are typical bacteria found in soils and are well documented in soil microbiology (Zhang et al., 2019; Mhete et al., 2020). The relative abundances of the dominant bacterial classes were consistent across the treatments over time apart from day 30, where there were marked differences (Figure 7.8A). Microplastics have previously been reported to enrich the proportions of *Actinobacteria* and *Bacteroidia* in soil (Zhang et al., 2019), which was the case in this study in the day 30 samples for treatments which contained polyethylene microfilms (Figure 7.8A). Furthermore, *Bacilli*, *Actinobacteria*, and *Alphaproteobacteria* have been reported to have the potential to degrade PAHs in soil (Lu et al., 2019; Mandree et al., 2021), therefore, it was anticipated that these classes may be enriched in chrysene contaminated treatments. However, there was no obvious enrichment in relative abundance of these bacterial classes observed in Figure 7.8A.

Examining microbial relative abundances at the family level (Figure 7.8B) further highlighted the shifts in microbial communities, both over time and between treatments. This indicates the effects of the treatments were more pronounced at a lower taxonomic level. Of interest, there was a noticeable

Figure 7.8: Stacked bar charts of (A) class and (B) family abundances in the different treatments. The 34 most abundant classes and families are listed, respectively. Days are labelled for each replicate per treatment.

increase in relative abundance of *Proteobacteria* in the CHR treatments at the family level, e.g., OTUs classified as *Burkholderiaceae* (1.9-2.9% in relative abundance at day 30 compared to 0-0.1% in all non-CHR treatments, with relative abundance ranging from 0.7-1.0% in PE-CHR treatments). As discussed, these are bacteria active in PAH degradation (Lu et al., 2019; Mandree et al., 2021), which indicates that the enrichment of these bacterial families in CHR may be a direct response to the presence of chrysene contamination in those soil environments. The abundance of *Burkholderiaceae* was markedly

less in PE-CHR suggesting that the sorption of chrysene to polyethylene microfilms indeed limited the availability of chrysene to soil micro-organisms and may alleviate the immediate effects of chrysene.

A non-metric multidimensional scaling (nMDS) plot was generated to evaluate the similarity in community compositions between treatments for day 30 and factors driving dissimilarity were assessed (Figure 7.9). The plot indicated that at day 30, the microbial community compositions for each treatment were different and had a 2D stress value of 0.19, providing confidence in the results. ANOSIM confirmed that AMP ($R = 0.407$), PE-CHR2 ($R = 0.370$), PE-CHR3 ($R = 0.185$), CHR1 ($R = 0.815$), and CHR3 ($R = 0.852$) were statistically different to SOIL ($p < 0.1$), suggesting that microbial community composition significantly differed between these treatments. These shifts in microbial community composition likely reflects the reduction in soil respiration and microbial biomass observed in section 7.3.1 and 7.3.2, respectively. Horizontal variability was predominantly driven by the microbial communities' ability to utilise D-(+)-glucose and D-(-)-fructose (which were two substrates highlighted in the MicroResp^{TM} discussion in section 7.3.2), as well as other harder to utilise substrates (e.g., p-coumaric acid), while vertical variability was driven by soil respiration.

Noticeably, there was a significance in changes in microbial community compositions between treatments compared to that observed for soil respiration and substrate-induced respiration. This suggests that the treatments markedly changed microbial community compositions, but overall ecosystem function was less changed. This may reflect functional redundancy in the microbial population to allow ecosystem function to continue similarly to its original community or resilience of the population to recover from disturbance in the form of added pollutants (Allison and Martiny, 2008). Results from this study suggest that it would be beneficial to assess these factors in future studies to further understand the impact of microplastic and organic pollutant amendments on microbial community and their functionality in soil.

7.4 Conclusion

This study investigated the impact of chrysene, microfilms, and chrysene-bound microfilms on ecosystem function (soil respiration), microbial activity (substrate-induced respiration) and changes in soil microbial community composition. Amendment of soil with chrysene was observed to cause a significant reduction in soil respiration and substrate-induced respiration compared to the soil control. Using glucose-induced respiration as an indicator for microbial biomass, chrysene likely caused a
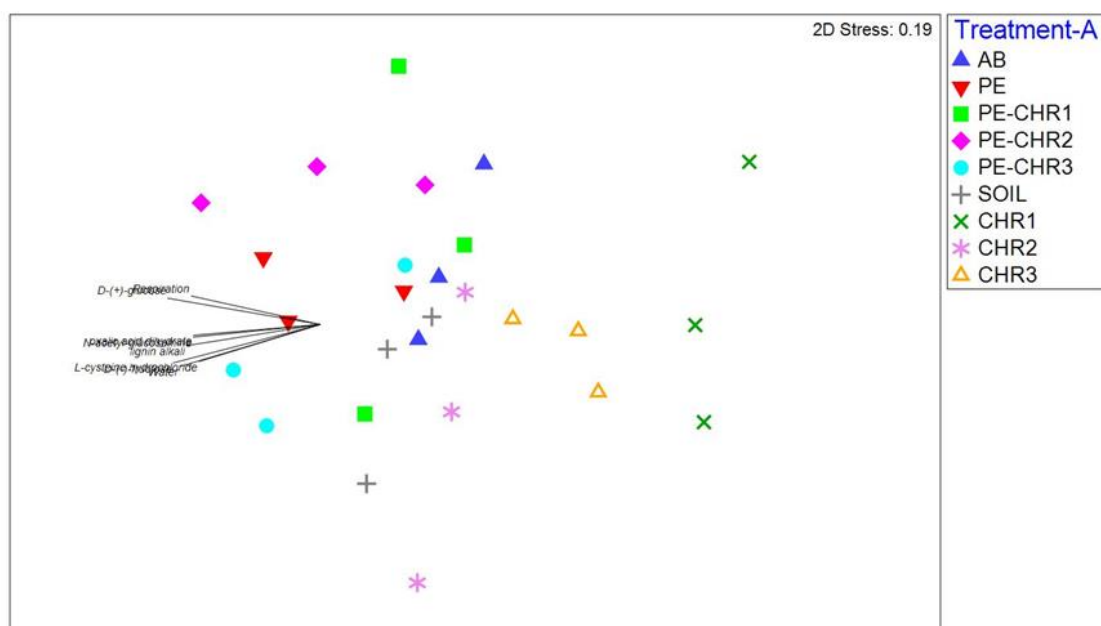
Figure 7.9: Non-metric multidimensional scaling (nMDS) plot of the soil microbial community compositions by treatment for day 30 with Pearson's correlations overlaid (where r > 0.5).

reduction in microbial biomass, suggesting that the decrease in respiration was attributed to a loss in biomass. Polyethylene microfilms resulted in a slight increase in soil and substrate-induced respiration, but this was not significant. This was attributed to an increase in microbial biomass, rather than due to a stress response. The chrysene-sorbed microfilms treatment resulted in not significant decrease in soil respiration but a not significant increase in substrate-induced respiration. Glucose-induce respiration suggested that the presence of the microfilms promoted microbial biomass, however, the decrease in soil respiration compared to soil indicated that ecosystem function was hindered through the presence of the pollutant, chrysene. The ability of the microbial communities to utilise carbon sources under the different treatment groups was assessed by principal components analysis which confirmed the findings of the soil respiration measurements.

Furthermore, changes in microbial community compositions between treatments was assessed. Beta diversity analysis highlighted changes in microbial diversity between treatments, while assessment of the microbial community compositions highlighted that the effects of the treatments was more pronounced at a lower taxonomic level. There was evidence of rarer species enrichment pertaining to chrysene degradation in the chrysene treatments and, to a lesser degree, in the chrysene-bound microfilm treatments. This further suggested that the sorption of chrysene to polyethylene microfilms

indeed limited the availability of chrysene to soil micro-organisms and may alleviate the immediate effects of chrysene as suspected from evidence gathered in Chapter 6.

The results of this study indicate that the potential for polyethylene microfilms to easily sequester chrysene in soil, as well as other PAHs (Chapter 6), can markedly lead to the negation of the negative impacts of chrysene on soil micro-organisms. However, the sorption of these contaminants to microplastics may further prolonged their exposure to the terrestrial environment.

7.5 References

Allison S.D., Martiny J.B.H. Resistance, resilience, and redundancy in microbial communities. *PNAS*. 2008; 105, 11512-11519. DOI: https://doi.org/10.1073/pnas.0801925105

Anderson J.P.E, Domsch K.H. Quantification of bacterial and fungal contributions to soil respiration. *Archiv für Mikrobiologie*. 1973; 93, 113-127. DOI: https://doi.org/10.1007/BF00424942

Bender J.M., Li F., Adisetiyo H., Lee D., Zabih S., Hung L., Wilkinson T.A., Pannaraj P.S., She R.C., Bard J.D., Tobin N.H, Aldrovandi G.M. Quantification of variation and the impact of biomass in targeted 16S rRNA gene sequencing studies. *Microbiome*. 2018; 6, 155. DOI: https://doi.org/10.1186/s40168-018-0543-z

Bérard A., Mozzia C., Sappin-Didier V., Capowiez L., Capowiez Y. Use of the MicroResp™ method to assess Pollution-Induced Community Tolerance in the context of metal soil contamination. *Ecological Indicators*. 2014; 40, 27-33. DOI: https://doi.org/10.1016/j.ecolind.2013.12.024

Bolyen E., Rideout, J.R., Dillon, M.R., et al. Reproducible, interactive, scalable and extensible microbiome data science using QIIME 2. *Nature Biotechnology*. 2019; 37, 852-857. DOI: https://doi.org/10.1038/s41587-019-0209-9

Bonin A.M., Rosario C.A., Duke C.C., Baker R.S.U., Ryan A.J., Holder G.M. The mutagenicity of dibenz[*a,j*]acridine, some metabolites and other derivatives in bacteria and mammalian cells. *Carcinogenesis*. 1989; 10, 1079-1084. DOI: https://doi.org/10.1093/carcin/10.6.1079

British Standards Institution (2009) *BS EN ISO 13320:2009: Particle size analysis – laser diffraction methods*. Available at: https://www.iso.org/standard/44929.html (Accessed: 02 February 2021).

Burns E.E., Boxall A.B.A. Microplastics in the aquatic environment: evidence for or against adverse impacts and major knowledge gaps. *Environmental Toxicology and Chemistry*. 2018; 37, 2776-2796. DOI: https://doi.org/10.1002/etc.4268

Campbell C.D., Chapman S.J., Cameron C.M., Davidson M.S., Potts J.M. A rapid microtiter plate method to measure carbon dioxide evolved from carbon substrate amendments so as to determine the physiological profiles of soil microbial communities by using whole soil. *Applied and Environmental Microbiology*. 2003; 69, 3593-3599. DOI: https://doi.org/10.1128/AEM.69.6.3593-3599.2003

Cao J., Li C., Gao X., Cai Y., Song X., Siddique K.H.M., Zhao X. Agricultural soil plastic as a hidden carbon source stimulates microbial activity and increases carbon dioxide emissions. *Resources, Conservation and Recycling*. 2023; 198, 107151. DOI: https://doi.org/10.1016/j.resconrec.2023.107151

Cao L., Shen G., Lu Y. Combined effects of heavy metal and polycyclic aromatic hydrocarbon on soil microorganism communities. *Environmental Geology*. 2008; 54, 1531-1536. DOI: https://doi.org/10.1007/s00254-007-0934-0

Chen H., 2016. *Synergistic effects of glyphosate and microplastic on soil microbial activities in Chinese loess soil*. [online]. MSc thesis, Wageningen University. Available from: https://edepot.wur.nl/386619 [accessed 19 March 2024].

Chen L., Wang C., Su J. Understanding the Effect of Different Glucose Concentrations in the Oligotrophic Bacterium *Bacillus subtilis* BS-G1 through Transcriptomics Analysis. *Microorganisms*. 2023; 11, 2401. DOI: https://doi.org/10.3390/microorganisms11102401

Cui W., Hale R.C., Huang Y., Zhou F., Wu Y., Liang X., Liu Y., Tan H., Chen D. Sorption of representative organic contaminants on microplastics: Effects of chemical physicochemical properties, particle size, and biofilm presence. *Ecotoxicology and Environmental Safety*. 2023; 251, 114533. DOI: https://doi.org/10.1016/j.ecoenv.2023.114533

de Souza Machado A.A., Lau C.W., Kloas W., Bergmann J., Bachelier J.B., Faltin E., Becker R., Görlich A.S., Rillig M.C. Microplastics Can Change Soil Properties and Affect Plant Performance. *Environmental Science and Technology*. 2019; 53, 6044-6052. DOI: https://doi.org/10.1021/acs.est.9b01339

de Souza Machado A.A., Lau C.W., Till J., Kloas W., Lehmann A., Becker R., Rillig M.C. Impacts of Microplastics on the Soil Biophysical Environment. *Environmental Science and Technology*. 2018; 52, 9656-9665. DOI: https://doi.org/10.1021/acs.est.8b02212

Evans R., Alessi A.M., Bird S., McQueen-Mason S.J., Bruce N.C., Brockhurst M.A. Defining the functional traits that drive bacterial decomposer community productivity. *The ISME Journal*. 2017; 11, 1680-1687. DOI: https://doi.org/10.1038/ismej.2017.22

Evans S.E., Wallenstein M.D. Soil microbial community response to drying and rewetting stress: does historical precipitation regime matter? *Biogeochemistry*. 2012; 109, 101-116. DOI: https://doi.org/10.1007/s10533-011-9638-3

Feyissa A. Chen R., Cheng X. Afforestation inhibited soil microbial activities along the riparian zone of the upper Yangtze River of China. *Forest Ecology and Management*. 2023; 538, 120998. DOI: https://doi.org/10.1016/j.foreco.2023.120998

Hedfi A., Ali M.B., Korkobi M., Allouche M., Harrath A.H., Beyrem H., Pacioglu O., Badraoui R., Boufahja F. The exposure to polyvinyl chloride microplastics and chrysene induces multiple changes in the structure and functionality of marine meiobenthic communities. *Journal of Hazardous Materials*. 2022; 436, 129161. DOI: https://doi.org/10.1016/j.jhazmat.2022.129161

Huang Y., Zhao Y., Wang J., Zhang M., Jia W., Qin X. LDPE microplastic films alter microbial community composition and enzymatic activities in soil. *Environmental Pollution*. 2019; 254, 112983. DOI: https://doi.org/10.1016/j.envpol.2019.112983

Hüffer T., Hofmann T. Sorption of non-polar organic compounds by micro-sized plastic particles in aqueous solution. *Environmental Pollution*. 2016; 214, 194-201. DOI: https://doi.org/10.1016/j.envpol.2016.04.018

Kim S.W., Liang Y., Zhao T., Rillig M.C. Indirect Effects of Microplastic-Contaminated Soils on Adjacent Soil Layers: Vertical Changes in Soil Physical Structure and Water Flow. *Frontiers in Environmental Science*. 2021; 9, 681934. DOI: https://doi.org/10.3389/fenvs.2021.681934

Li X., Qu C., Bian Y., Gu C., Jiang X., Song Y. New insights into the responses of soil microorganisms to polycyclic aromatic hydrocarbon stress by combining enzyme activity and sequencing analysis with metabolomics. *Environmental Pollution*. 2019; 255, 113312. DOI: https://doi.org/10.1016/j.envpol.2019.113312

Li Y., Hou Y., Hou Q., Long M., Wang Z., Rillig M.C., Liao Y., Yong T. Soil microbial community parameters affected by microplastics and other plastic residues. *Frontiers in Microbiology*. 2023; 14, 1258606. DOI: https://doi.org/10.3389%2Ffmicb.2023.1258606

Ling J., Jiang Y.S., Dong J.D., Zhang Y.Y., Zhang Y.Z. Responses of bacterial communities in seagrass sediments to polycyclic aromatic hydrocarbon-induced stress. *Ecotoxicology*. 2015; 24, 1517-1528. DOI: https://doi.org/10.1007/s10646-015-1493-x

Liu J., Liu Y., Dong W., Li J., Yu S., Wang J., Zuo R. Shifts in microbial community structure and function in polycyclic aromatic hydrocarbon contaminated soils at petrochemical landfill sites revealed by metagenomics. *Chemosphere*. 2022; 293, 133509. DOI: https://doi.org/10.1016/j.chemosphere.2021.133509

Lou Y., Zhou X., 2006. *Soil Respiration and the Environment*. Cambridge, MA: Academic Press. DOI: https://doi.org/10.1016/B978-0-12-088782-8.X5000-1

Lozano Y.M., Lehnert T., Linck L.T., Lehmann A., Rillig M.C. Microplastic Shape, Polymer Type, and Concentration Affect Soil Properties and Plant Biomass. *Frontiers in Plant Science*. 2021; 12, 616645. DOI: https://doi.org/10.3389/fpls.2021.616645

Lu C., Hong Y., Liu J., Gao Y., Ma Z., Yang B., Ling W., Waigi M.G. A PAH-degrading bacterial community enriched with contaminated agricultural soil and its utility for microbial bioremediation. *Environmental Pollution*. 2019, 251, 773-782. DOI: https://doi.org/10.1016/j.envpol.2019.05.044

Ma Y., Yang K., Yu H, Tan W., Gao Y., Lv B. Effects and mechanism of microplastics on organic carbon and nitrogen cycling in agricultural soil: A review. *Soil Use and Management*. 2023; 40, e12971. DOI: https://doi.org/10.1111/sum.12971

Maliszewska-Kordybach B., Smreczak B. Changes in soil properties in the course of PAH dissipation in soils artificially contaminated with these compounds. *Polycyclic Aromatic Compounds*. 2003b; 23, 1-12. DOI: https://doi.org/10.1080/10406630390163080

Maliszewska-Kordybach B., Smreczak B. Habitat function of agricultural soils as affected by heavy metals and polycyclic aromatic hydrocarbons contamination. *Environment International*. 2003a; 28, 719-728. DOI: https://doi.org/10.1016/S0160-4120(02)00117-4

Mandree P., Masika W., Naicker J., Moonsamy G., Ramchuran S., Lalloo R. Bioremediation of Polycyclic Aromatic Hydrocarbons from Industry Contaminated Soil Using Indigenous *Bacillus* spp. *Processes*. 2021; 9, 1606. DOI: https://doi.org/10.3390/pr9091606

Mayer M., Sandén H., Rewald B., Godbold D.L., Katzensteiner K. Increase in heterotrophic soil respiration by temperature drives decline in soil organic carbon stocks after forest windthrow in a mountainous ecosystem. *Functional Ecology*. 2017; 31, 1162-1172. DOI: https://doi.org/10.1111/1365-2435.12805

Mhete M., Eze P.N., Rahube T.O., Akinyemi F.O. Soil properties influence bacterial abundance and diversity under different land-use regimes in semi-arid environments. *Scientific African*. 2020; 7, e00246. DOI: https://doi.org/10.1016/j.sciaf.2019.e00246

Miao L., Wang P., Hou J., Yao Y., Liu Z., Liu S., Li T. Distinct community structure and microbial functions of biofilms colonizing microplastics. *Science of The Total Environment*. 2019; 650, 2395-2402. DOI: https://doi.org/10.1016/j.scitotenv.2018.09.378

Mingorance M.D., Peña A. A methodological approach to measure soil respiration. *Journal of Geochemical Exploration*. 2016; 169, 187-191. DOI: https://doi.org/10.1016/j.gexplo.2016.07.019

Nakamoto T., Wakahara S. Development of substrate induced respiration (SIR) method with selective inhibition for estimating fungal and bacterial biomass in humic andosols. *Plant Production Science*. 2004; 7, 70-76. DOI: https://doi.org/10.1626/pps.7.70

Nurjanah S., Sulistyanti S.T., Dewanti-Hariyadi R. Application of GFPuv labeled *Cronobacter sakazakii* for evaluation of its survival during cornstarch processing. *World Journal of Engineering and Technology*. 2015; 3, 1-6. DOI: http://dx.doi.org/10.4236/wjet.2015.33B001

Pella E., Colombo B. Study of carbon, hydrogen and nitrogen by combustion gas-chromatography. *Mikrochim Acta*. 1973; 1973, 697-719. DOI: https://doi.org/10.1007/BF01218130

Pérez-Leblic M.I., Turmero A., Hernández M., Hernández A.J., Pastor J., Ball A.S., Rodríguez J., Arias M.E. Influence of xenobiotic contaminants on landfill soil microbial activity and diversity. *Journal of Environmental Management*. 2012; 95, S285-S290. DOI: https://doi.org/10.1016/j.jenvman.2010.07.017

Picariello E., Baldantoni D., De Nicola F. Acute effects of PAH contamination on microbial community of different forest soils. *Environmental Pollution*. 2020; 262, 114378. DOI: https://doi.org/10.1016/j.envpol.2020.114378

Querejeta G.A. Sterilize Methods Comparison for Soils: Cost, Time, and Efficiency. *International Journal of Methodology*. 2023; 2, 34-40. DOI: http://dx.doi.org/10.21467/ijm.2.1.6263

Rhind S.M., Kyle C.E., Kerr C., Osprey M., Zhang Z.L., Duff E.I., Lilly A., Nolan A., Hudson G., Towers W., Bell J., Coull M., McKenzie C. Concentrations and geographic distribution of selected organic pollutants in Scottish surface soils. *Environmental Pollution*. 2013; 182, 15-27. DOI: https://doi.org/10.1016/j.envpol.2013.06.041

Rillig M.C., Leifheit E., Lehmann J. Microplastic effects on carbon cycling processes in soils. *PLoS Biology*. 2021; 19, e3001130. DOI: https://doi.org/10.1371/journal.pbio.3001130

Schindlbacher A., Rodler A., Kuffner M., Kitzler B., Sessitsch A., Zechmeister-Boltenstern S. Experimental warming effects on the microbial community of a temperate mountain forest soil. *Soil Biology & Biochemistry*. 2011; 43, 1417-1425. DOI: https://doi.org/10.1016%2Fj.soilbio.2011.03.005

Shen Q., Fu W., Chen B., Zhang X., Xing S., Ji C., Zhang X. Community response of soil microorganisms to combined contamination of polycyclic aromatic hydrocarbons and potentially toxic elements in a typical coking plant. *Frontiers in Microbiology*. 2023; 14, 1143742. DOI: https://doi.org/10.3389/fmicb.2023.1143742

Sun Y., Li X., Cao N., Duan C., Ding C., Huang Y., Wang J. Biodegradable microplastics enhance soil microbial network complexity and ecological stochasticity. *Journal of Hazardous Materials*. 2022; 439, 129610. DOI: https://doi.org/10.1016/j.jhazmat.2022.129610

The James Hutton Institute, 2024. *UK Crop Diversity Bioinformatics HPC Resource*. [online]. Aberdeen: Information & Computational Sciences, The James Hutton Institute. Available from: https://www.cropdiversity.ac.uk/

Unger I.M., Goyne K.W., Kennedy A.C., Kremer R.J., McLain J.E.T., Williams C.F. Antibiotic Effects on Microbial Community Characteristics in Soils under Conservation Management Practices. *Soil Science Society of America Journal*. 2013; 77, 100-112. DOI: https://doi.org/10.2136/sssaj2012.0099

Wang T., Wang L., Chen Q., Kalogerakis N., Ji R., Ma Y. Interactions between microplastics and organic pollutants: Effects on toxicity, bioaccumulation, degradation, and transport. *Science of The Total Environment*. 2020; 748, 142427. DOI: https://doi.org/10.1016/j.scitotenv.2020.142427

Xu B., Liu F., Cryder Z., Huang D., Lu Z., He Y., Wang H., Lu Z., Brookes P.C., Tang C., Gan J., Xu J. Microplastics in the soil environment: occurrence, risks, interactions and fate – a review. *Critical Reviews in Environmental Science and Technology*. 2020; 50, 2175-2222. DOI: https://doi.org/10.1080/10643389.2019.1694822

Xu M., Du W., Ai F., Xu F., Zhu J., Yin Y., Ji R., Guo H. Polystyrene microplastics alleviate the effects of sulfamethazine on soil microbial communities at different CO_2 concentrations. *Journal of Hazardous Materials*. 2021; 413, 125286. DOI: https://doi.org/10.1016/j.jhazmat.2021.125286

Yao Y. Lili W., Shufen P., Gang L., Hongmei L., Weiming X., Lingxuan G., Jianning Z., Guilong Z., Dianlin Y. Can microplastics mediate soil properties, plant growth and carbon/nitrogen turnover in the terrestrial ecosystem? *Ecosystem Health and Sustainability*. 2022; 8, 2133638. DOI: https://doi.org/10.1080/20964129.2022.2133638

Zhang M., Zho Y., Qin X., Jia W., Chai L., Huang M., Huang Y. Microplastics from mulching film is a distinct habitat for bacteria in farmland soil. *Science of the Total Environment*. 2019; 688, 470-478. DOI: https://doi.org/10.1016/j.scitotenv.2019.06.108

Zhao T., Lozano Y.M., Rillig M.C. Microplastics Increase Soil pH and Decrease Microbial Activities as a Function of Microplastic Shape, Polymer Type, and Exposure Time. *Frontiers in Environmental Science*. 2021; 9, 675803. DOI: https://doi.org/10.3389/fenvs.2021.675803

Zhu Y.G., Peng J.J., Wei Z., Shen Q.R., Zhang F.S. Linking the soil microbiome to soil health. *Scientia Sinica Vitae*. 2021; 51, 1-11. DOI: https://doi.org/10.1360/SSV-2020-0320

Zoppini A., Ademollo N., Amalfitano S., Capri S., Casella P., Fazi S., Marxsen J., Patrolecco L. Microbial responses to polycyclic aromatic hydrocarbon contamination in temporary river sediments: Experimental insights. *Science of The Total Environment*. 2016; 541, 1364-1371. DOI: https://doi.org/10.1016/j.scitotenv.2015.09.144

Chapter 8: Conclusions and future work

8.1 Thesis overview

It is clear that microplastic pollution in our natural environment is a global and significant issue, with many unknowns regarding the extent or impact these anthropogenic pollutants cause, particularly in the terrestrial environment where there is considerably less research compared to the marine environment despite estimations of microplastic abundance to be significantly higher.

It was the overarching aim of this project to determine the extent of macro- and microplastics in Scottish surface soils, both spatially and temporally, and evaluate the impact of microplastics on soil function and ecosystem services. Discussion of how this aim was fulfilled using the following objectives is discussed below and future work identified as a result of this research is also discussed within each objective.

8.2 Objective 1: Develop a novel method for improved extraction of microplastics from soil to be applied to soil samples throughout the project

Chapter 3 focused on the development of a novel methodology for the recovery of microplastics from soil samples, as well as their enumeration through optical microscopy and identification through FTIR microscopy. To date, most microplastic extraction methods rely on the differences in density between microplastics and soil particles (namely density separation or flotation). Typically, density separation fails to recover high-density microplastics due to their closeness in density to the salt solutions used. Density separation is also incapable of recovering microplastics which are incorporated into soil aggregates due to the overall heavier weight of the complex.

In this thesis, a novel method was developed which coupled the use of the high-gradient magnetic separation (HGMS) and hydrophobised iron nanoparticles for binding to the surface of microplastics to facilitate high-gradient magnetic separation from soils and their subsequent recovery. The method involved three stages: Stage 1 – initial removal of inherently present magnetic soil particles; Stage 2 – tagging of microplastics with modified iron nanoparticles to render them magnetic; and Stage 3 – recovery of surface modified microplastics. Tests were performed to compare the HGMS method's capability to extract several microplastic morphologies, sizes, and compositions against the commonly

used density separation method using spiked samples in different soil types, as well as testing on an environmental sample. The developed HGMS method was found to achieve significantly higher recoveries of all microplastics tested in all soil types tested compared to density separation (p < 0.05) and was not affected by properties which hinder density separation. Fibres partially embedded in soil aggregates were also recovered using the developed HGMS method, aiding to improve the accuracy and confidence in reporting microplastic abundance. Furthermore, the process only took ~30 min to process one sample, compared to 2-3 days for density separation. HGMS removed the need for toxic salts by using ethanol instead, thus reducing impacts to both health and cost. The use of an electromagnet allowed the system to be controlled and allowed microplastics to be optimally recovered easily without damage. A potential drawback of the novel HGMS method is that some knowledge of the soil composition and particle size may be required prior to microplastic extraction as this influences the parameters required for separation. However, it is possible to identify broad soil types relatively easily by hand texturing.

The developed HGMS method was latterly applied to two studies in this thesis (Chapters 4 and 5). The feasibility and use of HGMS for microplastic extraction from sewage sludges, which is a different complex matrix to soil, was also successfully tested and implemented in Chapter 4.

Post-extraction, microplastics were enumerated by optical microscopy. However, the use of a counter-staining approach was investigated for its use in improving the detection of microplastics. The use of fluorescent dyes (Nile Red for microplastics and DAPI for organic matter) offered a substantial improvement in micro- and nanoplastic detection following HGMS extraction using fluorescent microscopy. However, the investment in the set up and optimisation of this was deemed to be out of scope for this project but warrants further investigation and implementation for future work.

8.3 Objective 2: Measure microplastics in archived soils collected from sewage sludge-treated land (1994-2019) to investigate their fate over time

Chapter 4 described the investigation into the accumulation, persistence, and degradation of microplastics in soils treated with sewage sludge. A field at the former research farm facility at Hartwood, Lanarkshire was part of a UK wide long-term sludge experiment (25 years), whereby various sewage sludges were added to plots over the first four years of the experiment (1994-1997) then soil samples were collected biennially for monitoring over time (1997-2019) and subsequently archived in

the National Soils Archive. The fate of microplastic pollution as a result of sewage sludge treatment over time was tracked at a high temporal resolution in these archived soil samples. Microplastics were extracted from the soil using the developed HGMS method. The HGMS method was also successfully applied to the sewage sludge samples to recover microplastics. Macroplastics were recovered from the sludge samples by hand following visual inspection.

Quantitative data showed that the application of sewage sludges resulted in huge increase in microplastic levels in the treatment plots ($p < 0.05$) and demonstrated how sewage sludges are a significant source and pathway of microplastics into soils. Data also showed that microplastics persisted at relatively constant levels across the 25-year period, and possibly beyond. Evidence of microplastic accumulation in the untreated control plots highlighted the potential for microplastics to be carried through surface run-off from the treated plots to uncontaminated areas, or be deposited atmospherically from additional sources.

Through size measurements and SEM imaging, fibres, fragments, and films were found to be more susceptible to degradation compared to other microplastic morphologies such as flakes or fragments, indicating that these microplastics may actively release micro- and potentially nanoplastics into the surrounding soil. Further investigation and development of methodologies to study nanoplastic pollution would be beneficial given the reported higher toxicity of nanoplastics to soil biota. Dye loss from fibres was also evident, although, the fate of these dyes is unknown. Given the environmental toxicity of some dyes, this may be of concern and warrants further investigation.

Determining the composition of microplastics was a useful tool in this study as it enabled the source of microplastics to be traced. For example, the presence of rarely observed high-density microplastics such as polymethyl methacrylate and polyurethane could be linked to industrial waste rather than municipal waste. Microplastic fragments and films were similar in composition to the macroplastics recovered directly from the applied sewage sludges and microplastics were also similar to those recovered from their respective sludge samples.

Of further interest is the potential for these microplastics to act as vectors for other pollutants present in sewage sludge (e.g., organic pollutants, pathogens, and heavy metals), causing further effects on soil

ecosystem functions, and potentially animal and human health. The interactions of microplastics with organic pollutants was explored in Chapters 7 and 8 (see section 8.6).

8.4 Objective 3: Measure microplastics in soils archived in the National Soils Inventory for Scotland to determine the prevalence of microplastics in Scotland on a national spatial scale

Surface soils were subsampled from the National Soils Inventory for Scotland (NSIS) and subjected to HGMS microplastic extraction as discussed in Chapter 5. Microplastics were then enumerated, categorised by their morphologies, measured in size, and their compositions identified through FTIR analysis.

Microplastics in Scottish soils were dominated by synthetic fibres which were predominantly white or colourless, however, there was also a high proportion of fibres with evidence of dye loss, whereby the loss of their dyes (potentially into the surrounding soil) may have an unknown impact on the soil environment. Spectral analysis revealed that microplastics recovered from all soil samples displayed signs of weathering (i.e., high carbonyl indices). Weathered microplastics have been reported to increase the potential severity of impacts on soil health and function.

Future work could include assessment of microplastic pollution in the corresponding samples in the first NSIS collection (1978-1987) to compare how microplastic abundance has changed over time at a national scale. Furthermore, the current NSIS dated from between 2007 to 2009 so may not accurately reflect present day pollution levels and would be worth investigating how microplastic pollution has progressed at the current day. Nonetheless, this study provides precedence for future national scale studies on microplastics in soils both within and out with Scotland.

8.5 Objective 4: Map microplastic distribution and investigate factors that influence microplastic distribution (e.g., land use, soil type, environmental and biological factors) using multivariate statistics

After enumeration and categorisation of microplastics, their distribution was mapped, highlighting areas of 'cold- and hotspots', where microplastic abundance was very low or very high, respectively. This allowed factors which may influence microplastic distribution in Scottish soils to be identified for

further investigation through various statistical tests, e.g., Kruskal-Wallis, Spearman's rank correlation, and non-metric multidimensional scaling.

Several factors were found to correlate with microplastic pollution and influence their distribution. Land use was identified as a significant factor, whereby soils from high-intensity land management such as arable land contained a higher abundance of microplastics as well as those of larger sizes. The close proximity of the sampling location to highly populated areas and roadways similarly correlated with increased microplastic abundance and size.

Evaluation of the data indicated that slope bearing at sampling locations influenced microplastic abundance and size. Areas facing into the direction of prevailing winds were more susceptible to atmospheric deposition of microplastics (and of a smaller size) than areas that were sheltered or faced away from the direction of prevailing winds. This is the first study to the author's knowledge to investigate the role soil topography plays in influencing microplastic distribution. Furthermore, slope gradient also had a significant negative relationship with microplastic abundance, indicating that microplastics may be potentially translocated through processes such as horizontal surface run-off which may lead to accumulation at flatter, lower altitude areas. Microplastic size and abundance had a significant relationship with altitude, with smaller microplastic sizes being present at high altitudes likely due to the preferential atmospheric transportation and deposition of these smaller microplastics.

Soil physicochemical properties were also found to correlate with microplastic abundance and size, however, these were likely reflections of their corresponding land uses. Furthermore, evidence from this study suggested that the vegetation present significantly influenced microplastic abundance and size. For example, dense semi-natural vegetation (e.g., heather) may physically impede microplastics reaching the surface of soils, particularly larger microplastics, and warrants further investigation. This study only assessed microplastics in the surface soils (0-5 cm) and the findings suggest that future work would be beneficial in measuring and assessing microplastic pollution in the lower soil horizons, and the factors which affect their distribution such as root depth and soil drainage, since results for this study suggested these factors may play an important role.

Lastly, there were significant correlations with persistent organic pollutants, including plasticisers, additives, and by-products, which each have links to plastic manufacturing and degradation, suggesting that microplastics may contribute to soil pollution of these contaminants through leaching or that they share a common anthropogenic source. This was further investigated in this project – see section 8.6.

The generation of this background microplastic data allowed for the understanding and assessment of the scale of microplastic pollution in Scottish surface soils at a national scale, enabling the identification of potential mitigation strategies for preventing further significant terrestrial microplastic pollution.

8.6 Objective 5: Determine the sorption and desorption kinetics of organic contaminants with microplastics and investigate the impact of microplastics carrying organic pollutants on soil function and ecosystem services using microbial respiration, microbial activity (MicroResp^{TM}), and microbial community structure (16S rRNA gene sequencing)

Chapter 6 reported on the determination of the sorption and desorption kinetics for 16 priority polycyclic aromatic hydrocarbons (PAHs) with two different sizes of polyethylene microfilms mixed in an agricultural soil. PAHs correlated with microplastic abundance across Scotland in Chapter 5 (see section 8.5) which raised concerns to the consequences of their potential interactions in soils. Typically, studies elucidating sorption kinetics of chemical pollutants with microplastics utilise a soil suspension experimental set up, however, this study aimed to investigate sorption kinetics using a true soil matrix, simulating environmental conditions.

Sorption data fitted a first order equilibrium model while desorption data fitted an exponential decay model. Results indicated that sorption and desorption kinetics were influenced by the molecular weight, water solubility, and logK_{ow} values of PAHs, and there were no significant differences between the rate of sorption or desorption observed. Smaller microfilm sizes reached higher estimated equilibrium concentrations during desorption but no significant difference between the different microfilm sizes was observed during sorption (p > 0.05).

Organic carbon content in soil was increased following PAH amendment and was observed to decrease over the time course as the PAHs sorbed to the microfilms. The greater reduction in organic carbon content in soil containing the smaller sized microfilms indicated that these microfilms sorbed a greater

amount of PAHs as expected due to their higher surface area. Soils undergoing sorption underwent significant acidification throughout the 30-day period ($p < 0.05$) likely due to the production of acidic degradation products (e.g., naphthoic acid) through microbial degradation. This suggests that PAH sorption to microfilms decreased their availability for degradation, thereby alleviating the soil from acidification which could negatively impact on crop production. Additional experiments will be required to understand the isotherms and thermodynamics of the PAHs tested.

Subsequently, the combined effect of microfilms and chrysene on soil microbial function and community composition were investigated. Chrysene was one of the most abundant PAHs in the NSIS dataset due to its greater chemical stability and persistence. Soil respiration was used as a proxy for ecosystem function while MicroResp™ was used to as a proxy to measure microbial activity through substrate-induced respiration. In both tests, the microfilm only treatment resulted in an increase in respiration (but this was not significant), while chrysene only treatments resulted in a significant decrease in respiration ($p < 0.05$). Chrysene-bound microfilms did not result in a significant change in respiration for either test compared to a soil negative control indicating that the sorption of chrysene to microfilms reduced the bioavailability of chrysene to soil microbes, thereby alleviating the negative impact of chrysene. Glucose-induced respiration suggested that the increased respiration observed in both tests for microfilm treatments was a result of increased microbial biomass and, opposingly, the reduction in respiration in the chrysene treatments was a result of decreased microbial biomass. Principal component analysis confirmed that the microbial communities' ability to utilise carbon substrates in the microfilm and chrysene treatments, respectively, was different to the soil negative control, while soil and chrysene-sorbed microfilms were similar.

Soils for each treatment were processed for bacterial 16S rRNA gene sequencing to determine whether the incorporation of microplastics, chrysene, or both had an effect on soil microbial community composition, particularly given the effects observed with microbial activity. Beta diversity of the microbial community compositions showed changes in the microbial communities between the treatments. Differences in the microbial communities was more pronounced at lower taxonomic levels (i.e., family level) and there was evidence of rarer species enrichment pertaining to chrysene degradation in the chrysene treatments and, to a lesser degree, in the chrysene-bound microfilm treatments. This further suggested that the sorption of chrysene to polyethylene microfilms indeed limited the availability of chrysene to soil micro-organisms and may alleviate the immediate effects of chrysene as suspected from evidence gathered in Chapter 6.

Despite microfilms alleviating the negative impact of chrysene, the interaction of PAHs with microfilms in agricultural soils may lead to prolonged exposure of PAHs to the soil environment, crops intended for human consumption, livestock, and humans, and warrants further investigation in long-term studies.

8.7 Thesis Synthesis

This project aimed to determine the prevalence of microplastics over time and space as well as elucidate their interactions and impacts in the terrestrial environment. The data generated from this project will have impacts from academia through to industry as well as the public. This includes setting precedence for future microplastic studies and pollution monitoring and informing policy on the prevention of future microplastic pollution and formulate remediation strategies to tackle the current risks to the environment, food security, and human health. It will also be beneficial for educating the public on the consequences of the misuse and poor waste disposal of plastics and how the risks of microplastic pollution are far-reaching, not only across the natural environment, but to humans themselves.

It is important to establish microplastic prevalence to learn how humans impact soil microplastic pollution, but also how soil microplastic pollution can impact human health and activity. Firstly, the extraction of microplastics from soil is arguably the most important step in microplastic analyses. In this project, a novel high-gradient magnetic separation (HGMS) extraction method was developed and applied throughout this project which significantly improved microplastic recoveries (particularly high density microplastics) and eliminated limiting factors experienced with the commonly used density separation method. Efficient extraction of all microplastic compositions, sizes, and morphologies is important to generate accurate data on microplastic pollution. HGMS systems are commercially available and scalable, therefore, it is recommended that future studies implement the use of the HGMS method to ensure improved and accurate microplastic investigations. The principal for extraction could be further researched and modified to be used as a tool for soil remediation.

The data generated from the spatial distribution study in this project highlighted that microplastics were ubiquitous across the whole of Scotland and emphasised that higher intensity human interaction with the land greatly influenced their distribution. In the first instance, plastic pollution in the natural environment is predominantly the consequence of human consumerism and poor waste management

or littering. It identified that the synergistic relationship between Scotland's wet and windy climate and soil topography had an influence on microplastic distribution in rural soils. However, the impact of human influence on microplastic pollution was further evidenced in soils where the reliance of plastic in land management was greatest, e.g., mulch film in agriculture or tree covers in forestry. Furthermore, the data generated from the temporal distribution of microplastics in soil following sewage sludge amendment study reinforced how human activity further increases microplastic pollution and demonstrated how the potential risks of microplastic pollution are long-lasting. Evidence suggested microplastics could persist relatively unchanged for over 25 years following addition to the soil, increasing their potential to damage soil health which can lead to the decline in crop yield and quality. The presence of microplastics in food production systems pose a possible exposure pathway to humans through the consumption of microplastic-contaminated crops.

While the influences of the environment on microplastic distribution may be beyond intervention, the data generated from these spatial and temporal studies made it clear that continued and future use of plastic by humans must be addressed through the introduction of alternative and sustainable materials and land management practices, as well as improved waste management and recycling. Moreover, it is evident from the findings of this project that further regulations on the use of biosolids is required to encompass restrictions on their use based on their microplastic content, similar to existing legislation on metal content in sludges. The incorporation of microplastic removal procedures from sludges during wastewater treatment would be recommended to improve on safeguarding crops, the environment, and humans from the growing release of microplastics through wastewater systems. Furthermore, policy regulators must continue to target and educate different sectors (from farmers to manufacturers to the public) on plastic misuse and the risks associated with microplastic pollution, but importantly, invest in suitable alternative materials for replacing plastics in agriculture and daily life to support these sectors in transitioning and mitigating future microplastic pollution. The generation of soil archives is also highly recommended for future spatio-temporal microplastic monitoring in order to collect vast and invaluable microplastic data not only on a national scale, but globally.

While it is highly valuable to establish the spatio-temporal distribution of microplastics, it is equally important to understand comprehensively how microplastics interact within the soil environment and the impact of these interactions on soil function. Hence this project concluded by elucidating the interaction of persistent organic pollutants, polycyclic aromatic hydrocarbons (PAHs), with microplastics and their impact on microbial activity and community structure. While PAHs can be

naturally occurring through wildfires for instance, their prevalence in the environment is largely driven, again, through harmful human activities. Sorption studies within this project suggested that PAH sorption to microplastics prevented their degradation, therefore, alleviated the soil from acidification but also prolongs their longevity, potentially alleviating the soil environment from the direct detrimental impacts of PAHs but increasing the chronic exposure of PAHs to soil flora and fauna as well as livestock and humans. PAH uptake to larger-sized microplastics may increase the likelihood of ingestion during grazing by livestock or dermal contact to humans through occupational exposure, while sorption to smaller-sized micro(nano)plastics may increase the uptake and slow release of PAHs in crops posing a significant risk to human and animal health through ingestion. By studying the impact of chrysene (a model PAH) sorption to microplastics, it was confirmed that sorption alleviated the negative impact of chrysene to microbial activity and biomass, indicating that this interaction was in fact beneficial. However, it is recommended that future long-term studies are conducted given that the sorption study suggested that increased PAH longevity is possible, meaning long-term effects may be more profound. A change in microbial community structure was also observed which has the potential to negatively impact soil health and ecosystem function (e.g., nutrient cycling) leading to issues with factors including crop production and disease suppression, relating back to implications on human health and our reliance on healthy soils for sustainability. Currently, there are no universally effective methods for remediation of soils from either microplastics or persistent organic pollutants, therefore, it is timely to further investigate the interactions of anthropogenic pollutants (i.e., microplastics and (in)organic pollutants) and identify methods of remediation in affected soil systems.